Lectures in Turbulence for the 21st Century

William K. George
Department of Aeronautics
Imperial College of London
London, UK
and
Professor of Turbulence Emeritus
Department of Applied Mechanics
Chalmers University of Technology
Gothenburg, Sweden

16 January 2013

Preface These notes have evolved over many years and are offered freely to students and researchers everywhere. In my own personal history I came from rather humble beginnings, and was the beneficiary of very generous scholarship and fellowship support, even with books provided. Without this generosity on the part of the taxpayers of the State of Maryland, the USA Federal Goverment and the Johns Hopkins University, I could never be where I am today. So these notes are my gift to all those who come behind, and especially those who find the cost of most books to be a real financial struggle. If you reference them, please refer to the website where others can find them (www.turbulence-online.com). They will probably never stop evolving, so it might be a good idea to check once in a while for updated versions.

These notes actually started as book on turbulence I was writing in the early 1980's, and which was nearly finished and ready to be published. I had taught turbulence classes for more than a decade (at SUNY/Buffalo) and thought I had found a way to improve the available texts. Fortunately (or unfortunately for publication), one day I ended up in class without my notes, and in trying to answer questions asked to me by the class, I ended up in a very different place than I expected. Some of the results have been published in various places, and some are referred to herein. But it was clear to me from the very first moment that the book had to go: I no longer believed to be true what I was saying in it. The last 30 years have been an interesting journey as successive waves of students have asked even more difficult questions, and as I wrestled to figure out what was true and not true. I have tried in these notes to provide to the best of my ability an honest account of turbulence and what I think we know for sure and what we do not. I remember despairing as a student that it seemed that all the problems were solved, and there was really nothing fundamental left to do. I doubt any careful reader of these notes will come to that erroneous conclusion. The goal was not to be comprehensive, so there is much left out. But instead the goal is to inspire continued study, and to provide a foundation for it.

I have also tried to make these notes fun to read. If you are expecting a totally serious account, you will probably be disappointd. I have included my opinions when I thought it would help in understanding, and also anedotes when I could think of them. The point is that turbulence (like all research) is done by people. It is probably true that the ones who do the best work are also having the most fun. I hope the newcomers to the field find that inspirational.

Please do not hesitate to ask me questions or point out places where I have screwed up. My email address is georgewilliamk@gmail.com. Whenever possible I will try to respond.

Contents

Chapter 1

The Nature of Turbulence

1.1 The turbulent world around us

The turbulent motion of fluids has captured the fancy of observers of nature for most of recorded history. From howling winds to swollen floodwaters, the omnipresence of turbulence paralyzes continents and challenges our quest for authority over the world around us. But it also delights us with its unending variety of artistic forms. Subconsciously we find ourselves observing exhaust jets on a frosty day; we are willingly hypnotized by licking flames in an open hearth. Babbling brooks and billowing clouds fascinate adult and child alike. From falling leaves to the swirls of cream in steaming coffee, turbulence constantly competes for our attention.

Turbulence by its handiwork immeasurably enriches the lives of even those who cannot comprehend its mysteries. Art museums are filled with artists attempts to depict turbulence in the world around us. The classic sketch of Italian renaissance artist and engineer, Leonardo da Vinci, shown in Figure 1.1 represents both art and early science. And as the tongue-in-cheek poem below by Corrsin (one of the turbulence greats of the past century) shows, even for those who try, the distinction between art and research is often difficult to make.

SONNET TO TURBULENCE
by
S. Corrsin[1]
(For Hans Liepmann [2] on the occasion of his 70th birthday,
with apologies to Bill S. and Liz B.B.)

Shall we compare you to a laminar flow?
You are more lovely and more sinuous.

[1]Stan Corrsin was a famous and much beloved turbulence researcher and professor at the Johns Hopkins University.

[2]Hans Liepmann was another famous turbulence researcher and professor at Cal Tech, who was Corrsin's Ph.D. dissertation advisor.

Rough winter winds shake branches free of snow,
And summer's plumes churn up in cumulus.

How do we perceive you? Let me count the ways.
A random vortex field with strain entwined.
Fractal? Big and small swirls in the maze
May give us paradigms of flows to find.

Orthonormal forms non-linearly renew
Intricate flows with many free degrees
Or, in the latest fashion, merely few —
As strange attractor. In fact, we need Cray 3's[3].

Experiment and theory, unforgiving;
For serious searcher, fun ... and it's a living!

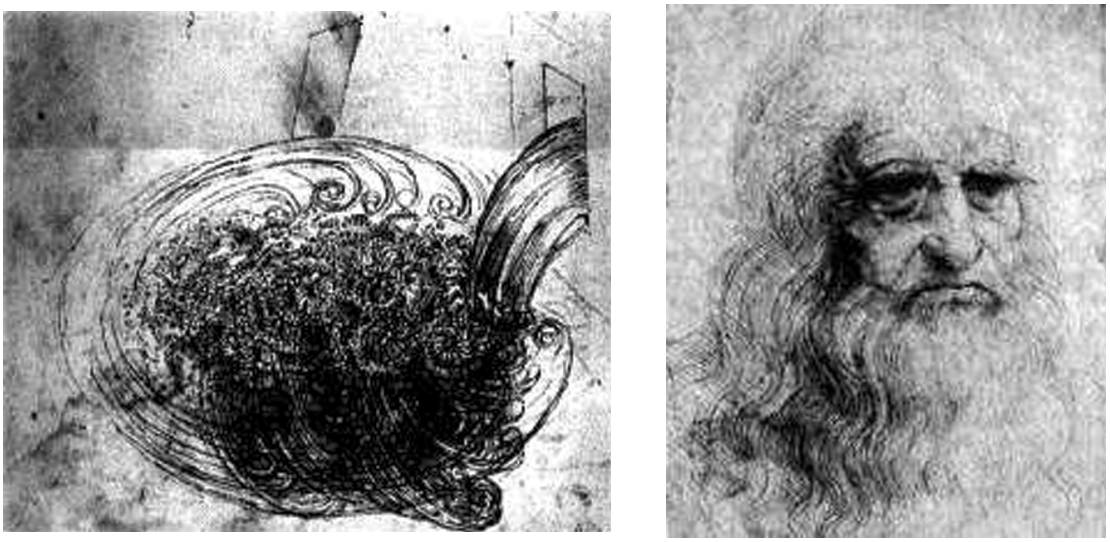

Figure 1.1: Leonardo da Vinci's observation of turbulent flow: Drawing of a free water jet issuing from a square hole into a pool (courtesy of eFluids.com).

These lectures will mostly deal with the equations used to describe the mechanics of turbulence. It is only equations which can give us the hope of predicting turbulence. But your study of this subject will be missing a great deal if this is all you learn. The advantage of studying turbulence is that you truly can see it almost everywhere as it mixes and diffuses, disrupts and dissipates the world around us.

So teach yourself to observe the natural and manmade processes around you. Not only will your life become more interesting, but your learning will be enhanced as well. Be vigilant. Whenever possible relate what you are learning to what you see. Especially note what you do not understand, and celebrate when and if you do. Then you will find that the study of turbulence really is fun.

[3]At the time this poem was written, the Cray 2 was the world's most powerful computer.

1.2 What is turbulence?

Turbulence is that state of fluid motion which is characterized by apparently random and chaotic three-dimensional vorticity. When turbulence is present, it usually dominates all other flow phenomena and results in increased energy dissipation, mixing, heat transfer, and drag. If there is no three-dimensional vorticity, there is no real turbulence. The reasons for this will become clear later; but briefly, it is ability to generate new vorticity from old vorticity that is essential to turbulence. And only in a three-dimensional flow is the necessary stretching and turning of vorticity by the flow itself possible.

For a long time scientists were not really sure in which sense turbulence is "random", but they were pretty sure it was. Like anyone who is trained in physics, we believe the flows we see around us must be the solution to some set of equations which govern. (This is after all what mechanics is about — writing equations to describe and predict the world around us.) But because of the nature of the turbulence, it wasn't clear whether the equations themselves had some hidden randomness, or just the solutions. And if the latter, was it something the equations did to them, or a consequence of the initial conditions?

All of this began to come into focus as we learned about the behavior of strongly non-linear dynamical systems in the past few decades. Even simple non-linear equations with deterministic solutions and prescribed initial conditions were found to exhibit chaotic and apparently random behavior. In fact, the whole new field of chaos was born in the 1980's[4], complete with its new language of strange attractors, fractals, and Lyapunov exponents. Such studies now play a major role in analyzing dynamical systems and control, and in engineering practice as well.

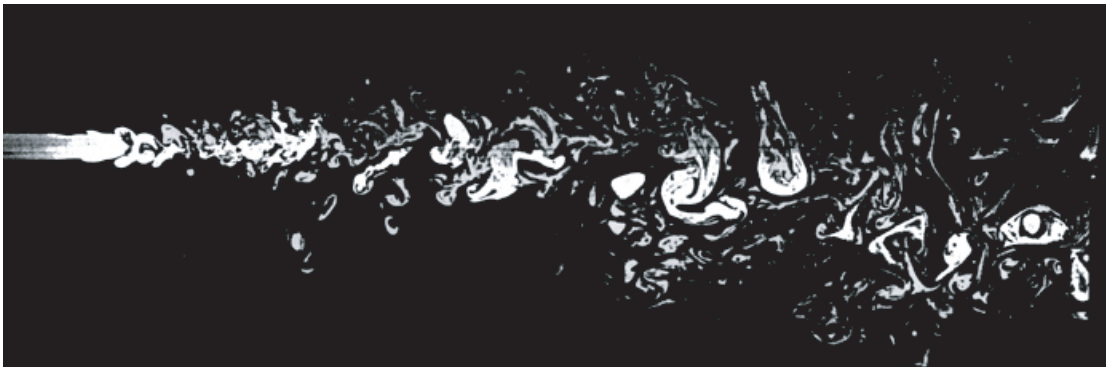

Figure 1.2: Turbulence in a water jet. Photo from Dimotakis, Miake-Lye and Papantoniou, *Phys. Flds., 26* (11), 3185 – 3192.

Turbulence is not really chaos, at least in the sense of the word that the dynamical systems people use, since turbulent flows are not only time-dependent but space dependent as well. But as even the photos of simple turbulent jets

[4]The delightful book by James Gleik "Chaos: the making of a new science" provides both interesting reading and a mostly factual account.

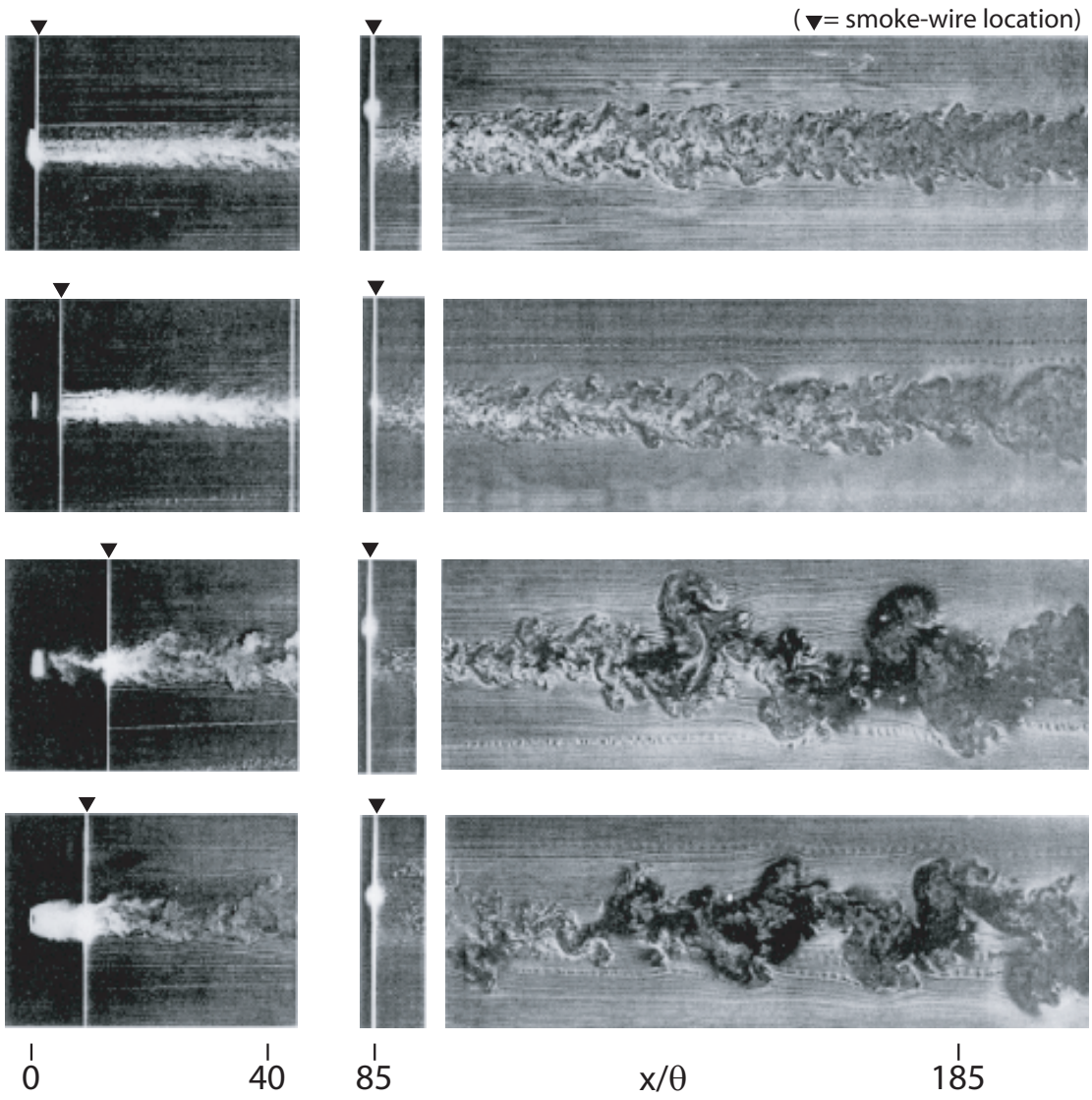

Figure 1.3: Axisymmetric wakes from four different generators. Photo from S.C. Cannon, Ph.D. Dissertation., U.of Ariz, 1991.

and wakes shown in Figures 1.2 and 1.3 make clear, turbulence has many features that closely resemble chaos. Obvious ones include spatial and temporal intermittency, dissipation, coherent structures, sensitive dependence of the instantaneous motions on the initial and upstream conditions, and even the near-fractal distribution of scales. In fact, the flows we see themselves bear an uncanny resemblance to the phase plane plots of strange attractors. No one would ever confuse a jet with a wake, but no two wakes seem to be quite alike either.

Because of the way chaos has changed our world view, most turbulence researchers now believe the solutions of the fluid mechanical equations to be deterministic. Just like the solutions of non-linear dynamical systems, we believe turbulent solutions to be determined (perhaps uniquely) by their boundary and

initial conditions[5]. And like non-linear dynamical systems, these deterministic solutions of the non-linear fluid mechanics equations exhibit behavior that appears for all intents and purposes to be random. We call such solutions *turbulent*, and the phenomenon *turbulence*. Because of this chaotic-like and apparently random behavior of turbulence, we will need statistical techniques for most of our study of turbulence.

This is a course about the mechanical mysteries of turbulence. It will attempt to provide a perspective on our quest to understand it. The lack of a satisfactory understanding of turbulence presents one of the great remaining fundamental challenges to scientists — and to engineers as well, since most technologically important flows are turbulent. The advances in understanding over the past few decades, together with the advent of large scale computational and experimental capabilities, present the scientist and engineer with the first real capabilities for understanding and managing turbulent flows. As a result, this is a really wonderful time to study this subject.

1.3 Why study turbulence?

There really are the *TWO* reasons for studying turbulence — engineering and physics! And they are not necessarily complementary, *at least in the short run.*

Certainly a case can be made that we don't know enough about turbulence to even start to consider engineering problems. To begin with (as we shall see very quickly over the next few lectures), we always have fewer equations than unknowns in any attempt to predict anything other than the instantaneous motions. This is the famous **turbulence closure problem**.

Of course, closure is not a problem with the so-called DNS (Direct Numerical Simulations) in which we numerically produce the instantaneous motions in a computer using the exact equations governing the fluid. Unfortunately we won't be able to perform such simulations for real engineering problems until at least a few hundred generations of computers have come and gone. And this won't really help us too much, since even when we now perform a DNS simulation of a really simple flow, we are already overwhelmed by the amount of data and its apparently random behavior. This is because without some kind of theory, we have no criteria for selecting from it in a single lifetime what is important.

The engineer's counter argument to the scientists' lament above is:

- airplanes must fly,
- weather must be forecast,
- sewage and water management systems must be built,

[5]If it comes as a surprise to you that we don't even know this for sure, you might be even more surprised to learn that there is a million dollar prize for the person who proves it.

- society needs ever more energy-efficient hardware and gadgets.

Thus, the engineer argues, no matter the inadequate state of our knowledge, **we have the responsibility as engineers to do the best we can with what we have**. Who, considering the needs, could seriously argue with this? Almost incredibly — some physicists do!

The same argument happens in reverse as well. Engineers can become so focused on their immediate problems they too lose the big picture. The famous British aerodynamicist M. Jones captured this well when he said,

> "A successful research enables problems which once seemed hopelessly complicated to be expressed so simply that we soon forget that they ever were problems. Thus the more successful a research, the more difficult does it become for those who use the result to appreciate the labour which has been put into it. This perhaps is why **the very people who live on the results of past researches are so often the most critical of the labour and effort which, in their time, is being expended to simplify the problems of the future"**[6]

It seems evident then that there must be at least two levels of assault on turbulence. At one level, the very nature of turbulence must be explored. At the other level, our current state of knowledge — however inadequate it might be — must be stretched to provide *engineering solutions* to *real problems*.

The great danger we face is of being deceived by the successes and good fortune of our "engineering solutions" into thinking we really understand the "physics". But the real world has a way of shocking us back to reality when our "tried and tested" engineering model fails miserably on a completely new problem for which we have not calibrated it. This is what happens when we really don't understand the "physics" behind what we are doing. Hopefully this course will get you excited about both the physics and the applications, so you won't fall into this trap.

1.4 The cost of our ignorance

It is difficult to place a price tag on the cost of our limited understanding of turbulence, but it requires no imagination at all to realize that it must be enormous. Try to estimate, for example, the aggregate cost to society of our limited turbulence prediction abilities which result in inadequate weather-forecasts alone. Or try to place a value on the increased cost to the consumer of the need of the designer of virtually every fluid-thermal system —from heat exchangers to hypersonic planes— to depend on empiricism and experimentation, with the resulting need for abundant safety factors and non-optimal performance by all but the crudest measures. Or consider the frustration to engineers and cost to management of the never-ending need for "code-validation" experiments every time a new class

[6] Jones, B.M. (1934) "Stalling", The Wilbur Wright Memorial Lecture". *J. Aeron. Sci*

of flows is encountered or major design change contemplated. The whole of idea of "codes" in the first place was to be able to evaluate designs without having to do experiments or build prototypes.

Some argue that our quest for knowledge about turbulence should be driven solely by the insatiable scientific curiosity of the researcher, and not by the applications. Whatever the intellectual merits of this argument, it is impossible to consider the vastness and importance of the applications and not recognize a purely financial imperative for fundamental turbulence research. The problem is, of course, that the cost of our ignorance is not confined to a single large need or to one segment of society, but is spread across the entire economic spectrum of human existence. If this were not the case, it would be easy to imagine federal involvement at the scale of America's successful moon venture or the international space station, or at very least a linear accelerator or a Galileo telescope. Such a commitment of resources would certainly advance more rapidly our understanding.

But the turbulence community — those who study and those who use the results — have failed ourselves to recognize clearly the need and nature of what we really do. Thus in turbulence, we have been forced to settle for far, far less than required to move us forward very fast, or maybe at all. Hopefully you will live to see this change. Or even better, perhaps you will be among the ones who change it.

1.5 What do we really know for sure?

Now even from these brief remarks, you have probably already figured out that the study of turbulence might be a little different than most of the subjects you have studied. This is a subject we are **still** studying. Now not everyone who teaches courses on this subject (and especially those who write books about it) will tell you this, but the truth is: *we really don't know a whole lot* **for sure** *about turbulence.* And worse, we even disagree about what we think we know!

Now, as you will learn in this course (or maybe heard somewhere before), there are indeed some things some researchers think we understand pretty well — like for example the Kolmogorov similarity theory for the dissipative scales and the Law of the Wall for wall-bounded flows, ideas you will soon encounter. These are based on assumptions and logical constructions about how we believe turbulence behaves in the limit of infinite Reynolds number. But even these ideas have never really been tested in controlled laboratory experiments in the limits of high Reynolds number, because no one has ever had the large scale facilities required to do so.[7]

It seems to be a characteristic of humans (and contrary to popular belief, scientists and engineers are indeed human) that we tend to accept ideas which

[7]The proposal to build the Nordic Wind Tunnel at Chalmers back at the beginning of this millenium was an attempt to fill this gap.

have been around a while as *fact*, instead of just *working hypotheses* that are still waiting to be tested. One can reasonably argue that the acceptance of **most** ideas in turbulence is perhaps more due to the time lapsed since they were proposed and found to be in reasonable agreement with a **limited** data base, than that they have been subjected to experimental tests over the range of their assumed validity.[8] Thus it might be wise to view most 'established' laws and theories of turbulence as more like religious creeds than matters of fact.

The whole situation is a bit analogous to the old idea that the sun and stars revolved around the earth — it was a fine idea, and even good today for navigational purposes. The only problem was that one day someone (Copernicus, Brahe and Galileo among them) looked up and realized it wasn't true. So it may be with a lot of what we believe today to be true about turbulence — some day you may be the one to look at evidence in a new way and decide that things we thought to be true are wrong.

1.6 Our personal adventure

This is a *turbulence course*. You are enthused I hope, at least for the moment, to learn about turbulence. But since no two people could be in complete agreement about something like turbulence about which we know so little, this will be perhaps a pretty unusual course. I will try really hard to be honest in what I tell you. Even so, you should not trust me entirely, nor anyone else for that matter. It will really be up to you to distinguish among what you wish to consider as *fact*, *working hypothesis*, or to dismiss as *fantasy*. It is also very important that you try to keep track of which is which in your mind, and be willing to let ideas move from one category to the other as your understanding and information grows.

Like different artists painting the same scene, the pictures you and I paint will as much reflect our own personalities and histories, as the facts. But, like real works of art, both my picture of turbulence and yours might enable others to see things that they would have otherwise missed. This does *not* imply, however, that there are not real truths to be found — only that we at this point can not say with confidence what they are. Above all, we must not forget that we seek truth and understanding, the first step toward which is learning and admitting what we do not know.

Of course we will try to never completely forget that there are real problems to be solved. Throughout these lectures I will try to use many illustrations from my own experience. But the real goal is to help you develop enough fundamental understanding that you can sort through the many options available to you for the particular problems you will encounter in the real world. And maybe, with a little luck, you will even be able to make your own contribution to the state of our knowledge about turbulence. But at very least I hope the result of this course

[8] This point was made rather forcefully by Robert R. Long, (Professor Emeritus, Johns Hopkins University) in his famous footnoted Journal of Fluid Mechanics paper in 1982.

will be to make you open to new ideas, however uncomfortable they make make you feel initially.

I encourage you to not be lazy. Too many study turbulence hoping for easy and quick answers, general formulas, and word pictures. The fact is the study of turbulence is quite difficult, and demands serious commitment on the part of the student. The notations are sometimes complex, and they must be this way to succinctly express the real physics. The equations themselves are extremely difficult, yet only by using them to express ideas can we say we understand the physics. Word pictures and sketches can help us, but they cannot be extrapolated to real problems. Of course we must resort to simplifications and at times even heuristic reasoning to understand what our equations are telling us. But be careful to never confuse these simplifications and pedagogical tools with the real flows you are likely to encounter. Sometimes they are useful in understanding, yet sometimes they can be misleading. There is no substitute for actually looking at a flow and analyzing exactly which terms in the governing equations are responsible for what you see.

If this all seems a bit discouraging, look at it this way. If the turbulence problem were easy, it would have been solved years ago. Like applying Newton's law (or even relativity) to point masses with known forces, every engineer could do turbulence on his laptop.[9] The turbulence problem has been worked on for over a century by many very smart people. There has certainly been progress, some would even say great progress. But not enough to make the study of turbulence easy. This problem is difficult. Even so, the equations require no more skills than undergraduate mathematics — just a lot of it. So be of brave heart and persevere. Do not quit before the end of an analysis. Actually carrying things out yourself is the only road to complete understanding. The difference between the success and failure of your effort will be almost entirely measured by your willingness to spend time and think difficult and complex thoughts. In other words, you can't be lazy and learn turbulence.

1.7 A brief outline

Now for some specifics: this book will provide an introduction to the fundamentals of turbulent flow. The focus will be on understanding the averaged equations of motion and the underlying physics they contain. The goal will be to provide you with the tools necessary to continue the study of turbulence, whether in the university or industrial setting. Topics covered include: what is turbulence; the Reynolds-averaged equations; instability and transition; simple closure models; the Reynolds stress equations; simple decaying turbulence; homogeneous shear flow turbulence; free turbulent shear flows; wall-bounded turbulent flows; multi-point and spectral considerations; and multi-point similarity in turbulence.

[9]Some indeed might now think this is possible, and for some very simple problems, it is.

Study questions for Chapter 1

1. Observe your surroundings carefully and identify at least ten different turbulent phenomena for which you can actually see flow patterns. Write down what you find particularly interesting about each.

2. Talk to people (especially engineers) you know (or even don't know particularly well) about what they think the *turbulence problem* is. Decide for yourself whether they have fallen into the trap that Professor Jones talks about in the quotation used in this text.

3. In 1990 I wrote an ASME paper entitled "The nature of turbulence". (You can download a copy for yourself from the TRL website.) In this paper I suggested that most turbulence researchers wouldn't recognize a solution to the turbulence problem, even if they stumbled across it. My idea was that if you don't know what you are looking for, you aren't likely to know when you find it. What do you think about this, especially in light of your interviews above?

4. Some believe that computers have already (or at least soon will) make experiments in turbulence unnecessary. The simplest flow one can imagine of sufficiently high Reynolds number to really test any of the theoretical ideas about turbulence will require a computational box of approximately $(10^5)^3$, because of the large range of scales needed. The largest simulation to-date uses a computational box of $(10^3)^3$, and takes several thousand hours of processor time. Assuming computer capacity continues to double every 1.5 years, calculate how many years it will be before even this simple experiment can be done in a computer.

5. The famous aerodynamicist Theordore von Karman once said: "A scientist studies what is; an engineer creates what has never been." Think about this in the context of the comments in Chapter 1, and about the differing goals of the scientist and the engineer. Then try to figure out how you can plot a life course that will not trap you into thinking your own little corner of the world is all there is.

6. The instructor has essentially told you that you really should believe nothing he says (or anyone else says, for that matter), just because he (or they) said it. Think about what the scientific method really is, and how you will apply it to your study of the material in this course.

7. Think about the comments that ideas become accepted simply because they have been around awhile without being disproved. Can you think of examples from history, or from your own personal experience? Why do you think this happens? And how can we avoid it, at least in our work as scientists and engineers?

Chapter 2

The Elements of Statistical Analysis

Original version February 26, 1987, last revised 11 Feb 2010.

2.1 Foreword

Much of the study of turbulence requires statistics and stochastic processes, simply because the instantaneous motions are too complicated to understand. This should not be taken to mean that the governing equations (usually the Navier-Stokes equations) are stochastic. Even simple non-linear equations can have deterministic solutions that look random. In other words, even though the solutions for a given set of initial and boundary conditions can be perfectly repeatable and predictable at a given time and point in space, it may be impossible to guess from the information at one point or time how it will behave at another (at least without solving the equations). Moreover, a slight change in the initial or boundary conditions may cause large changes in the solution at a given time and location; in particular, changes that we could not have anticipated.

In this chapter we shall introduce the simple idea of the *ensemble average*. Most of the statistical analyses of turbulent flows are based on the idea of an ensemble average in one form or another. In some ways this is rather inconvenient, since it will be obvious from the definitions that it is impossible to ever really measure such a quantity. Therefore we will spend the last part of this chapter talking about how the kinds of averages we can compute from data correspond to the hypothetical ensemble average we wish we could have measured. In later chapters we shall introduce more statistical concepts as we require them. But the concepts of this chapter will be all we need to begin a discussion of the averaged equations of motion in Chapter 3.

2.2 The Ensemble and Ensemble Averages

2.2.1 The mean (or ensemble) average

The concept of an *ensemble average* is based upon the existence of independent statistical events. For example, consider a number of individuals who are simultaneously flipping unbiased coins. If a value of one is assigned to a head and the value of zero to a tail, then the *arithmetic average* of the numbers generated is defined as:

$$X_N = \frac{1}{N}\Sigma x_n \tag{2.1}$$

where our nth flip is denoted as x_n and N is the total number of flips.

Now if all the coins are the same, it doesn't really matter whether we flip one coin N times, or N coins a single time. The key is that they must all be *independent events* — meaning the probability of achieving a head or tail in a given flip must be completely independent of what happens in all the other flips. Obviously we can't just flip one coin once and count it N times; these clearly would not be independent events.

Exercise Carry out an experiment where you flip a coin 100 times in groups of 10 flips each. Compare the values you get for X_{10} for each of the 10 groups, and note how they differ from the value of X_{100}.

Unless you had a very unusual experimental result, you probably noticed that the value of the X_{10}'s was also a random variable and differed from ensemble to ensemble. Also the greater the number of flips in the ensemble, the closer you got to $X_N = 1/2$. Obviously the bigger N, the less fluctuation there is in X_N.

Now imagine that we are trying to establish the nature of a random variable, x. The nth *realization* of x is denoted as x_n. The *ensemble average* of x is denoted as X (or $\langle x \rangle$), and *is defined as*

$$X = \langle x \rangle \equiv \lim_{N\to\infty} \frac{1}{N} \sum_{n=1}^{N} x_n \tag{2.2}$$

Obviously it is impossible to obtain the ensemble average experimentally, since we can never have an infinite number of independent realizations. The most we can ever obtain is the arithmetic mean for the number of realizations we have. For this reason the arithmetic mean can also referred to as the *estimator* for the true mean or ensemble average.

Even though the true mean (or ensemble average) is unobtainable, nonetheless, the idea is still very useful. Most importantly, we can almost always be sure the ensemble average exists, even if we can only estimate what it really is. Note that in some particularly difficult cases this may require imagining that we can sum our random variable at a given instant and time across an infinite number of universes which are governed by the same statistical rules. So the fact of the existence of the ensemble average does not always mean that it is easy to obtain in practice.

Nonetheless, unless stated otherwise, all of the theoretical deductions in this book will use this ensemble average; and therefore are completely general. Obviously this will mean we have to account for these "statistical differences" between true means and estimates of means when comparing our theoretical results to actual measurements or computations.

In general, the x_n could be realizations of any random variable. The X defined by equation 2.2 represents the ensemble average of it. The quantity X is sometimes referred to as the *expected value* of the random variable x, or even simply its *mean.*

For example, the velocity vector at a given point in space and time, $\vec{x}, t$, in a given turbulent flow can be considered to be a random variable, say $u_i(\vec{x}, t)$. If there were a large number of identical experiments so that the $u_i^{(n)}(\vec{x}, t)$ in each of them were identically distributed, then the ensemble average of $u_i^{(n)}(\vec{x}, t)$ would be given by

$$\langle u_i(\vec{x}, t)\rangle = U_i(\vec{x}, t) \equiv \lim_{N\to\infty} \frac{1}{N} \sum_{n=1}^{N} u_i^{(n)}(\vec{x}, t) \tag{2.3}$$

Note that this ensemble average, $U_i(\vec{x}, t)$, will, in general, vary with the independent variables $\vec{x}$ and t. It will be seen later that under certain conditions the ensemble average is the same as the average which would be generated by averaging in time, or even space. But even when a time (or space) average is not meaningful, however, the ensemble average can still be defined; e.g., as in an non-stationary or periodic flow. Only ensemble averages will be used in the development of the turbulence equations in this book unless otherwise stated. Thus the equations derived will be completely general, and quite independent of the particular nature of the flow, or even its statistical character.

2.2.2 Fluctuations about the mean

It is often important to know how a random variable is distributed about the mean. For example, Figure 2.1 illustrates portions of two random functions of time which have identical means, but are obviously members of different ensembles since the amplitudes of their fluctuations are not distributed the same. It is possible to distinguish between them by examining the statistical properties of the fluctuations about the mean (or simply the fluctuations) defined by:

$$x' = x - X \tag{2.4}$$

It is easy to see that the average of the fluctuation is zero, i.e.,

$$\langle x'\rangle = 0 \tag{2.5}$$

On the other hand, the ensemble average of the square of the fluctuation is *not* zero. In fact, it is such an important statistical measure we give it a special name, the **variance**, and represent it symbolically by either $var[x]$ or $\langle (x')^2\rangle$. The

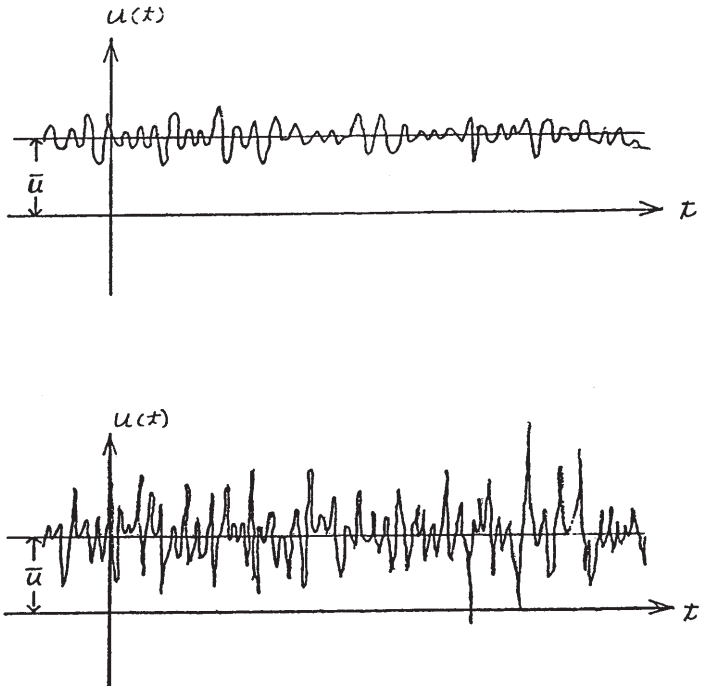

Figure 2.1: A typical random function of time with non-zero mean value.

variance is defined as:

$$var[x] \equiv \langle (x')^2 \rangle = \langle [x - X]^2 \rangle \tag{2.6}$$

$$= \lim_{N\to\infty} \frac{1}{N} \sum_{n=1}^{N} [x_n - X]^2 \tag{2.7}$$

Note that the variance, like the ensemble average itself, can never really be measured, since it would require an infinite number of members of the ensemble.

It is straightforward to show from equation 2.2 that the variance in equation 2.6 can be written as:

$$var[x] = \langle x^2 \rangle - X^2 \tag{2.8}$$

Thus the variance is the *second-moment* minus the square of the *first-moment* (or mean). In this naming convention, the ensemble mean is the *first moment.*

Exercise Use the definitions of equations 2.2 and 2.7 to derive equation 2.8.

The variance can also referred to as the *second central moment of x.* The word central implies that the mean has been subtracted off before squaring and averaging. The reasons for this will be clear below. If two random variables are identically distributed, then they must have the same mean and variance.

The variance is closely related to another statistical quantity called the *standard deviation* or root mean square (*rms*) value of the random variable x,which is

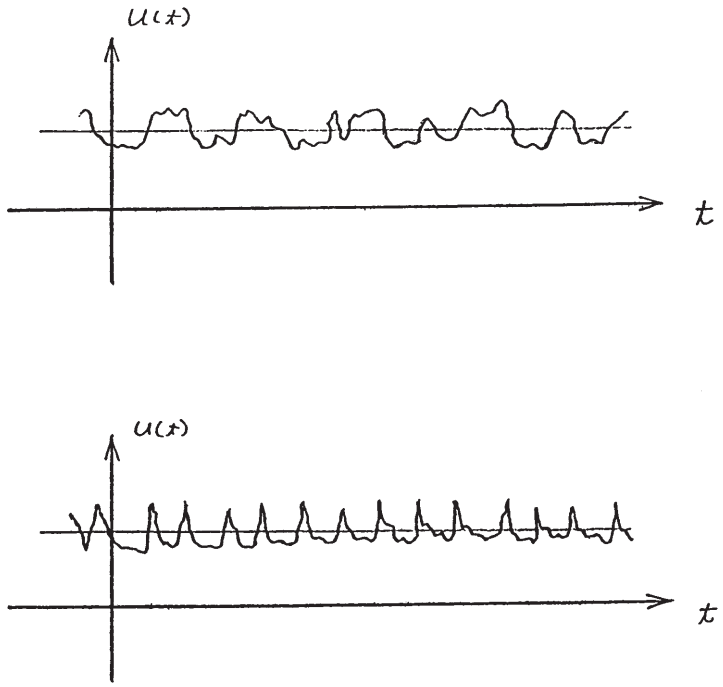

Figure 2.2: Two random functions of time having the same mean and variance, but very different higher moments.

denoted by the symbol, σ_x. Thus,

$$\sigma_x \equiv (var[x])^{1/2} \tag{2.9}$$

or $\sigma_x^2 = var[x]$.

2.2.3 Higher moments

Figure 2.2 illustrates two random variables of time which have the same mean and also the same variances, but clearly they are still quite different. It is useful, therefore, to define higher moments of the distribution to assist in distinguishing these differences.

The m-th moment of the random variable is defined as:

$$\langle x^m \rangle = \lim_{N\to\infty} \frac{1}{N} \sum_{n=1}^{N} x_n^m \tag{2.10}$$

It is usually more convenient to work with the *central moments* defined by:

$$\langle (x')^m \rangle = \langle (x - X)^m \rangle = \lim_{N\to\infty} \frac{1}{N} \sum_{n=1}^{N} [x_n - X]^m \tag{2.11}$$

The central moments give direct information on the distribution of the values of the random variable about the mean. It is easy to see that the variance is the second central moment (i.e., $m = 2$).

2.3 Probability

2.3.1 The histogram and probability density function

The frequency of occurrence of a given *amplitude* (or value) from a finite number of realizations of a random variable can be displayed by dividing the range of possible values of the random variables into a number of slots (or windows). Since all possible values are covered, each realization fits into only one window. For every realization a count is entered into the appropriate window. When all the realizations have been considered, the number of counts in each window is divided by the total number of realizations. The result is called the **histogram** (or *frequency of occurrence* diagram). From the definition it follows immediately that the sum of the values of all the windows is exactly one.

The shape of a histogram depends on the *statistical distribution of the random variable*, but it also depends on the total number of realizations, N, and the size of the slots, Δc. The histogram can be represented symbolically by the function $H_x(c, \Delta c, N)$ where $c \leq x < c + \Delta c$, Δc is the slot width, and N is the number of realizations of the random variable. Thus the histogram shows the relative frequency of occurrence of a given value range in a given ensemble. Figure 2.3 illustrates a typical histogram. If the size of the sample is increased so that the number of realizations in each window increases, the diagram will become less erratic and will be more representative of the actual *probability* of occurrence of the amplitudes of the signal itself, as long as the window size is sufficiently small.

If the number of realizations, N, increases without bound as the window size, Δc, goes to zero, the histogram divided by the window size goes to a limiting curve called the *probability density function*, $B_x(c)$. That is,

$$B_x(c) \equiv \lim_{\substack{N \to \infty \\ \Delta c \to 0}} H(c, \Delta c, N)/\Delta c \tag{2.12}$$

Note that as the window width goes to zero, so does the number of realizations which fall into it, NH. Thus it is only when this number (or relative number) is divided by the slot width that a meaningful limit is achieved.

The **probability density function** (or **pdf**) has the following properties:

- Property 1:

$$B_x(c) > 0 \tag{2.13}$$

  always.

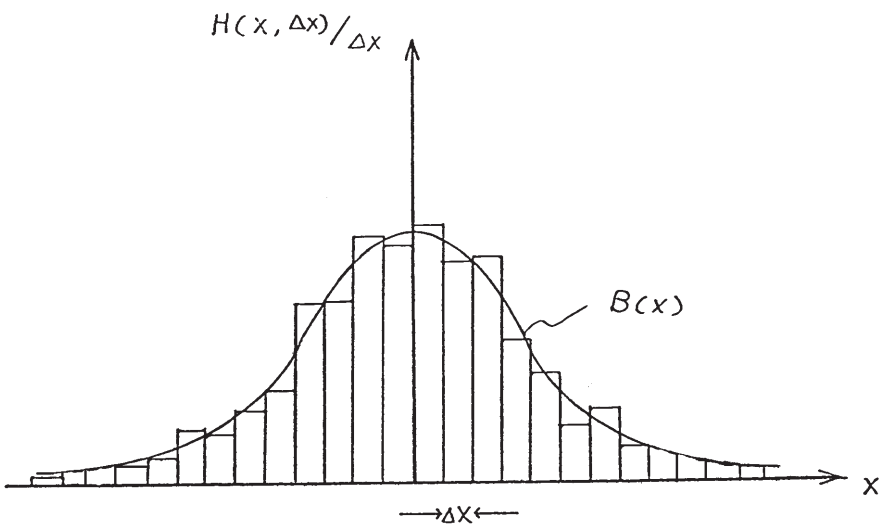

Figure 2.3: Histogram, together with it's limiting probability density function.

- Property 2:
$$Prob\{c < x < c + dc\} = B_x(c)dc \tag{2.14}$$
where $Prob\{\ \}$ is read "the probability that".

- Property 3:
$$Prob\{c < x\} = \int_{-\infty}^{x} B_x(c)dc \tag{2.15}$$

- Property 4:
$$\int_{-\infty}^{\infty} B_x(x)dx = 1 \tag{2.16}$$

The condition imposed by property (1) simply states that negative probabilities are impossible, while property (4) assures that the probability is unity that a realization takes on some value. Property (2) gives the probability of finding the realization in a interval around a certain value, while property (3) provides the probability that the realization is less than a prescribed value. Note the necessity of distinguishing between the running variable, x, and the integration variable, c, in equations 2.14 and 2.15.

Since $B_x(c)dc$ gives the probability of the random variable x assuming a value between c and $c + dc$, any moment of the distribution can be computed by integrating the appropriate power of x over all possible values. Thus the n-th moment is given by:
$$\langle x^n \rangle = \int_{-\infty}^{\infty} c^n B_x(c)dc \tag{2.17}$$

Exercise: Show (by returning to the definitions) that the value of the moment determined in this manner is exactly equal to the ensemble average defined earlier in equation 2.10. (Hint: use the definition of an integral as a limiting sum.)

If the probability density is given, the moments of all orders can be determined. For example, the variance can be determined by:

$$var\{x\} = \langle (x - X)^2 \rangle = \int_{-\infty}^{\infty} (c - X)^2 B_x(c) dc \tag{2.18}$$

The central moments give information about the shape of the probability density function, and *vice versa*. Figure 2.4 shows three distributions which have the same mean and standard deviation, but are clearly quite different. Beneath them are shown random functions of time which might have generated them. Distribution (b) has a higher value of the fourth central moment than does distribution (a). This can be easily seen from the definition

$$\langle (x - X)^4 \rangle = \int_{-\infty}^{\infty} (c - X)^4 B_x(c) dc \tag{2.19}$$

since the fourth power emphasizes the fact that distribution (b) has more weight in the tails than does distribution (a).

It is also easy to see that because of the symmetry of pdf's in (a) and (b), all the odd central moments will be zero. Distributions (c) and (d), on the other hand, have non-zero values for the odd moments, because of their asymmetry. For example,

$$\langle (x - X)^3 \rangle = \int_{-\infty}^{\infty} (c - X)^3 B_x(c) dc \tag{2.20}$$

is equal to zero if B_x is an even function.

2.3.2 The probability distribution

Sometimes it is convenient to work with the **probability distribution** instead of with the probability density function. The probability distribution is defined as the probability that the random variable has a value less than or equal to a given value. Thus from equation 2.15, the probability distribution is given by

$$F_x(c) = Prob\{x < c\} = \int_{-\infty}^{c} B_x(c') dc' \tag{2.21}$$

Note that we had to introduce the integration variable, c', since c occurred in the limits.

Equation 2.21 can be inverted by differentiating by c to obtain

$$B_x(c) = \frac{dF_x}{dc} \tag{2.22}$$

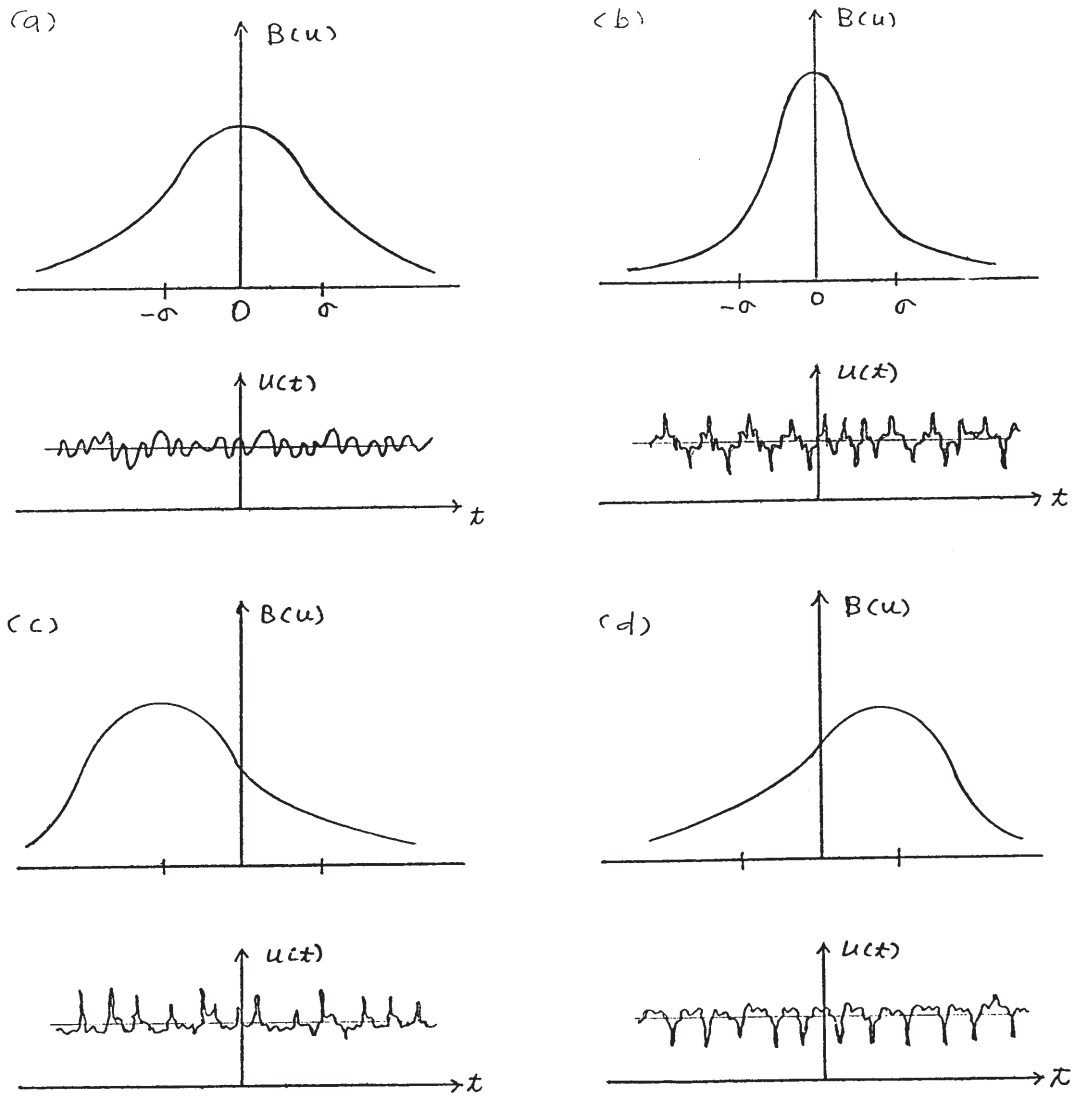

Figure 2.4: Relation of skewness to the shape of the pdf and nature of the signal.

2.3.3 Gaussian (or normal) distributions

One of the most important pdf's in turbulence is the Gaussian or Normal distribution defined by

$$B_{xG}(c) = \frac{1}{\sqrt{2\pi}\sigma_x} e^{-(c-X)^2/2\sigma_x^2} \tag{2.23}$$

where X is the mean and σ_x is the standard derivation. The factor of $1/\sqrt{2\pi}\sigma_x$ insures that the integral of the pdf over all values is unity as required. It is easy to prove that this is the case by completing the squares in the integration of the exponential (see problem 2.2).

The Gaussian distribution is unusual in that it is completely determined by its first two moments, X and σ. This is *not* typical of most turbulence distributions. Nonetheless, it is sometimes useful to approximate turbulence as being Gaussian, often because of the absence of simple alternatives.

It is straightforward to show by integrating by parts that all the even central moments above the second are given by the following recursive relationship,

$$\langle (x-X)^n \rangle = (n-1)(n-3)...3.1\sigma_x^n \tag{2.24}$$

Thus the fourth central moment is $3\sigma_x^4$, the sixth is $15\sigma_x^6$, and so forth.

Exercise: Prove this.

The probability distribution corresponding to the Gaussian distribution can be obtained by integrating the Gaussian pdf from $-\infty$ to $x = c$; i.e.,

$$F_{xG}(c) = \frac{1}{\sqrt{2\pi}\sigma_x} \int_{-\infty}^{c} e^{-(c'-X)^2/2\sigma_x^2} dc' \tag{2.25}$$

The integral is related to the erf-function tabulated in many standard tables and function subroutines, but usually with the independent variable normalized by σ_x; i.e., $c' = c/\sigma_x$. Alternatively we can subtract $F_{xG}(c)$ from unity to obtain the probability that $x \geq c$ as $1 - F_{xG}(c)$. This is related to the complementary error function, erfc(c), also usually easily available.

2.3.4 Skewness and kurtosis

Because of their importance in characterizing the shape of the pdf, it is useful to define scaled (or normalized) versions of third and fourth central moments: the *skewness* and *kurtosis* respectively. The *skewness* is defined as third central moment divided by the three-halves power of the second; i.e.,

$$S = \frac{\langle (x-X)^3 \rangle}{\langle (x-X)^2 \rangle^{3/2}} \tag{2.26}$$

The *kurtosis* is defined as the fourth central moment divided by the square of the second; i.e.,

$$K = \frac{\langle (x-X)^4 \rangle}{\langle (x-X)^2 \rangle^2} \tag{2.27}$$

Both these are easy to remember if you note the S and K must be dimensionless.

The pdf's in Figure 2.4 can be distinguished by means of their skewness and kurtosis. The random variable shown in (b) has a higher kurtosis than that in (a). Thus the kurtosis can be used as an indication of the tails of a pdf, a higher kurtosis indicating that relatively larger excursions from the mean are more probable. The skewnesses of (a) and (b) are zero, whereas those for (c) and (d) are non-zero. Thus, as its name implies, a non-zero skewness indicates a skewed or asymmetric pdf, which in turn means that larger excursions in one direction are more probable than in the other. For a Gaussian pdf, the skewness is zero and the kurtosis is equal to three (see problem 2.4). The flatness factor, defined as $(K-3)$, is sometimes used to indicate deviations from Gaussian behavior.

Exercise: Prove that the skewness and kurtosis of a Gaussian distributed random variable are 0 and 3 respectively.

2.4 Multivariate Random Variables

2.4.1 Joint pdfs and joint moments

Often it is important to consider more than one random variable at a time. For example, in turbulence the three components of the velocity vector are interrelated and must be considered together. In addition to the *marginal* (or single variable) statistical moments already considered, it is necessary to consider the **joint** statistical moments.

For example if u and v are two random variables, there are three second-order moments which can be defined $\langle u^2 \rangle$, $\langle v^2 \rangle$, and $\langle uv \rangle$. The product moment $\langle uv \rangle$ is called the *cross-correlation* or *cross-covariance*. The moments $\langle u^2 \rangle$ and $\langle v^2 \rangle$ are referred to as the *covariances*, or just simply the *variances*. Sometimes $\langle uv \rangle$ is also referred to as the *correlation*.

In a manner similar to that used to build-up the probability density function from its measurable counterpart, the histogram, a **joint probability density function** (or **jpdf**), B_{uv}, can be built-up from the *joint histogram*. Figure 2.5 illustrates several examples of jpdf's which have different cross-correlations. For convenience the fluctuating variables u' and v' can be defined as

$$u' = u - U \tag{2.28}$$

$$v' = v - V \tag{2.29}$$

where as before capital letters are used to represent the mean values. Clearly the fluctuating quantities u' and v' are random variables with zero mean.

A positive value of $\langle u'v' \rangle$ indicates that u' and v' tend to vary together. A negative value indicates that when one variable is increasing the other tends to be decreasing. A zero value of $\langle u'v' \rangle$ indicates that there is no correlation between

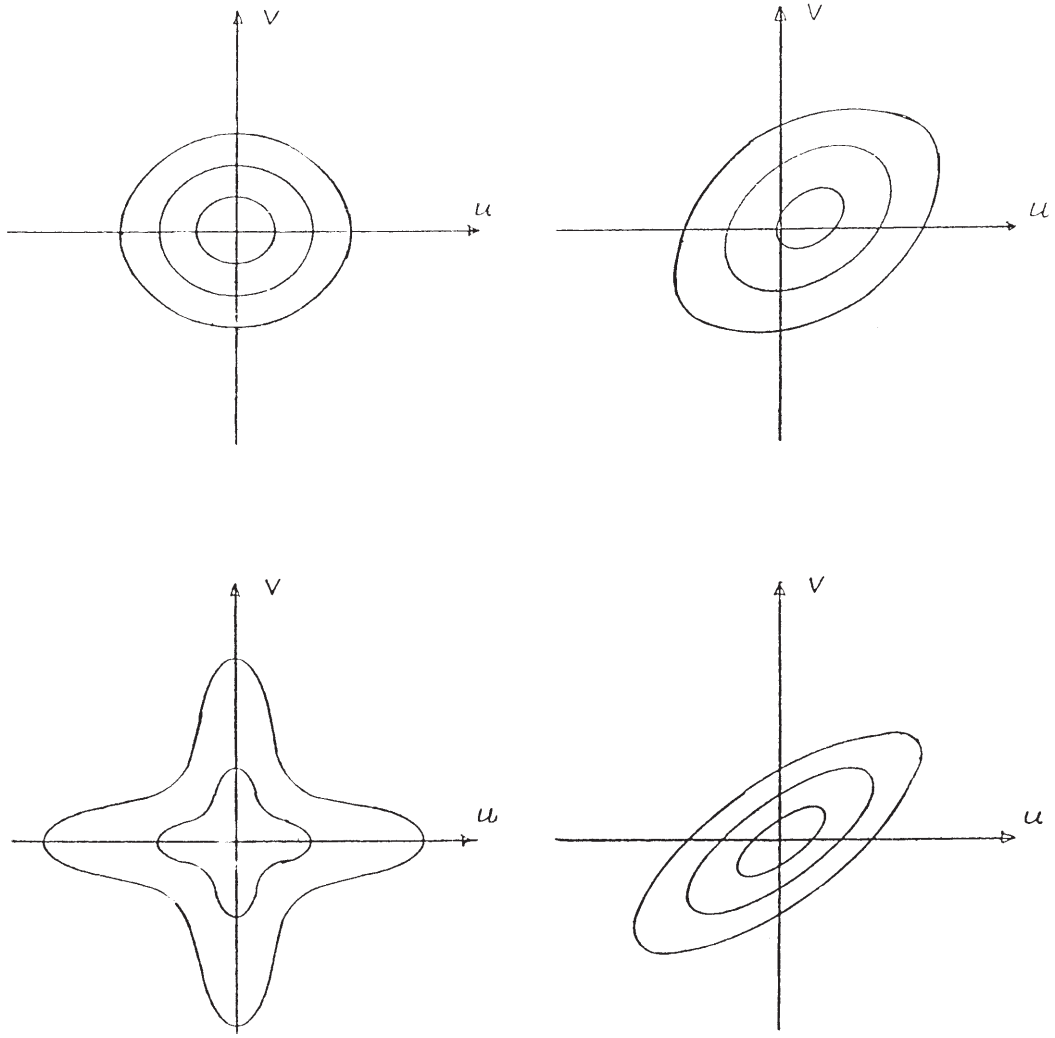

Figure 2.5: Contours of constant probability for four different joint probability density functions. Try to figure out what the moments would be for each and how they would differ.

u' and v'. As will be seen below, it does *not* mean that they are statistically independent.

It is sometimes more convenient to deal with values of the cross-variances which have been normalized by the appropriate variances. Thus the *correlation coefficient* is defined as:

$$\rho_{uv} \equiv \frac{\langle u'v' \rangle}{[\langle u'^2 \rangle \langle v'^2 \rangle]^{1/2}} \tag{2.30}$$

The correlation coefficient is bounded by plus or minus one, the former representing perfect correlation and the latter perfect anti-correlation.

As with the single-variable pdf, there are certain conditions the joint probability density function must satisfy. If $B_{uv}(c_1, c_2)$ indicates the jpdf of the random variables u and v, then:

- Property 1:

$$B_{uv}(c_1, c_2) > 0 \tag{2.31}$$

  always.

- Property 2:

$$Prob\{c_1 < u < c_1 + dc_1, c_2 < v < c_2 + dc_2\} = B_{uv}(c_1, c_2)dc_1, dc_2 \tag{2.32}$$

- Property 3:

$$\int_{-\infty}^{\infty} \int_{-\infty}^{\infty} B_{uv}(c_1, c_2)dc_1 dc_2 = 1 \tag{2.33}$$

- Property 4:

$$\int_{-\infty}^{\infty} B_{uv}(c_1, c_2)dc_2 = B_u(c_1) \tag{2.34}$$

  where B_u is a function of c_1 only.

- Property 5:

$$\int_{-\infty}^{\infty} B_{uv}(c_1, c_2)dc_1 = B_v(c_2) \tag{2.35}$$

  where B_v is a function of c_2 only.

The functions B_u and B_v are called the *marginal probability density functions*, and they are simply the single variable pdf's defined earlier. The subscript is used to indicate which variable is left after the others are integrated out. Note that $B_u(c_1)$ is not the same as $B_{uv}(c_1, 0)$. The latter is only a slice through the c_2-axis, while the marginal distribution is weighted by the integral of the distribution of the other variable. Figure 2.6 illustrates these differences.

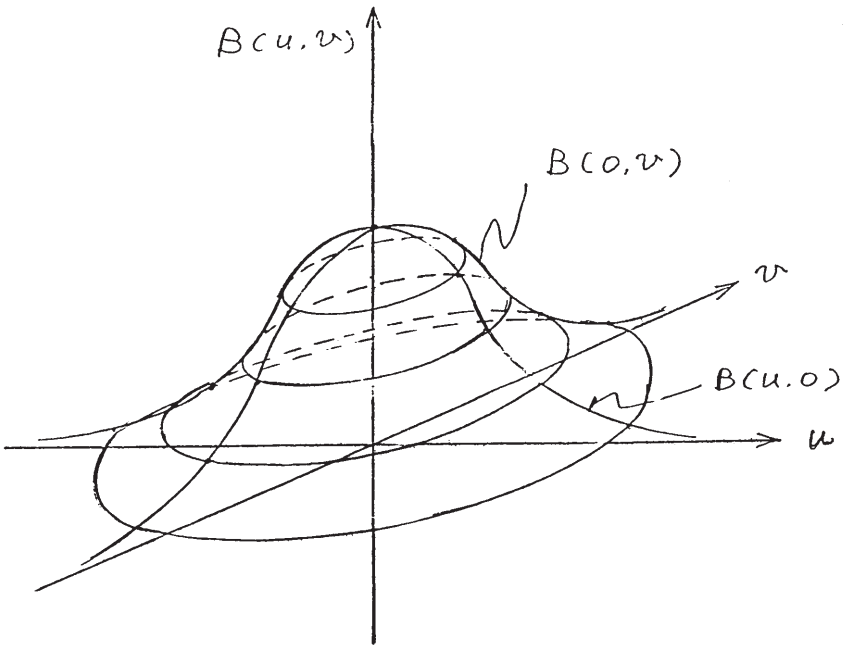

Figure 2.6: Surface representation of a joint probability density function.

If the joint probability density function is known, the *joint moments* of all orders can be determined. Thus the m, n-th joint moment is

$$\langle u^m v^n \rangle = \int_{-\infty}^{\infty} \int_{-\infty}^{\infty} c_1^m c_2^n B_{uv}(c_1, c_2) dc_1 dc_2 \tag{2.36}$$

where m and n can take any value. The corresponding central-moment is:

$$\langle (u - U)^m (v - V)^n \rangle = \int_{-\infty}^{\infty} \int_{-\infty}^{\infty} (c_1 - U)^m (c_2 - V)^n B_{uv}(c_1, c_2) dc_1 dc_2 \tag{2.37}$$

In the preceding discussions, only two random variables have been considered. The definitions, however, can easily be generalized to accommodate any number of random variables. In addition, the joint statistics of a single random variable at different times or at different points in space could be considered. This will be discussed later when stationary and homogeneous random processes are considered.

2.4.2 The bi-variate normal (or Gaussian) distribution

If u and v are *normally* distributed random variables with standard deviations given by σ_u and σ_v, respectively, with correlation coefficient ρ_{uv}, then their joint

probability density function is given by

$$B_{uvG}(c_1, c_2) = \frac{1}{2\pi\sigma_u\sigma_v} \exp\left[\frac{(c_1 - U)^2}{2\sigma_u^2} + \frac{(c_2 - V)^2}{2\sigma_v^2} - \rho_{uv}\frac{c_1 c_2}{\sigma_u\sigma_v}\right] \tag{2.38}$$

This distribution is plotted in Figure 2.7 for several values of ρ_{uv} where u and v are assumed to be identically distributed (i.e., $\langle u^2\rangle = \langle v^2\rangle$).

It is straightforward to show (by completing the square and integrating) that this yields the single variable Gaussian distribution for the marginal distributions (see problem 2.5). It is also possible to write a *multivariate Gaussian* probability density function for any number of random variables.

Exercise: Prove that equation 2.23 results from integrating out the dependence of either variable using equations 2.34 or 2.35.

2.4.3 Statistical independence and lack of correlation

Definition: Statistical Independence Two random variables are said to be *statistically independent* if their joint probability density is equal to the product of their marginal probability density functions. That is,

$$B_{uv}(c_1, c_2) = B_u(c_1)B_v(c_2) \tag{2.39}$$

It is easy to see that statistical independence implies a complete lack of correlation; i.e., $\rho_{uv} \equiv 0$. From the definition of the cross-correlation,

$$\begin{aligned}
\langle (u-U)(v-V)\rangle &= \int_{-\infty}^{\infty}\int_{-\infty}^{\infty}(c_1 - U)(c_2 - V)B_{uv}(c_1, c_2)dc_1 dc_2 \\
&= \int_{-\infty}^{\infty}\int_{-\infty}^{\infty}(c_1 - U)(c_2 - V)B_u(c_1)B_v(c_2)dc_1 dc_2 \\
&= \int_{-\infty}^{\infty}(c_1 - U)B_u(c_1)dc_1 \int_{-\infty}^{\infty}(c_2 - V)B_v(c_2)dc_2 \\
&= 0
\end{aligned} \tag{2.40}$$

where we have used equation 2.39 since the first central moments are zero by definition.

It is important to note that the inverse is not true — *lack of correlation does not imply statistical independence!* To see this consider two identically distributed random variables, u' and v', which have zero means and a non-zero correlation $\langle u'v'\rangle$. From these two correlated random variables two other random variables, x and y, can be formed as:

$$x = u' + v' \tag{2.41}$$

$$y = u' - v' \tag{2.42}$$

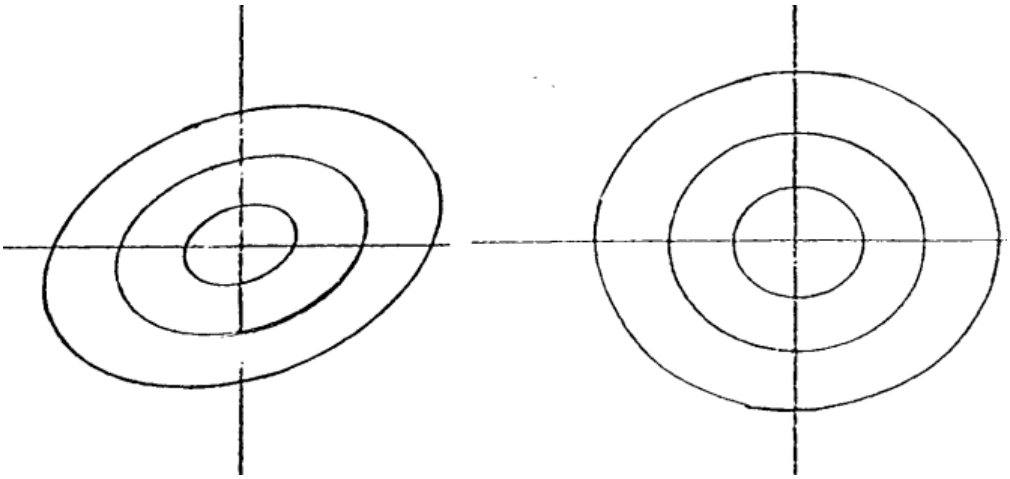

Figure 2.7: Jpdf on left (symmetry around slanted lines through the origin) shows correlation while the jpdf on the right (symmetry about both axes) formed by summing and differencing the two variables does not.

Clearly x and y are *not* statistically independent since the quantities from which they were formed are not statistically independent. They are, however, *uncorrelated* because:

$$\begin{aligned} \langle xy \rangle &= \langle (u' + v')(u' - v') \rangle \\ &= \langle u'^2 \rangle + \langle u'v' \rangle - \langle u'v' \rangle - \langle v'^2 \rangle \\ &= 0 \end{aligned} \tag{2.43}$$

since u' and v' are identically distributed (and as a consequence $\langle u'^2 \rangle = \langle v'^2 \rangle$).

Figure 2.7 illustrates the change of variables carried out above. The jpdf resulting from the transformation is symmetric about both axes, thereby eliminating the correlation. Transformation, however, does not insure that the distribution is separable, i.e., we did not insure that $B_{x,y}(a_1, a_2) = B_x(a_1)B_y(a_2)$, as required for statistical independence.

Exercise: Apply the transformation above, equation 2.41, to the jointly Gaussian pdf given by equation 2.38 with $\rho_{uv} \neq 0$. Then use it to determine whether in fact x and y are statistically independent.

2.5 Estimation from a Finite Number of Realizations

2.5.1 Estimators for averaged quantities

Since there can never an infinite number of realizations from which ensemble averages (and probability densities) can be computed, it is essential to ask: *How*

many realizations are enough? The answer to this question must be sought by looking at the statistical properties of estimators based on a finite number of realizations. There are two questions which must be answered. The first one is:

- Is the expected value (or mean value) of the estimator equal to the true ensemble mean? Or in other words, is the estimator *unbiased?*

The second question is:

- Does the difference between the value of the estimator and that of the true mean decrease as the number of realizations increases? Or in other words, does the estimator *converge* in a statistical sense (or converge in probability). Figure 2.8 illustrates the problems which can arise.

2.5.2 Bias and convergence of estimators

A procedure for answering these questions will be illustrated by considering a simple **estimator** for the mean, the arithmetic mean considered above, X_N. For N independent realizations, x_n, $n = 1, 2, \cdots, N$ where N is finite, X_N is given by:

$$X_N = \frac{1}{N}\sum_{n=1}^{N} x_n \tag{2.44}$$

Now, as we observed in our simple coin-flipping experiment, since the x_n are random, so must be the value of the estimator X_N. For the estimator to be *unbiased*, the mean value of X_N must be the true ensemble mean, X; i.e.,

$$lim_{N\to\infty} X_N = X \tag{2.45}$$

It is easy to see that since the operations of averaging and adding commute,

$$\begin{aligned} \langle X_N \rangle &= \langle \frac{1}{N}\sum_{n=1}^{N} x_n \rangle & (2.46)\\ &= \frac{1}{N}\sum_{n=1}^{N} \langle x_n \rangle & (2.47)\\ &= \frac{1}{N} NX = X & (2.48) \end{aligned}$$

(Note that the expected value of each x_n is just X since the x_n are assumed identically distributed). Thus x_N is, in fact, an *unbiased estimator for the mean.*

The question of *convergence* of the estimator can be addressed by defining the square of **variability of the estimator**, say $\epsilon^2_{X_N}$, to be:

$$\epsilon^2_{X_N} \equiv \frac{var\{X_N\}}{X^2} = \frac{\langle (X_N - X)^2 \rangle}{X^2} \tag{2.49}$$

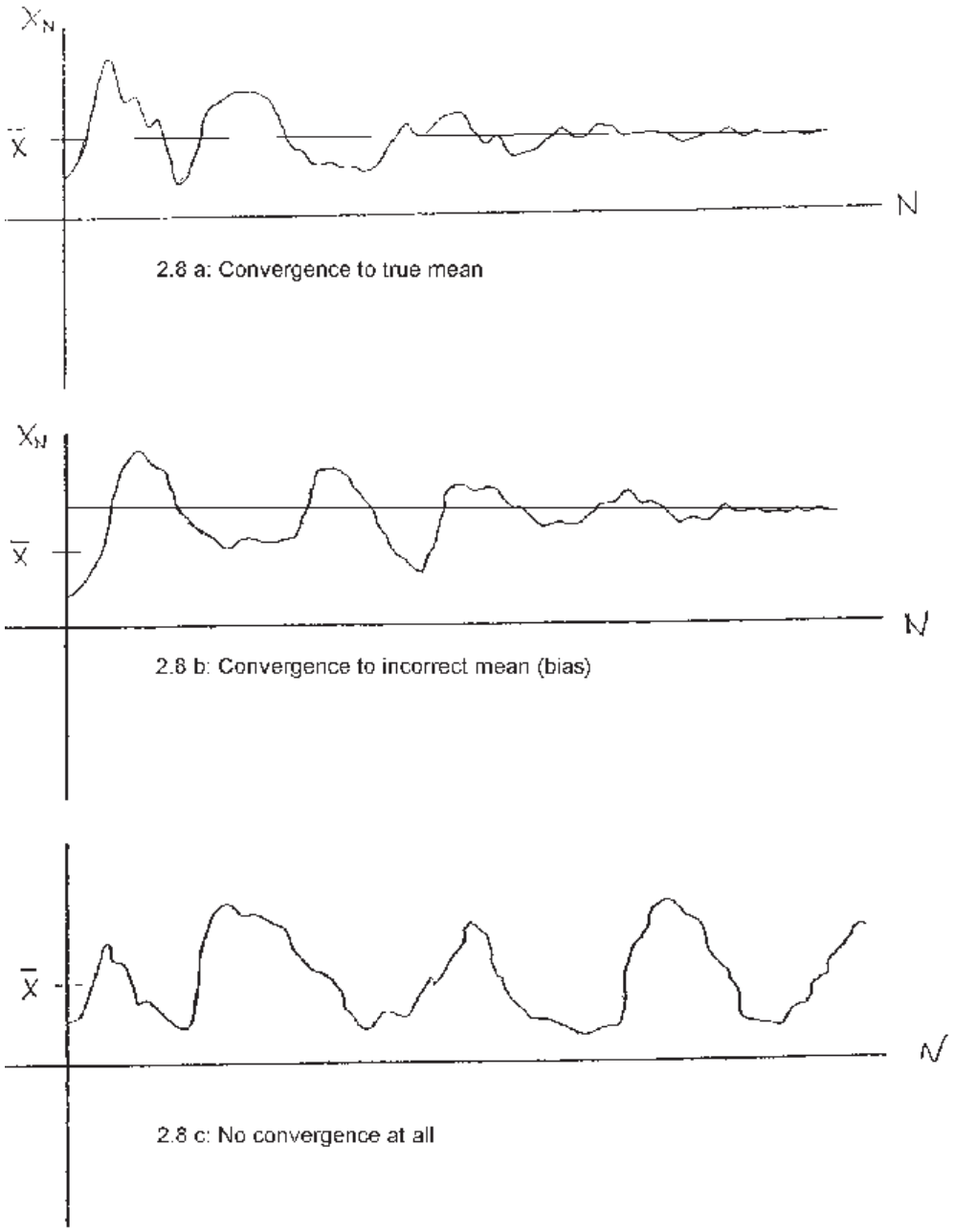

Figure 2.8: Three different estimators for the mean: The first of which converges to the mean with increasing number of samples, the middle converges to the wrong mean, and the bottom does not converge at all.

Now we want to examine what happens to ϵ_{X_N} as the number of realizations increases. For the estimator to converge it is clear that ϵ_x should decrease as the number of samples increases. Obviously, we need to examine the variance of X_N first. It is given by:

$$\begin{aligned} var\{X_N\} &= \langle (X_N - X)^2 \rangle \\ &= \langle \left[\frac{1}{N} \sum_{n=1}^{N} x_n \; - \; X) \right]^2 \rangle \qquad (2.50) \\ &= \langle \left[\frac{1}{N} \sum_{n=1}^{N} x_n - \frac{1}{N} \sum_{n=1}^{N} X) \right]^2 \rangle \qquad (2.51) \\ &= \langle \left[\frac{1}{N} \sum_{n=1}^{N} (x_n - X) \right]^2 \rangle \qquad (2.52) \end{aligned}$$

since $\langle X_N \rangle = X$ from equation 2.46. Using the fact that the operations of averaging and summation commute, the squared summation can be expanded as follows:

$$\begin{aligned} \langle \left[\sum_{n=1}^{N} (x_n - X) \right]^2 \rangle &= \frac{1}{N^2} \sum_{n=1}^{N} \sum_{m=1}^{N} \langle (x_n - X)(x_m - X) \rangle \\ &= \frac{1}{N^2} \sum_{n=1}^{N} \langle (x_n - X)^2 \rangle \\ &= \frac{1}{N} var\{x\}, \qquad (2.53) \end{aligned}$$

where the next to last step follows from the fact that the x_n are assumed to be statistically independent samples (and hence uncorrelated), and the last step from the definition of the variance. It follows immediately by substitution into equation 2.49 that the square of the variability of the estimator, X_N, is given by:

$$\begin{aligned} \epsilon_{X_N}^2 &= \frac{1}{N} \frac{var\{x\}}{X^2} \\ &= \frac{1}{N} \left[\frac{\sigma_x}{X} \right]^2 \qquad (2.54) \end{aligned}$$

Thus *the variability of the estimator depends inversely on the number of independent realizations, N, and linearly on the relative fluctuation level of the random variable itself, σ_x/X.* Obviously if the relative fluctuation level is zero (either because there the quantity being measured is constant and there are no measurement errors), then a single measurement will suffice. On the other hand, as soon as there is any fluctuation in the x itself, the greater the fluctuation (relative to the mean of x, $\langle x \rangle = X$), then the more independent samples it will take to achieve a specified accuracy.

Example: In a given ensemble the relative fluctuation level is 12% (i.e., $\sigma_x/X = 0.12$). What is the fewest number of independent samples that must be acquired to measure the mean value to within 1%?

Answer Using equation 2.54, and taking $\epsilon_{X_N} = 0.01$, it follows that:

$$(0.01)^2 = \frac{1}{N}(0.12)^2 \tag{2.55}$$

or $N \geq 144$.

The variability is of great value in estimating statistical error. But it is, of course, of no value when the mean value of the process itself if zero, or nearly so. In such cases we have to satisfy ourselves with simply the variance (or standard deviation) of X_N. This has proven to be quite terrifying to many investigators who have been afraid to show data because of what they believed to be its large relative errors. In fact were being fooled by the only apparently large scatter, since they were trying to measure a quantity whose average value was zero. This can happen quite easily since most the plotting routine are self-scaling. In most cases, a careful look at the actual numbers labelling the abscissa can put things into the proper perspective.

2.6 Generalization to the estimator of any quantity

Similar relations can be formed for the estimator of any function of the random variable, say $f(x)$. For example, an estimator for the average of f based on N realizations is given by:

$$F_N \equiv \frac{1}{N}\sum_{n=1}^{N} f_n \tag{2.56}$$

where $f_n \equiv f(x_n)$. It is straightforward to show that this estimator is unbiased, and its variability (squared) is given by:

$$\epsilon^2_{F_N} = \frac{1}{N}\frac{var\{F_N(x)\}}{\langle f(x)\rangle^2} \tag{2.57}$$

Example: Suppose it is desired to estimate the variability of an estimator for the variance based on a finite number of samples as:

$$var_N\{x\} \equiv \frac{1}{N}\sum_{n=1}^{N}(x_n - X)^2 \tag{2.58}$$

(Note that this estimator is not really the best that we could do since it presumes that the mean value, X, is known, whereas in fact usually only X_N is obtainable as in Problem 2.6 below. The errors this induces can be quite serious if the number of independent samples is quite small. The so-called 'Student-T' distribution is an attempt to deal with this problem. In modern turbulence research the number of independent samples in a properly designed experiment is usually very large, so the differences are slight.)

Answer Let $f = (x - X)^2$ in equation 2.57 so that $F_N = var_N\{x\}$, $\langle f \rangle = var\{x\}$ and $var\{f\} = var\{(x - X)^2\} = \langle \{(x - X)^2 - var[x - X]\}^2 \rangle$. Then:

$$\epsilon^2_{var_N} = \frac{1}{N} \frac{var\{(x - X)^2\}}{(var\{x\})^2} \tag{2.59}$$

This is easiest to understand if we first expand only the numerator to obtain:

$$var\{(x - X)^2\} = \langle \{(x - X)^2 - var[x]\}^2 \rangle = \langle (x - X)^4 \rangle - [var\{x\}]^2 \tag{2.60}$$

Thus

$$\epsilon^2_{var_N} = \frac{1}{N} \frac{\langle (x - X)^4 \rangle - [var\{x\}]^2}{[var\{x\}]^2} \tag{2.61}$$

Obviously to proceed further we need to know how the fourth central moment relates to the second central moment. As noted earlier, in general this is *not* known. If, however, it is reasonable to assume that x is a Gaussian distributed random variable, we know from section 2.3.4 that the kurtosis is 3. Then for Gaussian distributed random variables,

$$\epsilon^2_{var_N} = \frac{2}{N} \tag{2.62}$$

Thus the number of independent data required to produce the same level of convergence for an estimate of the variance of a Gaussian distributed random variable is $\sqrt{2}$ times that of the mean. It is easy to show that the higher the moment, the more the amount of data required (see Problem 2.7).

As noted earlier, turbulence problems are not usually Gaussian, and in fact values of the kurtosis substantially greater than 3 are commonly encountered, especially for the moments of differentiated quantities. Clearly the non-Gaussian nature of random variables can affect the planning of experiments, since substantially greater amounts of data can be required to achieved the necessary statistical accuracy.

Problems for Chapter 2

1. By using the definition of the probability density function as the limit of the histogram of a random variable as the internal size goes to zero and as the number of realizations becomes infinite (equation 2.12), show that the probability average defined by equation 2.17 and the ensemble average defined by equation 2.2 are the same.

2. By completing the square in the exponential, prove that the pdf for the normal distribution given by equation 2.23 integrates to unity (equation 2.16)

3. Prove equation 2.24.

4. Prove for a normal distribution that the skewness is equal to zero and that the kurtosis is equal to three.

5. Show by integrating over one of the variables that the Gaussian jpdf given by equation 2.38 integrates to the marginal distribution pdf given by equation 2.23, regardless of the value of the correlation coefficient.

6. Find the variability of an estimator for the variance using equation 2.60, but with the sample mean, X_N, substituted for the true mean, X.

7. Create a simple estimator for the fourth central moment — assuming the second to be known exactly. Then find its variability for a Gaussian distributed random variable.

8. You are attempting to measure a Gaussian distributed random variable with 12 bit A/D converter which can only accept voltage inputs between 0 and 10. Assume the mean voltage is +4, and the rms voltage is 4. Show what a histogram of your measured signal would look like assuming any voltage which is clipped goes into the first or last bins. Also compute the first three moments (central) of the measured signal.

Chapter 3

The Reynolds Averaged Equations and the Turbulence Closure Problem

3.1 The Equations Governing the Instantaneous Fluid Motions

All fluid motions, whether turbulent or not, are governed by the dynamical equations for a fluid. These can be written using Cartesian tensor notation as:

$$\rho\left[\frac{\partial\tilde{u}_i}{\partial t}+\tilde{u}_j\frac{\partial\tilde{u}_i}{\partial x_j}\right] = -\frac{\partial\tilde{p}}{\partial x_i}+\frac{\partial\tilde{T}_{ij}^{(v)}}{\partial x_j} \tag{3.1}$$

$$\left\{\frac{\partial\tilde{\rho}}{\partial t}+\tilde{u}_j\frac{\partial\tilde{\rho}}{\partial x_j}\right\} + \tilde{\rho}\frac{\partial\tilde{u}_j}{\partial x_j}=0 \tag{3.2}$$

where $\tilde{u}_i(\vec{x},t)$ represents the i-th component of the fluid velocity at a point in space, $[\vec{x}]_i = x_i$, and time, t. Also $\tilde{p}(\vec{x},t)$ represents the static pressure, $\tilde{T}_{ij}^{(v)}(\vec{x},t)$, the viscous (or deviatoric) stresses, and $\tilde{\rho}$ the fluid density. The tilde over the symbol indicates that an instantaneous quantity is being considered. Also the Einstein summation convention has been employed.[1]

In equation 3.1, the subscript i is a free index which can take on the values 1, 2, and 3. Thus equation 3.1 is in reality three separate equations. These three equations are just Newton's second law written for a continuum in a spatial (or Eulerian) reference frame. Together they relate the rate of change of momentum per unit mass (ρu_i), a vector quantity, to the contact and body forces.

Equation 3.2 is the equation for mass conservation in the absence of sources (or sinks) of mass. Almost all flows considered in this book will be incompressible, which implies that the derivative of the density following the fluid material (the

[1] Einstein summation convention: repeated indices in a single term are summed over 1,2, and 3.

term in brackets) is zero. Thus for incompressible flows, the mass conservation equation reduces to:

$$\frac{D\tilde{\rho}}{Dt} = \frac{\partial \tilde{\rho}}{\partial t} + \tilde{u}_j \frac{\partial \tilde{\rho}}{\partial x_j} = 0 \tag{3.3}$$

From equation 3.2 it follows that for incompressible flows,

$$\frac{\partial \tilde{u}_j}{\partial x_j} = 0 \tag{3.4}$$

The viscous stresses (the stress minus the mean normal stress) are represented by the tensor $\tilde{T}_{ij}^{(v)}$. From its definition, $\tilde{T}_{kk}^{(v)} = 0$. In many flows of interest, the fluid behaves as a Newtonian fluid in which the viscous stress can be related to the fluid motion by a constitutive relation of the form

$$\tilde{T}_{ij}^{(v)} = 2\mu \left[\tilde{s}_{ij} - \frac{1}{3} \tilde{s}_{kk} \delta_{ij} \right] \tag{3.5}$$

The viscosity, μ, is a *property of the fluid* that can be measured in an independent experiment. $\tilde{s}_{ij}$ is the instantaneous strain rate tensor defined by

$$\tilde{s}_{ij} \equiv \frac{1}{2} \left[\frac{\partial \tilde{u}_i}{\partial x_j} + \frac{\partial \tilde{u}_j}{\partial x_i} \right] \tag{3.6}$$

From its definition, $\tilde{s}_{kk} = \partial \tilde{u}_k / \partial x_k$. If the flow is incompressible, $\tilde{s}_{kk} = 0$ and the Newtonian constitutive equation reduces to

$$\tilde{T}_{ij}^{(v)} = 2\mu \tilde{s}_{ij} \tag{3.7}$$

Throughout this text, *unless explicity stated otherwise*, the density, $\tilde{\rho} = \rho$ and the viscosity μ will be assumed constant. With these assumptions, the instantaneous momentum equations for a Newtonian fluid reduce to:

$$\left[\frac{\partial \tilde{u}_i}{\partial t} + \tilde{u}_j \frac{\partial \tilde{u}_i}{\partial x_j} \right] = -\frac{1}{\tilde{\rho}} \frac{\partial \tilde{p}}{\partial x_i} + \nu \frac{\partial^2 \tilde{u}_i}{\partial x_j^2} \tag{3.8}$$

where the kinematic viscosity, ν, has been defined as:

$$\nu \equiv \frac{\mu}{\rho} \tag{3.9}$$

Note that since the density is assumed constant, the tilde is no longer necessary.

Sometimes it will be more instructive and convenient to *not* explicitly include incompressibility in the stress term, but to refer to the incompressible momentum equation in the following form:

$$\rho \left[\frac{\partial \tilde{u}_i}{\partial t} + \tilde{u}_j \frac{\partial \tilde{u}_i}{\partial x_j} \right] = -\frac{\partial \tilde{p}}{\partial x_i} + \frac{\partial \tilde{T}_{ij}^{(v)}}{\partial x_j} \tag{3.10}$$

This form has the advantage that it is easier to keep track of the exact role of the viscous stresses.

3.2 Equations for the Average Velocity

Turbulence is that chaotic state of motion characteristic of solutions to the equations of motion at high Reynolds number. Although laminar solutions to the equations often exist that are consistent with the boundary conditions, perturbations to these solutions (sometimes even infinitesimal) can cause them to become turbulent. To see how this can happen, it is convenient to analyze the flow in two parts, a mean (or average) component and a fluctuating component. Thus the instantaneous velocity and stresses can be written as:

$$\begin{aligned} \tilde{u}_i &= U_i + u_i \\ \tilde{p} &= P + p \\ \tilde{T}_{ij}^{(v)} &= T_{ij}^{(v)} + \tau_{ij}^{(v)} \end{aligned} \tag{3.11}$$

where U_i, p, and $T_{ij}^{(v)}$ represent the mean motion, and u_i, p, and τ_{ij} the fluctuating motions. This technique for decomposing the instantaneous motion is referred to as the *Reynolds decomposition*. Note that if the averages are defined as ensemble means, they are, in general, *time-dependent*. For the remainder of this book, unless otherwise stated, the density will be assumed constant so $\tilde{\rho} \equiv \rho$ and its fluctuation is zero.

Substitution of equations 3.11 into equations 3.10 yields

$$\rho \left[\frac{\partial (U_i + u_i)}{\partial t} + (U_j + u_j) \frac{\partial (U_i + u_i)}{\partial x_j} \right] = -\frac{\partial (P + p)}{\partial x_i} + \frac{\partial (T_{ij}^{(v)} + \tau_{ij}^{(v)})}{\partial x_j} \tag{3.12}$$

This equation can now be averaged to yield an equation expressing momentum conservation for the averaged motion. Note that the operations of averaging and differentiation commute; i.e., the average of a derivative is the same as the derivative of the average. Also, the average of a fluctuating quantity is zero.[2] Thus the equation for the averaged motion reduces to:

$$\rho \left[\frac{\partial U_i}{\partial t} + U_j \frac{\partial U_i}{\partial x_j} \right] = -\frac{\partial P}{\partial x_i} + \frac{\partial T_{ij}^{(v)}}{\partial x_j} - \rho \langle u_j \frac{\partial u_i}{\partial x_j} \rangle \tag{3.13}$$

where the remaining fluctuating product term has been moved to the right-hand side of the equation. Whether or not this last term is zero like the other fluctuating terms depends on the correlation of terms in the product. In general, these correlations are *not* zero.

The mass conservation equation can be similarly decomposed. In incompressible form, substitution of equations 3.11 into equation 3.4 yields:

$$\frac{\partial (U_j + u_j)}{\partial x_j} = 0 \tag{3.14}$$

[2]These are easily proven from the definitions of both.

of which the average is:

$$\frac{\partial U_j}{\partial x_j} = 0 \tag{3.15}$$

It is clear from equation 3.15 that the averaged motion satisfies the same form of the mass conservation equation as does the instantaneous motion, at least for incompressible flows. How much simpler the turbulence problem would be if the same were true for the momentum! Unfortunately, as is easily seen from equation 3.13, such is not the case.

Equation 3.15 can be subtracted from equation 3.14 to yield an equation for the instantaneous motion alone; i.e.,

$$\frac{\partial u_j}{\partial x_j} = 0 \tag{3.16}$$

Again, like the mean, the form of the original instantaneous equation is seen to be preserved. The reason, of course, is obvious: the continuity equation is linear. The momentum equation, on the other hand, is not; hence the difference.

Equation 3.16 can be used to rewrite the last term in equation 3.13 for the mean momentum. Multiplying equation 3.16 by u_i and averaging yields:

$$\langle u_i \frac{\partial u_j}{\partial x_j} \rangle = 0 \tag{3.17}$$

This can be added to $\langle u_j \partial u_i / \partial x_j \rangle$ to obtain:

$$\langle u_j \frac{\partial u_i}{\partial x_j} \rangle + 0 = \langle u_j \frac{\partial u_i}{\partial x_j} \rangle + \langle u_i \frac{\partial u_j}{\partial x_j} \rangle = \frac{\partial}{\partial x_j} \langle u_i u_j \rangle \tag{3.18}$$

where again the fact that arithmetic and averaging operations commute has been used.

The equation for the averaged momentum, equation 3.13 can now be rewritten as:

$$\rho \left[\frac{\partial U_i}{\partial t} + U_j \frac{\partial U_i}{\partial x_j} \right] = -\frac{\partial P}{\partial x_i} + \frac{\partial T_{ij}^{(v)}}{\partial x_j} - \frac{\partial}{\partial x_j} \rho \langle u_i u_j \rangle \tag{3.19}$$

The last two terms on the right-hand side are both divergence terms and can be combined; the result is:

$$\rho \left[\frac{\partial U_i}{\partial t} + U_j \frac{\partial U_i}{\partial x_j} \right] = -\frac{\partial P}{\partial x_i} + \frac{\partial}{\partial x_j} \left[T_{ij}^{(v)} - \rho \langle u_i u_j \rangle \right] \tag{3.20}$$

Now the terms in square brackets on the right have the dimensions of stress. The first term is, in fact, the *viscous stress*. The second term, on the other hand, is not a stress at all, but simply a re-worked version of the fluctuating contribution to the non-linear acceleration terms. The fact that it can be written this way, however, indicates that *at least as far as the mean motion is concerned*, it *acts* as though it were a *stress* — hence its name, the **Reynolds stress**. In the succeeding sections the consequences of this difference will be examined.

3.3 The Turbulence Problem

It is the appearance of the Reynolds stress which makes the turbulence problem so difficult — at least from the engineers perspective. Even though we can pretend it is a stress, the physics which give rise to it are very different from the viscous stress. The viscous stress can be related directly to the other flow properties by constitutive equations, which in turn depend only on the properties of the *fluid* (as in equation 3.5 for a Newtonian fluid). The reason this works is that when we make such closure approximations for a fluid, we are averaging over characteristic length and time scales much smaller than those of the *flows* we are interested in. Yet at the same time, these scales are much larger than the *molecular* length and time scales which characterize the molecular interactions that are actually causing the momentum transfer. (This is what the continuum approximation is all about.)

The *Reynolds stress*, on the other hand, arises directly from the *flow* itself! *Worse, the scales of the fluctuating motion which give rise to it* **are** *the scales we are interested in.* This means that the closure ideas which worked so well for the viscous stress, should not be expected to work too well for the Reynolds stress. And as we shall see, they do not.

This leaves us in a terrible position. Physics and engineering are all about writing equations (and boundary conditions) so we can solve them to make predictions. We don't want to have to build prototype airplanes first to see if they will fall out of the sky. Instead we want to be able to analyze our designs *before* building the prototype, both to save the cost in money and in lives if our ideas are wrong. The same is true for dams and bridges and tunnels and automobiles. If we had confidence in our turbulence models, we could even build huge one-offs and expect them to work the first time. Unfortunately, even though turbulence models have improved to the point where we can use them in design, we still cannot trust them enough to eliminate expensive wind tunnel and model studies. And recent history is full of examples to prove this.

The turbulence problem (from the engineers perspective) is then three-fold:

- **The averaged equations are not closed.** Count the unknowns in equation 3.20 above. Then count the number of equations. Even with the continuity equation we have at least six equations too few.

- **The simple ideas to provide the extra equations usually do not work.** And even when we can fix them up for a particular class of flows (like the flow in a pipe, for example), they will most likely not be able to predict what happens in even a slightly different environment (like a bend).

- **Even the last resort of compiling engineering tables for design handbooks carries substantial risk.** This is the last resort for the engineer who lacks equations or cannot trust them. Even when based on a wealth of experience, they require expensive model testing to see if they can

be extrapolated to a particular situation. Unfortunately so infinitely clever is Mother Nature in creating turbulence that is unique to a particular set of boundary conditions that often they cannot.

Turbulent flows are indeed flows!. And that is the problem.

3.4 The Origins of Turbulence

Turbulent flows can often be observed to arise from laminar flows as the Reynolds number, (or some other relevant parameter) is increased. This happens because small distubances to the flow are no longer damped by the flow, but begin to grow by taking energy from the original laminar flow. This natural process is easily visualized by watching the simple stream of water from a faucet (or even a pitcher). Turn the flow on very slowly (or pour) so the stream is very smooth initially, at least near the outlet. Now slowly open the faucet (or pour faster) and observe what happens, first far away, then closer to the spout. The surface begins to exhibit waves or ripples which appear to grow downstream. In fact, they are growing by extracting energy from the primary flow. Eventually they grow enough that the flow breaks into drops. These are capillary instabilities arising from surface tension. But regardless of the type of instability, the idea is the same: small (or even infinitesimal) disturbances have grown to disrupt the serenity (and simplicity) of laminar flow.

The manner in which instabilities grow naturally in a flow can be examined using the equations we have already developed above. We derived them by decomposing the motion into a mean and a fluctuating part. But suppose instead we had decomposed the motion into a *base* flow part (the initially laminar part) and into a *disturbance* which represents a fluctuating part superimposed on the base flow. The result of substituting such a decomposition into the full Navier-Stokes equations and averaging is precisely that given by equations 3.13 and 3.15. But the very important difference is the additional restriction that what was previously identified as *the mean (or averaged) motion is now also the base or laminar flow.*

Now if the base flow is really a laminar flow (which it must be by our original hypothesis), then our averaged equations governing the base flow must yield the same mean flow solution as the original laminar flow on which the disturbance was superimposed. But this can happen only if these new averaged equations reduce to **exactly** the same laminar flow equations without any evidence of a disturbance. Clearly from equations 3.13 and 3.15, this can happen *only if all the Reynolds stress terms vanish identically*! Obviously this requires that the disturbances be infinitesimal so the extra terms can be neglected — hence our interest in infinitesimal disturbances.

So we hypothesized a base flow which was laminar and showed that it is unchanged even with the imposition of infinitesimal disturbances on it — *but only as long as the disturbances* **remain** *infinitesimal!* What happens if the disturbance

starts to grow? Obviously before we conclude that all laminar flows are laminar forever we better investigate whether or not these infinitesimal disturbances can grow to *finite* size. To do this we need an equation for the fluctuation itself.

An equation for the fluctuation (which might be an imposed disturbance) can be obtained by subtracting the equation for the mean (or base) flow from that for the instantaneous motion. We already did this for the continuity equation. Now we will do it for the momentum equation. Subtracting equation 3.13 from equation 3.11 yields an equation for the fluctuation as:

$$\rho\left[\frac{\partial u_i}{\partial t}+U_j\frac{\partial u_i}{\partial x_j}\right]=-\frac{\partial p}{\partial x_i}+\frac{\partial \tau_{ij}^{(v)}}{\partial x_j}-\rho\left[u_j\frac{\partial U_i}{\partial x_j}\right]-\rho\left\{u_j\frac{\partial u_i}{\partial x_j}-\langle u_j\frac{\partial u_i}{\partial x_j}\rangle\right\} \quad (3.21)$$

It is very important to note the type and character of the terms in this equation. First note that the left-hand side is the derivative of the *fluctuating* velocity following the *mean* motion. This is exactly like the term which appears on the left-hand side of the equation for the mean velocity, equation 3.13. The first two terms on the right-hand side are also like those in the mean motion, and represent the fluctuating pressure gradient and the fluctuating viscous stresses. The third term on the right-hand side is new, and will be seen later to represent the primary means by which fluctuations (and turbulence as well!) extract energy from the mean flow, the so-called *production terms*. The last term is quadratic in the fluctuating velocity, unlike all the others which are linear. Note that all of the terms vanish identically if the equation is averaged, the last because its mean is subtracted from it.

Now we want to examine what happens if the disturbance is small. In the limit as the amplitude of the disturbance (or fluctuation) is *infinitesimal*, the bracketed term in the equation for the fluctuation vanishes (since it involves products of infinitesimals), and the remaining equation is *linear in the disturbance*. The study of whether or not such infinitesimal disturbances can grow is called **Linear Fluid Dynamic Stability Theory**. These linearized equations are very different from those governing turbulence. Unlike the equations for disturbances of *finite* amplitude, the linearized equations are well-posed (or closed) since the Reynolds stress terms are gone. Therefore, in principle, they can be solved exactly with no need for closure approximations.

The absence of the non-linear terms, however, constrains the validity of the linear analysis to only the initial stage of disturbance growth. This is because as soon as the fluctuations begin to grow, their amplitudes can no longer be assumed infinitesimal and the Reynolds stress (or more properly, the non-linear fluctuating terms), become important. As a result the base flow equations begin to be modified so that the solution to them can no longer be identical to the laminar flow (or base flow) from which it arose. Thus while linear stability theory can predict *when* many flows become *unstable*, it can say very little about *transition to turbulence* since this process is highly non-linear.

It is also clear from the above why the process of transition to turbulence is so dependent on the state of the background flow. If the disturbances present

in the base flow are small enough, then Linear Stability Theory will govern their evolution. On the other hand if the disturbances to the base flow are not small enough, Linear Stability Theory can never apply since the non-linear terms will never be negligible. This is so-called *by-pass transition*. It is not uncommon to encounter situations like this in engineering environments where the incoming flow has a modest turbulence level super-imposed upon it. In such cases, the nature of the disturbances present is as important as their intensities, with the consequence that a general transition criterion may not exist, and perhaps should not even be expected.

3.5 The importance of non-linearity

We saw in the preceding section that non-linearity was one of the essential features of turbulence. When small disturbances grow large enough to interact *with each other*, we enter a whole new world of complex behavior. Most of the rules we learned for linear systems do not apply. Since most of your mathematical training has been for linear equations, most of your mathematical intuition therefore will not apply either. On the other hand, you may surprise yourself by discovering how much your *non-mathematical* intuition already recognizes non-linear behavior and accounts for it.

Consider the following simple example. Take a long stick with one person holding each end and stand at the corner of a building. Now place the middle of the stick against the building and let each person apply pressure in the same direction so as to bend the stick. If the applied force is small, the stick deflects (or bends) a small amount. Double the force, and the deflection is approximately doubled. Quadruple the force and the deflection is quadrupled. Now you don't need a Ph.D. in Engineering to know what is going to happen if you continue this process. **The stick is going to break!**

But where in the equations for the deflection of the stick is there anything that predicts this can happen? Now if you are thinking only like an engineer, you are probably thinking: he's asking a stupid question. Of course you can't continue to increase the force because you will exceed first the yield stress, then the breaking limit, and of course the stick will break.

But pretend I am the company president with nothing more than an MBA.[3] I don't know much about these things, but you have told me in the past that your computers have equations to predict everything. So I repeat: Where in the equations for the deflection of this stick does it tell me this is going to happen?

[3]For some reason the famous O-ring disaster of the the Challenger space shuttle in 1983 comes to mind here. The decision by the manufacturer, Morton Thiokol, to launch at temperatures below that at which the O-ring seals had been tested was made entirely by MBA's and lawyers, over the objections of the scientists and engineers present. Aside from the tragedy of the lives lost, including Gregory Jarvis whom my former office building at University at Buffalo is named after, they blew up a billion dollar spacecraft.

The answer is very simple: **There is *nothing* in the equations that will predict this.** And the reason is also quite simple: You lost the ability to predict catastrophes like breaking when you linearized the fundamental equations – which started out as Newton's Law too. In fact, before linearization, they were exactly the same as those for a fluid, only the constitutive equation was different.

If we had NOT linearized these equations and had constitutive equations that were more general, then we possibly could apply these equation right to and past the limit. The point of fracture would be a bifurcation point for the solution.

Now the good news is that for things like reasonable deflections of beams, linearization works wonderfully since we hope most things we build don't deflect too much – especially if you are sitting on a geological fault as I am at the moment of this writing.[4] Unfortunately, as we noted above, for fluids the disturbances tend to quickly become dominated by the non-linear terms. This, of course, means our linear analytical techniques are pretty useless for fluid mechanics, and especially turbulence.

But all is not lost. Just as we have learned to train ourselves to anticipate when sticks break, we have to train ourselves to anticipate how non-linear fluid phenomena behave. Toward that end we will consider two simple examples: one from algebra – the logistic map, and one from fluid mechanics – simple vortex stretching.

Example 1: An experiment with the logistic map.

Consider the behavior of the simple equation:

$$y_{n+1} = r y_n (1 - y_n) \tag{3.22}$$

where $n = 1, 2, \cdots$, $0 < y < 1$ and $r > 0$. The idea is that you pick any value for y_1, use the equation to find y_2, then insert that value on the right-hand side to find y_3, and just continue the process as long as you like. Make sure you note any dependence of the final result on the initial value for y.

- First notice what happens if you linearize this equation by disregarding the term in parentheses; i.e., consider the simpler equation $y_{n+1} = r y_n$. My guess is that you won't find this too exciting – unless, of course, you are one of those individuals who likes watching grass grow (or golf on TV).

- Now consider the full equation and note what happens for $r < 3$, and especially what happens for very small values of r. Run as many iterations as necessary to make sure your answer has converged. Do NOT try to take short-cuts by programming all the steps at once. Do them one at a time so

[4] I am sitting at this moment of this writing at the Institute for Theoretical Physics at the University of California/Santa Barbara. If you are reading this, it is likely that an earthquake did not happen during the writing session.

you can see what is happening. Believe me, it will be much easier this way in the long run.

- Now research carefully what happens when $r = 3.1, 3.5$, and 3.8. Can you recognize any patterns.
- Vary r between 3 and 4 to see if you can find the boundaries for what you are observing.
- Now try values of $r > 4$. How do you explain this?

Example 2: Stretching of a simple vortex.
Imagine a simple vortex filament that looks about like a strand of spaghetti. Now suppose it is in an otherwise steady inviscid incompressible flow. Use the vorticity equation to examine the following:

- Examine first what happens to it in two-dimensional velocity field. Note particularly whether any new vorticity can be produced; i.e., can the material derivative of the vorticity ever be greater than zero? (Hint: look at the $\omega_j \partial u_i / \partial x_j$-term.)
- Now consider the same vortex filament in a three-dimensional flow. Note particularly the various ways new vorticity can be produced — if you have some to start with! Does all this have anything to do with non-linearities?

Now you are ready for a real flow.

A Simple Experiment: The Starbucks[5] problem

Go to the nearest coffee pot (or your favorite coffee shop) and get a cup of coffee. (Note that you are not required to drink it, just play with it.) Then slowly and carefully pour a little cream (or half and half, skim milk probably won't work) into it. Now ever so gently, give it a simple single stir with a stick or a spoon and observe the complex display that you see. Assuming that the cream and coffee move together, and that the vorticity (at least for a while) moves like fluid material, explain what you see in the light of Example 2 above.

3.6 The Turbulence Closure Problem and the Eddy Viscosity

From the point of view of the averaged motion, at least, the problem with the non-linearity of the instantaneous equations is that they introduce new unknowns,

[5]Starbucks is a very popular chain of coffee shops in the USA and many other countries who have only recently discovered what good coffee tastes like.

the so-called Reynolds stress, into the averaged equations. There are six new individual Reynolds stress components we must deal with to be exact: $\langle u_1^2 \rangle$, $\rangle u_2^2 \rangle$, $\langle u_3^2 \rangle$, $\langle u_1 u_2 \rangle$, $\langle u_1 u_3 \rangle$, and $\langle u_2 u_3 \rangle$. These have to be related to the mean motion itself before the equations can be solved, since the number of unknowns and number of equations must be equal. The absence of these additional equations is often referred to as **the Turbulence Closure Problem**.

A similar problem arose when the instantaneous equations were written (equations 3.1 and 3.2), since relations had to be introduced to relate the stresses (in particular, the viscous stresses) to the motion itself. These relations (or constitutive equations) *depended only on the properties of the fluid material, and not on the flow itself.* Because of this fact, it is possible to carry out independent experiments, called viscometric experiments, in which these fluid properties can be determined once and for all. Equation 3.5 provides an example of just such a constitutive relation, the viscosity, μ, depending only in the choice of fluid. For example, once the viscosity of water at given temperature is determined, this value can be used in all flows at that temperature, not just the one in which the evaluation was made. Or for another example, if we are working on a problem of air flow, we only need to go to reference book somewhere and we can find a complete specification of how the viscosity of air depends on temperature and pressure. Someone somewhere else has already compiled this information from independent experiments.

It is tempting to try such an approach for the turbulence Reynolds stresses (even though we know the underlying requirements of scale separation are not satisfied). For example, a Newtonian type closure for the Reynolds stresses, often referred to as an "eddy" or "turbulent" viscosity model, looks like:

$$-\rho\langle u_i u_j \rangle + \frac{1}{3}\langle u_i u_i \rangle = \mu_t \left[S_{ij} - \frac{1}{3} S_{kk}\delta_{ij} \right] \tag{3.23}$$

where μ_t is the turbulence "viscosity" (also called the eddy viscosity), and S_{ij} is the *mean* strain rate defined by:

$$S_{ij} = \frac{1}{2}\left[\frac{\partial U_i}{\partial x_j} + \frac{\partial U_j}{\partial x_i} \right] \tag{3.24}$$

The second term vanishes identically for incompressible flow. For the simple case of a two-dimensional shear flow, equation 3.23 for the Reynolds shear stress reduces to

$$-\rho\langle u_1 u_2 \rangle = \mu_t \frac{\partial U_1}{\partial x_2} \tag{3.25}$$

Note this "model" is the direct analogy to the Newtonian model for viscous stress in a fluid. The Reynolds stresses, $\langle -u_i u_j \rangle$ replaces the viscous stress, $\tau_{ij}^{(v)}$. The counterpart to the mechanical pressure is the mean normal Reynolds stress, $\langle u_i u_i \rangle / 3$. And like it's fluid counterpart it, the Reynolds stress can depend only on the mean strain rate at a single instant and single location in the flow, so has

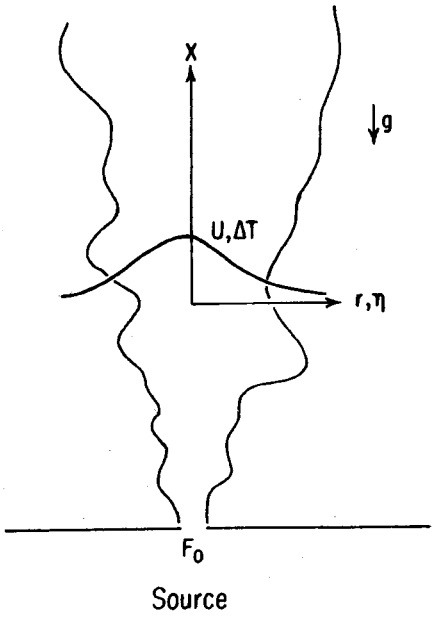

Figure 3.1: Schematic of axisymmetric plume

no history or non-local dependence. This absence will turn out to be fatal in most applications. Moreover, unlike like the viscosity, μ, which depends only on the fluid and not the motion itself, the "turbulence viscosity", μ_t, depends entirely on the motion.

That such a simple model can adequately describe the mean motion in at least one flow is illustrated by the axisymmetric buoyant plume sketched in Figure 3.1. Figures 3.2 and 3.3 show the calculation of the mean velocity and temperature profiles respectively. Obviously the mean velocity and temperature profiles are reasonably accurately computed, as are the Reynolds shear stress and lateral turbulent heat flux shown in Figures 3.4 and 3.5.

The success of the eddy viscosity in the preceding example is more apparent than real, however, since the value of the eddy viscosity and eddy diffusivity (for the turbulent heat flux) have been chosen to give the best possible agreement with the data. This, in itself, would not be a problem if that chosen values could have been obtained in advance of the computation, or even if they could be used to successfully predict other flows. In fact, the values used work only for this flow, thus the computation is *not a prediction at all, but a* **postdiction** *or* **hindcast** from which no extrapolation to the future can be made. In other words, our turbulence "model" is about as useful as having a program to predict yesterday's weather. Thus the closure problem still very much remains.

Another problem with the eddy viscosity in the example above is that it fails to calculate the vertical components of the Reynolds stress and turbulent heat flux. An attempt at such a computation is shown in Figure 3.6 where the vertical turbulent heat flux is shown to be severely underestimated. Clearly the value of the eddy viscosity in the vertical direction must be different than in the radial

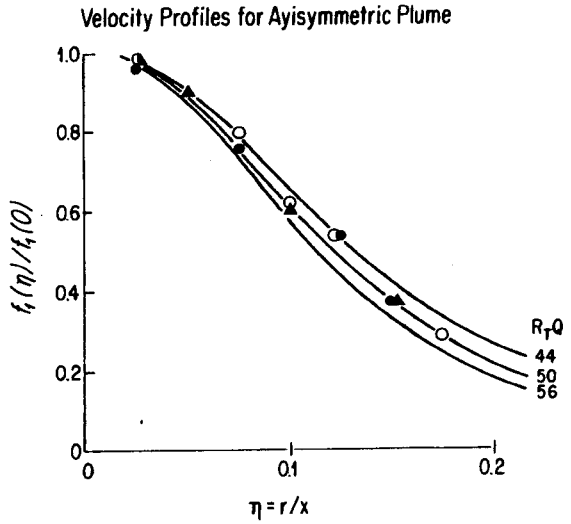

Figure 3.2: Mean velocity profiles for axisymmetric plume

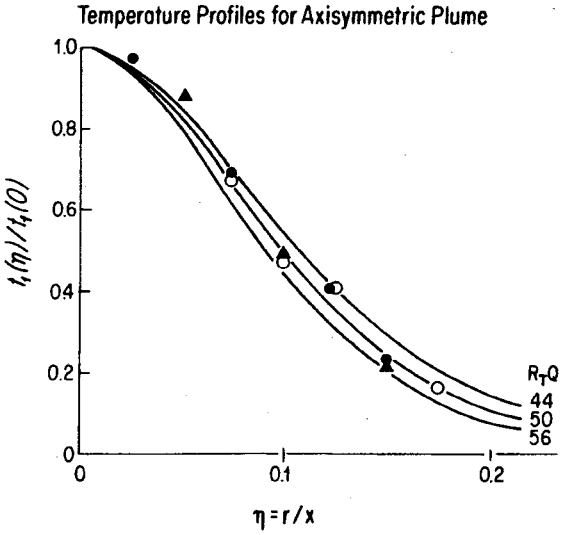

Figure 3.3: Mean temperature profiles for axisymmetric plume

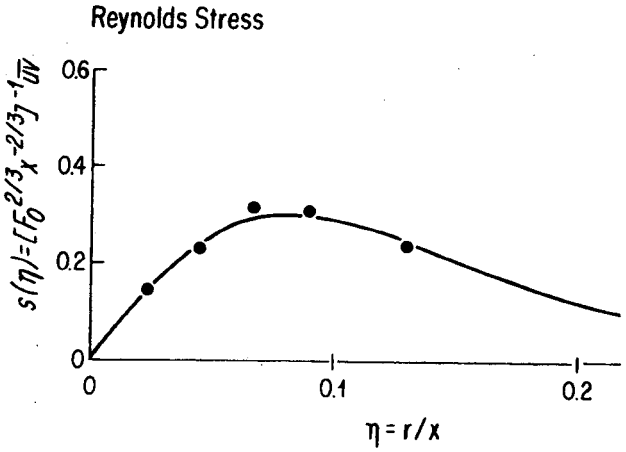

Figure 3.4: Reynolds shear stress profiles for axisymmetric plume

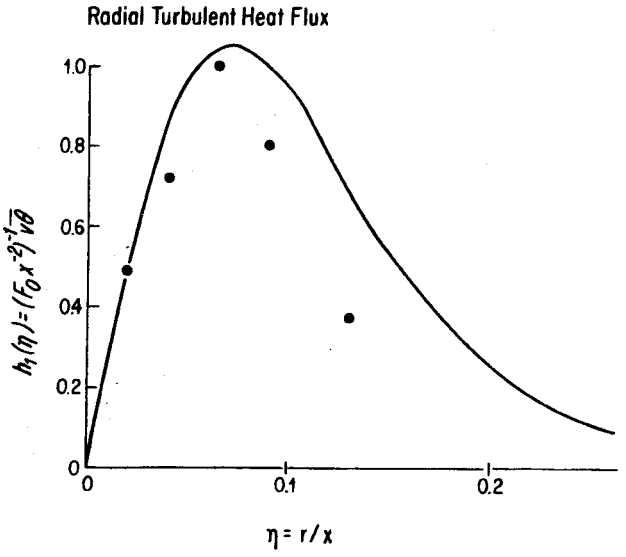

Figure 3.5: Radial turbulent heat flux for axisymmetric plume

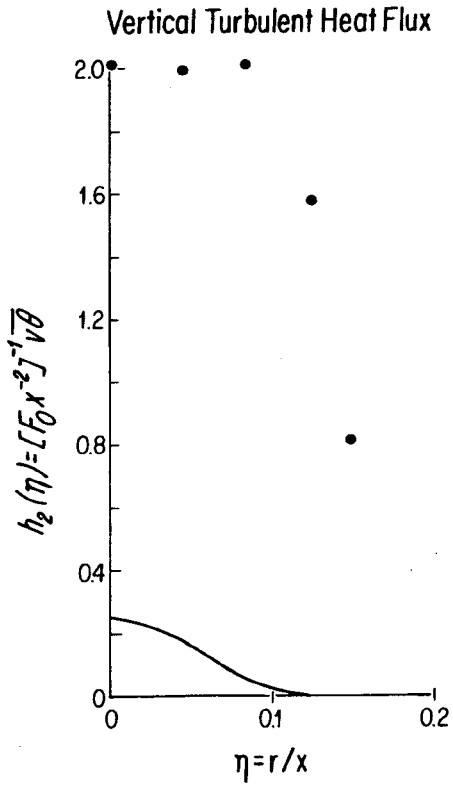

Figure 3.6: Vertical turbulent heat flux for axisymmetric plume

direction. In other words, the turbulence for which a constitutive equation is being written is *not an isotropic "medium"*. In fact, in this specific example the problem is that the vertical component of the heat flux is produced more by the interaction of buoyancy and the turbulence, than it is by the working of turbulence against mean gradients in the flow. We will discuss this in more detail in the next chapter when we consider the turbulence energy balances, but note for now that simple gradient closure models never work unless gradient production dominates. This rules out many flows involving buoyancy, and also many involving recirculations or separation where the local turbulence is convected in from somewhere else.

A more general form of constitutive equation which would allow for the non-isotropic nature of the "medium" (in this case the turbulence itself) would be

$$-\rho\langle u_i u_j\rangle + \frac{1}{3}\langle u_k u_k\rangle\delta_{ij} = \mu_{ijkl}\left[S_{kl} - \frac{1}{3}S_{mm}\delta_{kl}\right] \tag{3.26}$$

This closure relation allows each component of the Reynolds stress to have its own unique value of the eddy viscosity. It is easy to see that it is unlikely this will solve the closure problem since the original six unknowns, the $\langle u_i u_j\rangle$, have been traded for eighty-one new ones, μ_{ijkl}. Even if some can be removed by symmetries, the remaining number is still formidable. More important than the number of unknowns, however, is that there is no independent or general means for selecting them without considering a particular flow. This is because *turbulence is indeed a property of the flow, not of the fluid.*

3.7 The Reynolds Stress Equations

It is clear from the preceding section that the simple idea of an eddy viscosity might not be the best way to approach the problem of relating the Reynolds stress to the mean motion. An alternative approach is to try to derive dynamical equations for the Reynolds stresses from the equations governing the fluctuations themselves. Such an approach recognizes that the Reynolds stress is really a functional[6] of the velocity; that is, the stress at a point depends on the velocity everywhere and for all past times, not just at the point in question and at a particular instant in time.

The analysis begins with the equation for the instantaneous fluctuating velocity, equation 3.21. This can be rewritten for a Newtonian fluid with constant viscosity as:

$$\rho\left[\frac{\partial u_i}{\partial t} + U_j\frac{\partial u_i}{\partial x_j}\right] = -\frac{\partial p}{\partial x_i} + \frac{\partial \tau_{ij}^{(v)}}{\partial x_j} - \rho\left[u_j\frac{\partial U_i}{\partial x_j}\right] - \rho\left\{u_j\frac{\partial u_i}{\partial x_j} - \langle u_j\frac{\partial u_i}{\partial x_j}\rangle\right\} \tag{3.27}$$

Note that the free index in this equation is i. Also, since we are now talking about turbulence again, the capital letters represent mean or averaged quantities.

[6] A functional is a function of a function

Multiplying equation 3.27 by u_k and averaging yields:

$$\begin{aligned}\rho\left[\langle u_k\frac{\partial u_i}{\partial t}\rangle + U_j\langle u_k\frac{\partial u_i}{\partial x_j}\rangle\right] = & - \langle u_k\frac{\partial p}{\partial x_i}\rangle + \langle u_k\frac{\partial \tau_{ij}^{(v)}}{\partial x_j}\rangle \\ & -\rho\left[\langle u_k u_j\rangle\frac{\partial U_i}{\partial x_j}\right] - \rho\left\{\langle u_k u_j\frac{\partial u_i}{\partial x_j}\rangle\right\}\end{aligned} \tag{3.28}$$

Now since both i and k are free indices they can be interchanged to yield a second equation given by[7]:

$$\begin{aligned}\rho\left[\langle u_i\frac{\partial u_k}{\partial t}\rangle + U_j\langle u_i\frac{\partial u_k}{\partial x_j}\rangle\right] = & - \langle u_i\frac{\partial p}{\partial x_k}\rangle + \langle u_i\frac{\partial \tau_{kj}^{(v)}}{\partial x_j}\rangle \\ & - \rho\left[\langle u_i u_j\rangle\frac{\partial U_k}{\partial x_j}\right] - \rho\left\{\langle u_i u_j\frac{\partial u_k}{\partial x_j}\rangle\right\}\end{aligned} \tag{3.29}$$

Equations 3.28 and 3.29 can be added together to yield an equation for the Reynolds stress,

$$\begin{aligned}\frac{\partial\langle u_i u_k\rangle}{\partial t} + U_j\frac{\partial\langle u_i u_k\rangle}{\partial x_j} = & -\frac{1}{\rho}\left[\langle u_i\frac{\partial p}{\partial x_k}\rangle + \langle u_k\frac{\partial p}{\partial x_i}\rangle\right] \\ & - \left[\langle u_i u_j\frac{\partial u_k}{\partial x_j}\rangle + \langle u_k u_j\frac{\partial u_i}{\partial x_j}\rangle\right] \\ & + \frac{1}{\rho}\left[\langle u_i\frac{\partial \tau_{kj}^{(v)}}{\partial x_j}\rangle + \langle u_k\frac{\partial \tau_{ij}^{(v)}}{\partial x_j}\rangle\right] \\ & - \left[\langle u_i u_j\rangle\frac{\partial U_k}{\partial x_j} + \langle u_k u_j\rangle\frac{\partial U_i}{\partial x_j}\right]\end{aligned} \tag{3.30}$$

It is customary to rearrange the first term on the right hand side in the following way:

$$\begin{aligned}\left[\langle u_i\frac{\partial p}{\partial x_k}\rangle + \langle u_k\frac{\partial p}{\partial x_i}\rangle\right] = & \langle p\left[\frac{\partial u_i}{\partial x_k} + \frac{\partial u_k}{\partial x_i}\right]\rangle \\ & + \frac{\partial}{\partial x_j}\left[\langle p u_i\rangle\delta_{kj} + \langle p u_k\rangle\delta_{ij}\right]\end{aligned} \tag{3.31}$$

The first term on the right is generally referred to as the *pressure strain-rate* term. The second term is written as a divergence term, and is generally referred to as the *pressure diffusion* term. We shall see later that divergence terms can never create nor destroy anything; they can simply move it around from one place to another.

[7]Alternatively equation 3.21 can be rewritten with free index k, then multiplied by u_i and averaged

The third term on the right-hand side of equation 3.30 can similarly be re-written as:

$$\left[\langle u_i \frac{\partial \tau_{kj}^{(v)}}{\partial x_j}\rangle + \langle u_k \frac{\partial \tau_{ij}^{(v)}}{\partial x_j}\rangle\right] = - \left[\langle \tau_{ij}^{(v)} \frac{\partial u_k}{\partial x_j}\rangle + \langle \tau_{kj}^{(v)} \frac{\partial u_i}{\partial x_j}\rangle\right] + \frac{\partial}{\partial x_j}[\langle u_i \tau_{kj}^{(v)}\rangle + \langle u_k \tau_{ij}^{(v)}\rangle] \tag{3.32}$$

The first of these is also a divergence term. For a Newtonian fluid, the last is the so-called "dissipation of Reynolds stress" by the turbulence viscous stresses. This is easily seen by substituting the Newtonian constitutive relation to obtain:

$$\frac{1}{\rho}\left[\langle \tau_{ij}^{(v)} \frac{\partial u_k}{\partial x_j}\rangle + \langle \tau_{kj}^{(v)} \frac{\partial u_i}{\partial x_j}\rangle\right] = 2\nu \left[\langle s_{ij} \frac{\partial u_k}{\partial x_j}\rangle + \langle s_{kj} \frac{\partial u_i}{\partial x_j}\rangle\right] \tag{3.33}$$

It is not at all obvious what this has to do with dissipation, but it will become clear later on when we consider the trace of the Reynolds stress equation, which is the *kinetic energy* equation for the turbulence.

Now if we use the same trick from before using the continuity equation, we can rewrite the second term on the right-hand side of equation 3.30 to obtain:

$$\left[\langle u_i u_j \frac{\partial u_k}{\partial x_j}\rangle + \langle u_k u_j \frac{\partial u_i}{\partial x_j}\rangle\right] = \frac{\partial}{\partial x_j}\langle u_i u_k u_j\rangle \tag{3.34}$$

This is also a divergence term.

We can use all of the pieces we have developed above to rewrite equation 3.30 as:

$$\begin{aligned}\frac{\partial}{\partial t}\langle u_i u_k\rangle &+ U_j\frac{\partial}{\partial x_j}\langle u_i u_k\rangle = \langle\frac{p}{\rho}\left[\frac{\partial u_i}{\partial x_k}+\frac{\partial u_k}{\partial x_i}\right]\rangle \\ &+ \frac{\partial}{\partial x_j}\left\{-\frac{1}{\rho}[\langle pu_k\rangle\delta_{ij}+\langle pu_i\rangle\delta_{kj}]-\langle u_i u_k u_j\rangle\right. \\ &\qquad \left.+2\nu[\langle s_{ij}u_k\rangle+\langle s_{kj}u_i\rangle]\right\} \\ &- \left[\langle u_i u_j\rangle\frac{\partial U_k}{\partial x_j}+\langle u_k u_j\rangle\frac{\partial U_i}{\partial x_j}\right] \\ &- 2\nu\left[\langle s_{ij}\frac{\partial u_k}{\partial x_j}\rangle+\langle s_{kj}\frac{\partial u_i}{\partial x_j}\rangle\right] \qquad (3.35)\end{aligned}$$

This is the so-called **Reynolds Stress Equation** which has been the primary vehicle for much of the turbulence modeling efforts of the past few decades.

The left hand side of the Reynolds Stress Equation can easily be recognized as the rate of change of Reynolds stress following the mean motion. It seems to provide exactly what we need: nine new equations for the nine unknowns we cannot account for. The problems are all on the right-hand side. These terms are referred to respectively as

1. the pressure-strain rate term
2. the turbulence transport (or divergence) term
3. the "production" term, and
4. the "dissipation" term.

Obviously these equations do not involve only U_i and $\langle u_i u_j\rangle$, but depend on many more new unknowns.

It is clear that, contrary to our hopes, we have not derived a single equation relating the Reynolds stress to the mean motion. Instead, our Reynolds stress transport equation is exceedingly complex. Whereas the process of averaging the equation for the mean motion introduced only six new independent unknowns, the Reynolds stress, $\langle u_i u_j\rangle$, the search for a transport equation which will relate these to the mean motion has produced many more unknowns. They are:

$$\begin{aligned}\langle pu_i\rangle &- 3 \quad unknowns & (3.36)\\ \langle u_i s_{jk}\rangle &- 27 & (3.37)\\ \langle s_{ij}s_{jk}\rangle &- 9 & (3.38)\\ \langle u_i u_k u_j\rangle &- 27 & (3.39)\\ \langle p\frac{\partial u_i}{\partial x_j}\rangle &- 9 & (3.40)\\ TOTAL &- 75 & (3.41)\end{aligned}$$

Not all of these are independent, since some can be derived from the others. Even so, our goal of reducing the number of unknowns has clearly not been met.

Equations governing each of these new quantities can be derived from the original dynamical equations, just as we did for the Reynolds stress. Unfortunately new quantities continue to be introduced with each new equation, and at a faster rate than the increase in the number of equations. Now the full implications of the closure problem introduced by the Reynolds decomposition and averaging has become apparent. No matter how many new equations are derived, the number of new unknown quantities introduced will always increase more rapidly.

Our attempt to solve the turbulence problem by considering averages illustrates a general principle. Any time we try to fool Mother Nature by averaging out her details, she gets her revenge by leaving us with a closure problem — more equations than unknowns. In thermodynamics, we tried to simplify the consideration of molecules by averaging over them, and were left with the need for an equation of state. In heat transfer, we tried to simplify considerations by which molecules transfer their kinetic energy, and found we were lacking a relation between the heat flux and the temperature field. And in fluid mechanics, we tried to simplify consideration of the "mean" motion of molecules and ended up with viscous stress. In all of these cases we were able to make simple physical models which worked at least some of the time; e.g., ideal gas, Fourier-Newtonian fluid. And these models all worked because we were able to make assumptions about the underlying molecular processes and assume them to be independent of the macroscopic flows of interest. Unfortunately such assumptions are rarely satisfied in turbulence.

It should be obvious by now that the turbulence closure problem will not be solved by the straight-forward derivation of new equations, nor by direct analogy with viscous stresses. Rather, *closure attempts will have to depend on an intimate knowledge of the dynamics of the turbulence itself.* Only by understanding how the turbulence behaves can one hope to *guess* an appropriate set of constitutive equations **AND** *understand the limits of them.* This is, of course, another consequence of the fact that the *turbulence is a property of the flow itself, and not of the fluid*!

Chapter 4

The Turbulence Kinetic Energy

4.1 The Kinetic Energy of the Fluctuations

It is clear from the previous chapter that the straightforward application of ideas that worked well for viscous stresses do not work too well for turbulence Reynolds stresses. Moreover, even the attempt to directly derive equations for the Reynolds stresses using the Navier-Stokes equations as a starting point has left us with far more equations than unknowns. Unfortunately this means that the turbulence problem for engineers is not going to have a simple solution: we simply cannot produce a set of reasonably universal equations. Obviously we are going to have to study the turbulence fluctuations in more detail and learn how they get their energy (usually from the mean flow somehow), and what they ultimately do with it. Our hope is that by understanding more about turbulence itself, we will gain insight into how we might make closure approximations that will work, at least sometimes. Hopefully, we will also gain an understanding of when and why they will not work.

An equation for the fluctuating kinetic energy for constant density flow can be obtained directly from the Reynolds stress equation derived earlier, equation 3.35, by contracting the free indices. The result is:

$$\begin{aligned}\left[\frac{\partial}{\partial t}\langle u_i u_i\rangle \;+\; U_j\frac{\partial}{\partial x_j}\langle u_i u_i\rangle\right] \\ = \;\frac{\partial}{\partial x_j}\left\{-\frac{2}{\rho}\langle p u_i\rangle\delta_{ij} - \langle q^2 u_j\rangle + 4\nu\langle s_{ij}u_i\rangle\right\} \\ -2\langle u_i u_j\rangle\frac{\partial U_i}{\partial x_j} - 4\nu\langle s_{ij}\frac{\partial u_i}{\partial x_j}\rangle \qquad (4.1)\end{aligned}$$

where the incompressibility condition ($\partial u_j/\partial x_j = 0$) has been used to eliminate the pressure-strain rate term, and $q^2 \equiv u_i u_i$.

The last term can be simplified by recalling that the velocity deformation rate tensor, $\partial u_i/\partial x_j$, can be decomposed into symmetric and anti-symmetric parts;

i.e.,

$$\frac{\partial u_i}{\partial x_j} = s_{ij} + \omega_{ij} \tag{4.2}$$

where the symmetric part is the strain-rate tensor, s_{ij}, and the anti-symmetric part is the rotation-rate tensor, ω_{ij}, defined by:

$$\omega_{ij} = \frac{1}{2}\left[\frac{\partial u_i}{\partial x_j} - \frac{\partial u_j}{\partial x_i}\right] \tag{4.3}$$

Since the double contraction of a symmetric tensor with an anti-symmetric tensor is identically zero, it follows immediately that:

$$\begin{aligned} \langle s_{ij}\frac{\partial u_i}{\partial x_j}\rangle &= \langle s_{ij}s_{ij}\rangle + \langle s_{ij}\omega_{ij}\rangle \\ &= \langle s_{ij}s_{ij}\rangle \end{aligned} \tag{4.4}$$

Now it is customary to define a new variable k, the average fluctuating kinetic energy per unit mass, by:

$$k \equiv \frac{1}{2}\langle u_i u_i\rangle = \frac{1}{2}\langle q^2\rangle = \frac{1}{2}[\langle u_1^2\rangle + \langle u_2^2\rangle + \langle u_3^2\rangle] \tag{4.5}$$

By dividing equation 4.1 by 2 and inserting this definition, the equation for the average kinetic energy per unit mass of the fluctuating motion can be re-written as:

$$\begin{aligned} \left[\frac{\partial}{\partial t} + U_j\frac{\partial}{\partial x_j}\right]k &= \frac{\partial}{\partial x_j}\left\{-\frac{1}{\rho}\langle p u_i\rangle\delta_{ij} - \frac{1}{2}\langle q^2 u_j\rangle + 2\nu\langle s_{ij}u_i\rangle\right\} \\ &\quad -\langle u_i u_j\rangle\frac{\partial U_i}{\partial x_j} - 2\nu\langle s_{ij}s_{ij}\rangle \end{aligned} \tag{4.6}$$

The role of each of these terms will be examined in detail later. First note that an alternative form of this equation can be derived by leaving the viscous stress in terms of the strain rate. We can obtain the appropriate form of the equation for the fluctuating momentum from equation 3.21 by substituting the incompressible Newtonian constitutive equation into it to obtain:

$$\left[\frac{\partial}{\partial t} + U_j\frac{\partial}{\partial x_j}\right]u_i = -\frac{1}{\rho}\frac{\partial p}{\partial x_i} + \nu\frac{\partial^2 u_i}{\partial x_j^2} - \left[u_j\frac{\partial U_i}{\partial x_j}\right] - \left\{u_j\frac{\partial u_i}{\partial x_j} - \langle u_j\frac{\partial u_i}{\partial x_j}\rangle\right\} \tag{4.7}$$

If we take the scalar product of this with the fluctuating velocity itself and average, it follows (after some rearrangement) that:

$$\begin{aligned} \left[\frac{\partial}{\partial t} + U_j\frac{\partial}{\partial x_j}\right]k &= \frac{\partial}{\partial x_j}\left\{-\frac{1}{\rho}\langle p u_i\rangle\delta_{ij} - \frac{1}{2}\langle q^2 u_j\rangle + \nu\frac{\partial}{\partial x_j}k\right\} \\ &\quad - \langle u_i u_j\rangle\frac{\partial U_i}{\partial x_j} - \nu\langle\frac{\partial u_i}{\partial x_j}\frac{\partial u_i}{\partial x_j}\rangle \end{aligned} \tag{4.8}$$

Both equations 4.6 and 4.8 play an important role in the study of turbulence. The first form given by equation 4.6 will provide the framework for understanding the dynamics of turbulent motion. The second form, equation 4.8 forms the basis for most of the second-order closure attempts at turbulence modelling; e.g., the so-called k-ϵ models (usually referred to as the "**k-epsilon models**"). This because it has fewer unknowns to be modelled, although this comes at the expense of some extra assumptions about the last term. It is only the last term in equation 4.6 that can be identified as the true rate of dissipation of turbulence kinetic energy, unlike the last term in equation 4.8 which is only the dissipation when the flow is *homogeneous*. We will talk about homogeniety below, but suffice it to say now that it never occurs in nature. Nonetheless, many flows can be *assumed* to be homogeneous *at the scales of turbulence which are important to this term*, so-called *local homogeniety*.

Each term in the equation for the kinetic energy of the turbulence has a distinct role to play in the overall kinetic energy balance. Briefly these are:

- Rate of change of kinetic energy per unit mass due to non-stationarity; i.e., time dependence of the mean:
$$\frac{\partial k}{\partial t} \tag{4.9}$$

- Rate of change of kinetic energy per unit mass due to convection (or advection) by the mean flow through an inhomogenous field :
$$U_j \frac{\partial k}{\partial x_j} \tag{4.10}$$

- Transport of kinetic energy in an inhomogeneous field due respectively to the pressure fluctuations, the turbulence itself, and the viscous stresses:
$$\frac{\partial}{\partial x_j}\left\{-\frac{1}{\rho}\langle p u_i\rangle \delta_{ij} - \frac{1}{2}\langle q^2 u_j\rangle + 2\nu\langle s_{ij} u_i\rangle\right\} \tag{4.11}$$

- Rate of production of turbulence kinetic energy from the mean flow (gradient):
$$-\langle u_i u_j\rangle \frac{\partial U_i}{\partial x_j} \tag{4.12}$$

- Rate of dissipation of turbulence kinetic energy per unit mass due to viscous stresses:
$$\epsilon \equiv 2\nu\langle s_{ij} s_{ij}\rangle \tag{4.13}$$

These terms will be discussed in detail in the succeeding sections, and the role of each examined carefully.

4.2 The Rate of Dissipation of the Turbulence Kinetic Energy.

The last term in the equation for the kinetic energy of the turbulence has been identified as the rate of dissipation of the turbulence energy per unit mass; i.e.,

$$\epsilon = 2\nu\langle s_{ij}s_{ij}\rangle = \nu\left\{\langle\frac{\partial u_i}{\partial x_j}\frac{\partial u_i}{\partial x_j}\rangle + \langle\frac{\partial u_i}{\partial x_j}\frac{\partial u_j}{\partial x_i}\rangle\right\} \tag{4.14}$$

It is easy to see that $\epsilon \geq 0$ always, since it is a sum of the average of squared quantities only (i.e., $\langle s_{ij}s_{ij} \geq 0$). Also, since it occurs on the right hand side of the kinetic energy equation for the fluctuating motions preceded by a minus sign, it is clear that it can act only to *reduce* the kinetic energy of the flow. Therefore it causes a *negative* rate of change of kinetic energy; hence the name *dissipation*.

Physically, energy is dissipated because of the work done by the fluctuating viscous stresses in resisting deformation of the fluid material by the fluctuating strain rates; i.e.,

$$\epsilon = \langle\tau_{ij}^{(v)}s_{ij}\rangle \tag{4.15}$$

This reduces to equation 4.14 only for a Newtonian fluid. In non-Newtonian fluids, portions of this product may not be negative implying that it may not all represent an irrecoverable loss of fluctuating kinetic energy.

It will be shown in Chapter 5 that the dissipation of turbulence energy mostly takes place at the smallest turbulence scales, and that those scales can be characterized by the so-called Kolmogorov microscale defined by:

$$\eta_K \equiv \left(\frac{\nu^3}{\epsilon}\right)^{1/4} \tag{4.16}$$

In atmospheric motions where the length scale for those eddies having the most turbulence energy (and most responsible for the Reynolds stress) can be measured in kilometers, typical values of the Kolmogorov microscale range from $0.1-10$ *millimeters*. In laboratory flows where the overall scale of the flow is greatly reduced, much smaller values of η_K are not uncommon. The small size of these dissipative scales greatly complicates measurement of energy balances, since the largest measuring dimension must be about equal to twice the Kolmogorov microscale. And it is the range of scales, L/η, which makes direct numerical simulation of most interesting flows impossible, since the required number of computational cells is several orders of magnitude greater than $(L/\eta)^3$. This same limitation also affects experiments as well, which must often be quite large to be useful.

One of the consequences of this great separation of scales between those containing the bulk of the turbulence energy and those dissipating it is that *the dissipation rate is primarily determined by the large scales and not the small.* This is because the viscous scales (which operate on a time scale of $t_K = (\nu/\epsilon)^{1/2}$) dissipate rapidly any energy sent down to them by the non-linear processes of

scale to scale energy transfer. Thus the overall rate of dissipation is controlled by the rate of energy transfer *from* the energetic scales, primarily by the non-linear scale-to-scale transfer. This will be discussed later when we consider the energy spectrum. But for now it is important only note that a consequence of this is that the dissipation rate is given approximately as:

$$\epsilon \propto \frac{u^3}{L} \tag{4.17}$$

where $u^2 \equiv \langle q^2 \rangle / 3$ and L is something like an integral length scale. It is easy to remember this relation if you note that the time scale of the energetic turbulent eddies can be estimated as L/u. Thus $dk/dt = (3/2)du^2/dt$ can estimated as $(3u^2/2)/(L/u)$.

Sometimes it is convenient to just *define* the "length scale of the energy-containing eddies" (or the *pseudo-integral scale*) as:

$$l \equiv \frac{u^3}{\epsilon} \tag{4.18}$$

Almost always, $l \propto L$, but the relation is at most only exact theoretically in the limit of infinite Reynolds number since the constant of proportionality is Reynolds number dependent. Some just assume ratio to be constant (and even universal), and even refer to l as though it were the real integral scale. Others believe that the 'experimental' scatter observed in the constant is because of the differing upstream conditions and that the ratio may not be constant at all. It is really hard to tell who is right in the absence of facilities or simulations in which the Reynolds number can vary very much for fixed initial conditions. Nonetheless, there is really overwhelming evidence (experimental and theoretical) that this ratio depends very much on the type of flow being considered. This all may leave you feeling a bit confused, but that's the way turbulence is right now. It's a lot easier to teach if we just tell you one view, but that's not very good preparation for the future.

Here is what we can say for sure. Only the integral scale, L, is a physical length scale, meaning that it can be directly observed in the flow by spectral or correlation measurements (as shown later). The *pseudo-integral scale*, l, on the other hand is simply a definition; and it is only at infinite turbulence Reynolds number that it has any real physical significance. But it is certainly a useful approximation at large, but finite, Reynolds numbers. We will talk about these subtle but important distinctions later when we consider homogeneous flows, but it is especially important when considering similarity theories of turbulence. For now simply file away in your memory a note of caution about using equation 4.17 too freely. And do not be fooled by the cute description this provides. It is just that, a description, and not really an explanation of why all this happens — sort of like the weather man describing the weather.

Using equation 4.18, the Reynolds number dependence of the ratio of the

Kolmorgorov microscale, η_K, to the pseudo-integral scale, l, can be obtained as:

$$\frac{\eta_K}{l} = R_l^{-3/4} \tag{4.19}$$

where the *turbulence Reynolds number*, R_l, is defined by:

$$R_l \equiv \frac{ul}{\nu} = \frac{u^4}{\nu\epsilon} \tag{4.20}$$

Example Estimate the Kolmogorov microscale for $u = 1$ m/s and $L = 0.1$m for air and water.

air For air, $R_l = 1 \times (0.1)/15 \times 10^{-6} \approx 7 \times 10^3$. Therefore $l/\eta_K \approx 8 \times 10^2$, so $\eta_K \approx 1.2 \times 10^{-4}$m or 0.12mm.

water For water, $R_l = 1 \times (0.1)/10^{-6} \approx 10^5$. Therefore $l/\eta_K \approx 5 \times 10^3$, so $\eta_K \approx 2 \times 10^{-5}$m or 0.02mm.

Exercise: Find the dependence on R_l of the time-scale ration between the Kolmorogov microtime and the time scale of the energy-containing eddies.

Thus the dissipative scales are all much smaller than those characterizing the energy of the turbulent fluctuations, and their *relative size decreases with increasing Reynolds number*. Note that in spite of this, the Kolmogorov scales all *increase* with increasing energy containing scales for fixed values of the Reynolds number. This fact is very important in designing laboratory experiments at high turbulence Reynolds number where the finite probe size limits spatial resolution. The rather imposing size of some experiments is an attempt to cope with this problem by increasing the size of the smallest scales, thus making them larger than the resolution limits of the probes being used.

Exercise: Suppose the smallest probe you can build can only resolve 0.1 mm. Also to do an experiment which is a reasonable model of a real engineering flow (like a hydropower plant), you need (for reason that will be clear later) a scale separation of at least $L/\eta_K = 10^4$. If your facility has to be at least a factor of ten larger than L (which you estimate as l), what is its smallest dimension?

It will also be argued later that these small dissipative scales of motion at very high Reynolds number tend to be statistically nearly *isotropic*; i.e., their statistical character is independent of direction. We will discuss some of the implications of *isotropy* and *local isotropy* later, but note for now that it makes possible a huge reduction in the number of unknowns, particularly those determined primarily by the dissipative scales of motion.

4.3 The Kinetic Energy of the Mean Motion and the "Production" of Turbulence

An equation for the kinetic energy of the *mean motion* can be derived by a procedure exactly analogous to that applied to the fluctuating motion. The mean motion was shown in equation 3.19 to be given by:

$$\rho\left[\frac{\partial U_i}{\partial t}+U_j\frac{\partial U_i}{\partial x_j}\right]=-\frac{\partial P}{\partial x_i}+\frac{\partial T_{ij}^{(v)}}{\partial x_j}-\frac{\partial}{\partial x_j}(\rho\langle u_iu_j\rangle) \tag{4.21}$$

By taking the scalar product of this equation with the mean velocity, U_i, we can obtain an equation for the kinetic energy of the *mean* motion as:

$$U_i\left[\frac{\partial}{\partial t}+U_j\frac{\partial}{\partial x_j}\right]U_i=-\frac{U_i}{\rho}\frac{\partial P}{\partial x_i}+\frac{U_i}{\rho}\frac{\partial T_{ij}^{(v)}}{\partial x_j}-U_i\frac{\partial\langle u_iu_j\rangle}{\partial x_j} \tag{4.22}$$

Unlike the fluctuating equations, there is no need to average here, since all the terms are already averages.

In exactly the same manner that we rearranged the terms in the equation for the kinetic energy of the fluctuations, we can rearrange the equation for the kinetic energy of the mean flow to obtain:

$$\begin{aligned}\left[\frac{\partial}{\partial t}\right. &+ \left. U_j\frac{\partial}{\partial x_j}\right]K= \\ &\frac{\partial}{\partial x_j}\left\{-\frac{1}{\rho}\langle PU_i\rangle\delta_{ij}-\frac{1}{2}\langle u_iu_j\rangle U_i+2\nu\langle S_{ij}U_i\rangle\right\} \\ &+\langle u_iu_j\rangle\frac{\partial U_i}{\partial x_j}-2\nu\langle S_{ij}S_{ij}\rangle\end{aligned} \tag{4.23}$$

where

$$K\equiv\frac{1}{2}Q^2=\frac{1}{2}U_iU_i \tag{4.24}$$

The role of all of the terms can immediately be recognized since each term has its counterpart in the equation for the average fluctuating kinetic energy.

Comparison of equations 4.23 and 4.6 reveals that the term $-\langle u_iu_j\rangle\partial U_i/\partial x_j$ appears in the equations for the kinetic energy of BOTH the mean and the fluctuations. There is, however, one VERY important difference. This "production" term has the opposite sign in the equation for the mean kinetic energy than in that for the mean fluctuating kinetic energy! Therefore, *whatever its effect on the kinetic energy of the mean, its effect on the kinetic energy of the fluctuations will be the opposite.* Thus kinetic energy can be interchanged between the mean and fluctuating motions. In fact, the only other term involving fluctuations in the equation for the kinetic energy of the mean motion is a divergence term; therefore it can only move the kinetic energy of the mean flow from one place to another.

Therefore this "production " term provides the *only* means by which energy can be interchanged between the mean flow and the fluctuations.

Understanding the manner in which this energy exchange between mean and fluctuating motions is accomplished represents one of the most challenging problems in turbulence. The overall exchange can be understood by exploiting the analogy which treats $-\rho\langle u_i u_j\rangle$ as a stress, the Reynolds stress. The term:

$$-\rho\langle u_i u_j\rangle \partial U_i/\partial x_j \tag{4.25}$$

can be thought of as the working of the Reynolds stress against the mean velocity gradient of the flow, exactly as the viscous stresses resist deformation by the instantaneous velocity gradients. This energy expended against the Reynolds stress during deformation by the mean motion ends up in the fluctuating motions, however, while that expended against viscous stresses goes directly to internal energy. As we have already seen, the viscous deformation work from the fluctuating motions (or dissipation) will eventually send this fluctuating kinetic energy on to internal energy as well.

Now, just in case you are not all that clear exactly how the dissipation terms really accomplish this for the instantaneous motion, it might be useful to examine exactly how the above works. We begin by decomposing the mean deformation rate tensor $\partial U_i/\partial x_j$ into its symmetric and antisymmetric parts, exactly as we did for the instantaneous deformation rate tensor in Chapter 3; i.e.,

$$\frac{\partial U_i}{\partial x_j} = S_{ij} + \Omega_{ij} \tag{4.26}$$

where the mean strain rate S_{ij} is defined by

$$S_{ij} = \frac{1}{2}\left[\frac{\partial U_i}{\partial x_j} + \frac{\partial U_j}{\partial x_i}\right] \tag{4.27}$$

and the mean rotation rate is defined by

$$\Omega_{ij} = \frac{1}{2}\left[\frac{\partial U_i}{\partial x_j} - \frac{\partial U_j}{\partial x_i}\right] \tag{4.28}$$

Since Ω_{ij} is antisymmetric and $-\langle u_i u_j\rangle$ is symmetric, their contraction is zero so it follows that:

$$-\langle u_i u_j\rangle \frac{\partial U_i}{\partial x_j} = -\langle u_i u_j\rangle S_{ij} \tag{4.29}$$

Equation 4.29 is an analog to the mean viscous dissipation term given for incompressible flow by:

$$T_{ij}^{(v)} \frac{\partial U_i}{\partial x_j} = T_{ij}^{(v)} S_{ij} = 2\mu S_{ij} S_{ij} \tag{4.30}$$

It is easy to show that this term transfers (or dissipates) the mean kinetic energy directly to internal energy, since exactly the same term appears with the opposite

sign in the internal energy equations. Moreover, since $S_{ij}S_{ij} \geq 0$ always, this is a one-way process and kinetic energy is decreased while internal energy is increased. Hence it can be referred to either as "dissipation" of kinetic energy, or as "production" of internal energy. As surprising as it may seem, this direct dissipation of energy by the mean flow is usually negligible compared to the energy lost to the turbulence through the Reynolds stress terms. (Remember, there is a term exactly like this in the kinetic energy equation for the fluctuating motion, but involving only fluctuating quantities; namely, $2\mu\langle s_{ij}s_{ij}\rangle$.) We shall show later that for almost always in turbulent flow, $\langle s_{ij}s_{ij}\rangle >> S_{ij}S_{ij}$. What this means is that the energy dissipation in a turbulent flow is almost entirely due to the turbulence.

There is a very important difference between equations 4.29 and 4.30. Whereas the effect of the viscous stress working against the deformation (in a Newtonian fluid) is *always* to remove energy from the flow (since $S_{ij}S_{ij} > 0$ always), *the effect of the Reynolds stress working against the mean gradient can be of either sign*, at least in principle. That is, it can either transfer energy *from* the mean motion *to* the fluctuating motion, or *vice versa*.

Almost always (and especially in situations of engineering importance), $-\langle u_i u_j\rangle$ and S_{ij} have the opposite sign. Therefore, $-\langle u_i u_j\rangle S_{ij} > 0$ almost always, so kinetic energy is removed from the mean motion and added to the fluctuations. Since the term $-\langle u_i u_j\rangle \partial U_i/\partial x_j$ usually acts to increase the turbulence kinetic energy, it is usually referred to as the "rate of turbulence energy production", or simply the "*production*".

Now that we have identified how the averaged equations account for the 'production' of turbulence energy from the mean motion, it is tempting to think we have understood the problem. In fact, 'labeling' phenomena is not the same as 'understanding' them. The manner in which the turbulence motions cause this exchange of kinetic energy between the mean and fluctuating motions varies from flow to flow, and is really very poorly understood. Saying that it is the Reynolds stress working against the mean velocity gradient is true, but like saying that money comes from a bank. If we want to examine the energy transfer mechanism in detail we must look beyond the single point statistics, so this will have to be a story for another time.

Example: Consider how the production term looks if the Reynolds stress is modelled by an turbulent viscosity.

4.4 The Transport (or Divergence) Terms

The overall role of the transport terms is best understood by considering a turbulent flow which is completely confined by rigid walls as in Figure 4.1. First consider only the turbulence transport term. If the volume within the confinement is denoted by V_o and its bounding surface is S_o, then first term on the right-hand

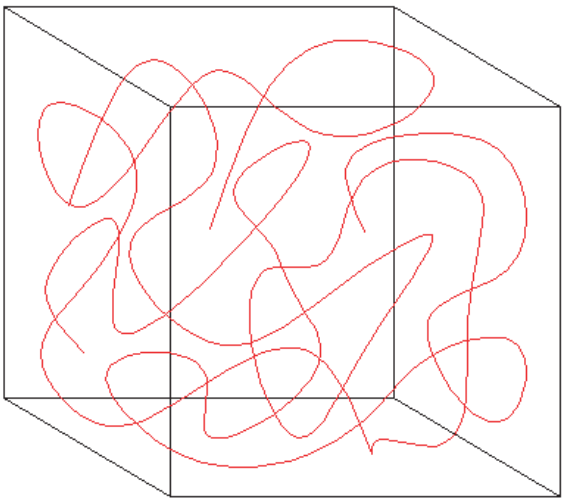

Figure 4.1: Turbulence confined by rigid walls.

side of equation 4.6 for the fluctuating kinetic energy can be integrated over the volume to yield:

$$\begin{aligned} & \int\int\int_{V_o} \frac{\partial}{\partial x_j}\left[-\frac{1}{\rho}\langle pu_i\rangle\delta_{ij} - \frac{1}{2}\langle q^2u_j\rangle + \nu\langle s_{ij}u_i\rangle\right] dV \\ = & \int\int_{S_o}\left[-\frac{1}{\rho}\langle pu_i\rangle\delta_{ij} - \frac{1}{2}\langle q^2u_j\rangle + \nu\langle s_{ij}u_i\rangle\right] n_j dS \end{aligned} \tag{4.31}$$

where we have used the divergence theorem — again!

We assumed our enclosure to have rigid walls; therefore the normal component of the mean velocity ($u_n = u_j n_j$) must be zero on the surface since there can be no flow through it (the kinematic boundary condition). This immediately eliminates the contributions to the surface integral from the $\langle pu_j n_j\rangle$ and $\langle q^2 u_j n_j\rangle$ terms. But the last term is zero on the surface also. This can be seen in two ways: either by invoking the no-slip condition which together with the kinematic boundary condition insures that u_i is zero on the boundary, or by noting from Cauchy's theorem that $\nu s_{ij} n_j$ is the viscous contribution to the normal contact force per unit area on the surface (i.e., $t_n^{(v)}$) whose scalar product with u_i must be identically zero since u_n is zero. Therefore the entire integral is identically zero and its net contribution to the rate of change of kinetic energy is zero.

Thus the only effect of the turbulence transport terms (in a fixed volume at least) can be to move energy from one place to another, neither creating nor destroying it in the process. This is, of course, why they are collectively called the *transport terms*. This spatial transport of kinetic energy is accomplished by the acceleration of adjacent fluid due to pressure and viscous stresses (the first

and last terms respectively), and by the physical transport of fluctuating kinetic energy by the turbulence itself (the middle term).

This role of these turbulence transport terms in moving kinetic energy around is often exploited by turbulence modellers. It is argued, that *on the average*, these terms will only act to move energy from regions of higher kinetic energy to lower. Thus a *plausible* first-order hypothesis is that this "diffusion" of kinetic energy should be proportioned to gradients of the kinetic energy itself. That is,

$$-\frac{1}{\rho}\langle pu_j\rangle - \frac{1}{2}\langle q^2 u_j\rangle + \nu\langle s_{ij}u_i\rangle = \nu_{ke}\frac{\partial k}{\partial x_j} \tag{4.32}$$

where ν_{ke} is an effective diffusivity like the eddy viscosity discussed earlier. If we use the alternative form of the kinetic energy equation (equation 4.8), there is no need to model the viscous term (since it involves only k itself). Therefore our model might be:

$$-\frac{1}{\rho}\langle pu_j\rangle - \frac{1}{2}\langle q^2 u_j\rangle = \nu_{kealt}\frac{\partial k}{\partial x_j} \tag{4.33}$$

These, of course, look much more complicated in a real model because of the need to insure proper tensorial invariance, etc., but the physics is basically the same.

If you think about it, that such a simple closure is worth mentioning at all is pretty amazing. We took 9 unknowns, lumped them together, and replaced their net effect by the simple gradient of something we did know (or at least wanted to calculate), k. And surprisingly, this simple idea works pretty well in many flows, especially if the value of the turbulent viscosity is itself related to other quantities like k and ϵ. In fact this simple gradient hypothesis for the turbulence transport terms is at the root of all engineering turbulence models.

There are a couple of things to note about such simple closures though, before getting too enthused about them. First such an assumption rules out a counter-gradient diffusion of kinetic energy which is known to exist in some flows. In such situations the energy appears to flow *up* the gradient. While this may seem unphysical, remember we only *assumed* it flowed *down* the gradient in the first place. This is the whole problem with a *plausibility* argument. Typically energy does tend to be transported from regions of high kinetic energy to low kinetic energy, but there is really no reason for it always to do so, especially if there are other mechanisms at work. And certainly there is no reason for it to always be true locally, and the gradient of anything is a local quantity.

Let me illustrate this by a simple example. Let's apply a gradient hypothesis to the economy — a plausibility hypothesis if you will. By this simple model, money would always flow from the rich who have the most, to the poor who have the least. In fact, as history has shown, in the absence of other forces (like revolutions, beheadings, and taxes) this almost never happens. The rich will always get richer, and the poor poorer. And the reason is quite simple, the poor are usually borrowing (and paying interest), while the rich are doing the loaning (and collecting interest). Naturally there are individual exceptions and

great success stories among the poor. And there are wealthy people who give everything away. But mostly in a completely free economy, the money flows in a counter-gradient manner. So society (and the rich in particular) have a choice — risk beheading and revolution, or find a peaceful means to redistribute the wealth — like taxes. While the general need for the latter is recognized (especially among those who have and pay the least), there is, of course, considerable disagreement of how much tax is reasonable to counter the natural gradient.

Just as the simple eddy viscosity closure for the mean flow can be more generally written as a tensor, so can it be here. In fact the more sophisticated models write it as second or fourth-order tensors. More importantly, they include other gradients in the model so that the gradient of one quantity can influence the gradient of another. Such models can sometimes even account for counter-gradient behavior. If your study of turbulence takes you into the study of turbulence models, watch for these subtle differences among them. And don't let yourself be annoyed or intimidated by their complexity. Instead marvel at the physics behind them, and try to appreciate the wonderful manner in which mathematics has been used to make them properly invariant so you don't have to worry about whether they work in any particular coordinate system. It is all these extra terms that give you reason to hope that it might work at all.

4.5 The Intercomponent Transfer of Energy

The objective of this section is to examine how kinetic energy produced in one velocity component of the turbulence can be transferred to the other velocity components of the fluctuating motion. This is very important since often energy is transferred from the mean flow to a only a single component of the fluctuating motion. Yet somehow all three components of the kinetic energy end up being about the same order of magnitude. The most common exception to this is very close to surfaces where the normal component is suppressed by the kinematic boundary condition. To understand what is going on, it is necessary to develop even a few more equations; in particular, equations for *each component of the kinetic energy*. The procedure is almost identical to that used to derive the kinetic energy equation itself.

Consider first the equation for the 1-component of the fluctuating momentum. We can do this by simply setting $i = 1$ and $k = 1$ in the equation 3.35, or derive it from scratch by setting the free index in equation 3.27 equal to unity (i.e. i=1); i.e.,

$$\left[\frac{\partial u_1}{\partial t} + U_j\frac{\partial u_1}{\partial x_j}\right] = -\frac{1}{\rho}\frac{\partial p}{\partial x_1} + \frac{1}{\rho}\frac{\partial \tau_{1j}^{(v)}}{\partial x_j} - \left[u_j\frac{\partial U_1}{\partial x_j}\right] - \left\{u_j\frac{\partial u_1}{\partial x_j} - \langle u_j\frac{\partial u_1}{\partial x_j}\rangle\right\} \quad (4.34)$$

Multiplying this equation by u_1, averaging, and rearranging the pressure-velocity gradient term using the chain rule for products yields:

1- component

$$\begin{aligned}\left[\frac{\partial}{\partial t} \;+\; U_j\frac{\partial}{\partial x_j}\right]\frac{1}{2}\langle u_1^2\rangle & \\ = \;+\; \langle p\frac{\partial u_1}{\partial x_1}\rangle & \\ +\; \frac{\partial}{\partial x_j}\left\{-\frac{1}{\rho}\langle pu_1\rangle\delta_{1j} - \frac{1}{2}\langle u_1^2u_j\rangle + 2\nu\langle s_{1j}u_1\rangle\right\} & \\ -\; \langle u_1u_j\rangle\frac{\partial U_1}{\partial x_j} - 2\nu\langle s_{1j}s_{1j}\rangle & \end{aligned} \tag{4.35}$$

All of the terms except one look exactly like the their counterparts in equation 4.6 for the average of the total fluctuating kinetic energy. The single exception is the first term on the right-hand side which is the contribution from the *pressure-strain rate*. This will be seen to be exactly the term we are looking for to move energy among the three components.

Similar equations can be derived for the other fluctuating components with the result that

2- component

$$\begin{aligned}\left[\frac{\partial}{\partial t} \;+\; U_j\frac{\partial}{\partial x_j}\right]\frac{1}{2}\langle u_2^2\rangle & \\ = \;+\; \langle p\frac{\partial u_2}{\partial x_2}\rangle & \\ +\; \frac{\partial}{\partial x_j}\left\{-\frac{1}{\rho}\langle pu_2\rangle\delta_{2j} - \frac{1}{2}\langle u_2^2u_j\rangle + 2\nu\langle s_{2j}u_2\rangle\right\} & \\ -\; \langle u_2u_j\rangle\frac{\partial U_2}{\partial x_j} - 2\nu\langle s_{2j}s_{2j}\rangle & \end{aligned} \tag{4.36}$$

and

3- component

$$\begin{aligned}\left[\frac{\partial}{\partial t} + U_j\frac{\partial}{\partial x_j}\right]\frac{1}{2}\langle u_3^2\rangle \\ = + \langle p\frac{\partial u_3}{\partial x_3}\rangle \\ + \frac{\partial}{\partial x_j}\left\{-\frac{1}{\rho}\langle pu_3\rangle\delta_{3j} - \frac{1}{2}\langle u_3^2 u_j\rangle + 2\nu\langle s_{3j}u_3\rangle\right\} \\ - \langle u_3u_j\rangle\frac{\partial U_3}{\partial x_j} - 2\nu\langle s_{3j}s_{3j}\rangle \end{aligned} \tag{4.37}$$

Note that in each equation a new term involving a *pressure-strain rate* has appeared as the first term on the right-hand side. It is straightforward to show that these three equations sum to the kinetic energy equation given by equation 4.6, the extra pressure terms vanishing for the incompressible flow assumed here. In fact, the vanishing of the pressure-strain rate terms when the three equations are added together gives a clue as to their role. Obviously they can neither create nor destroy kinetic energy, only move it from one component of the kinetic energy to another.

The precise role of the pressure terms can be seen by noting that incompressibility implies that:

$$\langle p\frac{\partial u_j}{\partial x_j}\rangle = 0 \tag{4.38}$$

It follows immediately that:

$$\langle p\frac{\partial u_1}{\partial x_1}\rangle = -\left[\langle p\frac{\partial u_2}{\partial x_2}\rangle + \langle p\frac{\partial u_3}{\partial x_3}\rangle\right] \tag{4.39}$$

Thus equation 4.35 can be written as:

$$\begin{aligned}\left[\frac{\partial}{\partial t} + U_j\frac{\partial}{\partial x_j}\right]\frac{1}{2}\langle u_1^2\rangle \\ = - \left[\langle p\frac{\partial u_2}{\partial x_2}\rangle + \langle p\frac{\partial u_3}{\partial x_3}\rangle\right] \\ + \frac{\partial}{\partial x_j}\left\{-\frac{1}{\rho}\langle pu_1\rangle\delta_{1j} - \frac{1}{2}\langle u_1^2 u_j\rangle + 2\nu\langle s_{1j}u_1\rangle\right\} \\ - \langle u_1u_j\rangle\frac{\partial U_1}{\partial x_j} - 2\nu\langle s_{1j}s_{1j}\rangle \end{aligned} \tag{4.40}$$

Comparison of equation 4.40 with equations 4.36 and 4.37 makes it immediately apparent that *the pressure strain rate terms act to exchange energy between components of the turbulence.* If $\langle p\partial u_2/\partial x_2\rangle$ and $\langle p\partial u_3/\partial x_3\rangle$ are both positive, then energy is removed from the 1-equation and put into the 2- and 3-equations since the same terms occur with opposite sign. Or vice versa.

The role of the pressure strain rate terms can best be illustrated by looking at a simple example. Consider a simple homogeneous shear flow in which $U_i = U(x_2)\delta_{1i}$ and in which the turbulence is homogeneous. For this flow, the assumption of homogeneity insures that all terms involving gradients of average quantities vanish (except for dU_1/dx_2). This leaves only the pressure-strain rate, production and dissipation terms; therefore equations 4.36, 4.37 and 4.40 reduce to:

1-component:

$$\frac{\partial\langle u_1^2\rangle}{\partial t} = -\left[\langle p\frac{\partial u_2}{\partial x_2}\rangle + \langle p\frac{\partial u_3}{\partial x_3}\rangle\right] - \langle u_1 u_2\rangle\frac{\partial U_1}{\partial x_2} - \epsilon_1 \tag{4.41}$$

2-component:

$$\frac{\partial\langle u_2^2\rangle}{\partial t} = \qquad +\langle p\frac{\partial u_2}{\partial x_2}\rangle \qquad - \epsilon_2 \tag{4.42}$$

3-component:

$$\frac{\partial\langle u_3^2\rangle}{\partial t} = \qquad +\langle p\frac{\partial u_3}{\partial x_3}\rangle \qquad - \epsilon_3 \tag{4.43}$$

where

$$\epsilon_1 \equiv 2\nu\langle s_{1j}s_{1j}\rangle \tag{4.44}$$
$$\epsilon_2 \equiv 2\nu\langle s_{2j}s_{2j}\rangle \tag{4.45}$$
$$\epsilon_3 \equiv 2\nu\langle s_{3j}s_{3j}\rangle \tag{4.46}$$

It is immediately apparent that only $\langle u_1^2\rangle$ can directly receive energy from the mean flow because only the first equation has a non-zero production term.

Now let's further assume that the smallest scales of the turbulence can be *assumed* to be *locally isotropic*. While not always true, this is a pretty good approximation for high Reynolds number flows. (Note that it *might* be exactly true in many flows in the limit of infinite Reynolds number, at least away from walls.) Local isotropy implies that the component dissipation rates are equal; i.e., $\epsilon_1 = \epsilon_2 = \epsilon_3$. But where does the energy in the 2 and 3-components come from? Obviously the pressure-strain-rate terms must act to remove energy from the 1-component and redistribute it to the others.

As the preceding example makes clear, the role of the pressure-strain-rate terms is to attempt to distribute the energy *among* the various components of the turbulence. An easy way to remember this is to think of the pressure strain rate terms as the 'Robin Hood' terms: they steal from the rich and give to the poor. In the absence of other influences, they are so successful that the dissipation by each component is almost equal, at least at high turbulence Reynolds numbers. In fact, because of the energy re-distribution by the pressure strain rate terms, it is uncommon to find a turbulent shear flow away from boundaries where the kinetic energy of the turbulence components differ by more than 30-40%, no matter which component gets the energy from the mean flow.

Example: In simple turbulent free shear flows like wakes or jets where the energy is primarily produced in a single component (as in the example above), typically $\langle u_1^2 \rangle \approx \langle u_2^2 \rangle + \langle u_3^2 \rangle$ where $\langle u_1^2 \rangle$ is the kinetic of the component produced directly by the action of Reynolds stresses against the mean velocity gradient. Moreover, $\langle u_2^2 \rangle \approx \langle u_3^2 \rangle$. This, of course, makes some sense in light of the above, since both off-axis components get most of their energy from the pressure-strain rate terms.

It is possible to show that the pressure-strain rate terms vanish in isotropic turbulence. This suggests (at least to some) that the natural state for turbulence in the absence of other influences is the isotropic state. This has also been exploited by the turbulence modelers. One of the most common assumptions involves setting these pressure-strain rate terms (as they occur in the Reynolds shear equation) proportional to the anisotropy of the flow defined by:

$$a_{ij} = \langle u_i u_j \rangle - \langle q^2 \rangle \delta_{ij}/3 \tag{4.47}$$

Models accounting for this are said to include a"*return-to-isotropy*" term. An additional term must also be included to account for the direct effect of the mean shear on the pressure-strain rate correlation, and this is referred to as the "*rapid term*". The reasons for this latter term are not easy to see from single point equations, but fall out rather naturally from the two-point Reynolds stress equations we shall discuss later.

Chapter 5

A First Look at Homogeneous Turbulence:

5.1 Introduction

The main purpose of this chapter is to examine the single point equations developed in the preceding chapters as they apply to homogeneous turbulence. Since we really haven't defined yet what we mean by '*homogenous*' let's do that now. By *homogeneous* we mean the statistics of the turbulence are independent of the physical origin in space. In other words, no matter where we put the coordinate system, we get the same numbers. For single point statistical quantities, this means they must be constant in the homogeneous directions (however many there are). For example, in a homogeneous flow which is homogeneous in all directions, $\langle u_1^2 \rangle(\vec{x}) = \langle u_1^2 \rangle(\vec{x}')$ for all $\vec{x}$ and $\vec{x'}$, so we could just drop the $\vec{x}$-argument completely and call it $\langle u_1^2 \rangle$. An obvious consequence of this which we have already noted in previous chapters is that all spatial gradients of a homogeneous process must be zero. We shall see later that another important consequence of this is that we can approximate true ensemble averages by averages over homogeneous directions in space instead.

A closely related concept to the concept of homogeneity is that of stationarity. A stationary random process is one in which the statistics are independent of origin in time. And this of course means all single-time averages must be time independent; i.e., $\langle u(t) \rangle = U$, $\langle [\tilde{u}(t) - U]^2 \rangle = \langle u^2 \rangle$, etc. Many experiments are approximately stationary random processes, or at least we try to perform them that way. The reason we shall see later in Chapter 8 is that it greatly simplifies averaging by allowing us to time-average instead of performing the experiment many times to build up an ensemble over which to average at an instant. This works for stationary process since in principle the statistics are time-independent. We only need to insure that we have enough independent pieces of information, since the variable at one instant can still be correlated with that at another. This is because stationarity does not imply that two-time statistics like $\langle u(t)u(t') \rangle$ are time-independent, only that they are independent of origin in time. Hence

they could be a function of the time difference $t' - t$. Analogously, homogeneous statistics involving two locations (e..g. two-point statistics like $\langle u(\vec{x})u(\vec{x}')\rangle$ can depend on the separation vector $\vec{x}' - \vec{x}$. We will have much more to say about this in later chapters, since two-point statistics are the key to understanding the different scales of turbulence motions and how they interact.

Homogeneous turbulence is an important subject in its own right but can only be properly discussed with much more powerful statistical tools than we have discussed so far. These will receive considerable attention later. Nonetheless it important to discuss homogeneous turbulencet here briefly since so many of the ideas commonly believed about turbulence come from our study of it. And another reason is that in fact you should be impressed by how little we actually know for sure about it. Most books and discussions on this subject present all of this 'believed' stuff as fact. Hopefully you will not only be convinced that little is really 'fact', but that there are plenty of opportunities for you to contribute to this field.[1] If nothing else, it should be obvious after reading this chapter that most of the simple turbulence models should not be expected to work too well, since they really can't predict much of the observed behavior, at least not without assuming the answer at the outset. And of course, this begs the bigger question: if the models don't work too well for simple homogeneous flows, can they ever be trusted for more complicated ones? The answer is: perhaps (in the absence of any alternatives) they are useful as engineering tools, but they certainly do not represent a scientific understanding of the observed phenomena.

5.2 Why are homogeneous flows important?

We have been able to gain considerable insight into how turbulent flows behave by considering in the preceding chapters the single point energy and Reynolds stress equations. For example, we now know how to recognize the difference between the unsteady (or non-stationary) contribution to the derivative following the mean motion and that due to convection through an inhomogeneous field by the mean flow (section 4.1. Obviously if the field is stationary or homogeneous, one or the other of these terms vanishes. We also learned that the so-called transport terms just move energy around, and that they vanish in homogeneous flows (section 4.4). Then we saw that there are some terms which can remain, even if the flow is homogeneous (e.g., sections 4.2 and 4.3).

We, in fact, already used a simple unsteady homogeneous example to illustrate how the turbulence obtains energy from the mean flow via the Reynolds stress working against the mean flow gradient (section 4.5). And we used the same exam-

[1] I remember my own experience as a student learning turbulence for the first time lamenting that there was nothing about this beautiful subject left for me to do, everything was known. So I turned my attention to free shear flows in the hopes I would find some small thing I could contribute. Imagine my surprise years later when I discovered the truth! I vowed that I would never leave students thiniking this way, at least until I was positive something was true.

ple to illustrate how the pressure strain-rate terms describe the process by which all the components are supplied with energy, even if all the energy is produced in only one of them. Finally, we saw saw that the energy is dissipated primarily by the turbulence at the very smallest scales of motion, which themselves have the least energy but are often nearly *locally homogeneous* (section 4.2).

Clearly homogeneous flows must be of considerable interest since they allow us to examine the behavior of the terms which do not vanish without additional complications of those which do. Unfortunately, like many of the flows we consider in this course, homogeneous turbulence is an ideal state which can at best be approximated in a wind tunnel or in the computer. Nonetheless it is still of considerable interest — to the engineer and the physicist, to the turbulence modeler and to the theoretician. It is of interest to engineers and turbulence modelers since it offers a simple way to test whether some terms have been modeled correctly without the complications of the others, or more importantly, without the complications of boundary conditions. But, by contrast, such flows are of interest to physicists and mathematicians because they appear to be anomalous, meaning the results do not seem to be completely consistent with our ideas about how they should behave.

These anomalies of homogeneous turbulence present a dilemma for the modelers and engineers: if they are truly anomalous, should they even try to account for the results at all with their models? Many think not, and many in fact do not. Even the ones who believe the results of homogeneous flows are important to modeling are very selective about which experimental results they use, and assume all the other experiments to be wrong or simply ignore the ones they don't like. But this creates a problem for those actually trying to find the truth, since new findings and insights can be treated quite harshly because these new ideas can be quite threatening to those who have invested so much time building models based the old ones.

These anomalies of homogeneous flows also present a real dilemma for the physicists and mathematicians. Anomalies in science sometimes mean there is something big is about to be discovered. One possibility is that we have been doing something very wrong in our experiments and computations, and we hopefully are about to learn what. Or even more exciting, there may be something very wrong with our ideas, and we might be about to have some new ones which may completely change our understanding of how the world is.

The best example of the latter possibility is illustrated by the general assessment of physics near the end of the 19th century. Scientists then thought they had learned all the fundamental ideas of physics, with nothing important left to be done but engineering applications of well-established principles. All that was left, some said, was to account for two anomalous experiments — the Rayleigh-Jeans experiment[2] and the Mickelson-Morley experiment[3] — and many thought

[2]The Rayleigh-Jeans experiment measured thermal radiation from a black box

[3]The Mickelson-Morley experiment measured the speed of light and showed it to be apparently independent of the speed of the source.

these experiments to be in error. The resolution of these two anomalies gave us quantum mechanics and relativity, both of which completely changed our picture of the world around us and had dramatic influences on engineering and life on this planet.

Will such be the case with our view of turbulence when we resolve the remaining dilemmas of homogeneous flows in turbulence? Or will we simply find out that most of the conflicting experiments have been wrong. The search for answers will be exhilarating for some, and frustrating for others, but necessary for all — especially for those like you entering the field now. If we find the answers, they may completely change how we do things, like quantum mechanics or relativity did. Or we may find they have little effect at all and our old way of doing things is the best we can do. A good example of this was the recognition by Copernicus that the earth was not the center of the universe. The new world view completely changed the way we think about the universe, but had no effect on navigation. Sailors still find their way across great oceans using the principles of Ptolemaic navigation which is based on the idea that the earth is at the center.[4]

My personal suspicion is that things will be changed a lot as our understanding of these anomalies grows, simply because our present turbulence models really don't extrapolate too well to new problems. Unlike the example of Ptolemaic navigation which works perfectly well on the surface of the earth, our turbulence models are really very reliable, especially at predicting new things we haven't built into them. This probably means we still have much to learn about turbulence, and as we learn our ideas will change and our models improve. So we might as well begin this learning process with the problem which is *at least in principle* the easiest: homogeneous turbulent flows.

5.3 Decaying turbulence: a brief overview

Look, for example, at the decay of turbulence which has already been generated. If this turbulence is homogeneous and there is no mean velocity gradient to generate new turbulence, the kinetic energy equation reduces to simply:

$$\frac{d}{dt}k = -\epsilon \tag{5.1}$$

Note that the time derivative is just an ordinary derivative, since there is no dependence of any single point quantity on position. This is often written (especially for isotropic turbulence) as:

$$\frac{d}{dt}\left[\frac{3}{2}u^2\right] = -\epsilon \tag{5.2}$$

where

$$k \equiv \frac{3}{2}u^2 \tag{5.3}$$

[4]I can personally testify that this works, since I arrived in Kinsale, Ireland after an arduous voyage across the Atlantic from America in my 42 foot sailboat *Wings* by exactly this method.

Now you can't get any simpler than this. Yet unbelievably we still don't have enough information to solve it. Let's try. Suppose we use the extended ideas of Kolmogorov we introduced in Chapter 4 to relate the dissipation to the turbulence energy, say:

$$\epsilon = f(Re)\frac{u^3}{l} \tag{5.4}$$

Already you can see we have two problems, what is $f(Re)$, and what is the time dependence of l? Now there is practically a different answer to these questions for every investigator in turbulence — most of whom will assure you their choice is the only reasonable one.

Figure 5.1 shows two attempts to correlate some of the grid turbulence data using the longitudinal integral scale for l, i.e., $l = L_{11}^{(1)}$, or simply L. The first thing you notice is the problem at low Reynolds number. The second is probably the possible asymptote at the higher Reynolds numbers. And the third is probably the scatter in the data, which is characteristic of most turbulence experiments, especially if you try to compare the results of one experiment to the other.

Let's try to use the apparent asymptote at high Reynolds number to our advantage by arguing that $f(Re) \to A$, where A is a constant. Note that this limit is consistent with the Kolmogorov argument we made back when we were talking about the dissipation earlier, so we might feel on pretty firm ground here, at least at high turbulent Reynolds numbers. But before we feel too comfortable about this, we should note that a careful examination of the data suggests that the asymptote depends on the details of how the experiment was forced at the large scales of motion (e.g. which grid was used, etc.) . This is not good, since if true it means that the answer depends on the particular flow — exactly what we wanted to avoid by modelling in the first place.

Nonetheless, let's proceed by *assuming* in spite of the evidence that $A \approx 1$ and L is the integral scale. Now how does L vary with time? Figure 5.2 shows the ratio of the integral scale to the Taylor microscale from the famous Comte-Bellot/Corrsin (1971) experiment. One might assume, with some theoretical justification, that $L/\lambda \to const.$ This would be nice since you will be able to show that if the turbulence decays as a power law in time, say $u^2 \sim t^n$, then $\lambda \sim t^{1/2}$. But as shown in Figure 5.3 from Wang et al (2000), this is not a very good assumption for the DNS data available at that time. Now I believe this is because of problems in the simulations, mostly having to do with the fact that turbulence in a box is not a very good approximation for truly homogeneous turbulence unless the size of the box is much larger than the energetic scales. Figure 5.4 shows what happens if you try to correct for the finite box size, and now the results look pretty good.

You can see immediately that if I am right and $L \sim \lambda \sim t^{1/2}$ then $u^2 \sim t^{-1}$. Now any careful study of the data will convince you that the energy indeed decays as a power law in time, but there is no question that $n \neq -1$, but $n < -1$, at least for most of the experiments. Most people have tried to fix this problem changing p. But I say the problem is in $f(Re)$ and the assumption that $\epsilon \sim u^3/L$

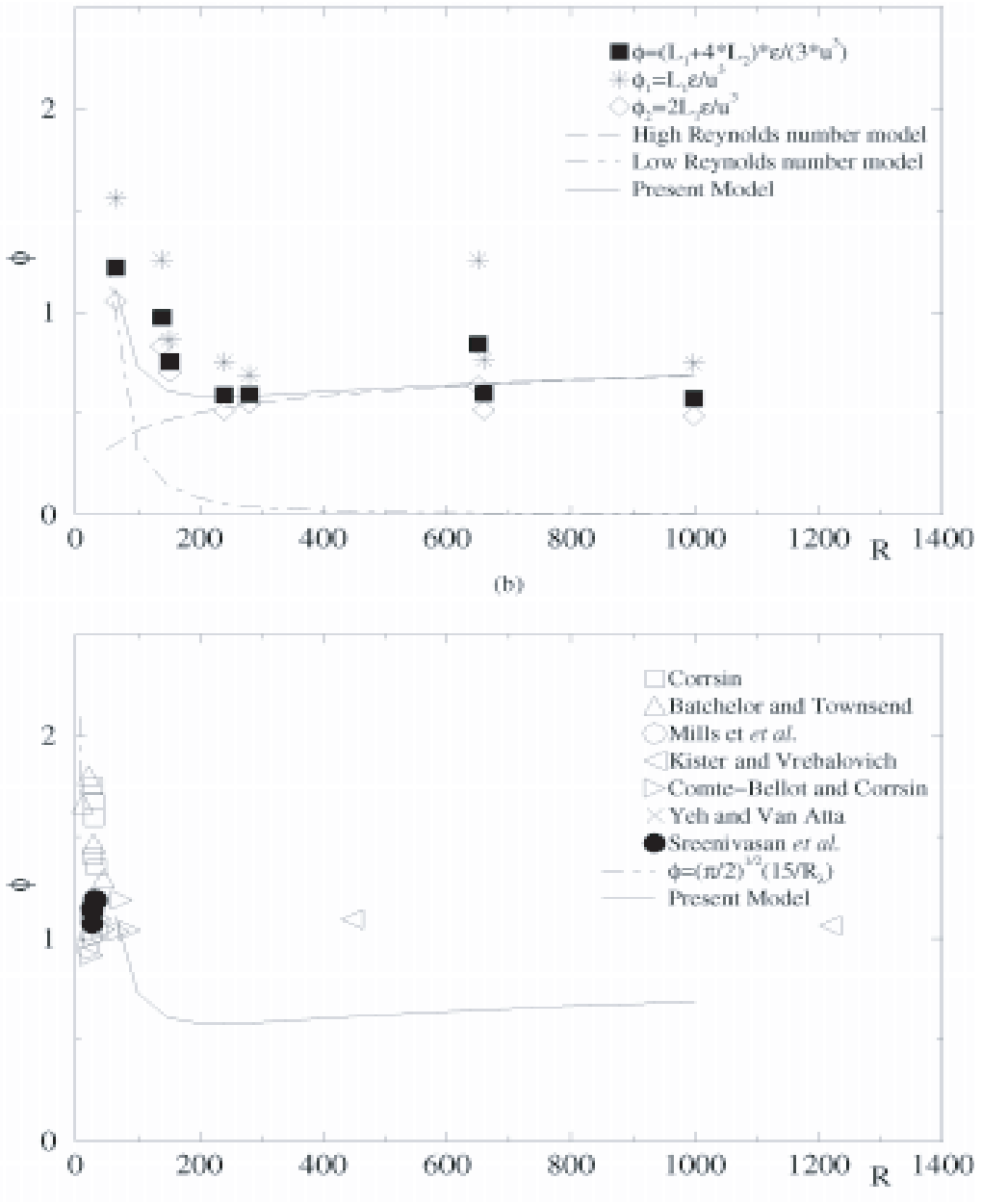

Figure 5.1: Collection of experimental data showing relation of the longitudianl integral scale, $L^{1)}_{1,1}$, to $l = u^3/\epsilon$; i.e., $\phi = L^{(1)}_{1,1}/l = L^{(1)}_{1,1}\epsilon/u^3$ (from Gamard and George 2000).

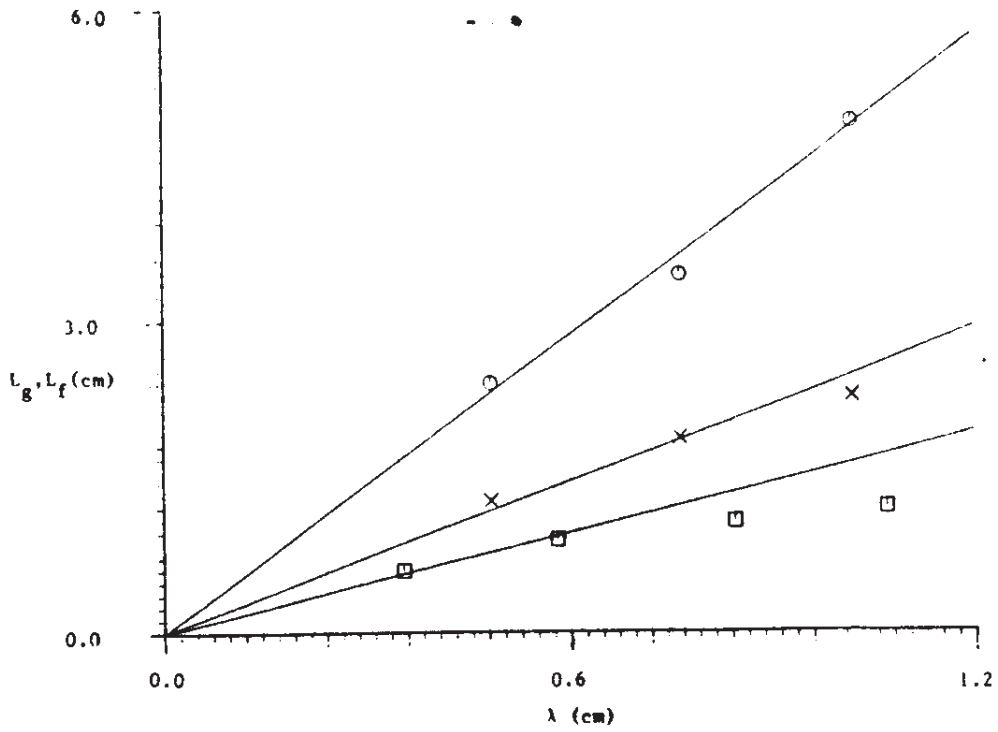

Figure 5.2: Plots of longitudinal integral scale ($L^{(1)}_{1,1} = L_f$) and lateral integral scale ($L^{(1)}_{2,2} = L_g$) to the Taylor microscale, λ_g (data of Comte-Bellot and Corrsin 1971).

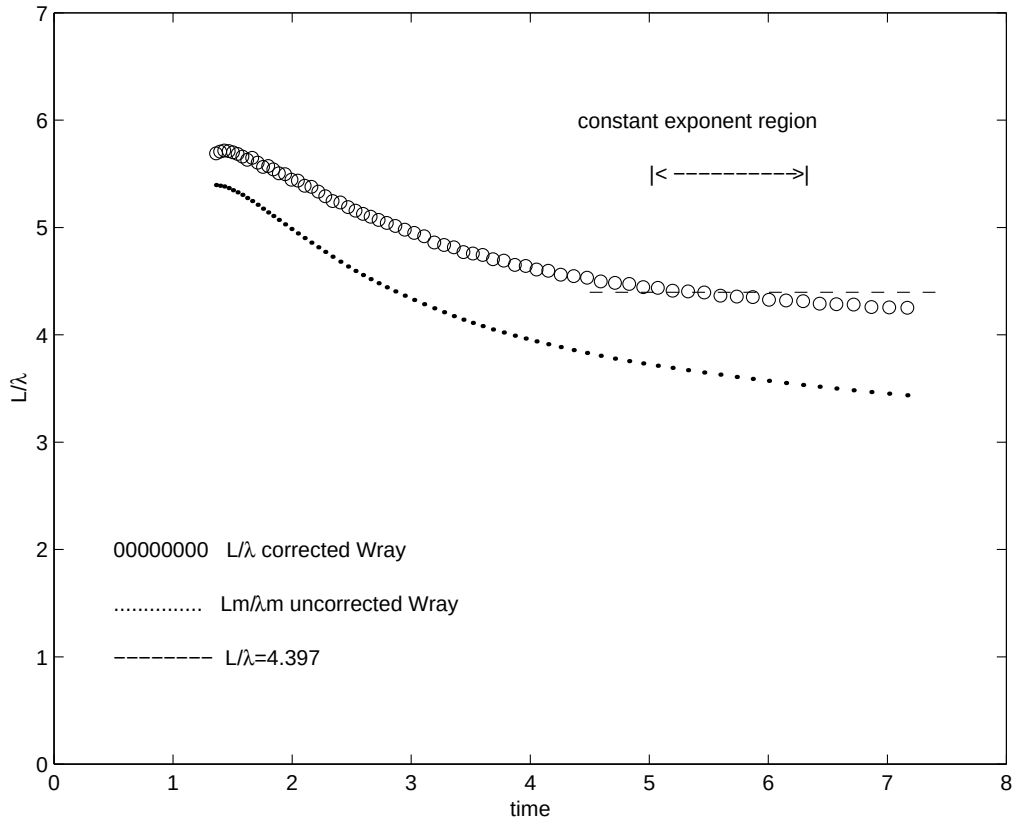

Figure 5.3: Ratio of longitudinal integral scale to the Taylor microscale, λ_g from recent DNS of isotropic decaying turbulence by Wray (1998), from Wang and George 2003). Note how different the results are when the large scales missing due to the finite computational box are accounted for.

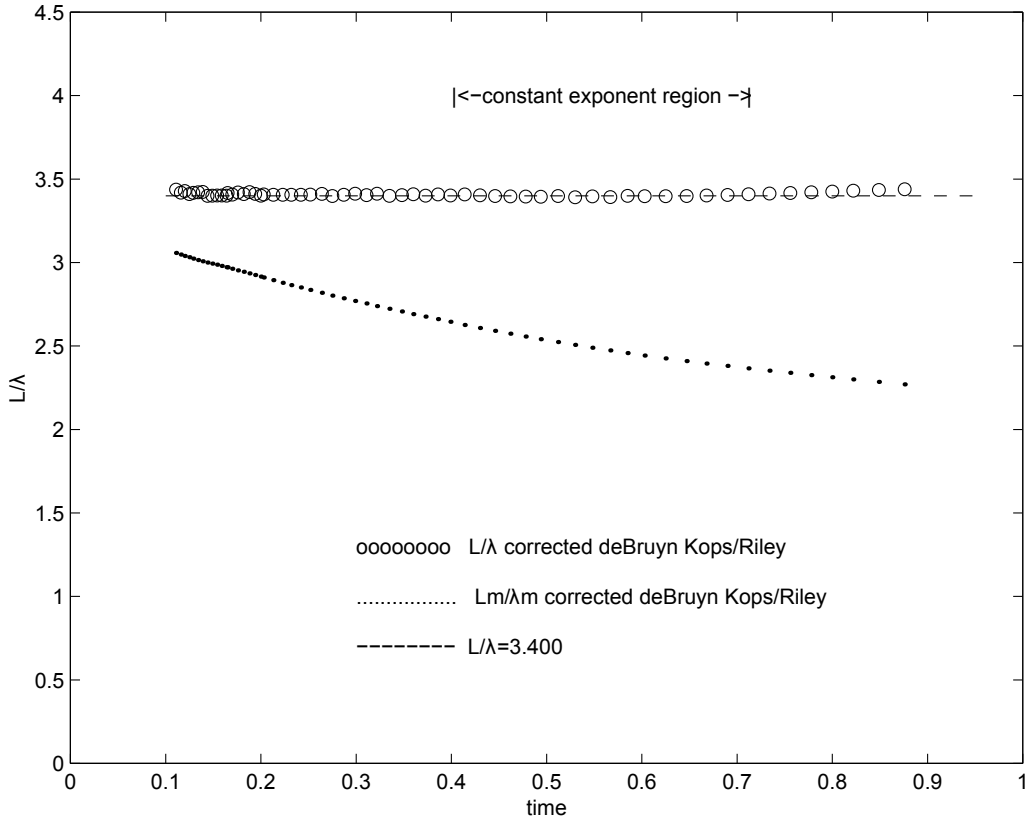

Figure 5.4: Ratio of longitudinal integral scale to the Taylor microscale, λ_g from recent DNS of isotropic decaying turbulence by DeBruyn Kops and Riley (1999), from Wang and George 2003). Note how different the results are when the large scales missing due to the finite computational box are accounted for.

at *finite* Reynolds numbers. I would argue that $n \to -1$ only in the limit of infinite Reynolds number.

To see why I believe this, try doing the problem another way. We will show in a later chapter that *if* the turbulence decays as a power law, *then* the Taylor microscale, λ_g, must be proportional exactly to $t^{1/2}$. Thus we must have (assuming isotropy):

$$\frac{dk}{dt} = -10\nu\frac{k}{\lambda_g^2} \propto \frac{k}{t} \tag{5.5}$$

It is easy to show that $k \propto t^n$ where n is given by:

$$\frac{d\lambda_g^2}{dt} = -\frac{10}{n} \tag{5.6}$$

and any value of $n \leq -1$ is acceptable. Obviously the difference lies in the use of the relation $\epsilon \propto u^3/L$ at finite Reynolds numbers.

Figure 5.5 shows data taken downstream of a grid by Genevieve Comte-Bellot and Stanley Corrsin in one of the most famous turbulence experiments ever. The experiments were carried out at the Johns Hopkins University while I was a student there, and I can still remember the huge hand-drawn graphs spread out over the long coffee table. Genevieve was using them to determine whether data satisfied a power law decay, which in the days before modern computer graphics was the way you had to do things. You can judge from yourself from the figure, but clearly a power law of $n = -1.28$ works pretty well.

Believe it or not, this whole subject is one of the really hot debates of the last decade, and may well be for the next as well. The reason, at least in part, is that the value of the decay exponent, n, seems to a function of how the flow started (e.g., which grid, what Reynolds number, etc.). Until quite recently actually (George 1992 Phys. Fluids was the turning point) people believed (hoped is perhaps a more accurate description) that such turbulence had universal decay characteristics. There is pretty convincing evidence that it does not. As figure **??** makes clear, there is even convincing evidence from recent experiments at Imperial College of London by Christos Vassilicos and his co-workers that some kinds of grids (a particular class of fractal grids) like the one shown in figure **??** don't decay as power-laws at all, but in fact decay exponentially. If you examine the equations above, you can see that this can happen only if the Taylor microscale remains constant during decay, so that the time derivative of the kinetic energy is proportional to the kinetic energy. Figure **??** show that this is exactly what happens.

Interestingly, as shown in George 1992 (Physics of Fluids) and George and Wang (2009), both kinds of decay, power-law and exponential, are consistent with an equilibrium similarity analysis of the spectral energy equations. And the theory even predicts the observed dependence on initial (or upstream) conditions. But while this shows that what we observe is consistent with the equations and how the turbulence generally evolves, we really don't have clue yet why it behaves one

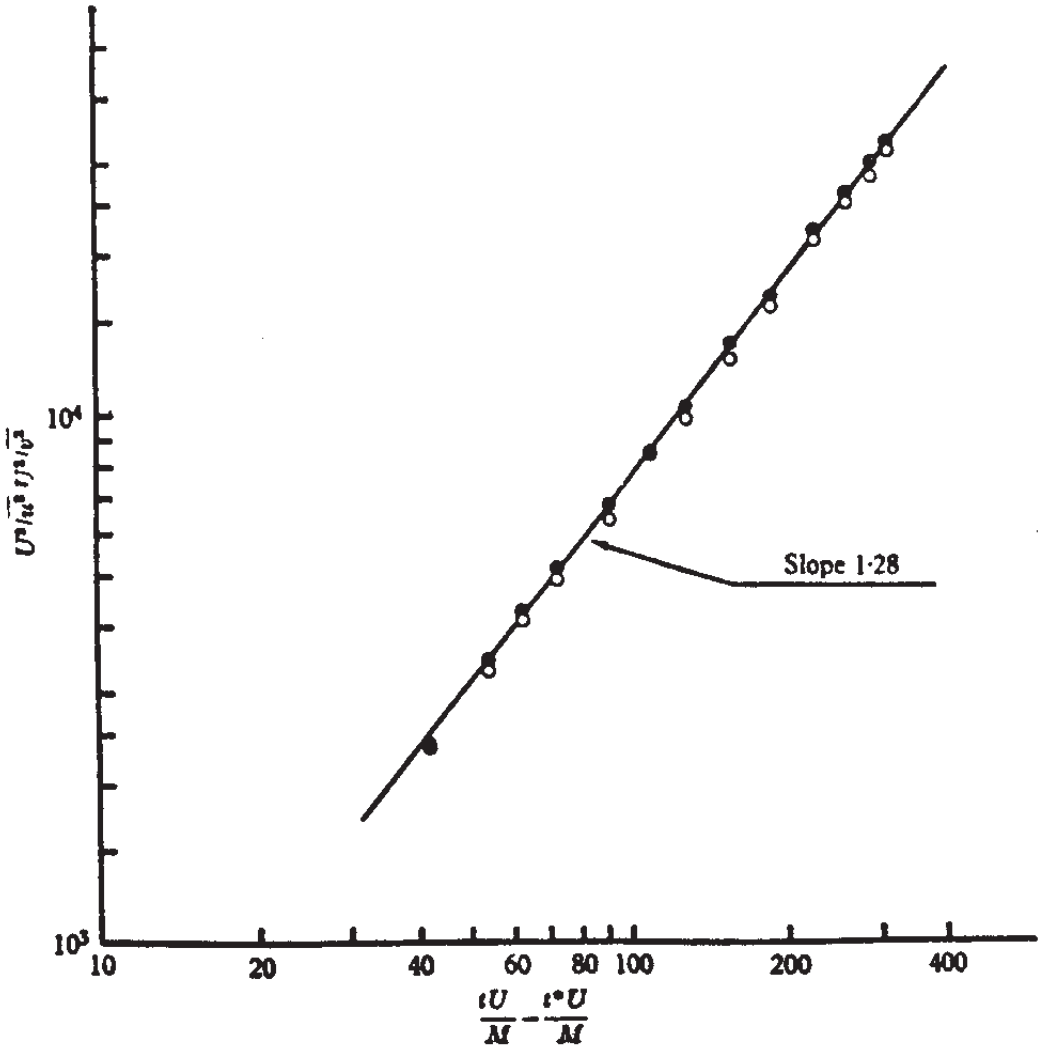

Figure 5.5: Turbulence intensity decay downstream of a square-rod grid with $M = 25.4mm$ and $U = 20m/s$ The open circles represent the mean square streamwise fluctuations and the plus signs the cross-stream (from Comte-Bellot and Corrsin 1971).

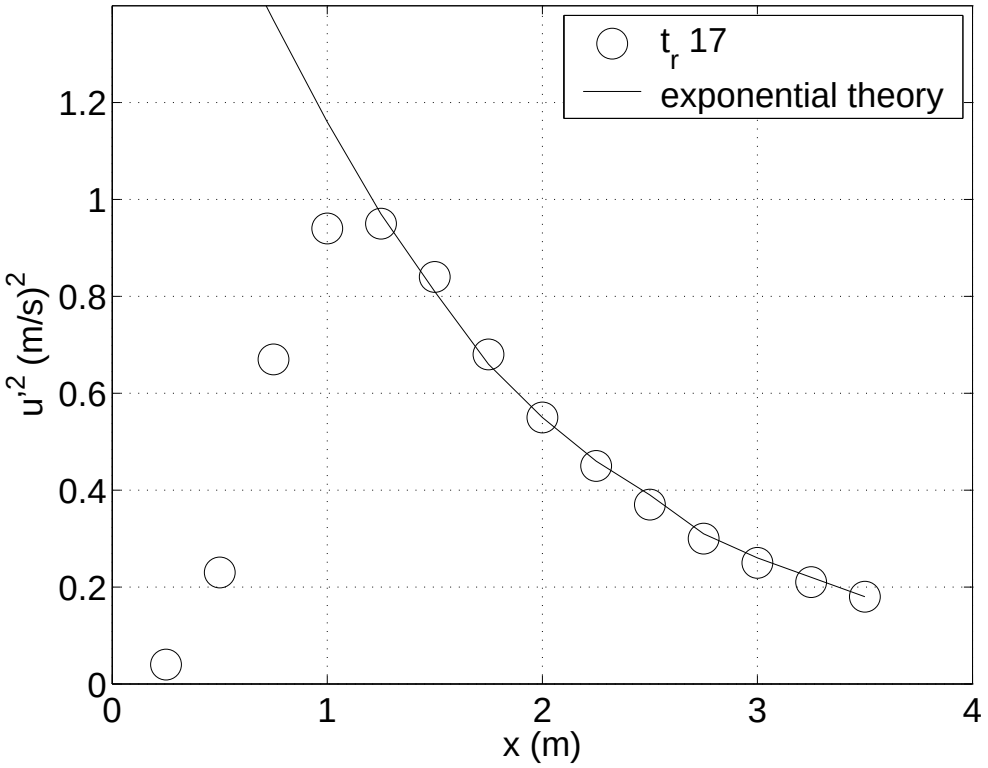

Figure 5.6: Variation of turbulence intensity with downstream position for one space-filling fractal grid. Solid line shows exponential fit (from Hurst and Vassilicos (2007)).

way or the other. Who knows, maybe some of you will be involved in resolving it, since it really is one of the most fundamental questions in turbulence.

5.4 A second look at simple shear flow turbulence

Let's consider another homogeneous flow that seems pretty simple at first sight, homogeneous shear flow turbulence with constant mean shear. We already considered this flow when we were talking about the role of the pressure-strain rate terms. Now we will only worry, for the moment, about the kinetic energy which reduces to:

$$\frac{\partial}{\partial t}\left[\frac{1}{2}k\right] = -\langle uv\rangle\frac{dU}{dy} - \epsilon \tag{5.7}$$

Now turbulence modelers (and most experimentalists as well) would love for the left-hand side to be exactly zero so that the production and dissipation exactly balance. Unfortunately Mother Nature, to this point at least, has not allowed such a flow to be generated. In every experiment to-date after some initial adjustments, the energy increases with time (or equivalently, increases with increasing

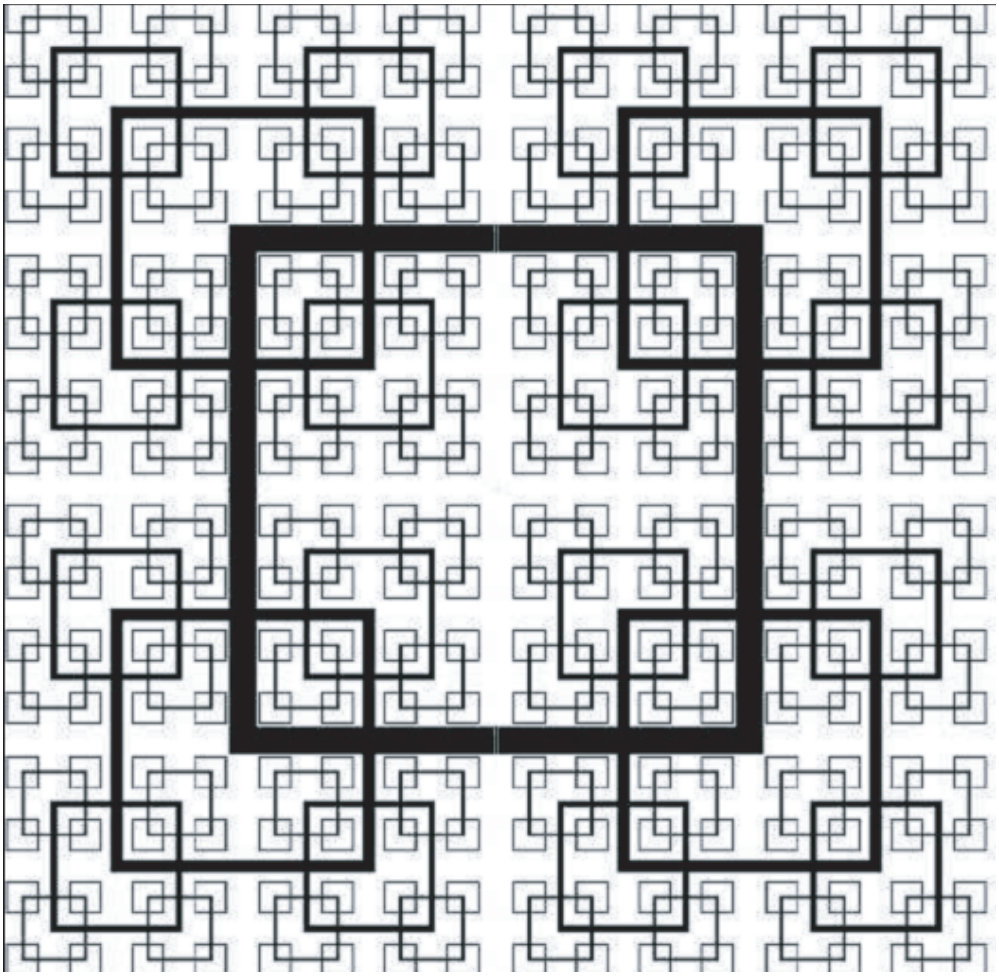

Figure 5.7: Diagram of space-filling square fractal grid, from figure 33 of Hurst and Vassilicos (2007).

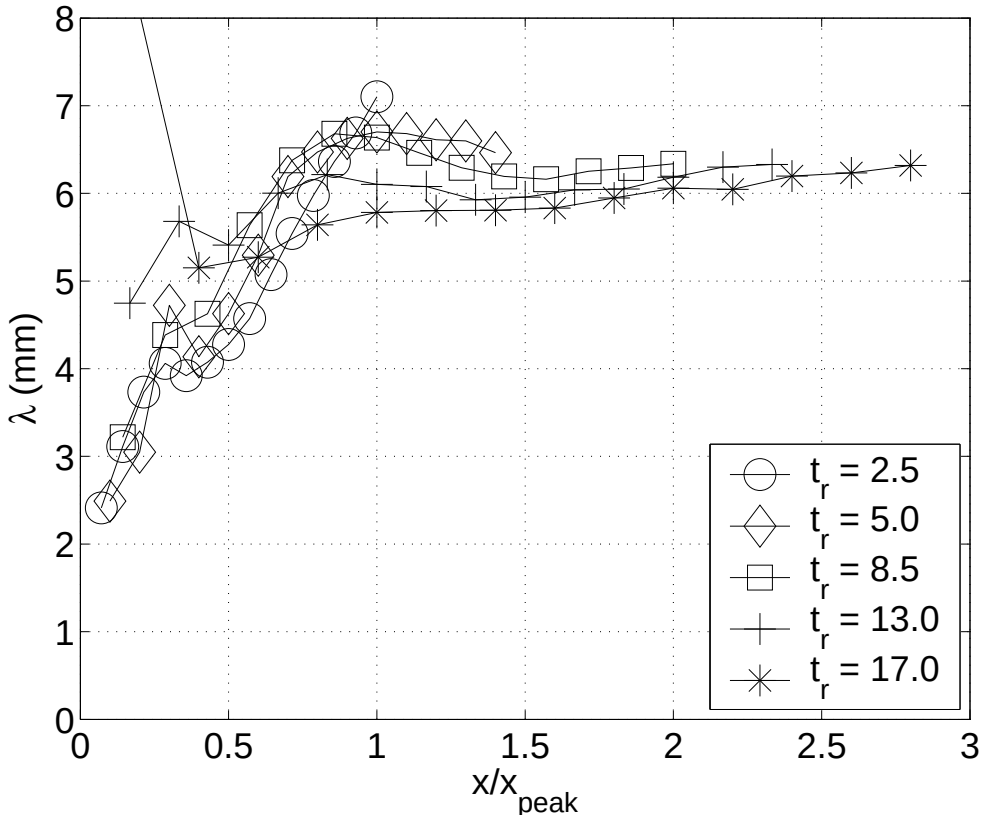

Figure 5.8: Downstream variation of Taylor microscale, λ, for different fractal grids showing approach to constant level as flow evolves downstream (from Hurst and Vassilicos (2007).)

downsteam distance as the turbulence is convected down the tunnel).

Let's make a few simple assumptions and see if we can figure out what is going on. Suppose we *assume* that the correlation coefficient $\langle uv\rangle/u^2 = C$ is a constant. Now, we could again *assume* that $\epsilon \sim u^3/l$, at least in the very high Reynolds number limit. But for reasons that will be obvious below, let's assume something else we know for sure about the dissipation; namely that:

$$\epsilon = D\frac{u^2}{\lambda^2} \tag{5.8}$$

where λ is the Taylor microscale and $D \approx 15$ (exact for isotropic turbulence). Finally let's assume that the mean shear is constant so $dU/dy = K$ is constant also. Then our problem simplifies to:

$$\frac{d}{dt}\frac{3}{2}u^2 = -KCu^2 - D\frac{u^2}{\lambda^2} \tag{5.9}$$

Even with all these simplifications and assumptions the problem still comes down to "What is $\lambda = \lambda(t)$?". Now the one thing that all the experiments agree on is that $\lambda = \lambda_o$ is approximately constant. (I actually have a theory about this, together with M. Gibson, and it even *predicts* this result, George and Gibson 1992 Experiments in Fluids) Now you have all you need to finish the problem, and I will leave it for you. But when you do you will find that the turbulence grows (or decays) exponentially. How fast it grows (or decays) depends on the ratio of the production to dissipation; i.e.,

$$\frac{P}{\epsilon} \equiv \frac{-\langle uv\rangle dU/dy}{\epsilon} \tag{5.10}$$

It is clear from the experiments that P/ϵ depends on the upstream or initial conditions, as the theory suggests it should. But it is not at all clear how. One possibiliy is that the higher Reynolds number characterising these initial conditions, the closer P/ϵ is to unity. If so, then you will only get $P/\epsilon \to 1$ as an infinite Reynolds number limit. Which in turn implies you can never really achieve the ideal flow many people would like where the production and dissipation exactly balance. But here we are again, with lots of questions and no definitive highl Reynolds number experiments to guide us, nor little hope for help from the low Reynolds number numerical simulations. So here is one more set of questions to add to the list of things about turbulence we would like to know and to which you might contribute.

Chapter 6

Turbulent Free Shear Flows

6.1 Introduction

Free shear flows are inhomogeneous flows with mean velocity gradients that develop in the absence of boundaries. As illustrated in Figures 6.1 and 6.2, turbulent free shear flows are commonly found in natural and in engineering environments. The jet of air issuing from one's nostrils or mouth upon exhaling, the turbulent plume from a smoldering cigarette, and the buoyant jet issuing from an erupting volcano — all illustrate both the omnipresence of free turbulent shear flows and the range of scales of such flows in the natural environment. Examples of the multitude of engineering free shear flows are the wakes behind moving bodies and the exhausts from jet engines. Most combustion processes and many mixing processes involve turbulent free shear flows.

Free shear flows in the real world are most often turbulent. Even if generated as laminar flows, they tend to become turbulent much more rapidly than the wall-bounded flows which we will discuss later. This is because the three-dimensional vorticity necessary for the transition to turbulence can develop much more rapidly in the absence of walls that inhibit the growth velocity components normal to them.

The tendency of free shear flows to become and remain turbulent can be greatly modified by the presence of density gradients in the flow, especially if gravitational effects are also important. Why this is the case can easily be seen by examining the vorticity equation for such flows in the absence of viscosity,

$$\left[\frac{\partial \omega_i}{\partial t} + \tilde{u}_j \frac{\partial \tilde{\omega}_i}{\partial x_j}\right] = \tilde{\omega_j} \frac{\partial \tilde{u_i}}{\partial x_j} + \epsilon_{ijk} \frac{\partial \tilde{\rho}}{\partial x_j} \frac{\partial \tilde{p}}{\partial x_k} \tag{6.1}$$

The cross-product of the density and pressure gradients of last term vanishes identically in constant density flows or barotropic[1] flows, but can act quite dramatically to either increase or decrease vorticity production. For example, in the

[1] A barotropic flow is one in which the gradients of density and pressure are co-linear, because the density is a function of the pressure only.

Figure 6.1: Left: Exhaust from smokestack. Right: Exhaust from rocket engine

vertically-oriented buoyant plume generated by exhausting a lighter fluid into a heavier one, the principal density gradient is across the flow and thus perpendicular to the gravitational force which is the principal contributor to the pressure gradient. As a consequence the turbulent buoyant plume develops much more quickly than its uniform density counterpart, the jet. On the other hand, horizontal vorticity (vertical motions) in a horizontal free shear flows in a stably stratified environment (fluid density decreases with height) can be quickly suppressed since the density and pressure gradients are in opposite directions.

Free turbulent shear flows are distinctly different from the homogeneous shear flows. In a free turbulent shear flow, the vortical fluid is spatially confined and is separated from the surrounding fluid by an interface, the turbulent-nonturbulent interface (also known as the "Corrsin superlayer" after itself discoverer). The turbulent/non-turbulent interface has a thickness which is characterized by the Kolmogorov microscale, thus its characterization as an interface is appropriate. The actual shape of the interface is random and it is severely distorted by the energetic turbulent processes which take place below it, with the result that at any given location the turbulence can be highly *intermittent*. This means that at a given location, it is sometimes turbulent, sometimes not.

It should not be inferred from the above that the non-turbulent fluid outside

Figure 6.2: Left: Steam engine. Right: Red Arrow Jets.

the superlayer is quiescent. Quite the opposite is true since the motion of the fluid at the interface produces motions in the surrounding stream just as would the motions of a solid wall. Alternately, the flow outside the interface can be viewed as being "induced" by the vortical motions beneath it. It is easy to show that these induced motions are irrotational. Thus since these random motions of the outer flow have no vorticity, they can not be considered turbulent.

Figure 6.3 shows records of the velocity versus time at two locations in the mixing layer of a round jet. When turbulent fluid passes the probes, the velocity signals are characterized by bursts of activity. The smooth undulations between the bursts in the lower figure are the irrotational fluctuations induced by the turbulent vorticity on the other side of the interface. Note that near the center of the mixing layer where the shear is a maximum, the flow is nearly always turbulent, while it becomes increasingly intermittent as one proceeds away from the region of maximum production of turbulence energy. This increasing intermittency toward the outer edge is a characteristic of all free shear flows, and is an indication of the fact that the turbulent/non-turbulent interface is constantly changing its position.

One of the most important features of free shear flows is that the amount of fluid which is turbulent is continuously increased by a process known as *entrainment*. No matter how little fluid is in the flow initially, the turbulent part of the flow will continue to capture new fluid by entrainment as it evolves. The photograph of an air jet in Figure 1.2 illustrates this phenomenon dramatically. The mass flow of the jet increases at each cross-section due to entrainment. Entrainment is not unique to turbulent flows, but is also an important characteristic of laminar flow, even though the actual mechanism of entrainment is quite different.

There are several consequences of entrainment. The first and most obvious is that free shear flows continue to spread throughout their lifetime. (That this is the case is obvious from the pictures of Figures 6.1 and 6.2. A second consequence of entrainment is that the fluid in the flow is being continuously diluted by the addition of fluid from outside it. This is the basis of many mixing processes, and without such entrainment our lives would be quite different. A third consequence

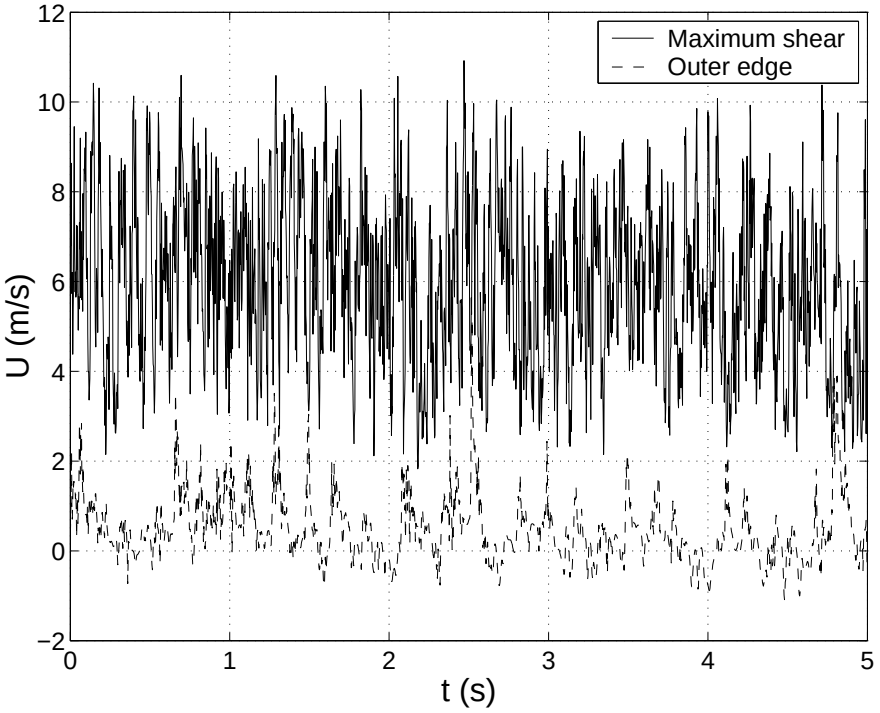

Figure 6.3: Velocity versus time, axisymmetric jet.

is that it will never be possible to neglect the turbulent transport terms in the dynamical equations, at least in the directions in which the flow is spreading. This is because the dilution process has ensured that the flow can never reach homogeneity since it will continue to entrain and spread through its lifetime (Recall that the transport terms were identically zero in homogeneous flows). Thus in dealing with free shear flows, all of the types of terms encountered in the turbulence kinetic energy equation of Chapter **??** must be dealt with — advection, dissipation, production, and turbulent transport.

Turbulent free shear flows have another distinctive feature in that they very often give rise to easily recognizable large scale structures or eddies. Figures 1.2 and 1.3 also illustrate this phenomenon, and coherent patterns of a scale equal to the lateral extent of the flow are clearly visible. The same features are are more difficult to see at higher Reynolds numbers because of the increasing energy of the smaller scales, but none-the-less they can still be discerned in the high Reynolds number jet of Figure 6.4. These large eddies appear to control the shape of the turbulent/non-turbulent interface and play an important role in the entrainment process. They stretch the small scale vorticity on the interface (the so-called Corrsin superlayer) so these are amplified, with the result that the vorticity diffuses rapidly into the non-turbulent fluid which has been engulfed by the large eddies. These large eddies are also important for the processes by which the turbulence gains and distributes energy from the mean flow.

A feature which free shear flows have in common with the homogeneous flows

Figure 6.4: Smoke visualization of jet mixing layer at Reynolds number of 65,000.

discussed in Chapter 5 is that their scales continue to grow as long as the flow remains turbulent. The dynamical equations and boundary conditions for many free shear flows can be shown to admit to similarity solutions in which the number of independent variables is reduced by one. According to the equilibrium similarity principle set forth in this chapter, such flows might be expected to asymptotically achieve such a state; and this, in fact, occurs. In the limit of infinite Reynolds number, some such flows can even be characterized by a single time and length scale, thus satisfying the conditions under which the simplest closure models might be expected to work. Care must be taken not to infer too much from the ability of a given closure model to predict such a flow, since any model which has the proper scale relations should work.

Finally there is the important question of whether free shear flows become asymptotically independent of their initial conditions (or source conditions). The conventional wisdom until very recently (and that presented in all texts prior to this one) has been that they do. If correct, this means that there is nothing that could be done to alter the far downstream flow. As we shall see later in this chapter, there is considerable theoretical and experimental evidence, however, that this traditional view is wrong. This opens up previously unimagined possibilities for flow control at the source.

In the remainder of this chapter, the averaged equations of motion will be simplified, and similarity solutions for several ideal shear flows will be derived and discussed in detail. The role of the large eddies will be discussed, and mechanisms for turbulent entrainment will be examined. The energy balance of several turbulent free shear flows will be studied in some detail. Finally, the effects of confinement and non-homogeneous external boundary conditions will be considered.

6.2 The averaged equations

6.2.1 The shear layer quations

One of the most important ideas in the history of fluid mechanics is that of the *boundary layer approximation.* These approximations to the Navier-Stokes equations were originally proposed by Prandtl in his famous theory for wall boundary

layers. By introducing a different length scale for changes perpendicular to the wall than for changes in the flow direction, he was able to explain how viscous stresses could survive near the wall at high Reynolds number. These allowed the no-slip condition at a surface to be satisfied, and resolved the paradox of how there could be drag in the limit of zero viscosity.

It may seem strange to be talking about Prandtl's boundary layer idea in a section about free shear flows, but as we shall see below, the basic approximations can be applied to all "thin" (or slowly growing) shear flows with or without a surface. In this section, we shall show that free shear flows, for the most part, satisfy the conditions for these "boundary layer approximations". Hence they belong to the general class of flows referred as "boundary layer flows".

One important difference will lie in whether momentum is being added to the flow at the source (as in jets) or taken out (by drag, as in wakes). A related influence is the presence (or absence) of a free stream in which our free shear flow is imbedded. We shall see that stationary free shear flows fall into two general classes, those with external flow and those without. One easy way to see why this makes a difference is to remember that these flows all spread by sharing their momentum with the surrounding flow, or by stealing momentum from it, almost always entraining mass from the surrounding fluid at the same time. (You don't have to think very hard to see that as mass is entrained, it is carries its own momentum with it into the shear flow.) You should expect (and find) that even a small free stream velocity (or pressure gradient or even free stream turbulence) can make a significant difference, since the momentum carried in is mixed in with that of the fluid particles which are already part of the turbulence. The longer the flow develops (or the farther downstream one looks), the more these simple differences can make a difference in how the flow spreads. In view of this, it should be no surprise that the presence or absence of an external stream plays a major role in determining which mean convection terms which must be retained in the governing equations. And also in determining whether an experiment or simulation is a valid approximation to a flow in an infinite environment, since both most be performed in a finite box or windtunnel.

We will consider here only flows which are plane (or two-dimensional) in the mean (although similar considerations can be applied to flows that are axisymmetric in the mean, see the exercises). In effect, this is exactly the same as assuming the flow is homogeneous in the third direction. Also we shall restrict our attention to flows which are statistically stationary, so that time derivatives of averaged quantities can be neglected. And, of course, we have already agreed to confine our attention to Newtonian flows at constant density.

It will be easier to abandon tensor notation for the moment, and use the symbols x, U, u for the streamwise direction, mean and fluctuating velocities respectively, and y, V, v for the cross-stream. Given all this, the mean momentum equations reduce to:

x-component:

$$U\frac{\partial U}{\partial x}+V\frac{\partial U}{\partial y}=-\frac{1}{\rho}\frac{\partial P}{\partial x}-\frac{\partial\langle u^2\rangle}{\partial x}-\frac{\partial\langle uv\rangle}{\partial y}+\nu\frac{\partial^2 U}{\partial x^2}+\nu\frac{\partial^2 U}{\partial y^2} \tag{6.2}$$

y-component:

$$U\frac{\partial V}{\partial x}+V\frac{\partial V}{\partial y}=-\frac{1}{\rho}\frac{\partial P}{\partial y}-\frac{\partial\langle uv\rangle}{\partial x}-\frac{\partial\langle v^2\rangle}{\partial y}+\nu\frac{\partial^2 V}{\partial x^2}+\nu\frac{\partial^2 V}{\partial y^2} \tag{6.3}$$

In addition, we have the two-dimensional mean continuity equation which reduces to:

$$\frac{\partial U}{\partial x}+\frac{\partial V}{\partial y}=0 \tag{6.4}$$

6.2.2 Order of magnitude estimates

Now let's make an order of magnitude estimate for each of the terms. This procedure may seem trivial to some, or hopeless hand-waving to others. The fact is that if you fall into either of these groups, you have missed something important. Learning to make good order-of-magnitude arguments and knowing when to use them (and when not to use them) are two of the most important skills in fluid mechanics, and especially turbulence. To do this right we will have to be very careful to make sure our estimates accurately characterize the terms we are making them for.

Naturally we should not expect changes of anything in the x-direction to scale the same as changes in the y-direction, especially in view of the above. (This, after all, is the whole idea of "thin" shear flow.) So let's agree that we will pick a length scale, say L, characteristic of changes or mean quantities in the x-direction; i.e.

$$\frac{\partial}{\partial x}\sim\frac{1}{L} \tag{6.5}$$

where for now '$\sim$ means "of the order of magnitude of". And we can do the same thing for changes of mean quantities in the y-direction by defining a second length scale, say δ, to mean:

$$\frac{\partial}{\partial y}\sim\frac{1}{\delta} \tag{6.6}$$

Note that both these scales will vary with the streamwise position where we evaluate them. A good choice for δ might be proportional to the local lateral extent of the flow (or its "width"), while L is related to the distance from the source.

Consider the mean velocity in equation 7.10. It occurs in five different terms: U alone; twice with x-derivatives, $\partial U/\partial x$ and $\partial^2 U/\partial x^2$; and twice with y-derivatives, $\partial U/\partial y$ and $\partial^2 U/\partial y^2$. Now it would be tempting to simply pick a scale velocity for U, say U_s, and use it to estimate all five terms, say as: U_s, U_s/L, U_s/L^2, U_s/δ, and U_s/δ^2. But this is much too naïve, and fails to appreciate the true role of the terms we are evaluating.

Look at the example shown in Figure 6.4. Our simple approach would provide an appropriate estimate for a jet if we took our velocity scale equal to the mean centerline velocity at a given streamwise location; i.e., $U_s(x) = U_{cl}(x)$. This is because both the mean velocity and the *changes* in the mean velocity across the flow are characterized by the centerline velocity. But by contrast, look at the wakes shown in Figure 1.3. If we denote the free stream velocity (i.e. far away from the wake) by U_o and the velocity at the wake centerline by U_{cl}, we can define a wake deficit by

$$\Delta U_{cl} = U_o - U_{cl} \tag{6.7}$$

Even relatively close to the wake generators, the wake deficit is small compared to the free stream velocity (i.e., $\Delta U_{cl} << U_o$). So the obvious choice to scale $U(x, y)$ would be U_o. On the other hand, an estimate for the velocity gradient across the flow of U_o/δ would be much too big, again because the deficit is so small. Obviously a better choice would be to use the centerline mean velocity *deficit*, ΔU_{cl}; i.e.,

$$\frac{\partial U}{\partial y} \sim \frac{\Delta U_{cl}}{\delta} \tag{6.8}$$

In the order of magnitude analysis below, we shall try to keep the discussion as general as possible by using U_s to characterize the mean velocity when it appears by itself, and ΔU_s to represent changes in the mean velocity. For the jet example of the preceding paragraph, both U_s and ΔU_s are the same; i.e., $U_s = U_{cl}$ and $\Delta U_s = U_{cl}$. But for the wake they are different because of the external stream; i.e., $U_s = U_o$ and $\Delta U_s = \Delta U_{cl}$. If you can keep in mind *why* these differences exist among the various flows, it will be a lot easier to both understand the results and not confuse them.

Now we could distinguish changes of velocity in the x-direction from those in the y-direction. But this level of complexity is not necessary (at least for the examples considered here), especially since we have left the precise definition of L rather nebulous. What we can do is to use the same estimate for changes in the velocity as for the y-direction, and *define* our length scale L to make the estimate based on both correct; i.e., $\partial U/\partial x \sim \Delta U_s/L$. To see why this makes sense physically and can be reasoned (as opposed to guessed), let's look at the wake. Pick a spot outside, near the edge of the wake fairly close the generator (say point A). Now proceed at constant y far downstream in x. Eventually the wake will have spread past you and you will be close enough to the centerline so the local mean velocity will be closer to U_{cl} than U_o. Obviously we have simply traveled far enough at constant y to insure that ΔU_{cl} is the proper scale for *the changes* in velocity in the x-direction. If the distance downstream over which this change occurred is taken as L, then the proper estimate is easily seen to be:

$$\frac{\partial U}{\partial x} \sim \frac{\Delta U_{cl}}{L} \tag{6.9}$$

But this is exactly what we would have gotten by taking $U_s = U_{cl}$ as we agreed above. We simply have absorbed any differences into our choice of L. When

considering specific problems and applying similarity techniques, the seemingly arbitrary choices here become quite precise constraints (as we shall see).

We still haven't talked about how to estimate the velocity scale for V, the cross-stream mean velocity component. From the continuity equation we know that:

$$\frac{\partial V}{\partial y} = -\frac{\partial U}{\partial x} \tag{6.10}$$

From our considerations above, we know that:

$$\frac{\partial U}{\partial x} \sim \frac{\Delta U_s}{L} \tag{6.11}$$

If there is no mean cross flow in the external stream, then the scale for V is the same as the scale for changes in V. Therefore,

$$\frac{\partial V}{\partial y} \sim \frac{V_s}{\delta} \tag{6.12}$$

It follows immediately that the order of magnitude of the cross-stream velocity is:

$$V_s \sim \Delta U_s \frac{\delta}{L} \tag{6.13}$$

We might have expected something like this if we had thought about it. If the V-velocity were of the same order as the U-velocity, how could the flow in any sense be a "thin shear flow". On the other hand, it also makes sense that $V_s/U_s \propto \delta/L$, since both are some measure of how the flow spreads. Note that equation 6.13 would not be the correct estimate for V_s if there were an imposed cross-flow, since then we would have to consider V and changes in V separately (exactly as for U).

The mean pressure gradient term is always a problem to estimate at the outset. Therefore it is better to simply leave this term alone, and see what is left at the end. In the estimates below you will see a question mark, which simply means we are postponing judgement until we have more information. Sometimes we will have to keep the term simply because we don't know enough to throw it away. Other times it will be obvious that it must remain because there is only one term left that must be balanced by something.

Now we have figured out how to estimate the order of magnitude of all the terms except the turbulence terms. For most problems this turns out to be pretty straightforward if you remember our discussion of the pressure strain-rate terms. They so effectively distribute the energy that even that the three components of velocity are usually about the same order of magnitude. So if we chose a turbulence scale as simply u, then $\langle u^2 \rangle \sim u^2$, $\langle v^2 \rangle \sim u^2$, and $\langle w^2 \rangle \sim u^2$. But what about the Reynolds shear stress components like $\langle uv \rangle$? When acting against the mean shear to produce energy, they tend to be well-correlated and the maximum value of $\langle uv \rangle / u_{rms} v_{rms} < 0.5$. Obviously the right choice for the order of magnitude is: $\langle uv \rangle \sim u^2$. This is not always the right choice though since some cross-stress like

$\langle uw \rangle$ are identically zero in plane flows because of homogeniety. Sometimes the Reynolds shear stress will be identically zero at some points in the flow (like when it is changing sign from one side to the other of a symmetry plane). When this happens terms you neglected can sneak back into the problem. The important point to remember is that you only estimating which terms might be the most important most of the time, and must look again after you have analyzed or solved the equations to see if your estimates were correct

6.2.3 The streamwise momentum equation

Let's look now at the x-component of the mean momentum equation and write below each term its order of magnitude.

$$\begin{array}{ccccccccc}
U\dfrac{\partial U}{\partial x} & + & V\dfrac{\partial U}{\partial y} & & & & & & \\
U_s\dfrac{\Delta U_s}{L} & & \left(\Delta U_s\dfrac{\delta}{L}\right)\dfrac{\Delta U_s}{\delta} & & & & & & \\
 & = & -\dfrac{1}{\rho}\dfrac{\partial P}{\partial x} & - & \dfrac{\partial\langle u^2\rangle}{\partial x} & - & \dfrac{\partial\langle uv\rangle}{\partial y} & + & \nu\dfrac{\partial^2 U}{\partial x^2} + \nu\dfrac{\partial^2 U}{\partial y^2} \\
 & & ? & & \dfrac{u^2}{L} & & \dfrac{u^2}{\delta} & & \nu\dfrac{\Delta U_s}{L^2} \quad \nu\dfrac{\Delta U_s}{\delta^2}
\end{array}$$

Now the survival of at least one of the terms on the left-hand side of the equation is the essence of free shear flow, since the flow is either being speeded up or slowed down by the external flow or surroundings. Since we have chosen the primary flow direction to be x, then the largest of these acceleration (or deceleration) terms is the first. Therefore to see the relative importance of the remaining terms, we need to re-scale the others by dividing all the estimates by $U_s\Delta U_s/L$. Doing this we have:

$$\begin{array}{ccccccccc}
U\dfrac{\partial U}{\partial x} & + & V\dfrac{\partial U}{\partial y} & & & & & & \\
1 & & \dfrac{\Delta U_s}{U_s} & & & & & & \\
 & = & -\dfrac{1}{\rho}\dfrac{\partial P}{\partial x} & - & \dfrac{\partial\langle u^2\rangle}{\partial x} & - & \dfrac{\partial\langle uv\rangle}{\partial y} & + & \nu\dfrac{\partial^2 U}{\partial x^2} + \nu\dfrac{\partial^2 U}{\partial y^2} \\
 & & ? & & \dfrac{u^2}{U_s\Delta U_s} & & \dfrac{u^2}{U_s\Delta U_s}\left(\dfrac{L}{\delta}\right) & & \dfrac{\nu}{U_sL} \quad \dfrac{\nu}{U_s\delta}\left(\dfrac{L}{\delta}\right)
\end{array}$$

So what do these mean? And how do we decide whether they are of the same order as our leading term, or much less? (Note that if any are bigger than our first term, it either means we have scaled it wrong, or that we guessed wrong about which term was the largest.) The beginning of the answer lies in remembering

that this is a book about turbulence. Therefore almost all the interesting flows are at high Reynolds number. But what does this mean? Now we can say. It could mean the viscous terms in the mean momentum equation are negligible, which in turn means that:

$$\frac{U_s L}{\nu} >> 1$$

and

$$\frac{U_s \delta}{\nu} >> \frac{L}{\delta}$$

Obviously the second criterion is much more stringent, since L/δ is typically of order 10 or less for our "thin" shear layers. When $U_s\delta/\nu > 1000$, the contributions of the viscous stresses are certainly negligible, at least as far as the x-component of the mean momentum equation is concerned. But if $U_s\delta/\nu \sim 100$ only, this is a pretty marginal assumption, and you might want to retain the last term in your analysis. Such is unfortunately the case in many experiments that are often at quite low Reynolds numbers.

So, what then, you ask, do we do about the turbulence terms? To repeat: this is a book about TURBULENCE! Which means there is no way we are going to throw away all the turbulence terms on the right-hand side of the equation. There is no magic or hocus-pocus about this; you simply can't have turbulence without at least one turbulence term. And if there is no turbulence, we really aren't too interested.

So, what does this tell us? It tells us about δ! Surprised? I bet you thought it would tell us about u, right? Not so. Look at the right-hand side of the second equation on the previous page and the orders of magnitude below it. Almost always, $u < U_s$, sometimes much less and almost never larger. Then the biggest turbulence term is the one involving the Reynolds shear stress, $\partial\langle -uv\rangle/\partial y$, which we have estimated as $[u^2/(U_s\Delta U_s)](L/\delta)$. Hence there can be no turbulence terms at all unless:

$$\frac{\delta}{L} \sim \frac{u^2}{U_s \Delta U_s}$$

Wow! Look what we have learned about turbulence without ever solving a single equation. We know how the growth of our free shear flow relates to the turbulence intensity – at least in terms of order of magnitude. The similarity theories described below will even be able to actually deduce the x-dependence of δ, again without actually solving the equations.

Does the argument above mean the other turbulence term is negligible since it is only of order $u^2/U_s\Delta U_s$? Well, no question we should expect it to be smaller, typically less than 5%. But unlike the viscous terms, this term often does not get smaller the farther we go in the streamwise direction. So the answer depends on the question we are asking and how accurate we want our answer to be. If

we are asking only first order questions and are willing to accept errors in our solutions (or experiments) to within a 5–10 percent, then this normal stress term is certainly negligible.

Before we go on, consider the following: since $\delta/L < 0.1$ typically, *to first order free shear flows do not grow at all!* So before you place your bets about whether $d\delta/dx$ for a particular shear flow, for example, is 0.095 instead of 0.09 (turbulence wars have been waged over less), then you better make sure you are dealing with a full deck — meaning these second order (and often neglected) terms had better be retained in any calculation or experimental verification (like momentum or energy balances).

Much of the confusion in the literature about free shear flows comes from the failure to use second order accuracy to make second order statements. And even more unbelievably, most attempts to do so-called 'code validation' of second-order turbulence models are based on measurements that are only first order accurate. Now I know you think I am kidding — but try to do a simple momentum balance on the data to within order $u^2/U_s\Delta U_s$. Did I hear you say it was ridiculous to use second-order equations (like the Reynolds stress equations or even the kinetic energy equation) and determine constants to three decimal places using first order accurate data?

Hopefully you have followed all this. If not, go forward and "faith" will come to you. I'll summarize how we do this:

- You have to look very carefully at the particular flow you wish to analyze.
- Then, based on physical reasoning and data (if you have it), you make estimates you think are appropriate.
- Then you use these estimates to decide which terms you have to keep, and which you can ignore.
- And when you are completely finished, you carefully look back to make sure that all the terms you kept really are important and remain important as the flow develops.

Finally, if you are really good at this, you look carefully to make sure that all the terms you kept do not all vanish at the same place (by going from positive to negative, for example). If this happens, then the terms you neglected may in fact be the only terms left in the equation that are not exactly zero — oops! This can make for some very interesting situations. (The famous "critical layer" of boundary layer stability theory is an example of this.)

Example: Turbulence through a contraction Consider the kinetic energy balance of a turbulence flow, homogeneous in lateral planes that is being accelerated through a contraction so that $\partial U/\partial x > 0$. First use the component Reynolds stress equations to show that the $\langle u^2 \rangle$ is *decreased* by the production term (and the pressure strain-rate term as well), and that $\langle v^2 \rangle$ is increased. Then

using the continuity equation together with l'Hôpital's rule show that to leading order at the centerline (assume symmetry around this line) the turbulence kinetic energy equation reduces to:

$$U\frac{\partial k}{\partial x} = -[\langle u^2\rangle - \langle v^2\rangle]\frac{\partial U}{\partial x} \tag{6.14}$$

Assuming that upstream $\langle u^2\rangle > \langle v^2\rangle$, re-examine your assessment of which terms are important near the points where k is maximal and where $\langle u^2\rangle = \langle v^2\rangle$. (Note that these points occur nearly, but not quite, in the same place.)

6.2.4 The transverse momentum equation

Now we must also consider the transverse or y-momentum equation. The most important thing we have to remember is that the y-equation can NOT be considered independently from the x-momentum equation. We would never consider trying to simplify a vector like (a, b, c) by dividing only one component by S say to produce (Sa, b, c), since this would destroy the whole idea of a vector as having a direction. Instead you would re-scale as (Sa, Sb, Sc) to preserve the direction. We must do the same for a *vector equation*. We have already decided that the first term on the left-hand side of the x-momentum equation was the term we had to keep, and we divided by its order of magnitude, $U_s\Delta U_s/L$, to make sure it was of order one. Thus we have already decided how we are going to scale *all* the components of the vector equation, and so we must do exactly the same thing here. But first we must estimate the order of magnitude of each term, exactly as before.

Using our previous results, here's what we get:

$$\begin{array}{cccccccccc}
U\dfrac{\partial V}{\partial x} & + & V\dfrac{\partial V}{\partial y} & & & & & & & \\
U_s\dfrac{\Delta U_s\delta/L}{L} & & \left(\Delta U_s\dfrac{\delta}{L}\right)\dfrac{\Delta U_s\delta/L}{\delta} & & & & & & & \\
 & = & -\dfrac{1}{\rho}\dfrac{\partial P}{\partial y} & - & \dfrac{\partial\langle uv\rangle}{\partial x} & - & \dfrac{\partial\langle v^2\rangle}{\partial y} & + & \nu\dfrac{\partial^2 V}{\partial x^2} & + & \nu\dfrac{\partial^2 V}{\partial y^2} \\
 & & ? & & \dfrac{u^2}{L} & & \dfrac{u^2}{\delta} & & \nu\dfrac{\Delta U_s\delta/L}{L^2} & & \nu\dfrac{\Delta U_s\delta/L}{\delta^2}
\end{array}$$

Now dividing each term by $U_s\Delta U_s/L$, exactly as before, we obtain:

$$\begin{array}{ccc}
U\dfrac{\partial V}{\partial x} & + & V\dfrac{\partial V}{\partial y} \\
\dfrac{\delta}{L} & & \dfrac{\Delta U_s}{U_s}\left(\dfrac{\delta}{L}\right)
\end{array}$$

$$= \quad -\frac{1}{\rho}\frac{\partial P}{\partial y} \quad - \quad \frac{\partial \langle uv \rangle}{\partial x} \quad - \quad \frac{\partial \langle v^2 \rangle}{\partial y} \quad + \quad \nu \frac{\partial^2 V}{\partial x^2} \quad + \quad \nu \frac{\partial^2 V}{\partial y^2}$$

$$? \qquad \frac{u^2}{U_s \Delta U_s} \qquad \frac{u^2}{U_s \Delta U_s}\left(\frac{L}{\delta}\right) \quad \frac{\nu}{U_s L}\left(\frac{\delta}{L}\right) \quad \frac{\nu}{U_s \delta}$$

Unless you have seen this all before, the left-hand side is probably a surprise: none of the mean convection terms are of order one! In fact the only estimated term that is of order one in the whole equation is $\partial\langle v^2 \rangle/\partial y$, and only because we have already agreed that $(u^2/U_s\Delta U_s)(L/\delta)$ had to be of order one to keep a turbulence term in the x-momentum equation. Of course, there cannot be an equation with only a single term equal to zero, unless we have badly over-estimated its order of magnitude. Fortunately there is the pressure term left to balance it, so to first order in $\delta/L \sim u^2/U_s\Delta U_s$, the y-momentum equation reduces to simply:

$$0 \approx -\frac{1}{\rho}\frac{\partial P}{\partial y} - \frac{\partial \langle v^2 \rangle}{\partial y} \tag{6.15}$$

This simple equation has an equally simple interpretation. It says that the change in the mean pressure is only due to the radial gradient of the transverse component of the Reynolds normal stress, $\langle v^2 \rangle$.

We can integrate equation 6.15 *across* the shear layer from a given value of y to infinity (or anywhere else for that matter) to obtain:

$$P(x, y) = P(x, \infty) - \rho\langle v^2 \rangle, \tag{6.16}$$

assuming of course the free stream value of $\langle v^2 \rangle$ to be zero. If the free stream is at constant (or zero) mean velocity, then $P(x, \infty) = P_\infty = constant$, so we can write simply:

$$P(x, y) = P_\infty - \rho\langle v^2 \rangle \tag{6.17}$$

Either of these can be substituted into the x-momentum equation to eliminate the pressure entirely, as we shall show below.

Now since $\langle v^2 \rangle << \Delta U_s^2$ typically, $P \approx P_\infty$, at least to first order in $u^2/\Delta U_s^2$. Therefore one might be tempted to conclude that the small pressure changes across the flow are not important. And they are not, of course, if only the streamwise momentum is considered. But without this small mean pressure gradient *across* the flow, there would be no entrainment and no growth of the shear layer. In other words, the flow would remain parallel. Clearly whether an effect is negligible or not depends on which question is being asked.

6.2.5 The free shear layer equations

If we assume the Reynolds number is always large enough that the viscous terms can be neglected, then as noted above, the pressure term in the x-momentum

equation can be evaluated in terms of P_∞ and $\langle v^2 \rangle$. Thus, *to second-order in* $u^2/U_s\Delta U_s$ *or* δ/L, the momentum equations for a free shear flow reduce to a single equation:

$$U\frac{\partial U}{\partial x} + \left\{ V\frac{\partial U}{\partial y} \right\} = -\frac{dP_\infty}{dx} - \frac{\partial}{\partial y}\langle uv \rangle - \left\{ \frac{\partial}{\partial x}\left[\langle u^2 \rangle - \langle v^2 \rangle \right] \right\} \tag{6.18}$$

As we have seen above, the second term on the left-hand side (in curly brackets) may or may not be important, depending on whether $U_s = \Delta U_s$ or $\Delta U_s/U_s << 1$. Clearly this depends on the velocity deficit (or excess) relative to the free stream. The second term in brackets on the right-hand side is also second-order (in $u^2/U_s\Delta U_s \sim \delta/L$) compared to the others, and so could rightly be neglected. It has been retained for now since in some flows it does not vanish with increasing distance from the source. Moreover, it can be quite important when considering integrals of the momentum equation, since the profiles of $\langle u^2 \rangle$ and $\langle v^2 \rangle$ do not vanish as rapidly with increasing y as do the other terms.

6.3 Two-dimensional Turbulent Jets

Turbulent jets are generated by a concentrated source of momentum issuing into an ambient environment. The state of the environment and the external boundary conditions are very important in determining how the turbulent flow evolves. The simplest case to consider is that in which the environment is at rest and unbounded, so all the boundary conditions are homogeneous. The jet itself can be assumed to issue from a line source or a slot as shown in Figure 6.5. The jet then evolves and spreads downstream by entraining mass from the surroundings which are at most in irrotational motion induced by the vortical fluid within the jet. But no new momentum is added to the flow downstream of the source, and it is this fact that distinguishes the jet from all other flows. As we shall see below, however, that the rate at which momentum crosses any x-plane is not quite constant at the source value due to the small streamwise pressure gradient arising from the turbulence normal stresses.

The averaged continuity equation can be integrated from the centerline (where it is zero by symmetry) to obtain V, i.e.,

$$V = -\int_0^y \frac{\partial U}{\partial x} d\tilde{y} \tag{6.19}$$

It immediately follows that the V velocity at $\pm\infty$ is given by:

$$V_\infty = -V_{-\infty} = -\frac{d}{dx}\int_0^\infty U(x,y)dy \tag{6.20}$$

Twice the integral represents the total volume flow rate crossing a given x-plane. Therefore it makes sense that the rate of increase of this integral is the entrainment velocity, V_∞. Obviously, V_∞ cannot be zero if the jet is to spread, at least in a

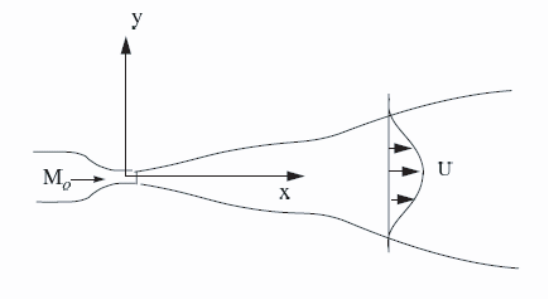

Figure 6.5: Sketch of plane jet showing jet source, coordinate system and typical mean velocity profile.

two-dimensional flow. It is easy to see that the entrainment velocity calculated from the integral is consistent with our order of magnitude estimate above (i.e., $V \sim \Delta U_s \delta / L$). Note that the integral makes no sense if the mean velocity U does *not* go to zero with increasing $|y|$.

If the free stream is assumed to have zero streamwise velocity, then the scales for the velocity and gradients of it are the same, so the equations reduce to simply equation 7.16 and the mean continuity equation. The latter can be multiplied by U to yield:

$$U \left\{ \frac{\partial U}{\partial x} + \frac{\partial V}{\partial y} \right\} = 0 \tag{6.21}$$

When this is added to equation 7.16 the terms can be combined to obtain:

$$\frac{\partial}{\partial x} U^2 + \frac{\partial}{\partial y} UV + \frac{\partial}{\partial y} \langle uv \rangle + \frac{\partial}{\partial x} \left[\langle u^2 \rangle - \langle v^2 \rangle \right] = 0 \tag{6.22}$$

This can be integrated across the flow for any given value of x to obtain:

$$\frac{d}{dx} \int_{-\infty}^{\infty} [U^2 + (\langle u^2 \rangle - \langle v^2 \rangle)] dy = 0 \tag{6.23}$$

where we have *assumed* that U, $\langle u^2 \rangle$, and $\langle v^2 \rangle$ vanish as $|y| \to \infty$. (Remember these assumptions the next time someone tries to tell you that a small co-flowing stream and modest background turbulence level in the external flow are not important.)

Equation 6.23 can in turn be integrated from the source, say $x = 0$, to obtain:

$$M_o = \int_{-\infty}^{\infty} [U^2 + (\langle u^2 \rangle - \langle v^2 \rangle)] dy \tag{6.24}$$

where M_o is the rate at which momentum per unit mass per unit length is added at the source. The first two terms of the integrand are the flux of streamwise momentum due to the mean flow and the turbulence. The last term is due to the streamwise pressure gradient obtained by integrating the y-momentum equation.

Equation 6.24 is a very powerful constraint, and together with the reduced governing equations allows determination of a similarity solution for this problem. It also is of great value to experimentalists, since it can be used to confirm whether their measurements are valid and whether the flow indeed approximates a plane jet in an infinite environment at rest. Be forewarned, most do not! And the explanations as to why range from hilarious to pathetic. Consider this, if you measure the velocity moments to within say 1%, then you should be able to estimate the integral even more accurately. The reason is that the random errors are reduced by the integration in proportion to the inverse of the square root of the number of points you used in the integration – if the errors are really random and statistically independent of each other. (Note that this is exactly like adding the statistically independent random numbers in Chapter 2.) So be very wary of measurements which have not been tested against the momentum integral — for this and all flows. Unfortunately there is usually a reason why the authors fail to mention it: they would rather you not know.

6.3.1 Similarity analysis of the plane jet

Foreword *The results of this section are VERY MUCH at odds with those in all texts, including the most recent. There is an increasing body of literature to support the position taken however, especially the multiplicity of solutions and the role of upstream or initial conditions. Since these ideas have a profound effect on how we think about turbulence, it is important that you consider both the old and the new, and be aware of why the conclusions are different.*[2]

The message you should take from the previous section is that regardless of how the plane jet begins, the momentum *integral* should be constant at M_o. Note that Schneider (1985) has shown that the nature of the entrained flow in the neighborhood of the source can modify this value, especially for plane jets. Also the term $\langle u^2 \rangle - \langle v^2 \rangle$, while important for accounting for the momentum balance in experiments, can be neglected in the analysis below with no loss in generality.

The search for similarity solutions to the averaged equations of motion is exactly like the approach utilized in laminar flows (e.g., Batchelor *Fluid Dynamics* 1967) except that here there are more unknowns than equations, i.e., the averaged equations are not closed. Thus solutions are sought which are of the form:

$$U = U_s(x) f(\overline{y}, *) \tag{6.25}$$

$$-\langle uv \rangle = R_s(x) g(\overline{y}, *) \tag{6.26}$$

$$\tag{6.27}$$

[2]This section has been taken in part from George 1995 "Some new ideas for similarity of turbulent flows", *Turbulence, Heat and Mass Transfer, Lisbon 1994*, (Hanjalic and Pereira, eds.), 24 - 49, Elsevier, Amsterdam. Also of interest might be the paper that started this line of thinking: George 1989 "The Self-Preservation of Turbulent Flows and Its Relation to Initial Conditions and Coherent Structures", in *Advances in Turbulence*, (George and Arndt, eds.), 39 – 73, Hemisphere (now Bacon and Francis), NY.

where

$$\overline{y} = y/\delta(x) \tag{6.28}$$

and where $*$ represents any dependence on upstream (or source) conditions we might not have thought of yet. The scale functions are functions of x only, i.e., $U_s = U_s(x)$ $R_s = R_s(x)$ and $\delta = \delta(x)$ only. Note that the point of departure from the traditional turbulence analyses was passed when it was *not* arbitrarily decided that $R_s = U_s^2$, etc. (c.f., Tennekes and Lumley 1972, Townsend 1976, Pope 2000).

Now lest you think there is something weird about the way we have written the form of the solutions we say we are looking for, consider this. Suppose you were looking for some x-dependent quantities with which you could normalize the profiles to make them all collapse together — like any experimentalist almost always does. Such a search is called the search for "*scales*", meaning "scales" which collapse the data. Now precisely what does "collapse the data" really mean? Exactly this: "collapse the data" means that the form of the solution must be an x-independent solution to the governing equations. But this is exactly what we are looking for in equations 6.25 and 6.26. Obviously we need to plug them into the averaged equations and see if such a solution is possible. We already know which terms in these equations are important. What we want to do now is to see if these governing equations admit to solutions for which these terms *remain* of equal importance throughout the jet development. These are called *equilibrium similarity solutions*. Note that for any other form of solution, one or more terms could die off, so that others dominate.

Differentiating equations 6.25 and 6.26 using the chain-rule, substituting into the averaged momentum equation, and clearing terms yields:

$$\left[\frac{\delta}{U_s}\frac{dU_s}{dx}\right] f^2 - \left[\frac{\delta}{U_s}\frac{dU_s}{dx} + \frac{d\delta}{dx}\right] f' \int_0^{\overline{y}} f(\overline{y}')d\overline{y}' = \left[\frac{R_s}{U_s^2}\right] g' \tag{6.29}$$

Now, all of the x-dependence is in the square bracketed terms, so equilibrium similarity solutions are possible only if all the bracketed terms have the same x-dependence, i.e.,

$$\frac{d\delta}{dx} \propto \frac{\delta}{U_s}\frac{dU_s}{dx} \propto \frac{R_s}{U_s} \tag{6.30}$$

We can define the coefficients of proportionality to be n and B respectively; i.e.,

$$\frac{d\delta}{dx} = n\frac{\delta}{U_s}\frac{dU_s}{dx} \tag{6.31}$$

$$\frac{d\delta}{dx} = B\frac{R_s}{U_s} \tag{6.32}$$

Note that n and B can at most depend on the details of how the flow began; i.e., the mystery argument "$*$".

Substitution into the momentum integral yields to first order,

$$AU_s^2\delta = M_o \tag{6.33}$$

where

$$A \equiv \int_0^\infty f^2(\overline{y}, *)d\overline{y} \tag{6.34}$$

A also can at most depend only on how the flow began (i.e., $*$), since every other dependence has been eliminated.

Now we learn somthing quite remarkable. Since M_o is independent of x, then the only possible value of n is $n = -1/2$. It follows immediately that:

$$U_s \propto M_o^{1/2}\delta^{-1/2} \tag{6.35}$$

It is easy to see that all of the relations involving U_s are proportional to $d\delta/dx$, leaving only

$$-\frac{1}{2}\left\{f^2 - f'\int_0^{\overline{y}} f(\overline{y}')d\overline{y}'\right\} = \left[\frac{R_s}{U_s^2 d\delta/dx}\right] g' \tag{6.36}$$

Thus the only remaining necessary condition for similarity is

$$R_s \propto U_s^2\frac{d\delta}{dx} \tag{6.37}$$

Note that, unlike the similarity solutions encountered in laminar flows, it is possible to have a jet which is similar *without* having some form of power law behavior. In fact, the x-dependence of the flow may not be known at all because of the closure problem. Nonetheless, the profiles will collapse with the local length scale.

In fact, it is easy to show that the profiles for *all* plane jets will be alike, if normalized properly, even if the growth rates are quite different and they began with quite different source conditions. To show this, define the scale velocity U_s to be the centerline velocity U_{cl} by absorbing an appropriate factor into the profile function $f(\overline{y})$. (In fact, it will now have the value unity at $\overline{y} = 0$.) Also, the entire factor in brackets on the right-hand side of equation 6.36 can be absorbed into the Reynolds stress profile,$g(\overline{y})$; i.e., by defining $\tilde{g}(\overline{y}, *)$ to be:

$$\tilde{g}(\overline{y}, *) = \left[\frac{R_s}{U_s^2 d\delta/dx}\right] g(\overline{y}, *) \tag{6.38}$$

Finally, if the length scale is chosen the same for all flows under consideration (e.g., the half-width, say $\delta_{1/2}$, defined as the distance between the center and where $U = U_{cl}/2$), then the similarity equation governing all jets reduces to:

$$f^2 + f'\int_0^{\overline{y}} f(\overline{y}')d\overline{y}' = -2\tilde{g}' \tag{6.39}$$

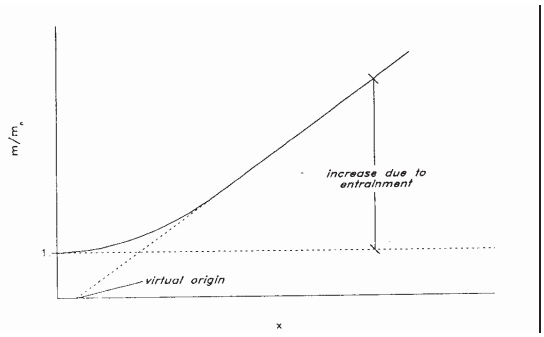

Figure 6.6: Sketch of net mass flow crossing any downstream plane for round jet as function of distance from the source.

Thus all jets, regardless of source conditions, will produce the same similarity velocity profile, when scaled with U_{cl} and $\delta_{1/2}$. This will not be true for the Reynolds stress, however, unless the coefficient of proportionality between R_s and $U_s^2 d\delta/dx$ is the same for *all* plane jets. In general, it is not; so here is where the dependence on source conditions shows up.

It is immediately obvious from equation 6.36 that the usual arbitrary choice of $R_s = U_s^2$ considerably restricts the possible solutions to those for which $d\delta/dx = constant$, or plane jets which grow linearly. However, even if the growth were linear under some conditions, there is nothing in the theory to this point which demands that the constant be universal and independent of how the jet began.

The idea that jets might all be described by the same asymptotic growth rate stems from the idea of a jet formed by a point source of momentum only, say ρM_o. Such a source must be infinitesimal in size, since any finite size will also provide a source of mass flow. In the absence of scaling parameters other than distance from the source, x, the only possibilities are $U_s \propto (M_o/x)^{1/2}$, $R_s \propto M_o/x$, and $\delta \propto x$. Obviously $R_s = U_s^2$, and the constants of proportionality can be assumed "universal" since there is only one way to create a point source jet.

The problem with the point source idea is not in the idea itself, but that it has been accepted for so long by so many without justification as the asymptotic state of *all* finite source jets. The usual line of argument (e.g., Monin and Yaglom 1972) (if one is presented at all) is the just a *plausiblity* argument that goes like this. The jet entrains mass, and the mass flow of the jet increases with distance downstream like that shown in Figure 6.6. Since the mass that has been entrained ultimately overwhelms that added at the source, it is argued that the latter can be neglected. Hence the far jet is indistinguishable from a point source jet.

And what is the experimental proof offered to substantiate this plausible sounding argument? Precisely that the profiles of U/U_{cl} collapse to a single profile for all types of initial conditions. But as was demonstrated above, the mean momentum equation tells us that the mean velocity profiles will collapse to a single profile *no matter what*! If there is a dependence on the initial conditions it

can only show up in the other turbulence moments, in profiles of the Reynolds shear stress normalized by U_{cl}^2 (instead of $d\delta/dx$), and, of course, in $d\delta/dx$ itself. And guess what quantities no two experiments ever seem to agree on? — All of the above! Could all those experiments plus this nice theory with virtually no assumptions be wrong? Many still think so. It is truly amazing how much good science people will throw away in order to hang-on to a couple of ideas that were never derived in the first place but only assumed: in this case, $R_s = U_s^2$ and the asymptotic independence of upstream conditions. But then there are still many people who believe the world is flat.

George (1989) demonstrated for an axisymmetric jet that even simple dimensional analysis suggests that the classical theory is wrong, and the same arguments apply here. Suppose that in addition to momentum, mass is added at the source at a rate of ρm_o. Now there is an additional parameter to be considered, and as a consequence, an additional length scale given by $L = m_0^2/M_o$. Thus the most that can be inferred from dimensional analysis is that δ/x, $U_s x^{1/2}/M_o^{1/2}$ and $R_s x/M_o$ are functions of x/L, with no insight offered into what the functions might be.

6.3.2 Implications of the Reynolds stress equations

George 1989 further argued that some insight into the growth rate of the jet can be obtained by considering the conditions for similarity solutions of the higher moment equations, in particular the kinetic energy equation. The choice of the kinetic energy equation for further analysis was unfortunate since it implicitly assumed that the three components of kinetic energy all scaled in the same manner. This is, in fact, true only if $d\delta/dx = const$, which is certainly not true *a priori* for turbulent shear flows. Therefore, here the individual component equations of the Reynolds stress will be considered (as should have been done in George 1989).

For the plane jet the equation for $\langle u^2 \rangle$ can be written to first order (Tennekes and Lumley 1972) as

$$\begin{aligned} U\frac{\partial\langle u^2\rangle}{\partial x} + V\frac{\partial\langle u^2\rangle}{\partial y} & \\ = \frac{2}{\rho}\langle p\frac{\partial u}{\partial x}\rangle \quad + \quad \frac{\partial}{\partial y}\left\{-\langle u^2 v\rangle\right\} - 2\langle uv\rangle\frac{\partial U}{\partial y} - 2\epsilon_u & \end{aligned} \tag{6.40}$$

where ϵ_u is the energy dissipation rate for $\langle u^2 \rangle$.

By considering similarity forms for the new moments like

$$\frac{1}{2}\langle u^2\rangle = K_u(x)k(\eta) \tag{6.41}$$

$$\langle p\frac{\partial u}{\partial x}\rangle = P_u(x)p_u(\eta) \tag{6.42}$$

$$-\frac{1}{2}\langle u^2 v\rangle = T_{u^2v}(x)t(\eta) \tag{6.43}$$

$$\epsilon_u = D_u(x)d(\eta) \tag{6.44}$$

and using $R_s = U_s^2 d\delta/dx$, it is easy to show that similarity of the $\langle u^2 \rangle$-equation is possible only if

$$K_u \propto U_s^2 \tag{6.45}$$

$$P_u \propto \frac{U_s^3}{\delta}\frac{d\delta}{dx} \tag{6.46}$$

$$T_{u^2v} \propto U_s^3 \frac{d\delta}{dx} \tag{6.47}$$

$$D_u \propto \frac{U_s^3}{\delta}\frac{d\delta}{dx} \tag{6.48}$$

All of these are somewhat surprising: The first (even though a second moment like the Reynolds stress) because the factor of $d\delta/dx$ is absent; the second, third and fourth because it is present.

Similar equations can be written for the $\langle v^2 \rangle$, $\langle w^2 \rangle$, and $\langle -uv \rangle$-equations; i.e.

$$U\frac{\partial \langle v^2 \rangle}{\partial x} + V\frac{\partial \langle v^2 \rangle}{\partial y} = 2\langle p\frac{\partial v}{\partial y}\rangle + \frac{\partial}{\partial y}\left\{-\langle v^3 \rangle - 2\langle pv \rangle\right\} - 2\epsilon_v \tag{6.49}$$

$$U\frac{\partial \langle w^2 \rangle}{\partial x} + V\frac{\partial \langle w^2 \rangle}{\partial y} = 2\langle p\frac{\partial w}{\partial z}\rangle + \frac{\partial}{\partial y}\left\{-\langle w^2 v \rangle\right\} - 2\epsilon_w \tag{6.50}$$

$$U\frac{\partial \langle uv \rangle}{\partial x} + V\frac{\partial \langle uv \rangle}{\partial y} = \langle p\left(\frac{\partial u}{\partial y} + \frac{\partial v}{\partial x}\right)\rangle + \frac{\partial}{\partial y}\left\{-\langle uv^2 \rangle\right\} - \langle v^2 \rangle\frac{\partial U}{\partial y} \tag{6.51}$$

When each of the terms in these equations is expressed in similarity variables, the resulting similarity conditions are:

$$D_v \propto P_v \propto \frac{U_s K_v}{\delta}\frac{d\delta}{dx} \tag{6.52}$$

$$D_w \propto P_w \propto \frac{U_s K_w}{\delta}\frac{d\delta}{dx} \tag{6.53}$$

$$T_{v^3} \propto \frac{U_s K_v}{\delta}\frac{d\delta}{dx} \tag{6.54}$$

$$T_{w^2v} \propto \frac{U_s K_w}{\delta}\frac{d\delta}{dx} \tag{6.55}$$

and the real surprise,

$$K_v \propto U_s^2 \left(\frac{d\delta}{dx}\right)^2 \tag{6.56}$$

There is an additional equation which must be accounted for: namely that the sum of the pressure strain-rate terms in the component energy equations be zero (from continuity). Thus,

$$\langle p\frac{\partial u}{\partial x}\rangle + \langle p\frac{\partial v}{\partial y}\rangle + \langle p\frac{\partial w}{\partial z}\rangle = 0 \tag{6.57}$$

or in similarity variables,

$$P_u(x)p_u(\eta) + P_v(x)p_v(\eta) + P_w(x)p_w(\eta) = 0 \tag{6.58}$$

This can be true for all η only if

$$P_u \propto P_v \propto P_w \tag{6.59}$$

An immediate consequence is that

$$D_u \propto D_v \propto D_w \tag{6.60}$$

From equations 6.46, 6.52 and 6.53 it also follows that the constraint imposed by 6.59 can be satisfied only if

$$K_u \propto K_v \propto K_w \tag{6.61}$$

But from equation 6.56, this can be true only if

$$\frac{d\delta}{dx} = constant \tag{6.62}$$

The relations given by equations 6.61 and 6.60 were assumed without proof in the George 1989 analysis. The additional constraint imposed by equation 6.62 was not derived, however, and arises from the additional information provided by the pressure strain-rate terms.

Hence, similarity solutions of the Reynolds stress equations are possible only if

$$D_s(x) \propto \frac{U_s^3}{\delta} \tag{6.63}$$

It is an immediate consequence of the earlier discussion on the nature of the dissipation that there are only two possibilities for this to occur:

i) Either the local Reynolds number of the flow is constant so that the effect of the dissipation on the energy containing eddies (and those producing the Reynolds stress as well) does not vary with downstream distance; or

ii) The local turbulence Reynolds number is high enough so that the relation $\varepsilon \propto q^3/L$ is approximately valid (for a *physical* length $L \propto \delta$!).

Unlike some flows (like the axisymmetric jet or plane wake) where the local Reynolds number is constant, for the plane jet it varies with downstream distance. Therefore the only possibility for similarity at the level of the Reynolds stresses is (ii). This can occur only when the turbulence Reynolds number is large enough, typically 10^4. Since the local Reynolds number for the plane jet continues to increase with increasing downstream distance, this state will eventually be reached. The higher the source Reynolds number, the closer to the exit plane the similarity of the moments will be realized.

6.4 Other Free Shear Flows

The plane jet is but one of the flows which can be analyzed in the manner described above. A few of the possibilities which have already been analyzed are the axisymmetric jet, plane and axisymmetric wakes (George 1989, 1995 Hussein et al. 1994, Moser et al. 1997, George and Davidson 2004, Johansson et al. 2005, Johansson and George 2006, Ewing et al. 2007). Other possibilities include free shear layers, thermal plumes and the self-propelled wake to mention but a few. All of these fall into the two categories described above: Flows which evolve at constant Reynolds number, and flows which do not. The axisymmetric jet and the plane wake are of the former type, and hence when properly scaled (using the techniques described above) will yield Reynolds number and source dependent solutions. These have been already discussed in detail in the cited papers and will not be discussed further here. The second type of flows (those for which the local Reynolds number varies with streamwise distances) also fall into two types: Those for which the local Reynolds number increases downstream (like the plane jet, plume or the shear layer), and those for which it decreases (like the axisymmetric wake).

When the Reynolds number is increasing with x, the flow will eventually reach the state of full similarity where all of the mean and turbulence quantities collapse. This state will be characterized by the infinite Reynolds number dissipation relation $\varepsilon \propto q^3/\delta$ which will be manifested in the approach of $d\delta/dx$ to its asymptotic value. (This has been shown above to be constant for the plane jet, but will be different for wakes, for example.) Generally this approach will coincide with a turbulent Reynolds number of $q^4/\varepsilon\nu \sim 10^4$ and the emergence in the spectra of the $k^{-5/3}$ range. Before this, the lack of collapse will be most evident in those quantities which depend directly on $d\delta/dx$, like $\langle -uv \rangle$, $\langle v^2 \rangle$, etc. Other quantities like the mean flow will collapse much earlier, and as noted above will collapse to profiles independent of source conditions. The latter will not be the case for the second moment quantities since a dependence in the asymptotic value of $d\delta/dx$ will result in differences in the Reynolds stress equations themselves.

Perhaps the most troubling (and for that reason the most interesting) flows

are those where the local Reynolds number is decreasing — like the axisymmetric wake. In these cases, the mean velocity profiles will collapse, assuming the Reynolds number to be large enough that the viscous terms in the mean momentum equation are negligible. The asymptotic growth rate (corresponding to $\varepsilon \propto q^3/\delta$ or in the case of the axisymmetric wake, $\delta \propto x^{1/3}$) will only be achieved as long as the local Reynolds number is high enough (again $q^4/\varepsilon\nu \propto 10^4$). As soon as it drops below this value, the growth rate and scale parameters will begin to deviate (perhaps substantially) from the asymptotic power law forms. The turbulence quantities will begin to reflect this in the lack of collapse — again first noticeable in quantities with v^2, etc. which have a direct dependence on $d\delta/dx$. The mean velocity profile, however, will continue to collapse when scaled in local variables. The same will be true for flows in which the source Reynolds number is not high enough for the flow to ever achieve the requisite turbulence Reynolds number — the mean velocity will collapse even though the x-dependence will be all wrong — at least if asymptotic behavior is expected. To further confuse matters, the axisymmetric wake eventually finds a new low Reynolds number similarity solution state, in which it stays for ever.

Chapter 7

WALL-BOUNDED TURBULENT FLOWS

7.1 Introduction

Without the presence of walls or surfaces, turbulence in the absence of density fluctuations could not exist. This is because it is only at surfaces that vorticity can actually be generated by an on-coming flow is suddenly brought to rest to satisfy the no-slip condition. The vorticity generated at the leading edge can then be diffused, transported and amplified. But it can only be generated at the wall, and then only at the leading edge at that. Once the vorticity has been generated, some flows go on to develop in the absence of walls, like the free shear flows we considered earlier. Other flows remained "attached" to the surface and evolve entirely under the influence of it. These are generally referred to as "*wall-bounded flows*" or "*boundary layer flows*".

The most obvious causes for the effects of the wall on the flow arise from the wall-boundary conditions. In particular,

- The **kinematic** boundary condition demands that the normal velocity of the fluid on the surface be equal to the normal velocity of the surface. This means there can be no flow through the surface. Since the velocity normal to the surface cannot just suddenly vanish, the kinematic boundary condition ensures that the normal velocity components in wall-bounded flows are usually much less than in free shear flows. Thus the presence of the wall reduces the entrainment rate. Note that viscosity is not necessary in the equations to satisfy this condition, and it can be met even by solutions to to the inviscid Euler's equations.

- The **no-slip** boundary condition demands that the velocity component tangential to the wall be the same as the tangential velocity of the wall. If the wall is at rest relative, then the no-slip condition demands the tangential flow velocity be identically zero at the surface.

Figure 7.1: Flow around a simple airfoil without separation.

It is the no-slip condition, of course, that led Ludwig Prandtl[1] to the whole idea of a boundary layer in the first place. Professor Prandtl literally saved fluid mechanics from d'Alembert's paradox: the fact that there seemed to be no drag in an inviscid fluid (not counting form drag). Prior to Prandtl, everyone thought that as the Reynolds number increased, the flow should behave more and more like an inviscid fluid. But when there were surfaces, it clearly didn't. Instead of behaving like those nice potential flow solutions (like around cylinders, for example), the flow not only produced drag, but often separated and produced wakes and other free shear flows. Clearly something was very wrong, and as a result fluid mechanics didn't get much respect from engineers in the 19th century. And with good reason: how useful could a bunch of equations be if they couldn't find viscous drag, much less predict how much? But Prandtl's idea of the *boundary layer* saved everything.

Prandtl's great idea was the recognition that the viscous no-slip condition could not be met without somehow retaining at least one viscous stress term in the equations. As we shall see below, this implies that there must be at least two length scales in the flow, unlike the free shear flows we considered in the previous chapter for which the mean flow could be characterized by only a single length scale. The second length scale characterizes changes normal to the wall, and make it clear precisely which viscous term in the instantaneous equations is important.

[1]Prandtl was a famous German professor at Göttingen in the early 19th century, and founder of the famous institute there which so dominated much of 20th century fluid dynamics thinking, well into the second half of the century. Among his most famous students were T. Von Karman, and H. Schlichting.

7.2 Review of laminar boundary layers

Let's work this all out for ourselves by considering what happens if we try to apply the kinematic and no-slip boundary conditions to obtain solutions of the Navier-Stokes equations in the infinite Reynolds number limit. Let's restrict our attention for the moment to the laminar flow of a uniform stream of speed, U_o, around a body of characteristic dimension, D, as shown in Figure 7.1. It is easy to see the problem if we non-dimensionalize our equations using the free stream boundary condition and body dimension. The result is:

$$\frac{D\tilde{\tilde{u}}_i}{D\tilde{\tilde{t}}} = -\frac{\partial\tilde{\tilde{p}}}{\partial\tilde{\tilde{x}}_i} + \frac{1}{Re}\frac{\partial^2\tilde{\tilde{u}}_i}{\partial\tilde{\tilde{x}}_j^2} \tag{7.1}$$

where $\tilde{\tilde{u}}_i \equiv u_i/U_o$, $\tilde{\tilde{x}}_i \equiv x_i/D$, $\tilde{\tilde{t}} \equiv U_o t/D$ and $\tilde{\tilde{p}} \equiv p/(\rho U_o^2)$. The kinematic viscosity, ν has disappeared entirely, and is included in the **Reynolds number** defined by:

$$Re \equiv \frac{U_o D}{\nu} \tag{7.2}$$

Now consider what happens as the Reynolds number increases, due to the increase of U_o or L, or even a decrease in the viscosity. Obviously the viscous terms become relatively less important. In fact, if the Reynolds number is large enough it is hard to see at first glance why any viscous term should be retained at all. Certainly in the limit as $Re \to \infty$, our equations must reduce to Euler's equations which have no viscous terms at all; i.e., in dimensionless form,

$$\frac{D\tilde{u}_i}{D\tilde{t}} = -\frac{\partial\tilde{p}}{\partial\tilde{x}_i} \tag{7.3}$$

Now if we replace the Navier-Stokes equations by Euler's equations, this presents no problem at all in satisfying the kinematic boundary condition on the body's surface. We simply solve for the inviscid flow by replacing the boundary of the body by a streamline. This automatically satisfies the kinematic boundary condition. If the flow can be assumed irrotational, then the problem reduces to a solution of Laplace's equation, and powerful potential flow methods can be used.

In fact, for potential flow, it is possible to show that the flow is entirely determined by the *normal* velocity at the surface. And this is, of course, the source of our problem. There is no role left for the *viscous* no-slip boundary condition. And indeed, the potential flow has a tangential velocity along the surface streamline that is not zero. The problem, of course, is the absence of viscous terms in the Euler equations we used. Without viscous stresses acting near the wall to retard the flow, the solution cannot adjust itself to zero velocity at the wall. But how can viscosity enter the equations when our order-of-magnitude analysis says they are negligible at large Reynolds number, and exactly zero in the infinite Reynolds

number limit? At the end of the nineteenth century, this was arguably the most serious problem confronting fluid mechanics.

Prandtl was the first[2] to realize that there must be at least one viscous term in the problem to satisfy the no-slip condition. Therefore he postulated that the strain rate very near the surface would become as large as necessary to compensate for the vanishing effect of viscosity, so that at least one viscous term remained. This very thin region near the wall became known as Prandtl's boundary layer, and the length scale characterizing the necessary gradient in velocity became known as the boundary layer "thickness".

Prandtl's argument for a laminar boundary layer can be quickly summarized using the same kind of order-of-magnitude analysis we used in Chapter 6. For the leading viscous term:

$$\nu \frac{\partial^2 u}{\partial y^2} \sim \nu \frac{U_s}{\delta^2} \tag{7.4}$$

where δ is the new length scale characterizing changes normal to the plate near the wall and we have assumed $\Delta U_s = U_s$. In fact, for a boundary layer next to walls driven by an external stream these can both be taken to be the free stream speed U_∞. For the leading convection term:

$$U \frac{\partial U}{\partial x} \sim \frac{U_s^2}{L} \tag{7.5}$$

The viscous term can survive only if it is the same order of magnitude as the convection term. Hence it follows that we must have:

$$\nu \frac{U_s}{\delta^2} \sim \frac{U_s^2}{L} \tag{7.6}$$

This in turn requires that the new length scale δ must satisfy:

$$\delta \sim \left[\frac{\nu L}{U_s}\right]^{1/2} \tag{7.7}$$

or

$$\frac{\delta}{L} \sim \left[\frac{\nu}{U_s L}\right]^{1/2} \tag{7.8}$$

Thus, for a *laminar flow*, δ grows like $L^{1/2}$. Now if you go back to your fluid mechanics texts and look at the similarity solution for a Blasius boundary layer, you will see this is exactly right if you take $L \propto x$, which is what we might have guessed anyway.

[2]Actually about the same time a Swedish meteorologist named Ekman realized the same thing must be true for rotating flows with a horizontal surface, like the earth's boundary layer, for example. He invented what we now call the *Ekman layer*, which had the really strange characteristic that the flow direction changed with height. You can actually observe this on some days simply by looking up and noting the clouds at different heights are moving in different directions.

It is very important to remember that the momentum equation is a vector equation, and therefore we have to scale all components of this vector equation the same way to preserve its direction. Therefore we must carry out the same kind of estimates for the cross-stream momentum equations as well. For a laminar boundary layer this can be easily be shown to reduce to:

$$\left[\frac{\delta}{L}\right]\left\{\frac{\partial\tilde{\tilde{u}}}{\partial\tilde{\tilde{t}}}+\tilde{\tilde{u}}\frac{\partial\tilde{\tilde{u}}}{\partial\tilde{\tilde{x}}}+\tilde{\tilde{v}}\frac{\partial\tilde{\tilde{v}}}{\partial\tilde{\tilde{y}}}\right\}=-\frac{\partial\tilde{\tilde{p}}_\infty}{\partial\tilde{\tilde{y}}}+\frac{1}{Re}\left[\frac{\delta}{L}\right]\left\{\frac{\partial^2\tilde{\tilde{v}}}{\partial\tilde{\tilde{y}}^2}\right\}+\frac{1}{Re}\left\{\frac{\partial^2\tilde{\tilde{v}}}{\partial\tilde{\tilde{x}}^2}\right\} \tag{7.9}$$

Note that a only single term survives in the limit as the Reynolds number goes to infinity, the cross-stream pressure gradient. Hence, for very large Reynolds number, the pressure gradient across the boundary layer equation is very small. Thus the pressure gradient *in the boundary layer* is imposed on it by the flow *outside* the boundary layer. And this flow **outside** the boundary layer is governed to first order by Euler's equation.

The fact that the pressure is *imposed* on the boundary layer provides us an easy way to calculate such a flow. First calculate the inviscid flow along the surface using Euler's equation. Then use the pressure gradient along the surface from this *inviscid* solution together with the boundary layer equation to calculate the boundary layer flow. If you wish, you can even use an iterative procedure where you recalculate the outside flow over a streamline which was been displaced from the body by the boundary layer displacement thickness, and then re-calculate the boundary layer, etc. Before modern computers, this was the only way to calculate the flow around an airfoil, for example. And even now it is still used for most calculations around aerodynamic and hydrodynamic bodies.

7.3 The "outer" turbulent boundary layer

The understanding of turbulent boundary layers begins with exactly the same averaged equations we used for the free shear layers of Chapter 7; namely,
x-component:

$$U\frac{\partial U}{\partial x}+V\frac{\partial U}{\partial y}=-\frac{1}{\rho}\frac{\partial P}{\partial x}-\frac{\partial\langle u^2\rangle}{\partial x}-\frac{\partial\langle uv\rangle}{\partial y}+\nu\frac{\partial^2 U}{\partial x^2}+\nu\frac{\partial^2 U}{\partial y^2} \tag{7.10}$$

y-component:

$$U\frac{\partial V}{\partial x}+V\frac{\partial V}{\partial y}=-\frac{1}{\rho}\frac{\partial P}{\partial y}-\frac{\partial\langle uv\rangle}{\partial x}-\frac{\partial\langle u^2\rangle}{\partial y}+\nu\frac{\partial^2 V}{\partial x^2}+\nu\frac{\partial^2 V}{\partial y^2} \tag{7.11}$$

two-dimensional mean continuity

$$\frac{\partial U}{\partial x}+\frac{\partial V}{\partial y}=0 \tag{7.12}$$

In fact, the order of magnitude analysis of the terms in this equation proceeds exactly the same as for free shear flows. If we take $U_s = \Delta U_s = U_\infty$, then the

ultimate problem again reduces to how to keep a turbulence term. And, as before this requires:

$$\frac{\delta}{L} \sim \frac{u^2}{U_s \Delta U_s}$$

No problem, you say, we expected this. But the problem is that by requiring this be true, we also end up concluding that even the *leading* viscous term is also negligible! Recall that the leading viscous term is of order:

$$\frac{\nu}{U_s \delta} \frac{L}{\delta} \tag{7.13}$$

compared to the unity.

In fact to leading order, there are *no viscous terms* in either component of the momentum equation. In the limit as $U_\infty \delta/\nu \to \infty$, they are exactly the same as for the free shear flows we considered earlier; namely,

$$U\frac{\partial U}{\partial x} + \left\{ V\frac{\partial U}{\partial y} \right\} = -\frac{1}{\rho}\frac{\partial P}{\partial x} - \frac{\partial}{\partial y}\langle uv \rangle - \left\{ \frac{\partial}{\partial x}\langle u^2 \rangle \right\} \tag{7.14}$$

and

$$0 = -\frac{1}{\rho}\frac{\partial P}{\partial y} - \frac{\partial}{\partial y}\langle v^2 \rangle \tag{7.15}$$

And like the free shear flows these can be integrated from the free stream to a given value of y to obtain a single equation:

$$U\frac{\partial U}{\partial x} + V\frac{\partial U}{\partial y} = -\frac{dP_\infty}{dx} - \frac{\partial}{\partial y}\langle uv \rangle - \left\{ \frac{\partial}{\partial x}\left[\langle u^2 \rangle - \langle v^2 \rangle \right] \right\} \tag{7.16}$$

The last term in brackets is the gradient of the difference in the normal Reynolds stresses, and is of order u^2/U^2 compared to the others, so is usually just ignored.

The bottom line here is that even though we have attempted to carry out an order of magnitude analysis for a *boundary layer*, we have ended up with exactly the equations for a free shear layer. Only the boundary conditions are different — most notably the kinematic and no-slip conditions at the wall. Obviously, even though we have equations that describe a turbulent boundary layer, we cannot satisfy the no-slip condition without a viscous term. In other words, we are right back where we were *before* Prandtl invented the boundary layer for laminar flow! We need a boundary layer within the boundary layer to satisfy the no-slip condition. In the next section we shall in fact show that such an *inner boundary layer* exists. And that everything we analyzed in this section applies only to the *outer boundary layer* — which is NOT to be confused with the *outer flow* which is non-turbulent and still governed by Euler's equation. Note that the presence of P_∞ in our outer boundary equations means that (to first order in the turbulence intensity), the pressure gradient is still imposed on the boundary layer by the flow outside it, exactly as for laminar boundary layers (and all free shear flows, for that matter).

7.4 The "inner" turbulent boundary layer

We know that we cannot satisfy the no-slip condition *unless* we can figure out how to keep a viscous term in the governing equations. And we know there can be such a term only if the mean velocity near the wall changes rapidly enough so that it remains, no matter how small the viscosity becomes. In other words, we need a length scale for changes in the y-direction very near the wall which enables us keep a viscous term in our equations. This new length scale, let's call it η. (Note that this choice of symbol is probably a bit confusing since it is very close to the symbol, η_K that we used for the Kolmogorov microscale. But we must make some compromises for the sake of history, since almost the whole world calls it η. In fact most use exactly the same symbol for the Kolmogorov microscale.) Obviously we expect that η is going to be much smaller than δ, the boundary layer thickness. But how much smaller?

Obviously we need to go back and look at the full equations again, and re-scale them for the near wall region. To do this, we need to first decide how the mean and turbulence velocities scale near the wall scale. We are clearly so close to the wall and the velocity has dropped so much (because of the no-slip condition) that it makes no sense to characterize anything by U_∞. But we don't have anyway of knowing yet what this scale should be, so let's just call it u_w (assuming $u_w << U_\infty$) and define it later. Also, we do know from experiment that the turbulence intensity near the wall is relatively high (30% or more). So there is no point in distinguishing between a turbulence scale and the mean velocity, we can just use u_w for both. Finally we will still use L to characterize changes in the x-direction, since these will vary even less rapidly than in the outer boundary layer above this very near wall region we are interested in (due to the wall itself).

For the complete x-momentum equation we estimate:

$$\begin{array}{ccccccccccc}
U\dfrac{\partial U}{\partial x} & + & V\dfrac{\partial U}{\partial y} & & & & & & & & \\
u_w\dfrac{u_w}{L} & & \left(u_w\dfrac{\eta}{L}\right)\dfrac{u_w}{\eta} & & & & & & & & \\
 & = & -\dfrac{1}{\rho}\dfrac{\partial P}{\partial x} & - & \dfrac{\partial\langle u^2\rangle}{\partial x} & - & \dfrac{\partial\langle uv\rangle}{\partial y} & + & \nu\dfrac{\partial^2 U}{\partial x^2} & + & \nu\dfrac{\partial^2 U}{\partial y^2} \\
 & ? & \dfrac{u_w^2}{\eta} & & \dfrac{u_w^2}{L} & & \nu\dfrac{u_w}{L^2} & & \nu\dfrac{u_w}{\eta^2} & &
\end{array}$$

where we have used the continuity equation to estimate $V \sim u_w\eta/L$ near the wall.

As always, we have to decide which terms we have to keep so we know what to compare the others with. But that is easy here: we MUST insist that at least one viscous term survive. Since the largest is of order $\nu u_w/\eta^2$, we can divide by it to obtain:

$$
\begin{array}{rcccccccc}
U\dfrac{\partial U}{\partial x} & + & V\dfrac{\partial U}{\partial y} & & & & & & \\
\left(\dfrac{u_w\eta}{\nu}\right)\dfrac{\eta}{L} & & \left(\dfrac{u_w\eta}{\nu}\right)\dfrac{\eta}{L} & & & & & & \\
 & = & -\dfrac{1}{\rho}\dfrac{\partial P}{\partial x} & - & \dfrac{\partial\langle u^2\rangle}{\partial x} & - & \dfrac{\partial\langle uv\rangle}{\partial y} & + & \nu\dfrac{\partial^2 U}{\partial x^2} + \nu\dfrac{\partial^2 U}{\partial y^2} \\
 & ? & \left(\dfrac{u_w\eta}{\nu}\right)\dfrac{\eta}{L} & & \dfrac{u_w\eta}{\nu} & & \dfrac{\eta^2}{L^2} & & 1
\end{array}
$$

Now we have an interesting problem. We have the power to decide whether the Reynolds shear stress term survives or not by our choice of η; i.e., we can pick $u_w\eta/\nu \sim 1$ or $u_w\eta/\nu \to 0$. Note that we can not choose it so this term blows up, or else our viscous term will not be at least equal to the leading term. The most general choice is to pick $\eta \sim \nu/u_w$ so the Reynolds shear stress remains too. (This is called the distinguished limit in asymptotic analysis.) By making this choice we eliminate the necessity of having to go back and find there is another layer in which only the Reynolds stress survives — as we shall see below. Obviously if we choose $\eta \sim \nu/u_w$, then all the other terms vanish, except for the viscous one. In fact, if we apply the same kind of analysis to the y-mean momentum equation, we can show that the pressure in our near wall layer is also imposed from the outside. Moreover, even the streamwise pressure gradient disappears in the limit as $u_w\eta/\nu \to \infty$. These are relatively easy to show and left as exercises.

So to first order in $\eta/L \sim \nu/(u_w L)$, our mean momentum equation for the *near wall region* reduces to:

$$0 \approx \frac{\partial}{\partial y}\left[-\langle uv\rangle + \nu\frac{\partial U}{\partial y}\right] \tag{7.17}$$

In fact, this equation is exact in the limit as $u_w\delta/\nu \to \infty$, **but only for the very near wall region!**

Equation 7.17 can be integrated from the wall to location y to obtain:

$$0 = -\langle uv\rangle - \langle uv\rangle|_{y=0} + \nu\frac{\partial U}{\partial y} - \nu\left.\frac{\partial U}{\partial y}\right|_{y=0} \tag{7.18}$$

From the kinematic and no-slip boundary conditions at the wall we immediately know that $\langle uv\rangle|_{y=0} \equiv 0$. We also know that the wall shear stress is given by:

$$\tau_w \equiv \mu\left.\frac{\partial U}{\partial y}\right|_{y=0} \tag{7.19}$$

Substituting this we obtain our equation for the very near wall (in the limit of infinite Reynolds number) as:

$$\frac{\tau_w}{\rho} = -\langle uv\rangle + \nu\frac{\partial U}{\partial y} \tag{7.20}$$

We immediately recognize one of the most important ideas in the history of boundary layer theory; namely that in the limit of infinite Reynolds number **the total stress in the wall layer is constant**. Not surprisingly, the wall layer is referred to quite properly as the **Constant Stress Layer**. It is important not to forget (as many who work in this field do) that this result is valid *only* in the limit of infinite Reynolds number. At finite Reynolds numbers the total stress is almost constant, but never quite so because of the terms we have neglected. This difference may seem slight, but it can make all the difference in the world if you are trying to build an asymptotically correct theory, or even just understand your experiments.

Before leaving this section we need to resolve the important questions of what is u_w, our inner velocity scale. It is customary to define something called the *friction velocity*, usually denoted as u_*, by:

$$u_*^2 \equiv \frac{\tau_w}{\rho} \tag{7.21}$$

Now using this, equation 7.20 can be rewritten as:

$$u_*^2 = -\langle uv \rangle + \nu \frac{\partial U}{\partial y} \tag{7.22}$$

It should be immediately obvious that the choice is $u_w = u_*$; in other words, the friction velocity is the appropriate scale velocity for the wall region. It follows immediately from our considerations above that the inner length scale is $\eta = \nu/u_*$. An interesting consequence of these choices is that the inner Reynolds number is unity; i.e., $u_*\eta/\nu = 1$, meaning that viscous and inertial terms are about the same. But then this is precisely why we defined η as we did in the first place — to ensure that viscosity was important.

It is important not to read too much into the appearance of the wall shear stress in our scale velocity. In particular, it is wrong to think that it is the shear stress that determines the boundary layer. In fact, it is just the opposite: the outer boundary layer determines the shear stress. If you have trouble understanding this, just think about what happens if turn off the outer flow: the boundary layer disappears. The wall shear stress appears in the scale velocity only because of the constant stress layer in which the Reynolds stress imposed by the outer flow is transformed into the viscous stress on the wall.

Finally we can use our new length scale to define where we are in this near wall layer. In fact, we can introduce a whole new dimensionless coordinate called y^+ defined as:

$$y^+ \equiv \frac{y}{\eta} = \frac{yu_*}{\nu} \tag{7.23}$$

When moments of the velocity field, for example, are normalized by u_* (to the appropriate power) and plotted as functions of y^+, they are said to be plotted in "inner" variables. Similarly, we can non-dimensionalize equation 7.20 using inner

variables and rewrite it as simply:

$$1 = r_i + \frac{df_i}{dy^+} \tag{7.24}$$

where if we suppress for the moment a possible x-dependence we can write:

$$f_i(y^+) \equiv \frac{U(x,y)}{u_*} \tag{7.25}$$

and

$$r_i(y^+) \equiv \frac{-\langle uv \rangle}{u_*^2} \tag{7.26}$$

By contrast an "outer" dimensionless coordinate, $\overline{y}$, is defined by:

$$\overline{y} = \frac{y}{\delta} \tag{7.27}$$

In terms of these coordinates the outer equations (for the mean flow) are generally considered valid outside of $y^+ = 30$ or so. And the inner equations are needed inside of $\overline{y} = 0.1$ if we take $\delta = \delta_{0.99}$, where $\delta_{0.99}$ is defined to be equal to the value of y at which the mean velocity in the boundary layer is 0.99% of its free stream value, U_∞.

It is easy to see that the ratio of y^+ to $\overline{y}$ is the local Reynolds number δ^+ where

$$\delta^+ = \frac{\delta u_*}{\nu} \tag{7.28}$$

Obviously the higher the value of δ^+, the closer the inner layer will be to the wall relative to δ. On the other hand, since the wall friction (and hence u_*) drops with increasing distance downstream, both the outer boundary layer and inner boundary grow in physical variables (i.e., the value of y marking their outer edge increases). Sorting all these things out can be very confusing, so it is very important to keep straight whether you are talking about inner, outer or physical variables.

7.5 The viscous sublayer

7.5.1 The linear sublayer

It should be clear from the above that the viscous stress and Reynolds stress cannot both be important all the way across the constant stress layer. In fact, inside $y^+ = 3$, the Reynolds stress term is negligible (to within a few percent), so very near the wall equation 7.20 reduces to:

$$u_*^2 \approx \nu \frac{\partial U}{\partial y} \tag{7.29}$$

or in inner variables:

$$1 \approx \frac{df_i}{dy^+} \tag{7.30}$$

This equation is exact right at the wall, for any Reynolds number. It can immediately be integrated to obtain the leading term in an expansion of the velocity about the wall as:

$$f_i(y^+) = y^+ \tag{7.31}$$

or in physical variables

$$U(x, y) = \frac{u_*^2 y}{\nu} \tag{7.32}$$

Note that some authors consider the extent of the linear sublayer to be $y^+ = 5$, but by $y^+ = 3$ the Reynolds stress has already begun to evolve, making the approximations above invalid. Or said another way, the linear approximation is only good to within about 10% at $y^+ = 5$; and the linear approximation deteriorates rapidly outside this. It should be obvious why this subregion very near the wall is usually referred to as the *linear sublayer*. It should not be confused with the term *viscous sublayer*, which extends until the mean flow is dominated by the Reynolds stress alone at about $y^+ = 30$.

This linear sublayer is one of the very few EXACT solutions in all of turbulence. There are NO adjustable constants! Obviously it can be used with great advantage as a boundary condition in numerical solutions — if the resolution is enough to resolve this part of the flow at all. And it has great advantages for experimentalists too. They need only resolve the velocity to $y^+ = 3$ to be able to get an excellent estimate of the wall shear stress. Unfortunately, few experiments can resolve this region. And unbelievably, even some who are able to measure all the way to the wall sometimes choose to ignore the necessity of satisfying equation 7.31 or 7.32. Look at it this way, if these equations are not satisfied by the data, then either the data is wrong, or the Navier-Stokes equations are wrong. If you think the latter and can prove it, you might win a Nobel prize.

The important point is that the mean velocity profile is *linear* at the wall! It is easy to show using the continuity equation and the wall boundary conditions on the instantaneous velocity at the wall that the Reynolds stress is cubic at the wall; i.e., $-\langle uv \rangle / u_*^2 = d_3 {y^+}^3$. See if you can now use equation 7.20 to show that this implies that a fourth order expansion of the mean velocity at the wall yields:

$$u^+ = y^+ + c_4 {y^+}^4 \tag{7.33}$$

where $c_4 = d_3/4$. It is not clear at this point whether c_4 (and d_3) are Reynolds number dependent or not. Probably not, but they are usually taken as constant anyway by turbulence modelers seeking easy boundary conditions. Note that this fourth order expansion is a good description of the mean velocity only out to $y^+ \approx 7$, beyond which the cubic expansion of the Reynolds stress (on which it is based) starts to be invalid.

Exercise: Show that the presence of a streamwise pressure gradient in the viscous sublayer equations introduces a quadratic term into the near wall mean velocity profile; i.e., $\lambda^+ y^{+2}/2$ where $\lambda^+ = (\nu/u_*^3)dP/dx$. See if you can use your ability to scale the y-momentum equation to show that it is imposed from the outer flow onto the near wall layer.

7.5.2 The sublayers of the constant stress region

As we move out of the linear region very close to the wall the Reynolds stress rapidly develops until it overwhelms the viscous stress. Also, as we move outward, the mean velocity gradient slowly drops until the viscous stress is negligible compared to the Reynolds shear stress. We call this region of adjustment where both the viscous and Reynolds stresses are important in the mean momentum equation, the *buffer layer* or *buffer region*. It roughly extends from about $y^+ = 3$ to $y^+ = 30$. On the inside viscous stresses dominate. By $y^+ = 30$, however, the viscous shear stress is less than 1 % percent or so of the Reynolds shear stress and therefore nearly negligible.

Outside approximately $y^+ = 30$, we have only:

$$u_*^2 \approx -\langle uv \rangle \tag{7.34}$$

In other words, the Reynolds shear stress is itself nearly constant. Viscous effects *on the mean flow* are gone, and only the inertial terms from the fluctuating motion remain. This remains true for increasing distance from the wall until the mean convection terms begin to be important, which is about $y/\delta_{99} \approx 0.1$ for boundary layers. Obviously a necessary condition for this to be true is that $\delta^+ = \delta_{99}/\eta >> 300$, since otherwise there will be no region where both the viscous stress and mean convection terms are negligible. When this condition is satisfied, the region of approximately constant Reynolds stress is referred to as the *constant Reynolds stress layer* or **inertial sublayer**.

We will have much more to say about the inertial sublayer later, after we consider boundary layers with pressure gradient and channel flows. But note for now that there are many in the turbulence community who ignore this necessary condition for its existence. This is especially true when interpreting the results of experiments and DNS, most of which are at low Reynolds number and thus never achieve a real inertial sublayer. In particular, you should be quite skeptical when you find conceptual and computational models based on them, as many are. High Reynolds number boundary layers with a true inertial sublayers quite possibly behave very differently; but at this writing we are only beginning to find out. But we have learned enough to be quite suspicious.

Figure 7.2 summarizes the important regions of a turbulent boundary layer. The constant stress layer has two parts: a viscous sublayer and an inertial sublayer. The viscous sublayer itself has two identifiable regions: the linear sublayer where

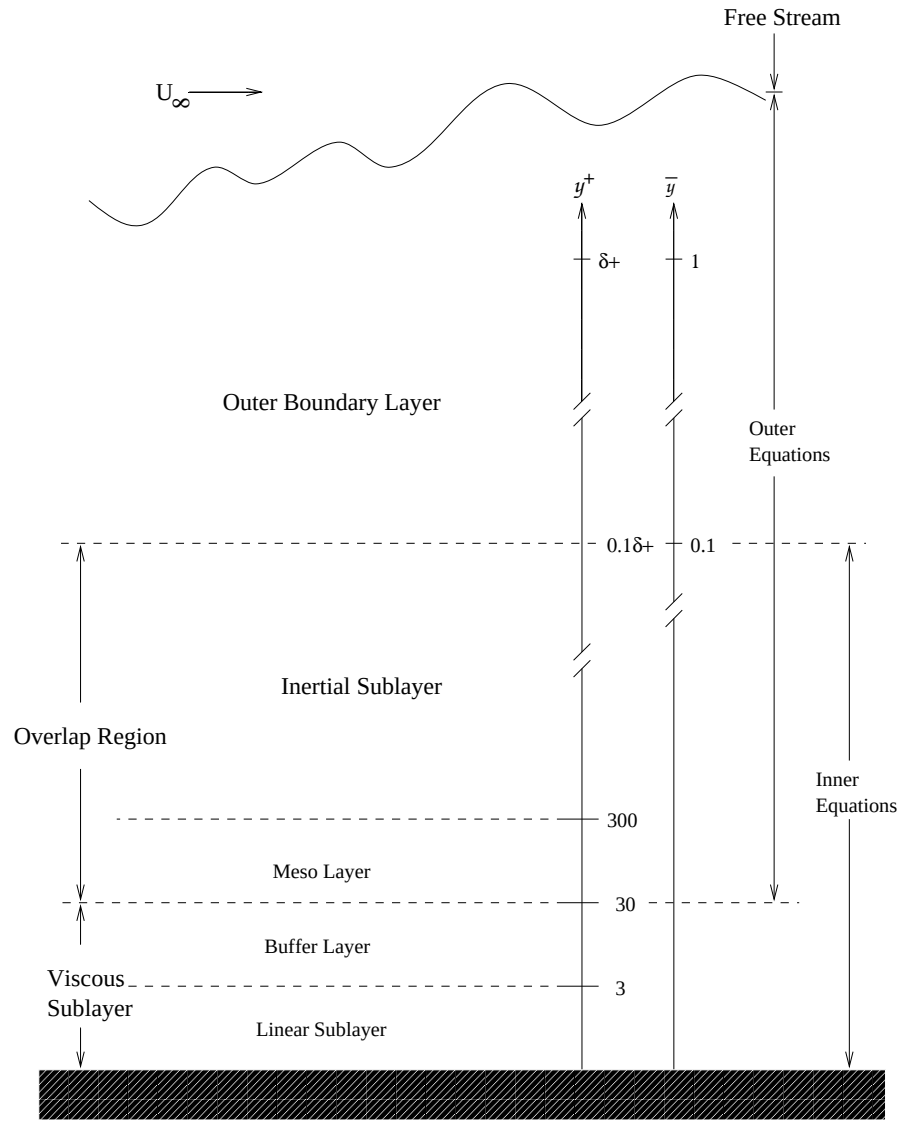

Figure 7.2: Sketch showing the various regions of the turbulent boundary layer in inner and outer variables. Note that in δ^+ is less than approximately 3000, then the inertial layer cannot be present, and for δ^+ less than about 300, the mesolayers extend into the outer layer.

only viscous shear stresses are important, and a buffer layer in which both viscous and Reynolds shear stresses are important. And as we shall see later, some (me among them) believe that the lower part of the inertial sublayer ($30 < y^+ < 300$ approximately) is really a *mesolayer* in which the Reynolds shear stress is constant at u_*^2, but the energetics of the turbulence (the multi-point equations) are still influenced by viscosity. Or said another way, the mean flow equations are indeed inviscid, but the multi-point equations for the turbulence are not. This close to the wall there simply is not the scale separation between the energy and dissipative scales required for viscosity to not directly affect the Reynolds stress producing motions.

7.6 Pressure gradient boundary layers and channel flow

We will consider the near wall regions of pressure gradient boundary layers and channel flows together, in part because many have been led to believe that the near wall regions of both are identical; and even that they are identical to the near wall region of the zero pressure gradient turbulent boundary layer we considered above. From an engineering perspective, the problem would be greatly simplified if this were true. You can decide for yourself whether this is reasonable or not.[3]

The averaged equations for a turbulent boundary layer (including pressure gradient) look like this:

$$U\frac{\partial U}{\partial x} + V\frac{\partial U}{\partial y} = -\frac{1}{\rho}\frac{dP_\infty}{dx} + \frac{\partial}{\partial y}\left[-\langle uv\rangle + \nu\frac{\partial U}{\partial y}\right] \tag{7.35}$$

where the y-momentum equation for the boundary layer has been integrated to replace the local pressure by that imposed from outside the boundary layer, P_∞, which is in turn assumed to be a function of the streamwise coordinate, x, only.

By contrast fully developed turbulent channel flows are homogeneous in the streamwise direction (only the pressure varies with x), so the convection terms (left hand side) are identically zero and the mean momentum equation reduces to:

$$0 = -\frac{1}{\rho}\frac{dP}{dx} + \frac{d}{dy}\left[-\langle uv\rangle + \nu\frac{dU}{dy}\right] \tag{7.36}$$

The cross-stream momentum equation can be used to argue that P is independent of y, to at least second order in the turbulence intensity.

Clearly equations 7.35 and 7.36 reduce to equation 7.17 only if the extra terms in each vanish; i.e., the mean convection terms on the left-hand side of equation 7.35 and the pressure gradient term in both. This is *presumed* to happen at

[3]This chapter was taken from a more extensive discussion of the issues raised in this section and the next by George, W.K. (2007) "Is there really a universal log law for turbulent wall-bounded flows?", *Phil. Trans. Roy. Soc. A, 365*, pp. 789 - 806.

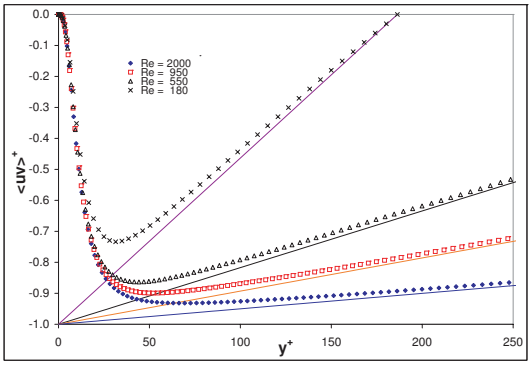

Figure 7.3: Plots of $\langle uv \rangle^+$ and $y^+/R^+ - 1$ for DNS of channel flow, $R^+ = 180$, 550, 950, and 2000.

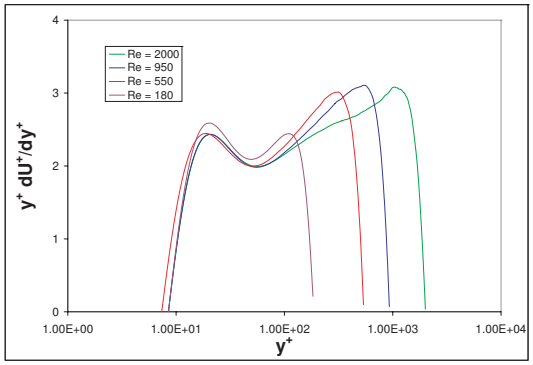

Figure 7.4: Plots of $y^+ dU^+/dy^+$ for DNS of channel flow, $R^+ = 180$, 550, 950, and 2000.

'sufficiently' high Reynolds number. But there is a problem which is seldom (if ever) addressed. It is obvious if equation 7.36 is integrated to obtain:

$$u_*^2 = \left[-\langle uv \rangle + \nu \frac{\partial U}{\partial y} \right] - \frac{y}{\rho} \frac{dP_\infty}{dx}, \tag{7.37}$$

or in so-called 'inner variables, $y^+ = y u_*/\nu$ and $U^+ = U/u_*$:

$$1 = -\langle uv \rangle^+ \frac{dU^+}{dy^+} - \lambda^+ y^+ \tag{7.38}$$

where λ^+ is a dimensionless pressure gradient defined as:

$$\lambda^+ = \frac{\nu}{\rho u_*^3} \frac{dP_\infty}{dx} \tag{7.39}$$

For a channel flow, the force exerted on the overall flow due to the streamwise pressure gradient is exactly balanced by the wall shear stress, so that:

$$\frac{\tau_w}{\rho} = u_*^2 = -\frac{R}{\rho} \frac{dP}{dx} \tag{7.40}$$

where R is the half-height of the channel. Therefore for a channel, $\lambda^+ = 1/R^+$, where $R^+ = u_* R/\nu$. Thus equation 7.38 becomes simply:

$$1 = -\langle uv \rangle^+ \frac{dU^+}{dy^+} + \frac{y^+}{R^+} \tag{7.41}$$

Since the viscous stress term is less than about 1% by $y^+ = 30$, this means that Reynolds shear stress drops linearly by 10% over the region of interest ($y/R \leq 0.1$), independent of the Reynolds number. Therefore only in the innermost part of the constant stress layer can the pressure gradient be assumed negligible, and nowhere if the Reynolds number is not extremely high.

The interplay of the Reynolds shear stress and the mean pressure gradient is illustrated in figure 7.3 using the recent DNS channel flow data from Jimenez and his co-workers (e.g., del Alamo *et al.* 2006). The values of R^+ are 180, 500, 950 and 2000. The linear drop of the total shear stress (viscous plus Reynolds) insures that there is no constant stress region, since its contribution is more than 1% of the total beyond $y^+ = 2$, 5, 10 and 20 respectively. And, contrary to popular belief, the situation will not improve with Reynolds number, since by $y^+ = 0.1R^+$ – $0.2R^+$ (the approximate outer limit of the inertial layer) the pressure gradient will always have reduced the Reynolds shear stress by 10 % - 20 %.

Many assume (mostly because they have been told) that the inertial region is described by a logarithmic profile, and that is built into many turbulence models. Figure 7.4 uses the same DNS data to illustrate that there is certainly not a logarithmic region for these data. If the velocity profile were really logarithmic, the quantity plotted, $y^+ dU^+/dy^+$ would be constant over some region. Clearly it is not, at least for Reynolds number range of DNS data currently available.

By contrast, the boundary layer at zero pressure gradient does not have this pressure gradient problem, since the pressure gradient term is identically zero. If the Reynolds number is high enough for the convection (advection) and viscous terms to be negligible over some region (e.g., $\delta^+ >> 300$), it truly does have a y-independent stress layer (even though it continues to vary slowly with x). Therefore it *can* (at least in principle) behave like the equation 7.17, even if pipe or channel flow cannot. Boundary layers *with* pressure gradient, however, do not behave like either a zero pressure gradient boundary layer or a channel (or pipe) flow, since over the range logarithmic behavior is expected the role of the pressure gradient depends on the value of λ^+. Therefore the effect of the pressure gradient over the overlap region will in principle be different for each imposed λ^+ (with presumably different log parameters for each).

Thus there is no reason *a priori* to believe boundary layers and pipes/channels to have identical inertial layers (or even mesolayers). The most that can be expected is that they might be identical only for the part of the flow which satisfies $y^+ << 0.1R^+$ or $y^+ << 0.1/\lambda^+$ (and even then only if the residual x-dependence of the boundary layer is ignored). For most boundary layer experiments, this is a very small region indeed. Therefore, while pipe/channel experiments (or DNS) may be of considerable interest in their own right, they can not be a substitute for high Reynolds number boundary layer experiments. This is especially true if the goal is to evaluate or substantiate theories to within 10% (since their underlying equations differ over the overlap region by this amount).

7.7 The inertial sublayer

7.7.1 Some history

The realization that the Reynolds stress might be nearly constant over some region of the flow led von Kármán (1930) and Prandtl (1932) to postulate that the velocity profile might be logarithmic there. The easiest derivation begins with using an eddy viscosity argument. Simply model the Reynolds shear stress with an eddy viscosity, say $-\langle uv\rangle = \nu_e \partial U/\partial y \approx u_*^2$ (since the viscous term is negligible in the inertial region). Then on dimensional grounds choose $\nu_e = \kappa u_* y$, where κ is a constant of proportionality. Integration yields immediately:

$$u^+ = \frac{1}{\kappa} \ln y^+ + B \tag{7.42}$$

where κ and B are assumed constant

This was originally believed to apply outside of $y^+ = 30$ out to about $y/\delta_{99} \approx 0.1 - 0.2$ or $y/R \approx 0.2$ for a channel or pipe flow. The results looked pretty good, especially given the data at the time. So not only was the idea of the 'log law' born, it came (on the basis of quite limited evidence) to be considered 'universal'. The subsequent refinements by Millikan (1938), Isakson (1937), Clauser (1954) and Coles (1956) were so strongly embraced by the community that they not only appear in virtually all texts, it is only in the past decade or so that serious challenges to the arguments are even publishable.

At this time (and over the past decade or so), the 'log' sublayer has been (and is) one of the most discussed and debated subjects in Fluid Mechanics. There is one whole school of thought that says the mean profile is logarithmic — quite independent of whether the external flow is a boundary layer, a pipe, a channel, or for that matter about anything you can think of. Moreover, it is usually argued that the three paramenters in this *universal* log profile are themselves *universal constants*.

This whole idea of a universal log law has pretty much been elevated to the level of the religion — and why not? Life becomes a lot simpler if some things can be taken as known to be true. And even the word, **universality** has a nice ring to it. For example, some go so far as to say that we can be so sure of these things that we don't even need to bother measure down below the "log" layer, since we already know the answer — we need only find the 'shear stress' which fits the universal log profile onto our data, and that's the shear stress. And if the measurements down in the linear region don't collapse when plotted as $U^+ = U/u_*$ versus $y^+ = yu_*/\nu$ and the *inferred value* of u_*, why then clearly the measurements of U or y must be wrong down there. The possibility that the log law might be wrong, or even that the parameters might not be constant is just too painful to contemplate. So no matter how much evidence piles up to the contrary, the *universalists* persist in their "beliefs" – a lot like the people who still believe that the earth is flat[4]. It just makes the earth so much easier to draw.

[4]There really are people who still believe the earth is flat, and they even have 'explanations'

Now you probably suspect from the tone of the above that I am not a member of the *universalist* school. And you are certainly right — and I don't believe the earth is flat either. But I am not one of the 'other' group either — the so-called *power-law* school who believe that the mean velocity profile in this region is given by a power law. The 'power law people' are at somewhat of a disadvantage since their parameters are Reynolds number dependent. The fact that their power laws may fit the data better is scoffed at, of course, by the universalists who naturally believe any data for which their universal log law does not fit perfectly must be wrong, or certainly in need of careful manipulation.

So where to these ideas come from? And why do people hold them so zealously? Well, the first is easy and we shall see below. The answer to the second question is probably the same as for every religious quarrel that has ever been — *the less indisputable evidence there is for an idea, the more people argue that there is.*

7.7.2 Channel and Pipe Flows

So back to question one. Here in a nutshell is the answer: Let's consider two simple changes to the closure solution presented above; i.e.,

$$u_*^2 = \nu_t \frac{\partial U}{\partial y} \tag{7.43}$$

Consider the following:

- We are in a flow region where the viscous stress is negligible.
- The only parameters we have to work with are the distance from the wall, y, and the friction velocity, u_*.

It follows immediately **on dimensional grounds alone** that:

$$\nu_t = C u_* [y + a] \tag{7.44}$$

where the coefficient C must be exactly constant in the limit of infinite Reynolds number as must the additive "offset" a. Note that an offset is necessary since we really don't have any idea how big an eddy is relative to the wall, nor what the effect of the viscous sublayer beneath us is.

For the flows homogeneous in x, we can take $C(Re)$ and $a = a(Re)$ to be Reynolds number dependent, but independent of y. This implies we can integrate equation 7.43 using equation 7.44 to obtain:
homogeneous flows

$$u^+ = C_i(Re) \ln[y^+ + a(RE)^+] + B_i(Re) \tag{7.45}$$

for all our observations that suggest it is not. Turbulence 'experts' are capable of these kinds of arguments too.

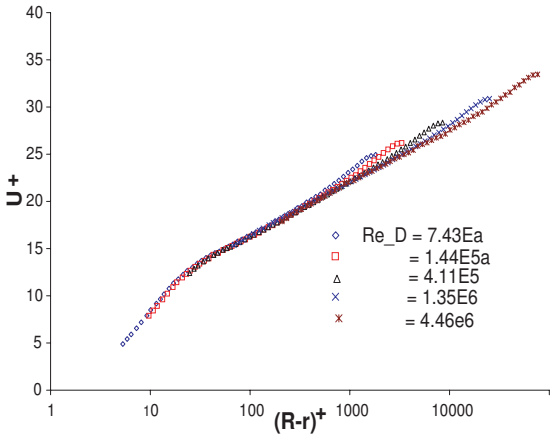

Figure 7.5: Five velocity profiles in inner variables. Superpipe data of McKeon *et al.* 2004a.

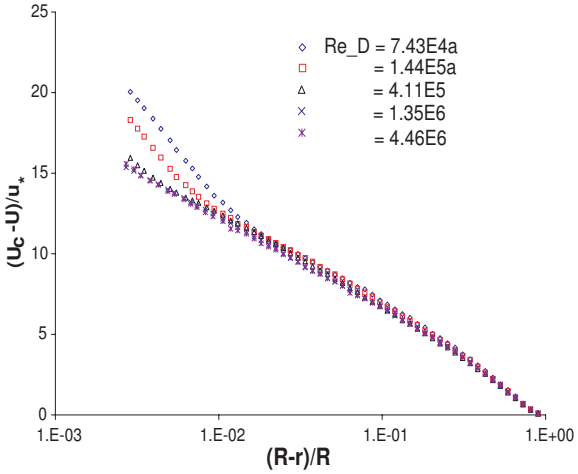

Figure 7.6: Five velocity profiles in outer variables. Superpipe data of McKeon *et al.* 2004a.

where $B(Re)$ is the integration constant. Since in the limit of infinite Reynolds number, our original momentum equation was independent of Reynolds number, then so must our solution be in the same limit; i.e.

$$B_i(Re) \rightarrow B_{i\infty} \tag{7.46}$$
$$C_i(Re) \rightarrow C_{i\infty} \tag{7.47}$$
$$a(Re)^+ \rightarrow a^+_\infty \tag{7.48}$$

This is, of course, the usual log law – but with an offset. And $C_{i\infty} = 1/\kappa$ is the inverse of the usual von Karman "constant". A much more formal derivation is included in the appendix to this chapter, which avoids both the problems raised earlier about the pressure gradient and the need to assume a particular turbulence model.

There really aren't many high Reynolds number channel simulations, but the same considerations can be applied to turbulent pipe flows. And there are some really impressively high Reynolds number pipe flow experiments that were conducted by Beverly McKeon, Lex Smits and their co-workers using the superpipe facility at Princeton. As can clearly be seen in Figures 7.5 and 7.6, the superpipe data really does show the expected logarithmic region, and it's extent increases with increasing Reynolds number. It can also be argued theoretically for channel and pipe flows that there should also be a logarithmic friction law. Figure 7.7 shows that this seems to be true also.

7.7.3 Boundary Layers

The evidence above for the logarithmic profile and friction laws would seem to be rather convincing, at least for a pipe or channel. So what's the problem?

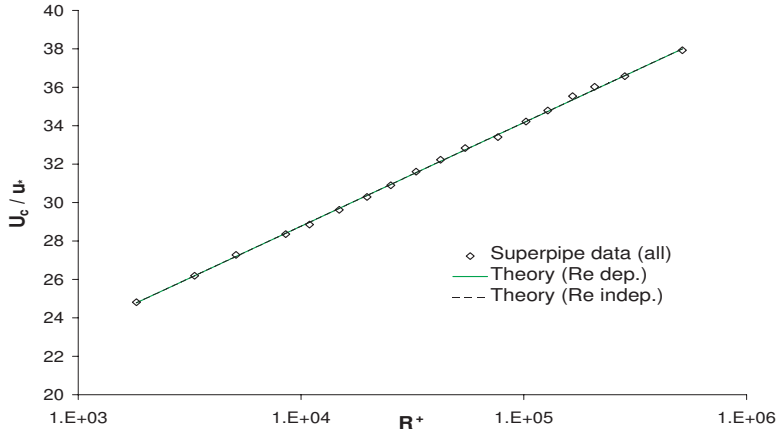

Figure 7.7: Plot of U_c/u_* versus R^+ using superpipe data of McKeon et al. (2004b).

The first problem we have to confront is what do we mean by infinite Reynolds number — which is of course the only limit in which our inner equations are valid anyway? For a parallel flow like a pipe or channel where all the x-derivatives of mean quantities are zero (i.e., homogeneous in x), this is no problem, since at least the local Reynolds number would not change with downstream distance. But for a developing flow like a boundary layer or wall jet it is a BIG problem since the further you go, the bigger the local Reynolds number gets, so you never stop evolving.

So we need to ask ourselves: how might things be different in a developing boundary layer. Many want to assume that nothing is different. But then the whole idea of a boundary layer is that it spreads, so it is the departures from a parallel flow that make it a boundary layer in the first place. The most obvious way (maybe the only way) to account for the variation of the local Reynolds number as the flow develops is to include a factor $y^{+\alpha}$ in our eddy viscosity; i.e.,

$$\nu_t = C(Re)[y^+]^\alpha \, u_* y \tag{7.49}$$

where α can depend on the local Reynolds number.

Since we know the flow very near the wall is almost parallel, it is obvious that α is going to be have to be quite small. But it is easy to show that no matter how small α is, unless it is identically zero our equation will never integrate to a logarithm. In fact, we obtain:

$$u^+ = C_i(Re)[y^+ + a^+]^\alpha + B_i(Re) \tag{7.50}$$

where as before all the parameters must be asymptotically constant. As you can see this is a power law. It can become a log law only if α is asymptotically zero, which of course would mean that the boundary layer has stopped growing. This seems unlikely, at least to me.

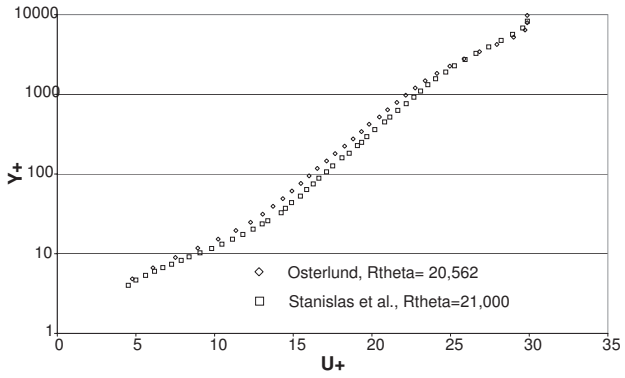

Figure 7.8: Comparison of mean velocity pro- files from Österlund (2000) at $R_\theta = 20,562$ and Stanislas *et al.* (2006) at $R_\theta = 21,000$.

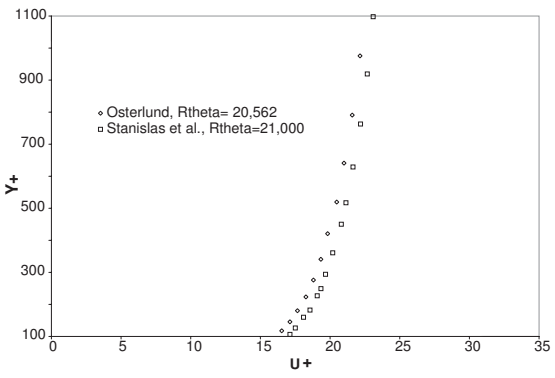

Figure 7.9: Expanded linear-linear plot of data in figure **??** from $100 < y^+ < 1,100$.

On the other hand, suppose the flow is exactly parallel, like a channel or a pipe. Then our α would be **exactly** zero, and we get a logarithmic profile. This is to me one of the great and beautiful mysteries of calculus: how a tiny infinitesimal can change a logarithm to a power law.

In fact, other arguments based on functional analysis and quite independent of closure models can produce the same results, and show that the additive parameter for the power law is identically zero. Moreover, it is possible using a powerful new method called *Near-asymptotics* to actually deduce the Reynolds number dependence of most of the parameters in both the log and the power laws. This is an area still undergoing development at the moment. My advice is: reject any simple argument which dismisses these new developments. They may not be as simple as the old log law, but they might have the advantage of being correct.

Boundary layer developments over the past decade have been discussed in detail in a recent paper (George 2006 AIAA Journal) from the perspective of the ideas presented here, so the very brief summary below will not suffice for a careful reading of that paper. The primary concerns are twofold: first the apparent lack of a consistent theory for the log law in boundary layers; and second, the validity of the experiments. Both these are discussed below.

First, there is good reason to believe that the underlying log theory utilized above so convincingly for pipe/channel flow does not apply to boundary layers. The theory for pipe and channel flows depends crucially on the existence of the Reynolds number independent limits of the scaled profiles. If the inner and outer profiles do not both scale with u_*, then there is no possibility of a logarithmic profile in the overlap region. Because the boundary layer is not homogeneous in the streamwise direction, there is no theoretical argument that can be used to justify an outer deficit law for boundary layers using u_* (as described in detail in George 2006 and George and Castillo 1997). Thus in the absence of supporting theory, any further inferences based on this deficit scaling are at most built on a

foundation of empiricism, no matter how good the empirical collapse over some range of the data.

In spite of the theoretical objections, there is still evidence that a log friction law with $\kappa = 0.38$ is an accurate description of at least the friction law for the boundary layer (e.g., Österlund 2000, Nagib *et al.* 2004), and perhaps even the velocity profiles. In an effort to resolve the apparent paradox, George (2006) suggested these might represent the leading terms in a logarithmic expansion of the power law solutions, and showed that a value near 0.38 was consistent with the power law coefficients. In fact, the dependence of the skin friction (or equivalently, u_*/U_∞) on Reynolds number (or δ^+) that results from a power law theory (which is theoretically defensible from first principles, George and Castillo 1997), are virtually indistinguishable from the log law fits to the same power law theoretical curves.

Whatever the reason for the apparent success of the log law in zero pressure gradient boundary layers, in the absence of a consistent log theory for the boundary layer (or any developing wall-bounded flow), there is no reason to believe that logarithmic friction and velocity laws for boundary layers should be linked to those for pipes and channels, no matter how good the empirical curve fits. The consequences of this are quite important, since it means that boundary layers could be quite well described by logarithms with $\kappa = 0.38$, independent of all other considerations.

Second, there are reasons to believe there are significant problems with at least some of the boundary layer mean velocity measurements that have been used to argue for the log law with $\kappa = 0.38$. George (2006) pointed out that the recent results from Nagib *et al.* (2004) are not consistent with the momentum integral, differing by as much as 30-40%.[5] Thus either the flow is not a two-dimensional incompressible smooth wall turbulent boundary layer, or the skin friction and/or velocity measurements are in error.

George (2006) also considered in detail the other extensive and relatively recent set of mean velocity measurements by Österlund 2000. Contrary to the claims made by Österlund *et al.* (2000), these data were shown to be equally consistent with either log or power law curve fits, and in fact the curve fits were indistinguishable. It was also pointed out that in the absence of Reynolds stress measurements, there was no way to confirm that any of the measured profiles were consistent with the mean equations of motion. This was of considerable concern, since unlike earlier boundary data (e.g., Smith & Walker (1959)), the Österlund data showed virtually no Reynolds number dependence in the overlap region, but did in the outer region of the flow (where one would least expect to find it).

The afore-mentioned concern about the Österlund experiment was considerably heightened by recent results from on-going experiments at the Lille boundary layer facility (mentioned above) by Stanislas and co-workers (see Carlier and

[5]This problem seems to have disappeared in more recently reported versions of this data, but with no explanation offered. The data have still not been made available to the general public as of this writing.

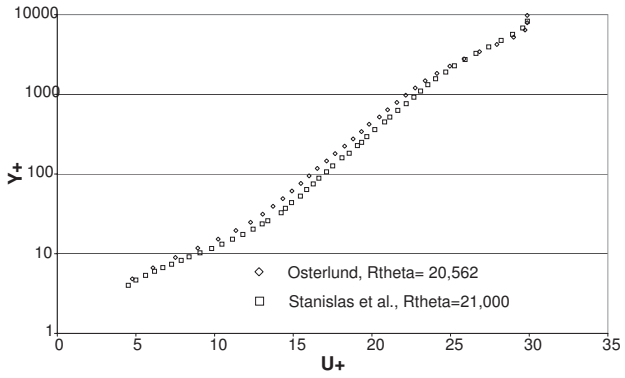

Figure 7.10: Comparison of mean velocity profiles from Österlund (2000) at $R_\theta = 20,562$ and Stanislas *et al.* (2006) at $R_\theta = 21,000$.

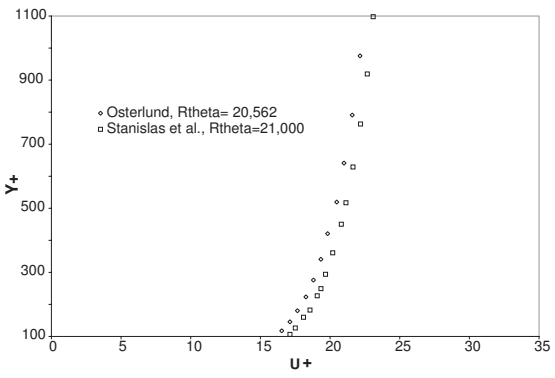

Figure 7.11: Expanded linear-linear plot of data in figure **??** from $100 < y^+ < 1,100$.

Stanislas *et al.* 2004), Stanislas *et al.* 2006), which became available to me in the course of preparing this paper. Their mean velocity profile obtained at $R_\theta = 21,000$ is plotted in Figure 7.10 along with the corresponding profile from Österlund (2000). The friction coefficients for the two experiments were almost exactly the same (meaning the normalized shear stresses were in agreement), as is evident from the near overlay of the curves at the largest distances from the wall (effectively U_∞/u_*). This is encouraging, since the Österlund shear stress was estimated using an oil film method, and the Lille result obtained by micro-PIV. Incidentally, the latter value differs by about 3.5% from the shear stress estimated using the Clauser chart on the Lille data, a substantial difference in view of the questions being asked.

By contrast to the data at large distances from the wall, the mean velocity profiles near the wall (inside $0.15\delta_{99}$ or $y^+ < 1200$) differ substantially until they come together again inside $y^+ = 10$. Figure 7.11 shows a linear-linear plot of both sets of data showing only the region from $100 < y^+ < 1,100$. The two profiles appear virtually identical over this range, but shifted in both velocity and position. This is difficult to understand. Both sets of measurements were obtained using hot-wire anemometry, so there is no obvious reason for the difference. The Lille profiles, however, were confirmed by more sparsely spaced PIV measurements. Moreover the Lille profiles are consistent with the measured Reynolds stress profiles (from PIV) and the differential equations of motion.

Both the log profile and power law profile, $U^+ = C_i(y^+ + a^+)^\gamma$, can be optimized to fit the Lille velocity profiles to within 0.2% for $50 < y^+ < 0.1\delta^+$. This was no surprise, since as pointed out by George (2006), the functional forms are indistinguishable, at least over the range of data available. The results for γ, C_o, C_i and a^+ were 0.119, 0.97, 9.87 and -8.3 respectively, different from the earlier estimates of George and Castillo (1997) as expected since the data were different than that previously considered. The values for the logarithmic fit, on the other

hand, were quite surprising given the difference in the measured profiles, since the optimal values were 0.384, 4.86, -2.03, and 4 for κ, B_i, B_o and a^+ respectively. By comparison, the log values for the Österlund profile were $\kappa = 0.384$, $B_i = 4.16$, and $a^+ = 0$.

In other words, the values of κ from the log curve fits to the Stanislas *et al.* and Österlund experiments were identical, even though the profiles and other constants differed substantially. Thus in spite of the differences and shortcomings of the various experiments (which remain to be explained and reconciled), there would appear to be increasing evidence for $\kappa = 0.38$ (or even 0.384) for boundary layers.

7.7.4 Summary and conclusions

So in summary, there is no justification, theoretical or experimental, for a *universal* log law for all wall-bounded flows, no matter how aesthetically appealing or potentially useful an idea. At very least, boundary layers and pipe/channel flows are fundamentally different. Or viewed another way, the 'log law' represents the inertial region of pipes, channels and boundary layers to about the same degree that their underlying equations have the same terms, which is to within about 10%. Thus the historical value of $\kappa = 0.41$ is probably best seen as a compromise for different flows, accurate to within these limits.

The log theory does apply quite rigorously to pipe flows with $\kappa = 0.43$, and perhaps to other wall-bounded flows homogeneous in horizontal planes (e.g., channels, Couette flow, the neutral planetary boundary layer, etc.). But it is a power law theory for the boundary layer that can be derived from first principles using equilibrium similarity analysis and near-asymptotics. This theory predicts (without additional assumptions) a number of things that have also been observed, but which require additional hypotheses with a log theory. Among them are: differing outer scales for the normal and shear stress components (U_o^2 and u_*^2 respectively), the consequent dependence of the turbulence properties of boundary layers in the overlap region on mixed scales, and the dependence of pressure fluctuations on the ratio U_o/u_*. Moreover, the same principles can be used to predict different results for different flows (like wall-jets and boundary layers with pressure gradient), again as observed.

Nonetheless, theoretical arguments notwithstanding, the log 'law' also appears to apply to developing boundary layers. If not the leading term in a logarithmic expansion of the power law solution, it is at least a local and empirical description And to the degree that developing boundary layers can be described this way, the value of κ for them appears (at least at this time) to be about 0.38.

Appendix: Formal derivation of log profiles for pipe flow

The derivation of the log law for pipe and channel flows can be carried out much more rigorously than presented above, and quite independent of any eddy viscosity model. This derivation also avoids any problems one might infer from the arguments above (and the DNS data) about the importance of the pressure gradient. The problem is that for pipe and channel flows is that there is really no constant Reynolds stress region nor any region where the pressure gradient can be ignored. We owe to Isakson (1937) and Millikan (1938) the original arguments that the contrary is true. The basic arguments have been presented in detail in many texts (e.g., Tennekes and Lumley 1972, Panton 1996 and in slightly more general form in Wosnik *et al.* 2000), and will only be summarized here. We will present them for pipe flow only, since experiments in pipes are much easier to realize at high Reynolds numbers than in channels, in part due to the difficulty of maintaining a two-dimensional mean flow in the latter. The superpipe data of Zagorola and Smits (1998), for example, go as high as $R^+ = 500,000$. The basic theoretical arguments for channels, however, are the same.

The counterpart to equation 7.36 for fully-developed flow in an axisymmetric pipe with smooth walls is:

$$0 = -\frac{1}{\rho}\frac{\partial P}{\partial x} + \frac{1}{r}\frac{\partial}{\partial r} r \left[-\langle uv \rangle + \nu \frac{\partial U}{\partial r} \right] \tag{7.51}$$

where r is measured from the pipe centerline, and U, u and v are to be interpreted as corresponding to the streamwise and radial velocity components respectively. Since P is nearly independent of r, we can multiply by r and integrate from the wall, R, to the running coordinate, r, to obtain the counterpart to equation 7.37 as:

$$u_*^2 = \left(\frac{r}{R}\right) \left[-\langle uv \rangle + \nu \frac{\partial U}{\partial r} \right] - \frac{1}{2} \frac{(R^2 - r^2)}{R} \frac{1}{\rho} \frac{dP}{dx} \tag{7.52}$$

Integration all the way to the centerline ($r = 0$) yields the relation between the pipe radius, the wall shear stress and the imposed pressure gradient as:

$$u_*^2 = -\frac{R}{2\rho} \frac{dP}{dx} \tag{7.53}$$

Thus of the four parameters in the equation, R, ν, $(1/\rho)dP/dx$ and u_*^2, only three are independent. It follows immediately from dimensional analysis that the mean velocity for the entire flow can be written in either of two ways:

$$\frac{U}{u_*} = f_i(r^+, R^+) \tag{7.54}$$

and

$$\frac{U - U_c}{u_*} = f_o(\overline{r}, R^+) \tag{7.55}$$

where U_c is the mean velocity at the centerline, $R^+ = u_* R/\nu$ is the ratio of outer to inner (or viscous) length scales, $r^+ = r u_*/\nu$ is an 'inner' normalization of r, and $\overline{r} = r/R$ is an 'outer' normalization of r. Note that the velocity difference from the centerline, or 'velocity deficit', is used in the last expression to avoid having to take account of viscous effects as $R^+ \to \infty$.

Figures 7.5 and 7.6 show some of the recent superpipe data of McKeon *et al.* (2004b) plotted in 'inner' and 'outer' variables respectively. (Note that the conventional labels 'inner' and 'outer' may appear opposite to the what they should be, since the 'outer' is really the core region for the pipe and 'inner' is a thin region closest to the pipe walls.) Clearly the inner scaled profiles appear to collapse near the wall, nearly collapse over a large intermediate range, and diverge when $(R - r)/R > 0.1$ or so. This means that the extent of the region of near-collapse *in inner variables* increases indefinitely as the Reynolds number, R^+, increases. One might easily infer that in this region of near-collapse, the collapse will also improve to some asymptotic limiting profile (in inner variables). Similarly the outer scaled profiles appear to nearly collapse as long as $R^+ - r^+ > 300 - 500$ approximately, and again one could infer that the region of collapse might improve and continue all the way to the wall if the Reynolds number increased without bound.

We can define hypothetical 'inner' and 'outer' limiting profiles as $f_{i\infty}(r^+)$ and $f_{o\infty}(\overline{r})$ respectively; i.e.,

$$lim_{R^+ \to \infty} f_i(r^+, R^+) = f_{i\infty}(r^+) \tag{7.56}$$

$$lim_{R^+ \to \infty} f_o(\overline{r}, R^+) = f_{o\infty}(\overline{r}) \tag{7.57}$$

For finite values of R^+, both equations 7.56 and 7.57 describe functionally the entire profile, and R^+ acts as a parameter to distinguish the curves when they diverge. To see how they differ, consider the limit as $R^+ \to \infty$. Clearly viscosity has disappeared entirely from $f_{o\infty}(\overline{r})$, so it can at most represent the mean velocity profile away from the near wall region where viscous effects are not important. By contrast, $f_{i\infty}(r^+)$ can only describe the very near wall region, since it has retained no information about R.

Now it is possible that the two limiting profiles, $f_{i\infty}$ and $f_{o\infty}$, don't link up; i.e., neither describes the flow far enough toward the pipe center in the first case and toward the wall in the latter that they both describe a common region. But suppose they do (Millikan's great idea), so that both the inner and outer scalings have a common (or overlap) region. Or thought of another way: can we 'stretch' the region over which the inner region collapses the data so that it overlaps a similar 'stretch' in the other direction of the outer scaled version?

In fact there are a variety of ways to show that the answer is yes. The traditional way is to set the inner limit of f_o equal to the outer limit of f_i and ask

whether there can be a solution in the limit of infinite Reynolds number. Similar results can be obtained by matching derivatives in the limit (c.f., Tennekes and Lumley 1972), or using matched asymptotic expansions (e.g., Panton 1996). Alternatively, Wosnik *et al.* (2000) used the methodology of near asymptotics to seek *not an overlap region*, but instead a common region which survives at finite Reynolds number as the limits are approached. Regardless, **all** of the methodologies conclude that the mean velocity profile in the common (or overlap) region should be logarithmic and given by the following equations:

$$\frac{U - U_c}{u_*} = \frac{1}{\kappa} \ln\left(1 - \overline{r} + \overline{a}\right) + B_o \tag{7.58}$$

$$\frac{U}{u_*} = \frac{1}{\kappa} \ln\left(R^+ - r^+ + a^+\right) + B_i \tag{7.59}$$

where $\overline{a} = a/R$, $a^+ = a u_*/\nu$ and a is a spatial offset which is a necessary consequence of the need for invariance (c.f., Oberlack 2001, Wosnik *et al.* 2000). In addition, the friction velocity and centerline velocity must be related by the following relationship (or friction law):

$$\frac{U_c}{u_*} = \frac{1}{\kappa} \ln\ R^+ + C \tag{7.60}$$

where

$$C = B_i - B_o \tag{7.61}$$

Thus it is not enough to simply draw a logarithmic curve on a friction plot or an inner velocity plot and conclude anything more than that an empirical fit is possible. In fact empirical log fits always always seem to work, at least over some limited range, for just about any curve. Therefore it is only when fits to all the three plots (friction, inner and outer mean velocity) can be linked together with common parameters using equations 7.58 to 7.61 that it can truly be concluded that pipe/channel flows are logarithmic and that theory and experiment agree.

The asymptotic theories conclude that κ, B_i, and B_o must be constant, but only because the matching is done in the limit as $R^+ \to \infty$. Near-asymptotics, by contrast tells how these limits are approached (inversely with powers of $\ln R^+$) and also how the different parameters are linked together; i.e., they must either be independent of R^+ or satisfy:

$$\ln R^+ \frac{d}{d \ln R^+}(1/\kappa) = \frac{d}{d \ln R^+}(B_i - B_o) \tag{7.62}$$

But regardless of whether κ, B_i or B_o are constants (i.e., independent of Reynolds number) or only asymptotically constant, only two of them can be chosen independently.

So how well does this work? Quite well actually. Figure 7.7 shows data for U_c/u_* from the superpipe experiments of McKeon *et al.* (2004a), along with

several logarithmic fits to the data, both with average rms errors of about 0.2%. One curve uses constant values of κ and C, and another the variable Reynolds number version proposed by Wosnik et al. 2000. The values of κ and $C = B_i - B_o$ were 0.427 and 7.19 for the constant parameter (Reynolds number *independent*) analysis, while the limiting values for κ_∞ and $C_\infty = B_{i\infty} - B_{o\infty}$ for the Reynolds number *dependent* analysis were 0.429 and 7.96 respectively. The reason for the difference between the two values of C can be seen by examining the Reynolds number dependence in the Wosnik et al. theory for which:

$$C_i = C_{i\infty} + \frac{(1+\alpha)A}{(\ln R^+)^\alpha} \tag{7.63}$$

$$\frac{1}{\kappa} = \frac{1}{\kappa_\infty} - \frac{\alpha A}{(\ln R^+)^{1+\alpha}} \tag{7.64}$$

Substituting these into equation 7.60 yields the refined friction law as:

$$\frac{U_c}{u_*} = \frac{1}{\kappa_\infty} \ln\ R^+ + C_\infty + \frac{A}{(\ln R^+)^\alpha}, \tag{7.65}$$

All of the extra Reynolds number dependence is in the last term of equation 7.65, and in fact it is this term which 'adjusts' C from its asymptotic value of 7.96 to 7.19 over the range of the experiments. For this data set the optimal values of α and A were given by -0.932 and 0.145 respectively, so the variation in κ over the entire range of the data was only from 0.426 to 0.427. The corresponding variation of the last term in the friction law, however, was from -0.690 to -0.635, enough to account for the slight lack of collapse of the mean velocity profiles in outer variables noted in figure 7.6.

Note that the constants determined by the Wosnik *et al.* 2000 used an earlier (and 'uncorrected') form of the superpipe data, which showed a slightly different Reynolds number dependence. The differences are due to the static hole corrections in the new data set. Unlike the conclusions from earlier versions of the superpipe data, there would appear to be little reason to consider the Reynolds number dependent version superior.

Table 7.1 summarizes the parameters from individual fits to five of the McKeon *et al.* (2004a) profiles selected to cover the entire range of the data. The value of κ determined from the friction data was taken as given, and the values of B_i and a were determined from a regression fit of each inner profile between $50 < (R-r)^+ < 0.1R^+$. The average rms errors are approximately 0.2% for all inner profiles. These same values, together with $C = B_i - B_o$, were then used to determine B_o, by optimizing the fit to the same profile in outer variables over the same range. The values of κ are remarkably constant, as are those of B_i. There might be a slight Reynolds number trend in the values of B_o. In view of the closest distance to the wall which can be measured (relative to a^+), the variation in a^+ is probably random positioning errors.

$Re_D \times 10^{-5}$	0.743	1.44	4.11	13.5	44.6
$R^+ \times 10^{-3}$	1.82	3.32	8.51	25.2	76.4
κ	0.426	0.426	0.427	0.427	0.427
B_i	5.62	5.50	5.64	5.87	5.85
B_o	-1.65	1.77	-1.65	-1.43	-1.46
a^+	-1.33	-1.34	-5.10	-11.9	-1.5
% errin	0.169	0.269	0.427	3.26e-04	0.188
% errout	0.657	1.13	1.71	1.37	1.55

Table 7.1: Parameters for fits of log law to inner and outer profiles of McKeon *et al.* (2004a) using friction law values for Reynolds number dependent parameters.

If the Reynolds number dependence is truly negligible, then the inner and outer mean velocity profiles should collapse when different Reynolds numbers are plotted together as in Figures 7.5 and 7.6. The collapse of the profiles in inner variables is excellent, consistent with the observations that κ is nearly constant, and B_i and a^+ are nearly so. The outer variable plot does not collapse quite so well, especially over the range for which the profiles are logarithmic. This lends support for the variable Reynolds number approach, which shows that the only significantly Reynolds number dependent parameter is B_o. This has implications for the asymptotic friction law, however, since the asymptotic values of $C = B_i - B_o$ are different, 7.19 versus 7.96.

So where does this leave us? These experiments (and most other pipe experiments as well) show an almost perfect agreement with the theoretical predictions, both the asymptotic and near-asymptotic versions. Not only does there appear to be a region of logarithmic behavior in the mean velocity profiles where we expected to find it ($30 - 50 < y^+ < 0.1 - 0.2R^+$), the parameters determined from fits to these and the logarithmic friction law satisfy the constraints among them. This is about the strongest experimental confirmation for a theory that can possibly be imagined.

So the analysis presented here (of part of the most recent version of the superpipe experiments) suggests strongly that the value of κ is about 0.43, a bit lower than the value of 0.44-0.45 suggested from the earlier uncorrected data and slightly higher than the estimate of McKeon *et al.* (2004a) of 0.42 using a larger set of the same data used herein. But all are higher than the earlier accepted value of 0.41, however, and most certainly not lower. The asymptotic value of the additive constant for the outer velocity profile (and friction law) can still be debated, but this debate in no way detracts from the overall conclusion. In spite of the absence of a constant total stress region (and hence the lack of validity of the early arguments for it), the logarithmic theory for a pipe flow can be taken as fact. One can infer this is probably also true for the channel, once data at sufficiently high Reynolds number becomes available to test it.

Part II: Two Point Equations of Turbulence

Chapter 8

Stationarity Random Processes

This chapter on stationary random processes does not really fit here if we were following the logical order of presentation of the material, since it has absolutely nothing to do with the chapters which immediately follow it. And it is a actually a bit dangerous to put it here, since it leads many people to the conclusion that the Reynolds-averaged equations of the next few chapters are valid only for stationary random processes. **This is absolutely false. The RANS equations are completely general, whether the under-lying statistical processes are stationary or not, since they have been averaged in the sense of the true (or ensemble) average of the preceding chapter.** Nonetheless there is an advantage pedagogically to putting this chapter here since many students at this point are trying to figure out how the results the preceding chapter apply to the time-varying (and often statistically) stationary processes they are seeing in the lab, or have seen in their experience. It is not hard to think of the finite time estimator for the time average, say U_T, as being related to the the finite sample estimator, X_N, of the preceding chapter, especially if the process is sampled digitally. It is not at all obvious, however, '*What constitutes an independent realization is the process is time-varying?*' This chapter both introduces the idea of a stationary random process, and answers this question. Much more detail about this important class of random process is included in the appendices, including a complete discussion of spectral analysis.

8.1 Processes statistically stationary in time

Many random processes have the characteristic that their statistical properties do not appear to depend directly on time, even though the random variables themselves are time-dependent. For example, consider the signals shown in Figures 2.2 and 2.5.

When the statistical properties of a random process are independent of time, the random process is said to be *stationary*. For such a process all the moments are time-independent, e.g., $\langle \tilde{u}(t) \rangle = U$, etc. Note that we have used a tilde

to represent the instantaneous value (i.e., $\tilde{u}(t)$), a capital letter to represent its average (i.e., $U = \langle\tilde{u}(t)\rangle$), and we define the fluctuation by a lower case letter (i.e., $u = \tilde{u}(t) - U$). Also since the process is assumed stationary, the mean velocity and velocity moments are time-independent. In fact, the probability density itself is time-independent, as should be obvious from the fact that the moments are time independent.

An alternative way of looking at *stationarity* is to note that *the statistics of the process are independent of the origin in time*. It is obvious from the above, for example, that if the statistics of a process are time independent, then $\langle u^n(t)\rangle = \langle u^n(t+T)\rangle$, etc., where T is some arbitrary translation of the origin in time. Less obvious, but equally true, is that the product $\langle u(t)u(t')\rangle$ depends only on the time difference $t' - t$ and not on t (or t') directly. This consequence of stationarity can be extended to any product moment. For example, $\langle u(t)v(t')\rangle$ can depend only on the time difference $t' - t$. And $\langle u(t)v(t')w(t'')\rangle$ can depend only on the two time differences $t' - t$ and $t'' - t$ (or $t'' - t'$) and not t, t' or t'' directly.

8.2 The autocorrelation

One of the most useful statistical moments in the study of stationary random processes (and turbulence, in particular) is the **autocorrelation** defined as the average of the product of the random variable evaluated at two times, i.e. $\langle u(t)u(t')\rangle$. Since the process is assumed stationary, this product can depend only on the time difference $\tau = t' - t$. Therefore the autocorrelation can be written as:

$$C(\tau) \equiv \langle u(t)u(t+\tau)\rangle \tag{8.1}$$

The importance of the autocorrelation lies in the fact that it indicates the "memory" of the process; that is, *the time over which a process is correlated with itself*. Contrast the two autocorrelations shown in Figure 8.1. The autocorrelation of a deterministic sine wave is simply a cosine as can be easily proven. Note that there is no time beyond which it can be guaranteed to be arbitrarily small since it always "remembers" when it began, and thus always remains correlated with itself. By contrast, a stationary random process like the one illustrated in the figure will eventually lose all correlation and go to zero. In other words it has a "finite memory" and "forgets" how it was. Note that one must be careful to make sure that a correlation really both goes to zero and *stays down* before drawing conclusions, since even the sine wave was zero at some points. Stationary random processes *always* have two-time correlation functions which eventually go to zero and stay there.

Example 1.

Consider the motion of an automobile responding to the movement of the wheels over a rough surface. In the usual case where the road roughness is ran-

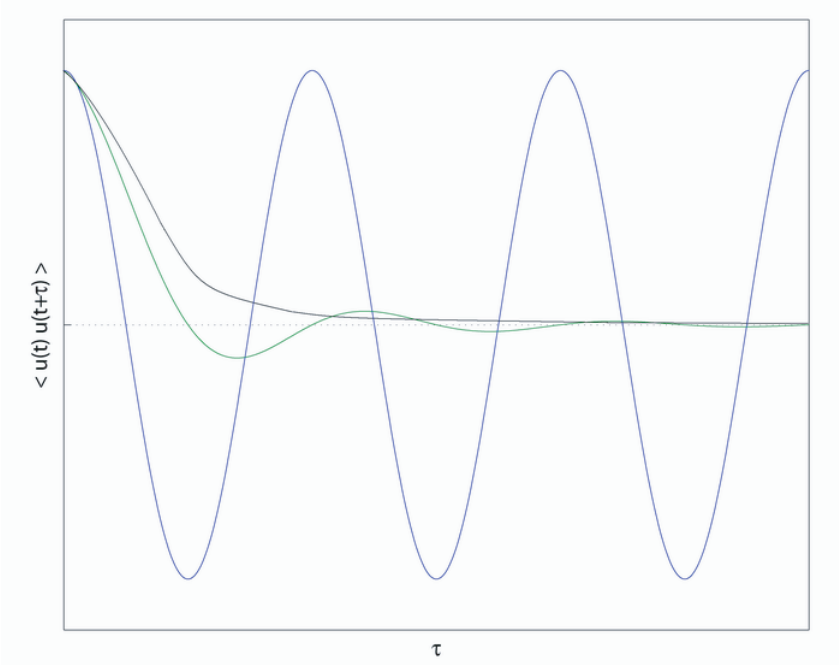

Figure 8.1: Autocorrelations for two random processes and a periodic one.

domly distributed, the motion of the car will be a weighted history of the road's roughness with the most recent bumps having the most influence and with distant bumps eventually forgotten. On the other hand if the car is traveling down a railroad track, the periodic crossing of the railroad ties represents a deterministic input and the motion will remain correlated with itself indefinitely. This can be a very bad thing if the tie crossing rate corresponds to a natural resonance of the suspension system of the vehicle.

Since a random process can never be more than perfectly correlated, it can never achieve a correlation greater than is value at the origin. Thus

$$|C(\tau)| \leq C(0) \tag{8.2}$$

An important consequence of stationarity is that the autocorrelation is symmetric in the time difference, $\tau = t' - t$. To see this simply shift the origin in time backwards by an amount τ and note that independence of origin implies:

$$\langle u(t)u(t+\tau)\rangle = \langle u(t-\tau)u(t)\rangle = \langle u(t)u(t-\tau)\rangle \tag{8.3}$$

Since the right hand side is simply $C(-\tau)$, it follows immediately that:

$$C(\tau) = C(-\tau) \tag{8.4}$$

8.3 The autocorrelation coefficient

It is convenient to define the *autocorrelation coefficient* as:

$$\rho(\tau) \equiv \frac{C(\tau)}{C(0)} = \frac{\langle u(t)u(t+\tau)\rangle}{\langle u^2\rangle} \tag{8.5}$$

where

$$\langle u^2\rangle = \langle u(t)u(t)\rangle = C(0) = var[u] \tag{8.6}$$

Since the autocorrelation is symmetric, so is its coefficient, i.e.,

$$\rho(\tau) = \rho(-\tau) \tag{8.7}$$

It is also obvious from the fact that the autocorrelation is maximal at the origin that the autocorrelation coefficient must also be maximal there. In fact from the definition it follows that

$$\rho(0) = 1 \tag{8.8}$$

and

$$\rho(\tau) \leq 1 \tag{8.9}$$

for all values of τ.

8.4 The integral scale

One of the most useful measures of the length of time a process is correlated with itself is the integral scale defined by

$$T_{int} \equiv \int_0^\infty \rho(\tau)d\tau \tag{8.10}$$

It is easy to see why this works by looking at Figure 8.2. In effect we have replaced the area under the correlation coefficient by a rectangle of height unity and width T_{int}.

8.5 The temporal Taylor microscale

The autocorrelation can be expanded about the origin in a MacClaurin series; i.e.,

$$C(\tau) = C(0) + \tau \left.\frac{dC}{d\tau}\right|_{\tau=0} + \frac{1}{2}\tau^2 \left.\frac{d^2C}{d\tau^2}\right|_{\tau=0} + \frac{1}{3!}\tau^3 \left.\frac{d^3C}{dt}\right|_{\tau=0} \tag{8.11}$$

But we know the autocorrelation is symmetric in τ, hence the odd terms in τ must be identically zero (i.e., $dC/d\tau|_{\tau=0} = 0$, $d^3/d\tau^3|_{\tau=0}$, etc.). Therefore the expansion of the autocorrelation near the origin reduces to:

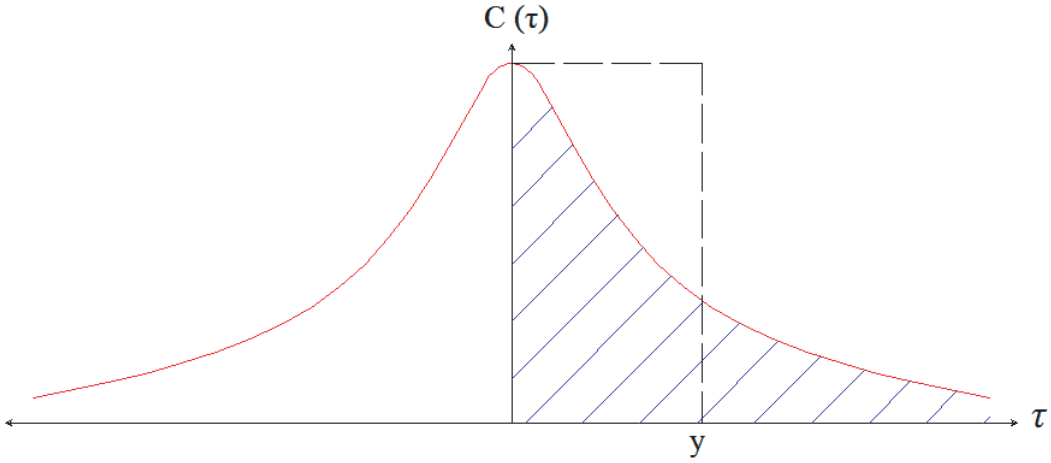

Figure 8.2: The autocorrelation coefficient showing relation of the integral scale to the area under the autocorrelation coefficient curve.

$$C(\tau) = C(0) + \frac{1}{2}\tau^2 \left.\frac{d^2C}{d\tau^2}\right|_{\tau=0} + \cdots \tag{8.12}$$

Similarly, the autocorrelation coefficient near the origin can be expanded as:

$$\rho(\tau) = 1 + \frac{1}{2} \left.\frac{d^2\rho}{d\tau^2}\right|_{\tau=0} \tau^2 + \cdots \tag{8.13}$$

where we have used the fact that $\rho(0) = 1$. If we define $' = d/d\tau$ we can write this compactly as:

$$\rho(\tau) = 1 + \frac{1}{2}\rho''(0)\tau^2 + \cdots \tag{8.14}$$

Since $\rho(\tau)$ has its maximum at the origin, obviously $\rho''(0)$ must be negative.

We can use the correlation and its second derivative at the origin to *define* a special time scale, λ_τ (called the Taylor microscale [1]) by:

$$\lambda_\tau^2 \equiv -\frac{2}{\rho''(0)} \tag{8.15}$$

Using this in equation 8.14 yields the expansion for the correlation coefficient near the origin as:

$$\rho(\tau) = 1 - \frac{\tau^2}{\lambda_\tau^2} + \cdots \tag{8.16}$$

[1]The Taylor microscale is named after the famous English scientist G.I. Taylor who invented it in the 1930's. Among his many other accomplishments he designed the CQR anchor which is still found on many boats today.

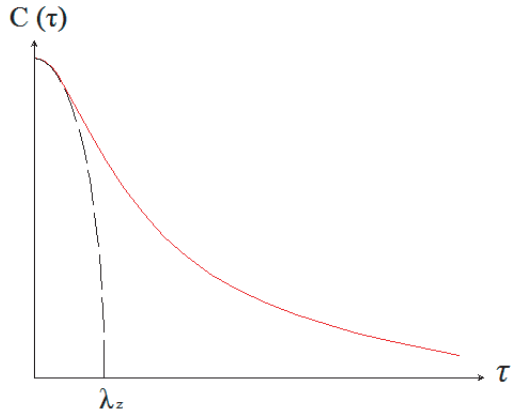

Figure 8.3: The autocorrelation coefficient for positive time lags together with its oscullating parabola showing the Taylor microscale.

Thus very near the origin the correlation coefficient (and the autocorrelation as well) simply rolls off parabolically; i.e.,

$$\rho(\tau) \approx 1 - \frac{\tau^2}{\lambda_\tau^2} \tag{8.17}$$

This parabolic curve is shown in Figure 8.3 as the osculating (or 'kissing') parabola which approaches zero exactly as the autocorrelation coefficient does. The intercept of this osculating parabola with the τ-axis is the Taylor microscale, λ_τ.

The Taylor microscale is significant for a number of reasons. First, for many random processes (e.g., Gaussian), the Taylor microscale can be proven to be the average distance between zero-crossing of a random variable in time. This is approximately true for turbulence as well. Thus one can quickly estimate the Taylor microscale by simply observing the zero-crossings using an oscilloscope trace.

The Taylor microscale also has a special relationship to the mean square time derivative of the signal, $\langle [du/dt]^2 \rangle$. This is easiest to derive if we consider two stationary random signals, say u and u', we obtain by evaluating the same signal at two different times, say $u = u(t)$ and $u' = u(t')$. The first is only a function of t, and the second is only a function of t'. The derivative of the first signal is du/dt and the second du'/dt'. Now lets multiply these together and rewrite them as:

$$\frac{du'}{dt'}\frac{du}{dt} = \frac{d^2}{dtdt'}u(t)u'(t') \tag{8.18}$$

where the right-hand side follows from our assumption that u is not a function of t' nor u' a function of t.

Now if we average and interchange the operations of differentiation and averaging we obtain:

$$\langle \frac{du'}{dt'} \frac{du}{dt} \rangle = \frac{d^2}{dtdt'} \langle u\ u' \rangle \tag{8.19}$$

Here comes the first trick: $u\ u'$ is the same as $u(t)u(t')$, so its average is just the autocorrelation, $C(\tau)$. Thus we are left with:

$$\langle \frac{du'}{dt'} \frac{du}{dt} \rangle = \frac{d^2}{dtdt'} C(t' - t) \tag{8.20}$$

Now we simply need to use the chain-rule. We have already defined $\tau = t' - t$. Let's also define $\xi = t' + t$ and transform the derivatives involving t and t' to derivatives involving τ and ξ. The result is:

$$\frac{d^2}{dtdt'} = \frac{d^2}{d\xi^2} - \frac{d^2}{d\tau^2} \tag{8.21}$$

So equation 8.23 becomes:

$$\langle \frac{du'}{dt'} \frac{du}{dt} \rangle = \frac{d^2}{d\xi^2} C(\tau) - \frac{d^2}{d\tau^2} C(\tau) \tag{8.22}$$

But since C is a function only of τ, the derivative of it with respect to ξ is identically zero. Thus we are left with:

$$\langle \frac{du'}{dt'} \frac{du}{dt} \rangle = -\frac{d^2}{d\tau^2} C(\tau) \tag{8.23}$$

And finally we need the second trick. Let's evaluate both sides at $t = t'$ (or $\tau = 0$ to obtain the *mean square derivative* as:

$$\langle \left(\frac{du}{dt} \right)^2 \rangle = - \left. \frac{d^2}{d\tau^2} C(\tau) \right|_{\tau=0} \tag{8.24}$$

But from our definition of the Taylor microscale and the facts that $C(0) = \langle u^2 \rangle$ and $C(\tau) = \langle u^2 \rangle \rho(\tau)$, this is exactly the same as:

$$\langle \left(\frac{du}{dt} \right)^2 \rangle = 2 \frac{\langle u^2 \rangle}{\lambda_\tau^2} \tag{8.25}$$

This amazingly simple result is very important in the study of turbulence, especially after we extend it to spatial derivatives.

8.6 Time averages of stationary processes

It is common practice in many scientific disciplines to define a time average by integrating the random variable over a fixed time interval, i.e.,

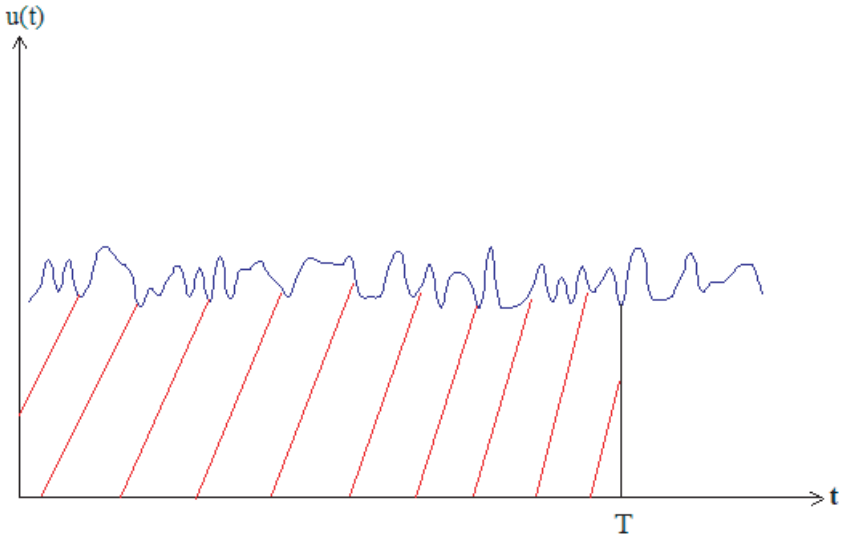

Figure 8.4: Integration of random time signal from 0 to T is area under the signal

$$U_T \equiv \frac{1}{T}\int_{T_1}^{T_2} \tilde{u}(t)dt \tag{8.26}$$

For the stationary random processes we are considering here, we can define T_1 to be the origin in time and simply write:

$$U_T \equiv \frac{1}{T}\int_{0}^{T} \tilde{u}(t)dt \tag{8.27}$$

where $T = T_2 - T_1$ is the integration time.

Figure 8.4 shows a portion of a stationary random signal over which such an integration might be performed. The time integral of $\tilde{u}(t)$ over the interval (O, T) corresponds to the shaded area under the curve. Now since $\tilde{u}(t)$ is random and since it forms the upper boundary of the shaded area, it is clear that our estimator for the time average over the interval $(0, T)$, U_T, is itself random and will depend on which particular section of the signal is being integrated. Thus, U_T is a lot like the estimator for the mean based on a finite number of independent realizations, X_N we encountered earlier in Section 2.5.

It will be shown in the analysis presented below that *if the signal is stationary*, the time average defined by equation 8.27 is an unbiased estimator of the true average U. Moreover, the estimator converges to U as the time becomes infinite; i.e., for stationary random processes

$$U = \lim_{T\to\infty} \frac{1}{T}\int_{0}^{T} \tilde{u}(t)dt \tag{8.28}$$

Thus the time and ensemble averages are equivalent in the limit as $T \to \infty$, *but only for a stationary random process.*

8.7 Bias and variability of time estimators

It is easy to show that the estimator, U_T, is unbiased by taking its ensemble average; i.e.,

$$\langle U_T \rangle = \langle \frac{1}{T} \int_0^T \tilde{u}(t)dt \rangle = \frac{1}{T} \int_0^T \langle \tilde{u}(t) \rangle dt \tag{8.29}$$

Since the process has been assumed stationary, $\langle u(t) \rangle$ is independent of time. It follows that:

$$\langle U_T \rangle = \frac{1}{T} \langle \tilde{u}(t) \rangle T = U \tag{8.30}$$

To see whether the estimate improves as T increases, the variability of U_T must be examined, exactly as we did for X_N earlier in Section 2.5.2. To do this we need the variance of U_T given by:

$$\begin{aligned} var[U_T] &= \langle [U_T - \langle U_T \rangle]^2 \rangle = \langle [U_T - U]^2 \rangle \\ &= \frac{1}{T^2} \langle \left\{ \int_0^T [\tilde{u}(t) - U]dt \right\}^2 \rangle \\ &= \frac{1}{T^2} \langle \int_0^T \int_0^T [\tilde{u}(t) - U][\tilde{u}(t') - U]dtdt' \rangle \qquad (8.31) \\ &= \frac{1}{T^2} \int_0^T \int_0^T \langle u(t)u(t') \rangle dtdt' \qquad (8.32) \end{aligned}$$

But since the process is assumed stationary $\langle u(t)u(t') \rangle = C(t'-t)$ where $C(t'-t) = \langle u^2 \rangle \rho(t'-t)$ is the correlation function defined earlier and $\rho(t'-t)$ is the correlation coefficient. Therefore the integral can be rewritten as:

$$\begin{aligned} var[U_T] &= \frac{1}{T^2} \int_0^T \int_0^T C(t'-t)dtdt' \qquad (8.33) \\ &= \frac{\langle u^2 \rangle}{T^2} \int_0^T \int_0^T \rho(t'-t)dtdt' \qquad (8.34) \end{aligned}$$

Now we need to apply some fancy calculus. If new variables $\tau = t' - t$ and $\xi = t' + t$ are defined, the double integral can be transformed to (see Figure 8.5):

$$var[U_T] = \frac{var[u]}{2T^2} \left[\int_0^T d\tau \int_\tau^{2T-\tau} d\xi \rho(\tau) + \int_{-T}^0 d\tau \int_{-\tau}^{2T+\tau} d\xi \rho(\tau) \right] \tag{8.35}$$

where the factor of 1/2 arises from the Jacobian of the transformation. The integrals over $d\xi$ can be evaluated directly to yield:

$$var[U_T] = \frac{var[u]}{2T^2} \left\{ \int_0^T [\rho(\tau)[T - \tau]d\tau + \int_{-T}^0 \rho(\tau)[T + \tau]d\tau \right\} \tag{8.36}$$

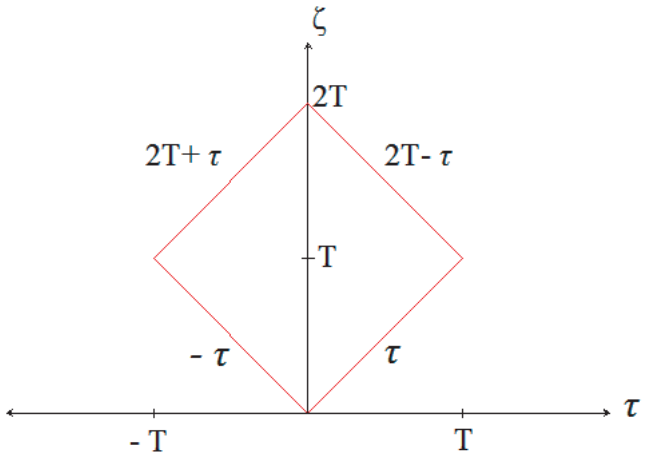

Figure 8.5: Integration domain for transformed variables.

By noting that the autocorrelation is symmetric, the second integral can be transformed and added to the first to yield at last the result we seek as:

$$var[U_T] = \frac{var[u]}{T} \int_{-T}^{T} \rho(\tau) \left[1 - \frac{|\tau|}{T}\right] d\tau \tag{8.37}$$

Now if our averaging time, T, is chosen so large that $|\tau|/T\langle < 1$ over the range for which $\rho(\tau)$ is non-zero, the integral reduces:

$$\begin{aligned} var[U_T] &\approx \frac{2var[u]}{T} \int_{0}^{T} \rho(\tau) d\tau \\ &= \frac{2T_{int}}{T} var[u] \end{aligned} \tag{8.38}$$

where T_{int} is the integral scale defined by equation 8.10. Thus the *variability* of our estimator is given by:

$$\epsilon^2_{U_T} = \frac{2T_{int}}{T} \frac{var[u]}{U^2} \tag{8.39}$$

Therefore the estimator does, in fact, converge (in mean square) to the correct result as the averaging time, T increases relative to the integral scale, T_{int}.

There is a direct relationship between equation 8.39 and equation 2.54 which gave the mean square variability for the ensemble estimate from a finite number of statistically independent realizations, X_N. Obviously the effective number of independent realizations for the finite time estimator is:

$$N_{eff} = \frac{T}{2T_{int}} \tag{8.40}$$

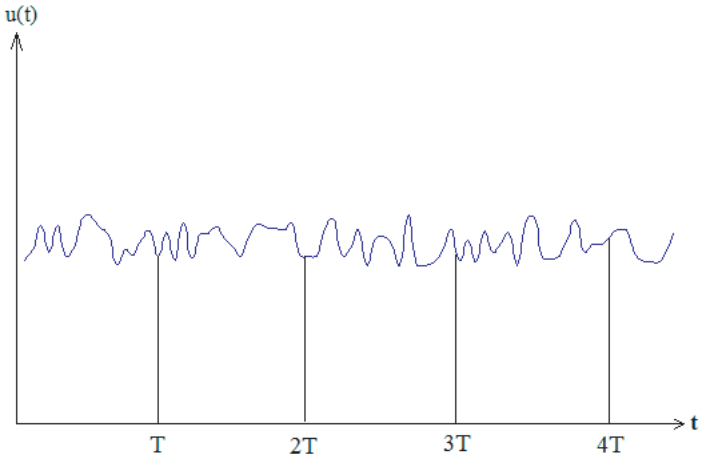

Figure 8.6: The integral for two integral scales in time effectively acts as an independent realization, at least for the time integral of a random signal.

so that the two expressions are equivalent. Thus, in effect, *portions of the record separated by two integral scales behave as though they were statistically independent, at least as far as convergence of finite time estimators is concerned.*

Thus what is required for convergence is again, many *independent* pieces of information. This is illustrated in Figure 8.6. That the length of the record should be measured in terms of the integral scale should really be no surprise since it is a measure of the rate at which a process forgets its past.

Example

It is desired to measure the mean velocity in a turbulent flow to within an rms error of 1% (i.e., $\epsilon = 0.01$). The expected fluctuation level of the signal is 25% and the integral scale is estimated as 100 ms. What is the required averaging time?

From equation 8.39

$$\begin{aligned} T &= \frac{2T_{int}}{\epsilon^2}\frac{var[u]}{U^2} \\ &= 2 \times 0.1 \times (0.25)^2/(0.01)^2 = 125sec \end{aligned} \tag{8.41}$$

Similar considerations apply to any other finite time estimator and equation 2.57 can be applied directly as long as equation 8.40 is used for the number of independent samples.

It is common experimental practice to not actually carry out an analog integration. Rather the signal is sampled at fixed intervals in time by digital means and the averages are computed as for an ensemble with a finite number of realizations. Regardless of the manner in which the signal is processed, only a finite portion of

a stationary time series can be analyzed and the preceding considerations always apply.

It is important to note that data sampled more rapidly than once every two integral scales do **not** contribute to the convergence of the estimator since they can not be considered independent. If N is the actual number of samples acquired and Δt is the time between samples, then the effective number of independent realizations is

$$N_{eff} = \begin{cases} N\Delta t/T_{int} & if \quad \Delta t < 2T_{int} \\ N & if \quad \Delta t \geq 2T_{int} \end{cases} \tag{8.42}$$

It should be clear that if you sample faster than $\Delta t = 2T_{int}$ you are processing unnecessary data which does not help your statistics converge.

You may wonder why one would ever take data faster than absolutely necessary, since it simply fills up your computer memory with lots of statistically redundant data. When we talk about measuring spectra you will learn that for spectral measurements it is necessary to sample much faster to avoid spectral aliasing. Many wrongly infer that they must sample at these higher rates even when measuring just moments. Obviously this is not the case if you are not measuring spectra.

Chapter 9

Homogeneous Random Processes

Acknowledgement: The figures in this chapter were prepared by Abolfazl Shiri.

9.1 Random fields of space and time

To this point only temporally varying random fields have been discussed. For turbulence however, random fields can be functions of both space and time. For example, the temperature θ could be a random scalar function of time t and position $\vec{x}$, i.e.,

$$\theta = \theta(\vec{x}, t) \tag{9.1}$$

The velocity is another example of a random vector function of position and time, i.e.,

$$\vec{u} = \vec{u}(\vec{x}, t) \tag{9.2}$$

or in tensor notation,

$$u_i = u_i(\vec{x}, t) \tag{9.3}$$

In the general case, the ensemble averages of these quantities are functions of both position and time; i.e.,

$$\langle \theta(\vec{x}, t) \rangle \equiv \Theta(\vec{x}, t) \tag{9.4}$$

$$\langle u_i(\vec{x}, t) \rangle \equiv U_i(\vec{x}, t) \tag{9.5}$$

If only *stationary* random processes are considered, then the averages do not depend on time and are functions of $\vec{x}$ only; i.e.,

$$\langle \theta(\vec{x}, t) \rangle \equiv \Theta(\vec{x}) \tag{9.6}$$

$$\langle u_i(\vec{x}, t) \rangle \equiv U_i(\vec{x}) \tag{9.7}$$

Now the averages may not be position dependent either. For example, if the averages are *independent of the origin in position*, then the field is said to be **homogeneous**. **Homogeneity** (the noun corresponding to the adjective homogeneous) is exactly analogous to stationarity except that position is now the variable, and not time.

It is, of course, possible (at least in concept) to have homogeneous fields which are either stationary or non-stationary. Since position, unlike time, is a vector quantity it is also possible to have only partial homogeneity. For example, a field might be homogeneous in the x_1- and x_3-directions, but not in the x_2-direction. In fact, it appears to be dynamically impossible to have flows in nature which are homogeneous in *all* variables and stationary as well, but the concept is useful, nonetheless. Such so-called 'forced' turbulence, however, can be generated in a computer, and is both stationary and approximately homogeneous.

Homogeneity will be seen to have powerful consequences for the equations governing the averaged motion, since the spatial derivative of any averaged quantity must be identically zero. Thus even homogeneity in only one direction can considerably simplify the problem. For example, in the Reynolds stress transport equation, the entire turbulence transport is exactly zero if the field is homogeneous.

9.2 Multi-point correlations

The concept of homogeneity can also be extended to multi-point statistics. Consider for example, the correlation between the velocity at one point and that at another as illustrated in Figure 9.1. If the time dependence is suppressed and the field is assumed statistically *homogeneous*, this correlation is a function only of the separation of the two points, i.e.,

$$\langle u_i(\vec{x},t)u_j(\vec{x'},t)\rangle \equiv B_{i,j}(\vec{r}) \tag{9.8}$$

where $\vec{r}$ is the separation vector defined by

$$\vec{r} = \vec{x'} - \vec{x} \tag{9.9}$$

or

$$r_i = x'_i - x_i \tag{9.10}$$

Note that the convention we shall follow for vector quantities is that the first subscript on $B_{i,j}$ is the component of velocity at the first position, $\vec{x}$, and the second subscript is the component of velocity at the second, $\vec{x'}$. For scalar quantities we shall simply put a symbol for the quantity to hold the place. For example, we would write the two-point temperature correlation in a homogeneous field as:

$$\langle \theta(\vec{x},t)\theta(\vec{x'},t)\rangle \equiv B_{\theta,\theta}(\vec{r}) \tag{9.11}$$

Figure 9.2 shows a typical example. Note how the correlation peaks at zero separation and dies off as the separation vector increases.

A mixed vector/scalar correlation like the two-point temperature velocity correlation would be written as:

$$\langle u_i(\vec{x},t)\theta(\vec{x'},t)\rangle \equiv B_{i,\theta}(\vec{r}) \tag{9.12}$$

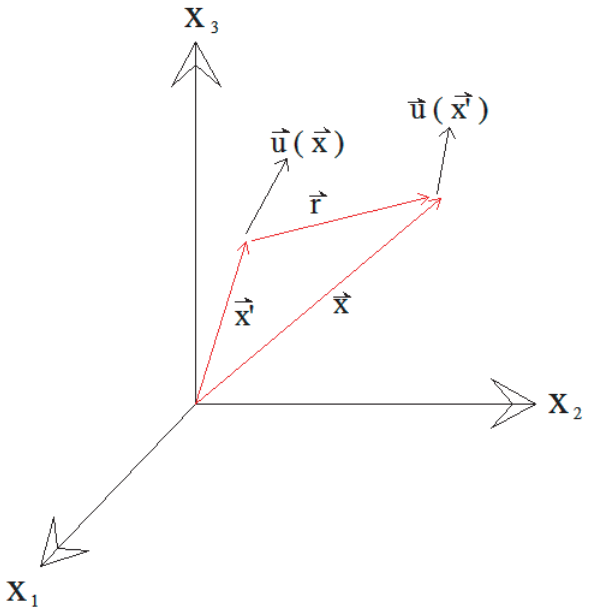

Figure 9.1: Velocity at two points separated by $\vec{r} = \vec{x'} - \vec{x}$.

On the other hand, if we meant for the temperature to be evaluated at $\vec{x}$ and the velocity at $\vec{x'}$ we would have to write:

$$\langle \theta(\vec{x}, t) u_i(\vec{x'}, t) \rangle \equiv B_{\theta,i}(\vec{r}) \tag{9.13}$$

Most books don't bother with this subscript notation, and simply give each new correlation a new symbol. At first this seems much simpler, and as long as you are only dealing with one or two different correlations, it is. But after we introduce a few more correlations and you read about a half-dozen pages, you find that you have completely forgotten which symbol stands for which correlation. Then because it is usually very important to know exactly what the forgotten symbol means, you thumb madly through the book trying to find where they were defined in the first place. Since we will use many different correlations and would like to avoid this useless waste of time thumbing through the book, we will use this comma system to help us remember[1].

9.3 Spatial integral and Taylor microscales

Just as for a stationary random process, correlations between spatially varying, but *statistically homogeneous*, random quantities ultimately go to zero; i.e., they

[1]For this system we can thank Professors Monin and Yaglom who wrote the famous two volume compendium translated into English by Professor John Lumley [**?**]

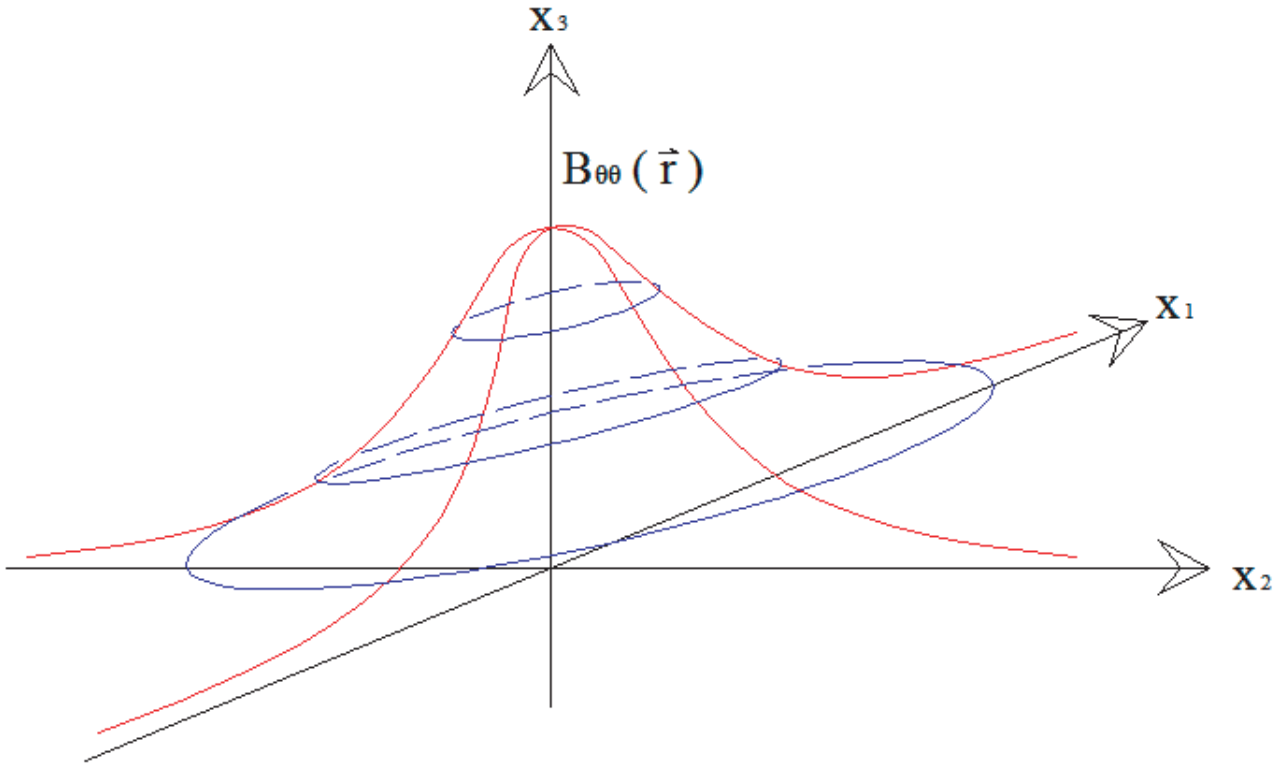

Figure 9.2: Two-point correlation of a scalar field with vector separation, $\vec{r} = (r_1, r_2, 0)$; i.e., in the x_1-x_2-plane.

become uncorrelated as their locations become widely separated. Statistical phenomena that behave this way are sometimes referred as *ergodic* processes. Because position (or relative position) is a vector quantity, however, the correlation may die off at different rates in different directions. Thus 'direction' must be an important part of any definition of 'scales' from correlation functions, both the directions associated with the quantities and the direction of the separation between them.

Consider for example the one-dimensional spatial correlation which is obtained by measuring the correlation between the temperature at two points along a line in the x-direction, say,

$$\begin{aligned} B^{(1)}_{\theta,\theta}(r) &\equiv \langle \theta(x_1, x_2, x_3, t)\theta(x_1 + r, x_2, x_3, t)\rangle \\ &= B_{\theta,\theta}(r, 0, 0) \end{aligned} \tag{9.14}$$

where $B_{\theta,\theta}$ is defined by equation 9.11. The superscript "(1)" denotes "the coordinate direction in which the scalar separation, r, has been chosen. This distinguishes it from the vector separation, $\vec{r}$ of $B_{\theta,\theta}(\vec{r})$. Also, note that the correlation at zero separation is just the variance; i.e.,

$$B^{(1)}_{\theta,\theta}(0) = \langle \theta^2 \rangle \tag{9.15}$$

Figure 9.3 shows a typical one-dimensional correlation.

For separations along the 2- and 3-axes we could define other correlations given by:

$$B^{(2)}_{\theta,\theta}(r) \equiv \langle \theta(x_1, x_2, x_3, t)\theta(x_1, x_2 + r, x_3, t)\rangle = B_{\theta,\theta}(0, r, 0) \tag{9.16}$$

$$B^{(3)}_{\theta,\theta}(r) \equiv \langle \theta(x_1, x_2, x_3, t)\theta(x_1, x_2, x_3 + r, t)\rangle = B_{\theta,\theta}(0, 0, r) \tag{9.17}$$

$$\tag{9.18}$$

In fact, we could define a one-dimensional correlation in an arbitrary direction, say given by the unit vector $\vec{r}/r$, but this would just be the original correlation function; i.e., $B^{(\vec{r}/r)}_{\theta,\theta}(r) = B_{\theta,\theta}(\vec{r})$.

9.3.1 Integral scales

The integral scale of $\theta(\vec{x}, t)$ in the x_1-direction can be defined as:

$$L^{(1)}_{\theta} \equiv \frac{1}{\langle \theta^2 \rangle} \int_0^\infty B^{(1)}_{\theta,\theta}(r) dr \tag{9.19}$$

Since the integral defined to be the area under positive values of the two-point correlation normalized by its value at zero separation, it has the simple geometrical interpretation shown in Figure 9.3. In particular, it is just equal to the intercept of the ordinate (separation axis) of a rectangle with the same area and abscissa intercept as the correlation function. It is easy to see from the figure that the integral scale can be a useful measure of how large a separation is required in

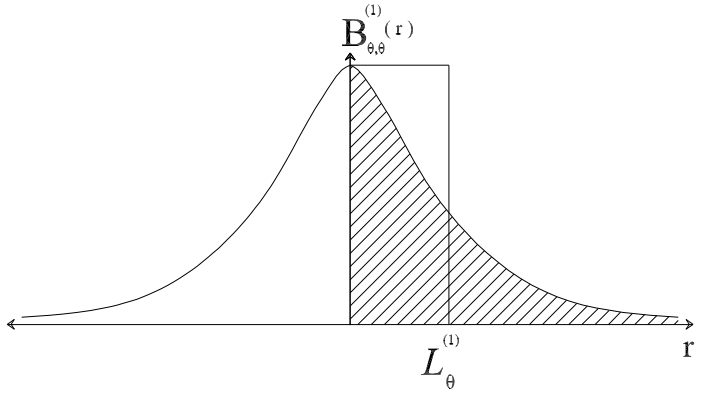

Figure 9.3: One-dimensional correlation of a scalar field, $B^{(1)}_{\theta,\theta}(r) = B_{\theta,\theta}(r,0,0)$. The intercept of the rectangle with the r-axis illustrates the integral scale, $L^{(1)}_\theta$.

order for the most of the process to become uncorrelated with itself, typically a few integral scales.

It is clear that there are at least two more integral scales which could be defined by considering separations in the 1- and 2 directions; i.e.,

$$L^{(2)}_\theta \equiv \frac{1}{\langle\theta^2\rangle}\int_0^\infty B^{(2)}_{\theta,\theta}(r)dr \tag{9.20}$$

and

$$L^{(3)}_\theta \equiv \frac{1}{\langle\theta^2\rangle}\int_0^\infty B^{(3)}_{\theta,\theta}(r)dr \tag{9.21}$$

In fact, an integral scale could be defined for *any* direction, say $\vec{r}/r$; i.e.,

$$L^{(\vec{r}/r)}_{\theta,\theta} = \frac{1}{\langle\theta^2\rangle}\int_0^\infty B_{\theta,\theta}(\vec{r})dr \tag{9.22}$$

where the integration is in the direction of the separation vector $\vec{r}$. Note that just because we can define an integral scale does not necessarily mean it exists, since the integral of the correlation function can be zero (e.g., if the correlation function changes sign). We'll see examples of this later.

The situation is even more complicated when correlations of vector quantities are considered. For example, consider the correlation of the velocity vectors at two points, $B_{i,j}(\vec{r})$. Clearly $B_{i,j}(\vec{r})$ is not a single correlation, but rather nine separate correlations: $B_{1,1}(\vec{r})$, $B_{1,2}(\vec{r})$, $B_{1,3}(\vec{r})$, $B_{2,1}(\vec{r})$, $B_{2,2}(\vec{r})$, etc. For each of these an integral scale can be defined once a direction for the separation vector

is chosen. For example, the integral scales associated with $B_{1,1}$ for the principal directions are

$$L_{1,1}^{(1)} \equiv \frac{1}{\langle u_1^2 \rangle} \int_0^\infty B_{1,1}(r,0,0)dr \tag{9.23}$$

$$L_{1,1}^{(2)} \equiv \frac{1}{\langle u_1^2 \rangle} \int_0^\infty B_{1,1}(0,r,0)dr \tag{9.24}$$

$$L_{1,1}^{(3)} \equiv \frac{1}{\langle u_1^2 \rangle} \int_0^\infty B_{1,1}(0,0,r)dr \tag{9.25}$$

Integral scales can similarly be defined for the other components of the correlation tensor. Two of particular importance in the historical development of turbulence theory are

$$L_{1,1}^{(1)} \equiv \frac{1}{\langle u_1^2 \rangle} \int_0^\infty B_{1,1}(r,0,0)dr \tag{9.26}$$

$$L_{2,2}^{(1)} \equiv \frac{1}{\langle u_2^2 \rangle} \int_0^\infty B_{2,2}(r,0,0)dr \tag{9.27}$$

In general, each integral scale will be different, unless restrictions beyond simple homogeneity are placed on the process (e.g., like *isotropy* discussed below). Thus, it is important to specify precisely which integral scale is being referred to, which components of the vector quantities are being used, and in which direction the integration is being performed.

Finally note that the integral scales defined in this section are all *physical integral scales*, meaning that they are directly obtainable from the two-point statistics. They should not confused with the *pseudo-integral scale*, u^3/ε, defined by equation 4.18 in Chapter 4. As noted there, the *pseudo-integral scale* is very much associated with the idea of a large gap in size between the energy-containing scales and those dissipating most of the energy. In the limit of infinite Reynolds numbers, it can be argued that the physical and pseudo-integral scales should be proportional, but the constants of proportionality can vary greatly from flow to flow. So MIND THE GAP when using or making arguments from either type.

The biggest problem in determining integral scales in the laboratory or from experimental data is most often with the experiment or simulation itself. In particular, the correlation at separations significantly greater than integral scale can affect the integration. This also means that unless the purpose is to examine the effect of the boundaries on the flow, the windtunnel or computational box must also much greater in size than the integral scale for the experiment or DNS to be valid at all. This is a serious problem with many experiments and especially DNS which purport to be simulations of homogeneous turbulence (and free shear flows like jets or wakes), but in fact are not.

9.3.2 Taylor microscales

Similar considerations apply to the Taylor microscales, regardless of whether they are being determined from the correlations at small separations, or from the mean

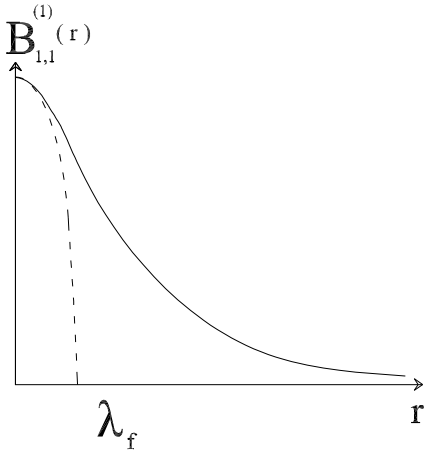

Figure 9.4: Sketch showing relation of Taylor microscale, λ_f to oscullating parabola of correlation, $f(r) = B^{(1)}_{1,1}(r)$.

square fluctuating gradients. The two most commonly used Taylor microscales are often referred to as λ_f and λ_g and are defined by:

$$\lambda_f^2 \equiv 2\frac{\langle u_1^2 \rangle}{\langle [\partial u_1/\partial x_1]^2 \rangle} \tag{9.28}$$

and

$$\lambda_g^2 \equiv 2\frac{\langle u_2^2 \rangle}{\langle [\partial u_2/\partial x_1]^2 \rangle} \tag{9.29}$$

The subscripts f and g are historical, and refer to the autocorrelation coefficients defined by:

$$f(r) \equiv \frac{\langle u_1(x_1, x_2, x_3) u_1(x_1 + r, x_2, x_3) \rangle}{\langle u_1^2 \rangle} = \frac{B_{1,1}(r, 0, 0)}{B_{1,1}(0, 0, 0)} \tag{9.30}$$

and

$$g(r) \equiv \frac{\langle u_2(x_1, x_2, x_3) u_1(x_2 + r, x_2, x_3) \rangle}{\langle u_1^2 \rangle} = \frac{B_{2,2}(r, 0, 0)}{B_{2,2}(0, 0, 0)} \tag{9.31}$$

It is straightforward to show from the definitions that λ_f and λ_g are related to the curvature of the f and g correlation functions at $r = 0$. Specifically,

$$\lambda_f^2 = \frac{2}{d^2 f/dr^2|_{r=0}} \tag{9.32}$$

and

$$\lambda_g^2 = \frac{2}{d^2 g/dr^2|_{r=0}} \tag{9.33}$$

Since both f and g are symmetrical functions of r, df/dr and dg/dr must be zero at $r = 0$. It follows immediately that the leading r-dependent term in the McClaurin series expansion about the origin of each autocorrelations is of parabolic form; i.e.,

$$f(r) = 1 - \frac{r^2}{\lambda_f^2} + \cdots \tag{9.34}$$

and

$$g(r) = 1 - \frac{r^2}{\lambda_g^2} + \cdots \tag{9.35}$$

This is illustrated in Figure 9.4 which shows that the Taylor microscales are the intersection with the r-axis of a parabola fitted to the appropriate correlation function at the origin. Fitting a parabola is a common way to determine the Taylor microscale, but to do so you must make sure you resolve accurately to scales much smaller than it (typically an order of magnitude smaller is required). Otherwise the Taylor microscale you determine is more related to the spatial filtering of the probe or numerical algorithm than to the actual flow.

9.4 Symmetries

It is easy to see that the consideration of vector quantities raises special considerations with regard to symmetries of two-point statistical quantities. These can be very different, depending on whether the quantities involved are scalars or vectors, or some combination of each. These symmetry conditions can be used to great advantage to reduce the quantity of measurements, and as well to confirm that the fields are truly homogenous and the the measured quantities correct.

For example, as illustrated in Figures 9.2 and 9.3, the correlation between a scalar function of position at two points is symmetrical in $\vec{r}$, i.e.,

$$B_{\theta,\theta}(\vec{r}) = B_{\theta,\theta}(-\vec{r}) \tag{9.36}$$

This is easy to show from the definition of $B_{\theta,\theta}$ and the fact that the field is homogeneous. Simply shift each of the position vectors by the same amount $-\vec{r}$ to obtain:

$$\begin{aligned} B_{\theta,\theta}(\vec{r}) &\equiv \langle\theta(\vec{x},t)\theta(\vec{x'},t)\rangle \\ &= \langle\vec{\theta}(\vec{x}-\vec{r},t)\theta(\vec{x'}-\vec{r},t)\rangle \\ &= \langle\vec{\theta}(\vec{x},t)\theta(\vec{x}-\vec{r},t)\rangle \\ &= B_{\theta,\theta}(-\vec{r}) \end{aligned} \tag{9.37}$$

since $\vec{x'} - \vec{r} = \vec{x}$. Clearly the positions are reversed and the separation vector is pointing the opposite way.

Such is not the case, in general, for *vector* functions of position. For example, see if you can prove to yourself the following for a scalar velocity correlation:

$$B_{\theta,i}(\vec{r}) = B_{i,\theta}(-\vec{r}) \tag{9.38}$$

Similarly, the velocity-velocity correlation must satisfy:

$$B_{i,j}(\vec{r}) = B_{j,i}(-\vec{r}) \tag{9.39}$$

Clearly the latter is symmetrical in the variable $\vec{r}$ only when $i = j$.

Exercise: Prove equations 9.38 and 9.39. (Hint: Note that $\langle\theta(\vec{x}-\vec{r})u_j(\vec{x},t)\rangle = \langle u_j(\vec{x},t)\theta(\vec{x}-\vec{r})\rangle = B_{j,\theta}(-\vec{r})$.)

These properties of the two-point correlation function will be seen to play an important role in determining the interrelations among the different two-point statistical quantities. They will be especially important when we talk about spectral quantities.

9.5 Implications of Continuity

The equations of mass conservation can be used to relate the derivatives of the correlations. These can be used to great advantage in reducing the number of correlations which must be measured to completely describe a turbulent field, and even to verify whether the measured correlations are internally consistent with each other. Also, continuity together with homogeniety has important implications for the dissipation, which we have already encountered in Section 4.1. We shall see another important application in the section below when we consider isotropy, where it reduces the number of correlations (or spectra) which must be measured to a single one.

9.5.1 Reduction of $B_{i,j}(\vec{r})$ to three independent components

To see how this works, first write the incompressible continuity equation at point $\vec{x}$ (i.e., $\partial u_i(\vec{x},t)/\partial x_i = 0$), then multiply it by the velocity at second point, say $u_j(\vec{x'},t)$, and average to obtain:

$$\langle u_j(\vec{x'},t)\frac{\partial u_i(\vec{x},t)}{\partial x_i}\rangle = 0 \tag{9.40}$$

But since $u_j(\vec{x'},t)$ does not depend on $\vec{x}$, it can be pulled inside the derivative, as can the average, yielding:

$$\begin{aligned}&\frac{\partial}{\partial x_i}\langle u_i(\vec{x},t)u_j(\vec{x'},t)\rangle \\ &= \frac{\partial}{\partial x_i}B_{i,j}(\vec{r},t) = 0,\end{aligned} \tag{9.41}$$

the last line following from the fact that homogeneity implies that $\langle u_i(\vec{x},t)u_j(\vec{x'},t)\rangle = B_{i,j}\vec{r})$ only.

For convenience let's define $\xi_i = x'_i + x_i$ together with $r_i = x'_i - x_i$, which in turn implies that $x'_i = (\xi_i + r_i)/2$ and $x_i = (\xi_i - r_i)/2$. Application of the chain-rule implies immediately that:

$$\begin{aligned}\frac{\partial}{\partial x_i} &= \frac{\partial \xi_m}{\partial x_i}\frac{\partial}{\partial \xi_m} + \frac{\partial r_m}{\partial x_i}\frac{\partial}{\partial r_m} \\ &= \delta_{mi}\frac{\partial}{\partial \xi_m} - \delta_{mi}\frac{\partial}{\partial r_m} \\ &= \frac{\partial}{\partial \xi_i} - \frac{\partial}{\partial r_i} \end{aligned} \tag{9.42}$$

Using the chain-rule result in equation 9.43 yields immediately:

$$\frac{\partial}{\partial r_i}B_{i,j}(\vec{r}) = 0 \tag{9.43}$$

since $B_{i,j}$ is a function of $\vec{r}$ only.

By writing the continuity equation at the point, $\vec{x'}$, and multiplying by the velocity at the point, $\vec{x}$, another three equations can be similarly derived. The result is:

$$\frac{\partial}{\partial r_j}B_{i,j}(\vec{r}) = 0 \tag{9.44}$$

It is clear that with both equations 9.43 and 9.44 together, we have six equations in nine unknowns. Since our equations are differential equations, this means that all correlations can be derived to within a constant if any of three are known. But since all the correlations go to zero with increasing separation, this means that only three of the components of the two-point Reynolds stress tensor are independent. Said another way, we only need to measure three of them to find all the others – but only if the flow is incompressible. These relations among the various components of the two-point Reynolds stress equations will especially useful when we consider spectra in the next section, since the differential equations will be replaced by algebraic ones.

9.6 Relations among the derivative moments

Homogeniety also considerably reduces the number of independent derivative moments. To see how, consider the average of the product of the velocity derivatives at two different points. By using the fact that $u_i(\vec{x},t)$ is not a function of $\vec{x'}$ nor is $u_j(\vec{x'},t)$ a function of $\vec{x}$, it follows that:

$$\langle\frac{\partial u_i(\vec{x},t)}{\partial x_m}\frac{\partial u_j(\vec{x'},t)}{\partial x'_n}\rangle = \frac{\partial^2}{\partial x_m \partial x_n}B_{i,j}(\vec{x'}-\vec{x},t) \tag{9.45}$$

$$= -\frac{\partial^2}{\partial r_m \partial r_n}B_{i,j}(\vec{r},t) \tag{9.46}$$

where we have used equation 9.41 twice in succession.

But since the order of differentiation is irrelevant in the last expression on the right-hand side, the same must be also true on the left-hand side. In particular it must be true for $\vec{r} = 0$ (i.e., $\vec{x'} = \vec{x}$). Thus the derivative moments must be related by:

$$\langle \frac{\partial u_i}{\partial x_m} \frac{\partial u_j}{\partial x_n} \rangle = \langle \frac{\partial u_i}{\partial x_n} \frac{\partial u_j}{\partial x_m} \rangle \tag{9.47}$$

where we have reversed the indices with respect to which we are differentiating.

9.7 Elimination of the cross-derivative moments

The incompressible continuity equation can be used together with homogeneity to deduce another important result for homogeneous flows: namely that $\langle s_{ij} s_{ij} \rangle = \langle \omega_i \omega_i \rangle$. And immediate consequence is that for homogeneous turbulence:

$$\epsilon = 2\nu \langle s_{ij} s_{ij} \rangle = \nu \langle \frac{\partial u_i}{\partial x_j} \frac{\partial u_i}{\partial x_j} \rangle \tag{9.48}$$

To see this, multiply the continuity equation by $\partial u_1/\partial x_1$, $\partial u_2/\partial x_2$, and $\partial u_3/\partial x_3$ respectively, then average to obtain:

$$\langle \left[\frac{\partial u_1}{\partial x_1}\right]^2 \rangle + \langle \frac{\partial u_1}{\partial x_1} \frac{\partial u_2}{\partial x_2} \rangle + \langle \frac{\partial u_1}{\partial x_1} \frac{\partial u_3}{\partial x_3} \rangle = 0 \tag{9.49}$$

$$\langle \frac{\partial u_2}{\partial x_2} \frac{\partial u_1}{\partial x_1} \rangle + \langle \left[\frac{\partial u_2}{\partial x_2}\right]^2 \rangle + \langle \frac{\partial u_2}{\partial x_2} \frac{\partial u_3}{\partial x_3} \rangle = 0 \tag{9.50}$$

$$\langle \frac{\partial u_3}{\partial x_3} \frac{\partial u_1}{\partial x_1} \rangle + \langle \frac{\partial u_3}{\partial x_3} \frac{\partial u_2}{\partial x_2} \rangle + \langle \left[\frac{\partial u_3}{\partial x_3}\right]^2 \rangle = 0 \tag{9.51}$$

Now by using equation 9.47 for the derivative moments, we can reverse the indices in the crossed moments and rewrite this as:

$$\langle \left[\frac{\partial u_1}{\partial x_1}\right]^2 \rangle + \langle \frac{\partial u_1}{\partial x_2} \frac{\partial u_2}{\partial x_1} \rangle + \langle \frac{\partial u_1}{\partial x_3} \frac{\partial u_3}{\partial x_1} \rangle = 0 \tag{9.52}$$

$$\langle \frac{\partial u_1}{\partial x_2} \frac{\partial u_2}{\partial x_1} \rangle + \langle \left[\frac{\partial u_2}{\partial x_2}\right]^2 \rangle + \langle \frac{\partial u_2}{\partial x_3} \frac{\partial u_3}{\partial x_2} \rangle = 0 \tag{9.53}$$

$$\langle \frac{\partial u_1}{\partial x_3} \frac{\partial u_3}{\partial x_1} \rangle + \langle \frac{\partial u_2}{\partial x_3} \frac{\partial u_3}{\partial x_2} \rangle + \langle \left[\frac{\partial u_3}{\partial x_3}\right]^2 \rangle = 0 \tag{9.54}$$

Since there are three independent equations, they can be solved to obtain the crossed moments in terms of the squared derivatives as:

$$\langle \frac{\partial u_1}{\partial x_2}\frac{\partial u_2}{\partial x_1}\rangle = -\frac{1}{2}\left\{+\langle\left[\frac{\partial u_1}{\partial x_1}\right]^2\rangle + \langle\left[\frac{\partial u_2}{\partial x_2}\right]^2\rangle - \langle\left[\frac{\partial u_3}{\partial x_3}\right]^2\rangle\right\} \tag{9.55}$$

$$\langle \frac{\partial u_1}{\partial x_3}\frac{\partial u_3}{\partial x_1}\rangle = -\frac{1}{2}\left\{+\langle\left[\frac{\partial u_1}{\partial x_1}\right]^2\rangle - \langle\left[\frac{\partial u_2}{\partial x_2}\right]^2\rangle + \langle\left[\frac{\partial u_3}{\partial x_3}\right]^2\rangle\right\} \tag{9.56}$$

$$\langle \frac{\partial u_2}{\partial x_3}\frac{\partial u_3}{\partial x_2}\rangle = -\frac{1}{2}\left\{-\langle\left[\frac{\partial u_1}{\partial x_1}\right]^2\rangle + \langle\left[\frac{\partial u_2}{\partial x_2}\right]^2\rangle + \langle\left[\frac{\partial u_3}{\partial x_3}\right]^2\rangle\right\} \tag{9.57}$$

We will use them immediately in the section immediately following to simplify the dissipation in homogeneous flows. These relations will also be found to be particularly useful when the additional constraints of axisymmetry or isotropy are imposed toward the end of this chapter.

9.7.1 The 'homogeneous' dissipation

The dissipation is given by $\epsilon = 2\nu\langle s_{ij}s_{ij}\rangle$, which can be expanded to obtain:

$$\begin{aligned}
\epsilon &= 2\nu\langle s_{ij}s_{ij}\rangle \\
&= \nu\left\{\langle\frac{\partial u_i}{\partial x_j}\frac{\partial u_i}{\partial x_j}\rangle + \langle\frac{\partial u_i}{\partial x_j}\frac{\partial u_j}{\partial x_i}\rangle\right\} \qquad (9.58)\\
&= \nu\left\{\langle\left[\frac{\partial u_1}{\partial x_1}\right]^2\rangle + \langle\left[\frac{\partial u_1}{\partial x_2}\right]^2\rangle + \langle\left[\frac{\partial u_1}{\partial x_3}\right]^2\rangle\right.\\
&\quad + \langle\left[\frac{\partial u_2}{\partial x_1}\right]^2\rangle + \langle\left[\frac{\partial u_2}{\partial x_2}\right]^2\rangle + \langle\left[\frac{\partial u_2}{\partial x_3}\right]^2\rangle\\
&\quad \left. + \langle\left[\frac{\partial u_3}{\partial x_1}\right]^2\rangle + \langle\left[\frac{\partial u_3}{\partial x_2}\right]^2\rangle + \langle\left[\frac{\partial u_3}{\partial x_3}\right]^2\rangle\right\}\\
&+ \nu\left\{\langle\left[\frac{\partial u_1}{\partial x_1}\right]^2\rangle + \langle\frac{\partial u_1}{\partial x_2}\frac{\partial u_2}{\partial x_1}\rangle + \langle\frac{\partial u_1}{\partial x_3}\frac{\partial u_3}{\partial x_1}\rangle\right.\\
&\quad + \langle\frac{\partial u_2}{\partial x_1}\frac{\partial u_1}{\partial x_2}\rangle + \langle\left[\frac{\partial u_2}{\partial x_2}\right]^2\rangle + \langle\frac{\partial u_2}{\partial x_3}\frac{\partial u_3}{\partial x_2}\rangle\\
&\quad \left. + \langle\frac{\partial u_3}{\partial x_1}\frac{\partial u_1}{\partial x_3}\rangle + \langle\frac{\partial u_3}{\partial x_2}\frac{\partial u_2}{\partial x_3}\rangle + \langle\left[\frac{\partial u_3}{\partial x_3}\right]^2\rangle\right\} \qquad (9.59)
\end{aligned}$$

From equations 9.52 to 9.54 it is immediately obvious the second bracketed term is identically zero for homogenous incompressible flow (since each line adds to zero). But the first bracketed term is just $\langle[\partial u_i/\partial x_j]^2\rangle$. Thus for homogeneous incompressible flow the dissipation is given by:

$$\epsilon = \nu\langle\frac{\partial u_i}{\partial x_j}\frac{\partial u_i}{\partial x_j}\rangle, \tag{9.60}$$

exactly as we surmised must be true from the various forms of the turbulence kinetic energy equation of section 4.1.

There are several other similar relations that appear in turbulent flow analyses and experiments. For example, application of the derivative symmetry conditions lead immediately to the conclusion that in homogeneous turbulence the mean square strain rate is equal the mean square rotation rate which is in turn equal to half the mean square vorticity (or enstrophy); i.e.,

$$\langle s_{ij} s_{ij} \rangle = \langle \Omega_{ij} \Omega_{ij} \rangle = \frac{1}{2} \langle \omega_i \omega_i \rangle \tag{9.61}$$

Execise: Prove that for homogeneous incompressible flow the mean square strain rate equals the mean square rotation rate and half the mean square vorticity for homogeneous incompressible flow; i.e., equations 9.61 above.

9.7.2 Pressure fluctuations in homogeneous turbulence

Equations 9.61 have an interesting application to the pressure fluctuatuations in homogeneous turbulence. By taking the divergence of the constant desnsity Navier-Stokes equations, it follows immediately that the pressure fluctuations are described by the solution to the following Poisson's equation:

$$-\frac{1}{\rho} \nabla^2 \tilde{p} = \frac{\partial \tilde{u}_i}{\partial x_j} \frac{\partial \tilde{u}_j}{\partial x_i} \tag{9.62}$$

Decomposing the velocity and pressure into mean and fluctuating parts (e.g., $\tilde{p} = P + p$, etc), and subtracting the mean equation leaves an equation for the pressure fluctuations, $p(\vec{x}, t)$, as:

$$-\frac{1}{\rho} \nabla^2 p = \left[\frac{\partial U_i}{\partial x_j} \frac{\partial u_j}{\partial x_i} + \frac{\partial U_i}{\partial x_j} \frac{\partial u_j}{\partial x_i} \right] + \left[\frac{\partial u_i}{\partial x_j} \frac{\partial u_j}{\partial x_i} - \langle \frac{\partial u_i}{\partial x_j} \frac{\partial u_j}{\partial x_i} \rangle \right] \tag{9.63}$$

The first two terms are usually referred to as *turbulence-mean shear interaction*, and the latter as the *turbulence-turbulence interaction* terms.

But we can further decompose the last fluctuating term into the difference between the strain-rate tensor squared and the rotation-rate tensor squared; i.e.,

$$\frac{\partial u_i}{\partial x_j} \frac{\partial u_j}{\partial x_i} = s_{ij} s_{ij} - \Omega_{ij} \Omega_{ij} \tag{9.64}$$

Thus equation 9.63 can be rewritten as:

$$-\frac{1}{\rho} \nabla^2 p = \left[\frac{\partial U_i}{\partial x_j} \frac{\partial u_j}{\partial x_i} + \frac{\partial U_i}{\partial x_j} \frac{\partial u_j}{\partial x_i} \right] + \left[(s_{ij} s_{ij} - (\langle s_{ij} s_{ij} \rangle) - (\Omega_{ij} \Omega_{ij} - \langle \Omega_{ij} \Omega_{ij} \rangle) \right] \tag{9.65}$$

Thus the turbulence turbulence interaction terms consist of the difference of two quantities (the square of the fluctuating strain and rotation rates) which individually can be quite large, but their difference quite small. And in fact, as we have seen above, in *homogenous* turbulence the difference of the averages of the squared strain-rate and rotation-rate tensors is exactly zero!

Exercise: Show that the square of the rotation rate is equal to half the square of the vorticity (i.e., $\Omega_{ij}\Omega_{ij} = \omega_i\omega_i/2$); and rewrite equation 9.65 using it.

9.8 Isotropy

It should be clear even at this point that two point statistical quantities can be quite complex, even to simply define which ones we are talking about. Fortunately there are symmetries which can both help us reduce the number, and also help us decide the degree to which real flows or numerically generated ones approximate homogenous ones. In addition to these basic symmetries imposed by homogeneity, it is sometimes convenient to make even more stringent assumptions about the statistical character of the turbulence; e.g., axisymmetry or isotropy. Axisymmetry in this context does not mean the same thing as the axisymmetric shear flows discussed earlier in which the statistical properties were constant in circular contours about a centerline. What *axisymmetry* means here is that the statistics *at every point* have a preferred direction about which the properties are symmetrical. And similarly *isotropic* means is that there is no preferred direction at all — in fact, the turbulence statistical properties at a point even have reflectional symmetry. In this section we shall consider only implications of isotropy.

9.8.1 An example from fluid mechanics: viscous stress

Before looking at turbulence, let's make a point of contact with what you should have already from your study of Fluid Mechanics. (If you haven't seen this before, pick up any good fluid mechanics book.) In order to relate the viscous (or deviatoric) stress tensor, say $\tau_{ij}^{(v)}(\vec{x},t)$, to the velocity field one begins by noting that the stress tensor must be a functional of the velocity at all points in the flow and at all times up to the present. Then by a serious of arguments that relate to how it must appear in different coordinate systems one decides that it can really only be a function of the strain-rate. Then by another series of assumptions we argue that there might be some flows in which history played no role, and in fact further, the stress might depend on only the first power of the strain-rate locally.

With all of these assumptions we can write: $\tau_{ij}^{(v)} = C_{ijkl}\, s_{kl}$, meaning that we still have 81 undetermined material coefficients. But we know immediately that some of these must be equal since both the stress tensor and the strain-rate

tensor are symmetrical; i.e., $\tau_{ij} = \tau_{ji}^{(v)}$ and $s_{ij} = s_{ji}$. This reduces the number of unknowns from 81 to 36. Now we begin to make assumptions about the material, in particular that it is an *isotropic* material. This means that it should be be independent of how we view it, or even independent of whether we view it in a mirror. So step by step we consider what happens if we rotate about the 1-axis, then the 2-axis, etc., and insist these remain invariant during the transformation. And then we examine what happens if we reflect about the axes; i.e,, the 1-axis becomes the negative 1-axis, etc. When have exhausted all the possibilities we end up with only two undetermined constant, our familiar Newtonian fluid model; i.e.,

$$\tau_{ij}^{(v)} = 2\mu[s_{ij} - s_{kk}\delta_{ij}/3] + \mu_2 s_{kk}. \tag{9.66}$$

Amazingly, by simply exploring the implications of symmetries and isotropy, we have reduced the number of unknowns to two simple material properties. And the second of these, the second viscosity, μ_2, can often be assumed to be zero.

The implications of isotropy for turbulence are at least as profound. Even though flows are never really quite isotropic, we can learn a great deal by exploring what they would be like if they were. And of course we will not be able to reduce our result to simple material constants, since it is the statistics of the flow that will be assumed to be isotropic, not the underlying material.

9.8.2 Isotropic single-point correlations

There are a number of statistical quantities we have seen already for which we stated the effects of isotropy. For example, consider the single point Reynolds stress tensor, $\langle u_i u_j \rangle$. First rotate the coordinate system 90° around the x_1-axis so the old x_3-axis becomes the new x_2' axis and the old negative x_2-axis becomes the new x_3'-axis. It is easy to see $\langle u_2' u_3' \rangle$ in the new coordinate system must be equal to $-\langle u_2 u_3 \rangle$ in the old. But isotropy requires that the form of $\langle u_i u_j \rangle$ be independent of coordinate system. This clearly is possible only if $\langle u_2 u_3 \rangle = 0$. Rotations and reflections about the other axis lead to similar conclusions for all the off-diagonal terms. Moreover they also imply that all the diagonal terms must be equal. Therefore isotropy implies that $\langle u_1^2 \rangle = \langle u_2^2 \rangle = \langle u_3^2 \rangle$ and $\langle u_i u_j \rangle = 0$ for $i \neq j$. Similar considerations apply to the other second order tensors we encountered as well.

We also encountered the scalar-vector correlations, like the pressure-velocity correlation, $\langle p u_j \rangle$. Consider a mirror image transformation in which the old x_1-axis becomes the negative of the new x_1' axis. It follows immediately that $\langle p' u_1' \rangle = -\langle p u_1 \rangle$ since the direction of the velocity is reversed. But isotropy requires that the correlation be independent of rotations and reflections of the coordinate system. Hence the only possible value of the single point pressure-velocity correlation is zero. Similar considerations apply to all *vector* statistical properties, including the

mean flow. So, for example, the only possible value of the mean flow in isotropic turbulence is zero; i.e., no mean flow at all.

9.8.3 Isotropic two-point statistics

If a turbulent field is assumed to be isotropic, this very much restricts the form of the two-point correlations (and their Fourier transforms as well). And as we shall see below, the consequences of isotropy for two-point statistical properties are considerably more interesting than for the single-point quantities. The presence of the separation vector $\vec{r} = \vec{x'} - \vec{x}$ makes the problem a bit more complicated than for the single point quantities considered above. First it introduces a whole new scalar invariant, $r = |\vec{r}| = (r_i r_i)^{1/2}$. Second, if some of the statistical properties under consideration are vectors, it introduces new 'angles' into consideration from the inner products that can be formed with it; e.g., $\vec{u} \cdot \vec{r} = u_i r_i = |\vec{u}||\vec{r}| \cos\theta$, where θ is the angle between them. It is clear that we should expect very different results depending on whether the correlations under consideration are scalars, vectors or tensors, and indeed this is the case.

Consider first the two-point correlation of an isotropic scalar field like $B_{\theta,\theta}(\vec{r})$ above. We already know that $B_{\theta,\theta}(\vec{r}) = B_{\theta,\theta}(-\vec{r})$ from homogeneity alone. But if the field is isotropic this correlation must be invariant no matter how the coordinate system is rotated or reflected about itself. Since the components of $\vec{r}$ change with coordinate system and only its length, $r = |\vec{r}|$ is invariant, $B_{\theta,\theta}(\vec{r})$ can be invariant only if depends only on r; i.e.,

$$B_{\theta,\theta}(\vec{r}) = B_\theta(r) \tag{9.67}$$

Now consider a two-point correlation comprised of a vector and a scalar quantity, like $B_{p,i}(\vec{r}) = \langle p(\vec{x} u_i(\vec{x}+\vec{r}) \rangle$. Again homogeneity alone implies that $B_{p,i}(\vec{r}) = B_{i,p}(-\vec{r})$, and *vice versa*, so this must also be true for an isotropic field as well. But as we rotate and reflect both the magnitude, r, and the angle between $\vec{r}$ and $\vec{u}$ must be invariant. It is not immediately obvious, but straightforward to show, that the most general form of a two-point scalar-vector correlation in an isotopic field is given by:

$$B_{p,i}(\vec{r}) = B_{pL}(r)\frac{r_i}{r} \tag{9.68}$$

$$B_{j,p}(\vec{r}) = B_{Lp}(r)\frac{r_j}{r} = -B_{pL}(r)\frac{r_j}{r} \tag{9.69}$$

Two-point correlations involving two vectors, say $u_i = u_i(\vec{x})$ and $u'_j = u_j(\vec{x}+\vec{r})$, in addition to the separation vector, $\vec{r}$ are even more interesting. The reasons can be seen in Figure 9.5. In addition to the symmetry requirements imposed by homogeneity, $B_{i,j}(\vec{r}) = B_{j,i}(-\vec{r})$, all of the angles between the vectors must be maintained as the coordinate system is rotated and reflected. Again it is complicated but straightforward to show that the most general form of a two-point vector-vector correlation in an isotropic field is given by:

$$B_{i,j}(\vec{r}) = A(r) r_i r_j + B(r)\delta_{ij} \tag{9.70}$$

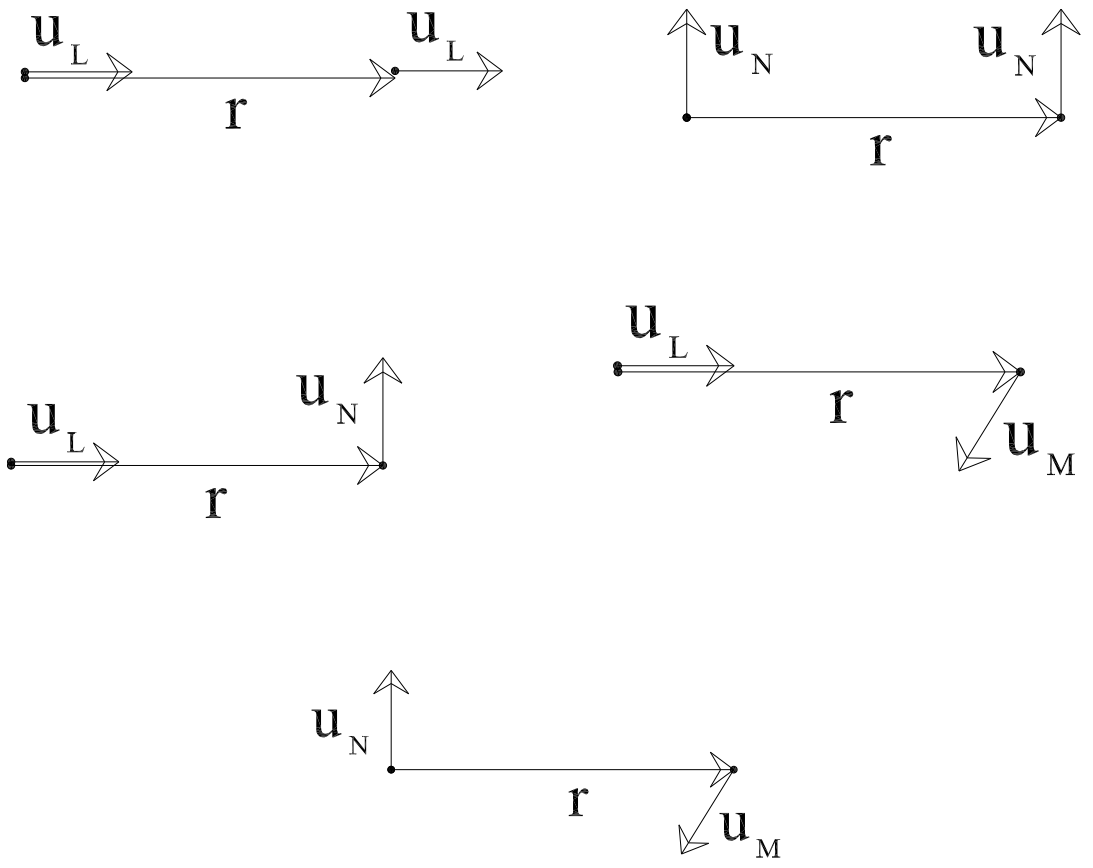

Figure 9.5: Sketches showing which velocity components are used to make up B_{LL}, B_{LL}, B_{NN}, B_{LM},B_{LN} and B_{NM} respectively, and their relation to the separation vector.

where $A(r)$ and $B(r)$ are two functions which depend on r only, and δ_{ij} is the isotropic tensor (or Kronecker delta tensor). We will find considerable use for the spectral equivalent of this result in the next chapter.

It is customary (and convenient) to express the functions A and B in terms of the two-point velocity correlations we commonly measure (see Figure 9.5). The first of these is denoted as $B_{LL}(r)$ and called the *longitudinal correlation* because the two-components of velocity are aligned with the separation vector. And the second is denoted as $B_{NN}(r)$ and called the *normal* or *transverse* correlation, since the two components of velocity are chosen to be in the same plane but perpendicular to the separation variable.

To see how these determine A and B simply follow the directions above. For example $B_{LL}(r)$ would have to be the same as $B_{1,1}(r,0,0)$, but $B_{2,2}(0,r,0)$ would also suffice (as would any choice for which the vectors are collinear). Substituting into equation 9.70 yields $B_{LL}(r)$ as:

$$B_{LL}(r) = B_{1,1}(r,0,0) = A(r)r^2 + B(r) \tag{9.71}$$

Similarly, $B_{NN}(r)$ can be determined from:

$$B_{NN}(r) = B_{2,2}(r,0,0) = B(r) \tag{9.72}$$

since $r_2 r_2 = 0$ if $\vec{r} = (r,0,0)$. We now have two equations in two unknowns, so we can solve for $A(r)$ and $B(r)$ to obtain the general form:

$$B_{i,j}(\vec{r}) = [B_{LL}(r) - B_{NN}(r)]\frac{r_i r_j}{r^2} + B_{NN}(r)\delta_{ij} \tag{9.73}$$

The number of unknown functions can be reduced to one (either B_{LL} or B_{NN}) by employing the continuity equations derived in above in Section 9.5

Exercise: Find B_{LL} in terms of B_{NN} Use the isotropic relation of equation 9.73 together with the incompressible continuity equations 9.43 and 9.44 to obtain:

$$B_{LL} = B_{NN} + r\frac{dB_{LL}}{dr} \tag{9.74}$$

(Hint: Note that $\partial B_{LL}/\partial r_i = dB_{LL}/dr\ (\partial r/\partial r_i)$ and that $\partial r/\partial r_j = r_j/r$. Show this by differentiating $r^2 = r_1^2 + r_2^2 + r_3^2$) term by term.)

9.8.4 Derivative moments in isotropic turbulence

Isotropy has a powerful influence on the velocity derivative moments. In fact, only one of them is independent, so all of the others can be expressed in terms of it. For example, if we choose to express the others in term of $\langle[\partial u_1/\partial x_1]^2\rangle$, the results are:

$$\langle\left[\frac{\partial u_1}{\partial x_1}\right]^2\rangle = \langle\left[\frac{\partial u_2}{\partial x_2}\right]^2\rangle = \langle\left[\frac{\partial u_3}{\partial x_3}\right]^2\rangle, \tag{9.75}$$

$$\begin{aligned}\langle\left[\frac{\partial u_1}{\partial x_1}\right]^2\rangle &= \frac{1}{2}\langle\left[\frac{\partial u_1}{\partial x_2}\right]^2\rangle = \frac{1}{2}\langle\left[\frac{\partial u_2}{\partial x_1}\right]^2\rangle \\ &= \frac{1}{2}\langle\left[\frac{\partial u_1}{\partial x_3}\right]^2\rangle = \frac{1}{2}\langle\left[\frac{\partial u_3}{\partial x_1}\right]^2\rangle \\ &= \frac{1}{2}\langle\left[\frac{\partial u_2}{\partial x_3}\right]^2\rangle = \frac{1}{2}\langle\left[\frac{\partial u_3}{\partial x_2}\right]^2\rangle \end{aligned} \tag{9.76}$$

and

$$\begin{aligned}\langle\left[\frac{\partial u_1}{\partial x_1}\right]^2\rangle &= -\langle\frac{\partial u_1}{\partial x_2}\frac{\partial u_2}{\partial x_1}\rangle \\ &= -\langle\frac{\partial u_2}{\partial x_3}\frac{\partial u_3}{\partial x_1}\rangle \\ &= -\langle\frac{\partial u_2}{\partial x_3}\frac{\partial u_3}{\partial x_2}\rangle \end{aligned} \tag{9.77}$$

It follows immediately the dissipation for isotropic turbulence can be quite simply expressed as:

$$\epsilon = 15\nu\langle\left[\frac{\partial u_1}{\partial x_1}\right]^2\rangle \tag{9.78}$$

But any of the other derivatives could have been used as well; e.g.,

$$\epsilon = \frac{15}{2}\nu\langle\left[\frac{\partial u_2}{\partial x_1}\right]^2\rangle. \tag{9.79}$$

9.8.5 Isotropic integral scale and Taylor microscales

It is straightforward to show from the form of the isotropic correlation function that the integral scales based on the longitudinal correlation, $B_{LL}(r)$, is double that of the normal correlation, $B_{NN}(r)$.

Exercise: Prove that $L^{(1)}_{2,2}$ and $L^{(2)}_{1,1}$ are twice $L^{(1)}_{1.1}$. (Hint: Use equation 9.74 and integrate by parts.)

It is similarly quite easy to show from the derivative relations and the definitions of the Taylor microscales that $\lambda_f = \sqrt{2}\lambda_g$. It follows immediately that the dissipation can be expressed in terms of the Taylor microscales for isotropic turbulence as:

$$\varepsilon = 30\nu\frac{u^2}{\lambda_f^2} = 15\nu\frac{u^2}{\lambda_g^2} \tag{9.80}$$

since $u^2 = \langle u_1^2 \rangle = \langle u_2^2 \rangle = \langle u_3^2 \rangle$.

Exercise: Prove that $\lambda_f^2 = 2\lambda_g^2$.

9.9 Axisymmetric Turbulence

A less restrictive hypothesis about turbulence than isotropy is that all statistical measures have rotational symmetry about a given axis. This is called *axisymmetric* turbulence.[2] In fact very few flows satisfy the conditions for isotropic turbulence, but many seem to satisfy the requirements and constraints for axisymmetric turbulence. For example, in turbulent shear flows, the produced component of the turbulence energy is larger than the other two components which are approximately equal. This is especially true for the derivative moments, where many flows appear to satisfy the axisymmetric relations but not the isotropic ones.[3] In spite of this axisymmetric turbulence has not been much exploited in modeling, perhaps because there is virtually nothing about it in texts. We shall to remedy that in this section.

We focus here only on the velocity derivatives. If we imagine the flow to have a preferred direction, say prescribed by the unit vector, $\vec{\gamma}$, then a Taylor expansion of the most general form of the two-point axisymmetric tensor around the point $\vec{r} = 0$ is given by:

$$\begin{aligned} B_{i,j}(\vec{r}) &= 2(\alpha_{02} - \alpha_{22} + \beta_{02}) r_i r_j - (2\alpha_{00} + \beta_{00}) + r^2 \{[-4\alpha_{02} + 2\alpha_{22} - 3\beta_{02}) \\ &\quad + \tilde{\mu}^2 (2\beta_{02} - \beta_{22} - 8\alpha_{22})\}\Big] \delta_{ij} + \Big[\beta_{00} + r^2(3\beta_{02} - 2\alpha_{22} + \beta_{22}\tilde{\mu}^2)\Big] \gamma_i \gamma_j \\ &\quad + 2r\tilde{\mu}(\gamma_i r_j + r_i \gamma_j)(2\alpha_{00} - \beta_{02}) \end{aligned} \tag{9.81}$$

where $\vec{\gamma}$ is a unit vector in the preferred direction and $\tilde{\mu} = \vec{\gamma} \cdot \vec{r}/r$ is the inner product of $\vec{\gamma}$ with a unit vector in the direction of the separation vector, $\vec{r}$. The two invariants, α_{00} and β_{00} can be related to the components of the turbulence energy by:

$$\alpha_{00} = -\frac{1}{2}\langle u_1^2 \rangle \tag{9.82}$$

$$\begin{aligned} \beta_{00} &= \langle u_1^2 \rangle - \langle u_2^2 \rangle \\ &= \langle u_1^2 \rangle - \langle u_3^2 \rangle \end{aligned} \tag{9.83}$$

where it is presumed that $\langle u_2^2 \rangle = \langle u_3^2 \rangle$. These will not enter the axisymmetric derivative relations.

[2]The theory of axisymmetric turbulence was first developed by Chrandresekhar in 1950.

[3]The idea of locally axisymmetric turbulence appears to have originated with George and Hussein (1991), J. Fluid Mechanics, vol. 233, pp 1 -23.

It is relatively easy to show that:

$$\begin{aligned} B_{1,1}(\vec{r}) &= -2\alpha_{00} - [2\alpha_{02} + 2\alpha_{022}]r_1^2 - 4\alpha_{02}(r_2^2 + r_3^2) && (9.84)\\ B_{2,2}(\vec{r}) &= -(2\alpha_{00} + \beta_{00}) - [4\alpha_{02} + 6\alpha_{22} + \beta_{02} + \beta_{22}]r_1^2 \\ &\quad -[2\alpha_{02} + \beta_{02}]r_2^2 - [4\alpha_{02} - 2\alpha_{22} + 3\beta_{02}]r_3^2 && (9.85)\\ B_{2,2}(\vec{r}) &= -(2\alpha_{00} + \beta_{00}) - [4\alpha_{02} + 6\alpha_{22} + \beta_{02} + \beta_{22}]r_1^2 \\ &\quad -[4\alpha_{02} - 2\alpha_{22} + 3\beta_{02}]r_2^2 - [2\alpha_{02} + \beta_{02}]r_3^2 && (9.86) \end{aligned}$$

Note that the last two just have r_2 and r_3 reversed, consistent with the symmetry about the 1-axis. The off-diagonal terms of $B_{i,j}$ reduce to:

$$\begin{aligned} B_{1,2}(\vec{r}) &= 2(\alpha_{02} + \alpha_{22})r_1 r_2 && (9.87)\\ B_{1,3}(\vec{r}) &= 2(\alpha_{02} + \alpha_{22})r_1 r_3 && (9.88)\\ B_{2,3}(\vec{r}) &= 2(\alpha_{02} - \alpha_{00} + \beta_{00})r_2 r_3 && (9.89) \end{aligned}$$

After some work the general derivative moments can be shown to be given by:

$$\begin{aligned} \langle \frac{\partial u_i}{\partial x_m}\frac{\partial u_j}{\partial x_n}\rangle &= (-2\alpha_{02} + 2\alpha_{22} - 2\beta_{02})(\delta_{in}\delta_{jm} + \delta_{im}\delta_{jn}) && (9.90)\\ &+ \{(8\alpha_{02} - 4\alpha_{22} + 6\beta_{02})\delta_{mn} - (4\beta_{02} - 2\beta_{22} - 16\alpha_{22})\delta_{1m}\delta_{1n}\}\,\delta_{ij} \\ &- (4\alpha_{02} - 2\beta_{02})[\gamma_i(\delta_{1m}\delta_{jn} + \delta_{jm}\delta_{1n}) + \gamma_j(\delta_{1m}\delta_{in} + \delta_{im}\delta_{1n})] \end{aligned}$$

It follows that of the 45 possible derivative moment combinations, all but 15 are zero in axisymmetric turbulence. The non-zero moments depend only on α_{02}, α_{22}, β_{02}, and β_{22}.

If the 1-axis is chosen as the axis of symmetry,then the non-zero moments are:

$$\begin{aligned} \langle\left[\frac{\partial u_1}{\partial x_1}\right]^2\rangle &= 4\alpha_{02} + 4\alpha_{22} && (9.91)\\ \langle\left[\frac{\partial u_2}{\partial x_2}\right]^2\rangle = \langle\left[\frac{\partial u_3}{\partial x_3}\right]^2\rangle &= 4\alpha_{02} + 4\beta_{02} && (9.92)\\ \langle\left[\frac{\partial u_1}{\partial x_2}\right]^2\rangle = \langle\left[\frac{\partial u_1}{\partial x_3}\right]^2\rangle &= 8\alpha_{02} && (9.93)\\ \langle\left[\frac{\partial u_2}{\partial x_1}\right]^2\rangle = \langle\left[\frac{\partial u_3}{\partial x_1}\right]^2\rangle &= 8\alpha_{02} + 12\alpha_{22} + 2\beta_{02} + 2\beta_{22} && (9.94)\\ \langle\left[\frac{\partial u_2}{\partial x_3}\right]^2\rangle = \langle\left[\frac{\partial u_3}{\partial x_2}\right]^2\rangle &= 8\alpha_{02} + 4\alpha_{22} + 6\beta_{02} && (9.95) \end{aligned}$$

The cross-derivative moments are:

$$\langle\frac{\partial u_1}{\partial x_2}\frac{\partial u_2}{\partial x_1}\rangle = \langle\frac{\partial u_1}{\partial x_3}\frac{\partial u_3}{\partial x_1}\rangle = -2(\alpha_{02}+\alpha_{22}) \tag{9.96}$$

$$\langle\frac{\partial u_2}{\partial x_3}\frac{\partial u_3}{\partial x_2}\rangle = -2(\alpha_{02}-\alpha_{22}+\beta_{02}) \tag{9.97}$$

It follows immediately by substitution into their definitions that the dissipation, ε, and enstrophy (mean square vorticity), $\langle\omega_i\omega_i\rangle$, are given by:

$$\varepsilon/\nu = \langle\omega_i\omega_i\rangle = [60\alpha_{02}+20\alpha_{22}+20\beta_{02}+4\beta_{22}] \tag{9.98}$$

There are a variety of ways to solve for the four invariants in terms of four independent derivative moments. These choice is generally made from what is easiest to obtain experimentally. For example, with hot-wire anemometers a particularly convenient choice of derivatives to measure are $\partial u_1/\partial x_1$, $\partial u_1/\partial x_3$, $\partial u_2/\partial x_1$ and $\partial u_3/\partial x_1$. It is easy to show the the relations above yield:

$$\alpha_{02} = \frac{1}{3}\langle\left[\frac{\partial u_1}{\partial x_3}\right]^2\rangle \tag{9.99}$$

$$\alpha_{22} = \frac{1}{4}\left\{\langle\left[\frac{\partial u_1}{\partial x_3}\right]^2\rangle - \frac{1}{2}\langle\left[\frac{\partial u_1}{\partial x_3}\right]^2\rangle\right\} \tag{9.100}$$

$$\beta_{02} = \frac{1}{6}\left\{\langle\left[\frac{\partial u_2}{\partial x_3}\right]^2\rangle + \langle\left[\frac{\partial u_1}{\partial x_1}\right]^2\rangle - \frac{3}{2}\langle\left[\frac{\partial u_1}{\partial x_3}\right]^2\rangle\right\} \tag{9.101}$$

$$\beta_{22} = \frac{1}{2}\left\{\langle\left[\frac{\partial u_2}{\partial x_1}\right]^2\rangle + \langle\left[\frac{\partial u_1}{\partial x_3}\right]^2\rangle - \frac{10}{3}\langle\left[\frac{\partial u_1}{\partial x_1}\right]^2\rangle - \frac{1}{3}\langle\left[\frac{\partial u_2}{\partial x_3}\right]^2\rangle\right\} \tag{9.102}$$

It follows that the dissipation and enstropy are given for this choice of independent derivatives as:

$$\varepsilon = \nu\left\{\frac{5}{3}\langle\left[\frac{\partial u_1}{\partial x_1}\right]^2\rangle + 2\langle\left[\frac{\partial u_1}{\partial x_3}\right]^2\rangle + 2\langle\left[\frac{\partial u_2}{\partial x_1}\right]^2\rangle + \frac{8}{3}\langle\left[\frac{\partial u_2}{\partial x_3}\right]^2\rangle\right\} \tag{9.103}$$

Exercise: Derive equations 9.102 and 9.103.

Alternatively one might choose derivatives depending only on measurements in the 1- and 2-directions; e.g., when using planar particle image velocimetry (PIV). The dissipation can be shown in this case to be given by:

$$\varepsilon = \nu\left\{-\langle\left[\frac{\partial u_1}{\partial x_1}\right]^2\rangle + 2\langle\left[\frac{\partial u_1}{\partial x_2}\right]^2\rangle + 2\langle\left[\frac{\partial u_2}{\partial x_1}\right]^2\rangle + 8\langle\left[\frac{\partial u_2}{\partial x_2}\right]^2\rangle\right\} \tag{9.104}$$

Exercise: Derive equation 9.104. Hint: first solve for the invariants in terms of these derivative moments.

Chapter 10

How do we decompose turbulence into 'scales of motion'?

10.1 Scales of turbulence

In the preceding chapter we have come to understand which terms do what in the incompressible Reynolds-averaged Navier-Stokes equations. We know now that it is the Reynolds stress working against the mean velocity gradient that accounts for taking energy from the mean flow and putting it into the turbulence (at least in most situations). And we know it is the dissipation (of turbulence energy) which takes this kinetic energy out from the turbulence and sends it along on an irreversible path to internal energy. So it seems there are no mysteries left, right? Actually there is quite a bit left to think about, especially if we want to know *how* these processes actually happen. And given all of the moments about which we need to make closure hypothesis to use the RANS e equations at all, we really all the "how" we possibly can.

Let me point something out again, something you probably just let slide by the first time. The Reynolds stresses are mostly associated with the large and energetic scales of motion, the so-called energy containing scales. But the dissipation takes place at the very smallest scales of motion, those characterized in high Reynolds number turbulence by the Kolmogorov microscale. If this picture is really true, how does the energy get from the large scales to the small scales? Or putting it another way: where in the equations is there a term (or terms) that accounts for this apparently necessary transfer of energy from large to small scales?

Obviously this whole "breakdown" of the energetic scales to smaller scales is the key to the entire role of turbulence as the primary mechanism for energy dissipation. If this didn't happen, then there would be no reason to expect $< s_{ij}s_{ij} > >> S_{ij}S_{ij}$. And thus no way the turbulence dissipation could dominate direct viscous dissipation by the mean flow, which it most certainly does in most instances where turbulence occurs.

But why does this really matter? Consider the following examples. If you

wanted to increase dissipation (e.g., to slow down an airplane) then you would want to increase the rate at which energy is transferred to the smaller scales. If you wanted to decrease dissipation (e.g., to save fuel in flight), then obviously you would like to interfere with and reduce this downward cascade. Regardless of its practical interest, the manner in which different scales of motion exchange energy is clearly VERY important.

But suppose you find you are not able to significantly alter the rate at which energy is sent from large to small scales? What can you do now? The obvious alternative is to prevent the energy from getting into the turbulence in the first place. But how do you do this? You know it is the Reynolds stress working against the mean velocity gradient that "produces" turbulence energy from the mean flow. But this is like saying that money comes from a bank. Where does the Reynolds stress come from? How does it accomplish this energy transfer from mean to fluctuation? You can guess that it must have something to do with the large scales of motion, since that's where the most energy is. But how and why did it get there? Clearly some kind of flow instability must be at work here. If so, is it the same kind of instabilities that transfer energy the from the large scales at which it is produced to the much smaller scales at which it is dissipated? Or is there something entirely different at work here?

An even more fundamental question is: what do we mean when we talk about 'scales' of motion at all? When we look up at the clouds or the exhaust from a smoke stack, we can certainly imagine that we see different 'scales' of motion. The same is true when we observe the breakdown of the smoke rising from a smoldering cigarette or match, or as we pour cream into a cup of coffee. But to carry out a physical analysis, we must somehow translate our visualization of 'scales' into mathematics of scale. And that is much more difficult.

There are many ways we can imagine spatially averaging, filtering (or 'windowing') the information about turbulence that we see or measure or simulate. For example, we can easily invent a 'volume-averaged' turbulent velocity field, $u_i^{(v)}(\vec{x},t)$ defined by

$$u_i^{(v)}(\vec{x},t) = \frac{1}{v}\int\int\int_v u_i(\vec{x}-\vec{x'},t)d\vec{x'} \tag{10.1}$$

This is just a convolution integral which produces a new velocity, u_i^v, from the original instantaneous field by averaging it around some neighborhood v of the point $\vec{x}$. And of course in doing so we will smooth out (or average out) fluctuations that are smaller than the characteristic dimension of the volume over which we have averaged. This would seem to be exactly what we are looking for, since simply by changing the volume, or looking at the differences between volumes of different sizes, we can look at any 'scale' of motion we please.

But now try to do the same volume-averaging to the Navier-Stokes equations. Immediately you will discover that you cannot compute anything without facing the same kind of closure problems that always result from averaging. No matter how we average, or over what scale, we are always left with trying to account for

what is affecting our averages by things that you thought we averaged out. When we made the continuum hypothesis, we ended up with stresses. When we used the Reynolds decomposition to produce the RANS equations, we ended up with Reynolds stresses. And no matter how we spatially average, we will always end up with 'sub-volume' stresses. Such volume averages are the basis most so-called 'large eddy simulations' (or LES), and finding suitable closure models for the sub-volume (or 'sub-grid') scale stresses represents one of the greatest challenges.

Unfortunately, in turbulence (like the stresses in many non-Newtonian fluids as well), often the effects of the sub-grid stresses are not local (in time or space), so simple gradient hypotheses do not work very well. Obviously, just as we must look at molecular structure to understand non-Newtonian effects in fluids, or look at grain structure to understand some solid materials, we need to figure out a way to literally tear the turbulence apart to understand what is really going on. This chapter and the ones that follow it are all how to do this, and do it in a way that leads us to dynamical equations. Only by analyzing such equations can we truly say we understand 'the physics'.

10.2 The anatomy of turbulent motions

Clearly we need a way to describe mathematically the different scales of motion. Moreover, it can only be useful to us (wearing our engineering hats) if it leads us to a set of equations that describe these different scales. And these equations must tell us how the different scales transfer energy to each other, and how they get energy from the mean flow in the first place. These are among the most difficult questions in turbulence for the physicists and mathematicians, and the successful resolution will be of enormous importance for engineers. In this chapter we will look at one very powerful approach to this problem.

Now it is really simple to see the evolution from large scales to small scales in nature. All you have to do is look into a coffee cup after you have added cream and stirred. But it is really difficult to try to quantify exactly how all this relates to simple vortical structures. Even when we succeed, it is not at all clear how these structures (or vortices) at different scales interact with (or evolve from) each other. Worse, though, it is almost impossible to write down equations to describe what we see.

Think of the following analogy with biology. It is one thing to talk about the anatomy of the human body, another to talk about its physiology. Anatomy describes what is there (like arms and legs and internal organs), physiology explains how things work. Both are essential, but anatomy alone would be pretty useless, and physiology alone impossible. But at the same time, imagine trying to even talk about physiology without having anatomical terms so we know which part of the body is being analyzed. So it is with turbulence: the 'anatomy' must allow us to do 'physiology'. Words that do not lead to equations are of very limited value, no matter how vivid and accurate their description of the flow.

So we need a mathematical way to break turbulent velocities down into various scales of motion. Now it is here that most introductory books simply give up, and either try to convince you (usually with lots of hand-waving and verbal descriptions) that it is all obvious. Or else they go immediately into spectral or structure function analysis, leaving you mostly on your own to figure out why these are important. The former approach cannot possibly succeed since you don't have to go very far to realize something is missing; namely any way to connect all these mental pictures with equations. And the latter leaves you shaking your head wondering what happened, why we switched to Fourier space, and how these powerful mathematical techniques could possibly have any relevance to real flows.

I am going to try something totally different in the history of introductory turbulence, so you have a chance here to either make me look like an educational pioneer or a complete fool. It is my view that most students are smart enough and know enough simple math that we can provide a satisfactory and correct answer to the question of scales in turbulence motion. This will eventually lead us to a subject that strikes terror into the hearts of even many senior turbulence investigators: **the POD**. But don't worry. We only need some rather simple calculus. Luckily for us, we will find it leads us to a gold mine of well-known mathematical results accumulated over the past 200 years.

Now the method we shall discuss is surely not the only way to decompose a turbulent flow. And it may not even ultimately prove to be the best way. But it certainly will be seen to be a sure way to both break the flow down into "things" which can be sometimes be interpreted as "scales of motion". From it, we shall see that spectral analysis falls out rather naturally as the ideal way to decompose a homogeneous flow. Most importantly, whether we can interpret the results as 'scales' or not, we can always end up with equations which describe how each piece evolves and interacts with the others.

The problem was originally posed for turbulence by John Lumley[1] in the following manner: suppose we have a random velocity field, $u_i(\cdot)$, where '$\cdot$' represents $\vec{x}, t$ or some subset of them. We seek to find a *deterministic* vector field, say $\phi_i(\cdot)$, which has the maximum projection on our *random* vector field, u_i, in a *mean square sense.* In other words, we would like to find a whole new deterministic field represented by $\phi_i(\cdot)$ for which $< |(u_i(\cdot), \phi_i^*(\cdot))|^2 >$ is maximized.

If we think of both u_i and ϕ_i as functions belonging to Hilbert space (I bet this sends most of you scurrying for those dusty old math books), then this inner product can be written as :

$$(u_i(\cdot), \phi_i^*(\cdot)) = \int\int\int_V u_i(\cdot)\phi_i^*(\cdot)d(\cdot) \tag{10.2}$$

where the integral is over the entire domain defined by the physical extent of the turbulent field.

[1]Professor John Lumley, now at Cornell, was (and still is) one of the leading turbulence experts in the last half of the 20th century. And he is rather special to me since he was my Ph.d dissertation advisor.

It is pretty easy to show by the calculus of variations[2] that the appropriate choice of $\phi_i(\cdot)$ to maximize its projection onto the velocity field is the solution to the following integral equation:

$$\int_{region} R_{ij}(\cdot,\cdot')\phi_j(\cdot')d(\cdot') = \lambda\phi_i(\cdot) \tag{10.3}$$

where $R_{i,j}(\cdot,\cdot')$ is the *two point* correlation function given by:

$$R_{i,j}(\cdot,\cdot') \equiv < u_i(\cdot)u_j(\cdot') > \tag{10.4}$$

and

$$\lambda =< |\alpha^2| > . \tag{10.5}$$

where α is defined by:

$$\alpha = \int_{region} u_i(\cdot)\phi_i(\cdot)d(\cdot) \tag{10.6}$$

Exercise: Prove that equations 10.3 to 10.5 result from maximizing the projection of $\phi(\cdot)$ onto $u_i(\cdot)$: in a mean square sense. Note that you must rule out simply making ϕ as large as possible by dividing by the square root of its projection on itself, $(\phi_i(\cdot), \phi_i(\cdot))$; i.e., maximize:

$$\frac{\int_{region} u_i(\cdot)\phi_i(\cdot)d(\cdot)}{\left[\int_{region} \phi_i(\cdot)\phi_i(\cdot)d(\cdot)\right]^{1/2}} \tag{10.7}$$

Alternatively, you can maximize $(u_i(\cdot), \phi_i^*(\cdot))$ subject to the constraint that $(\phi_i(\cdot), \phi_i^*(\cdot)) = 1$. Either way the result should be equation 10.3.

Equation 10.3 is an *integral equation* since the unknown function to be solved for, $\phi_i(\cdot)$, occurs on both sides, only one of them inside the integral. Also note that the value of λ is itself unknown, and must be determined as a part of the solution. This appears quite complicated, but luckily for us, integral equations are well-known to mathematicians who have spent a few hundred years learning and writing books about them. This particular integral equation is a member of the family of Fredholm integral equations.[3] Usually it does not have a single solution set ϕ_i, λ, but many. In general, the number, nature and character of these solutions depends on both the nature of the kernel *and* the type of region over which the integral is taken.

Thus, finding the very best choice of our special deterministic function, $\phi_i(\cdot)$, to represent the random velocity field, $u_i(\cdot)$, has reduced to finding a solution to an integral equation for $\phi_i(\cdot)$ in which the kernel is given by the two-point correlation function, $R_{i,j}(\cdot,\cdot')$. Now this might not have come as a surprise to you; but if not, you may well be the first person ever for which that is true.

[2]It only took me about 20 years, but it really is trivial

[3]Fredhom was a Swedish mathematician of the 19th century.

The two-point correlation is, of course, itself deterministic since it is obtained from averages of the velocity field. So all of the information about our particular solution to the Navier-Stokes equations (our flow of interest) is contained in this kernel. As we shall see, the big problem in applying equation 10.3 is in finding out sufficient information about $R_{i,j}(\cdot,\cdot')$ to make the integration possible (if it is possible at all).

10.3 Fields of Finite Extent

The most familiar application of equation 10.3 is to flows in which the region is of finite extent in one or more directions (or time), either naturally or because of artificially imposed boundaries. If the field is of finite total energy, then the classical Hilbert-Schmidt theory applies. (Another quick trip to the math books might help here too). According to the Hilbert-Schmidt theory of integral equations, there is not just a single solution to equation 10.3, but there are denumerably infinitely many solutions (or *eigenfunctions*), $\phi_i^{(n)}(\cdot)$, $n = 1, 2, \cdots$. For each eigenfunction, there is a corresponding eigenvalue, λ_n. Moreover, these solutions are *orthogonal*. (I sure this brings back lots of fond memories from your math courses, right?) All this means is that:

$$\int_{region} \phi_i^{(p)}(\cdot)\phi_i^{(n)^*}(\cdot)d(\cdot) = \delta_{pn} \tag{10.8}$$

Now since we have all of these solutions and they are orthogonal, we can reconstruct the original velocity field from them as:

$$u_i(\cdot) = \sum_{n=1}^{\infty} a_n \phi_i^{(n)}(\cdot) \tag{10.9}$$

The *random* coefficients a_n are functions of the variables *not* used in the integral, and must be determined by projection back onto the velocity field; *ie*

$$a_n = \int_{region} u_i(\cdot)\phi^{*(n)}_i(\cdot)d(\cdot) \tag{10.10}$$

It is easy to show using the fact that the $\phi^{(n)}(\cdot)$ are orthonormal that:

$$\lambda_n =< a_n a_m > \delta_{mn} \tag{10.11}$$

Thus the random coefficients are uncorrelated.

And, since we can reconstruct the velocity, of course we can reconstruct the two point Reynolds stress tensor, $R_{i,j}(\cdot,\cdot')$. The result after self-multiplication and averaging of equation 10.9 is:

$$R_{i,j}(\cdot,\cdot') = \sum_{n=1}^{\infty} \lambda_n \phi_i^{(n)}(\cdot)\phi_j^{(n)}(\cdot') \tag{10.12}$$

The eigenvalues are ordered (meaning that the lowest order eigenvalue is bigger that the next, and so on); i.e, $\lambda_1 > \lambda_2 > \lambda_3 \cdots$. Thus *the representation is optimal*

(or 'proper') in the sense that the fewest number of terms is required to capture the energy. This is VERY important, and frankly it is the only reason any one cares at all about the POD. It is truly the most efficient way to break-down a field of finite total energy into pieces, at least from the perspective of the *energy.*

Thus the POD has provided several insights and possibilities: First, because of the finite total energy it has produced a *denumerably infinite* set of *orthogonal* functions which optimally (in a mean square sense) describe the flow. This should make you feel VERY comfortable if you have had an applied math course, since you know lots of examples of orthogonal functions and can appreciate well what their advantages are. Don't be too bothered by the fact that we really don't know in general what our particular orthogonal functions are, and may not even be able to find them analytically. But we do know how to find them numerically and empirically — if we have enough information about the two point velocity correlation. We simply put our measured two-point correlation function into the integral of equation 10.18, and use some appropriate method method to calculate them. Usually this is by discretizing the integral first, so it becomes a matrix equation. Then with an appropriate subroutinue, out they pop.

Second a finite subset of these functions can be used to produce a finite number of equations for analysis. This is accomplished by using them in a Galerkin projection on the governing equations (in our case the instantaneous Navier-Stokes equations). By truncating after a specified number of modes, the infinitely dimensional governing equations are reduced to a finite set. We are not going to talk about this much in this course, but if you are into using the POD for control, or even if you are carrying out DNS (Direct Numerical Simulations) or LES (Large Eddy Simulations), you probably will find someone using them, even just to clean up numerical data. POD (Proper Orthogonal Decomposition) techniques are currently in vogue to generate appropriate bases for dynamical systems models of turbulence (*v* Holmes *et al* 1996, Glauser et al 1993), but they have been used for more than 30 years to investigate coherent structures in turbulence (*eg* Lumley 1967, George 1989b, Moin and Moser 1989).

10.4 Homogeneous Fields

Really interesting things happen to our optimal projection integral, equation 10.3, if the flow is homogeneous in $\vec{x}$. Recall that *homogeniety* means the statistics are independent of origin. In particular, the two point correlation with separation $\vec{r} = \vec{x'} - \vec{x}$ reduces to $R_{i,j}(\vec{x}, \vec{x'}) = B_{i,j}(\vec{r})$. Note that by definition homogeneous flows are not of finite total energy since they are of infinite extent, so the Hilbert-Schmidt theory cannot apply to them.

For fields homogeneous in $\vec{x}$, equation 10.3 can easily be shown to transform to:

$$\int\int\int_{-\infty}^{\infty} B_{i,j}(\vec{r}, t)\tilde{\phi}_j(\vec{x} + \vec{r})d\vec{r} = |\alpha^2|\tilde{\phi}_i(\vec{x}, t) \tag{10.13}$$

Since the $\phi(x)$ on the right hand side is a function of $\vec{x}$ only, it can be included in

the integral on the left so there is no x-dependence left on the right hand side; *ie*

$$\int\int\int_{-\infty}^{\infty} B_{i,j}(\vec{r},t)\left\{\frac{\tilde{\phi}_j(\vec{x}+\vec{r})}{\tilde{\phi}_i(\vec{x},t)}\right\}d\vec{r} = |\alpha^2| \tag{10.14}$$

It is immediately obvious that solution itself (the term in brackets) must eliminate the x-dependence on the left hand side.

There is really only one function which can accomplish this miracle, the exponential function. Therefore the eigenfunctions must be of the form $\phi(\vec{x}) \propto \exp[i\vec{k}\cdot\vec{x}]$ where $\vec{k}$ is a *wavenumber* vector and *all* values of it are possible; *ie* $-\infty < \vec{k} < \infty$. The coefficients of the exponential, say $\hat{u}_i(\vec{k},t)$, can be shown to be given by

$$\hat{u}_i(\vec{k},t) = \frac{1}{2\pi}\int\int\int_{-\infty}^{\infty} u_i(\vec{x},t)e^{-i\vec{k}\cdot\vec{x}}d\vec{x} \tag{10.15}$$

and the velocity field can be reconstructed from them by

$$u_i(\vec{x},t) = \int\int\int_{-\infty}^{\infty} \hat{u}_i(\vec{x},t)e^{i\vec{k}\cdot\vec{x}}d\vec{k} \tag{10.16}$$

Thus, unlike the finite total energy case considered above, the solutions to equation 10.3 for homogeneous fields do not need to be empirically determined. They are ordinary analytical functions and we know what they are; they are the familiar *Fourier transform* which depends on the continuous vector variable $\vec{k}$. This is indeed a wonderful surprise, mostly because over the past few hundred years we have learned more about the mathematics of Fourier transforms than just about any other function. Even though we are dealing with particularly nasty functions — these functions are not only random, but may not even go to zero at infinity (since the field is homogeneous) — there is a whole body of mathematics, the theory of *generalized* functions, to assure us that we are still able to proceed.

Exercise: Consider a random field of finite total energy which is a function of one variable only, say $u(r)$. Now the integral equation of equation 10.18 becomes:

$$\int_R R(r,r')\phi(r')dr' = \lambda\phi(r) \tag{10.17}$$

where the kernel is given by the cross-correlation, $R(r,r') = \langle u(r)u(r')\rangle$. Imagine that you only have data for a fixed number of points, say only $r, r' = n\Delta r$. Show how you can discretize this into a standard matrix eigenvalue problem which can be solved numerically.

Exercise: Now consider the same problem as above, but this time show how you might develop a solution by successive approximations, where you guess a solution, substitute it into the left-hand side and integrate to obtain the right hand side. Then use the new right-hand side to substitute into the the left-hand side again, etc. etc. For a simple example, let $R(r,r') = exp[-A(r+r')]$.

10.5 Are Homogeneous Fields and Periodic Fields the Same?

Contrary to popular assumption (especially in the DNS and LES communities), these are *not* the same thing. The velocity field is said to be *periodic* in the variable x if $u(x) = u(x + L)$ where L is the period and the dependence on the other variables has been suppressed for now, as has the fact that the field is a vector. *Homogeniety*, on the other hand, means the statistics are independent of origin. If a flow is homogeneous in a single variable, say x, then the two point correlation with separations in x reduces to $R(x, x') = \tilde{R}(r)$ where $r = x' - x$ is the separation. By definition, homogeneous flows are not of finite total energy since they are of infinite extent, so the Hilbert-Schmidt theory cannot apply to them. By oontrast, periodic fields are of finite total energy only if a single period is considered, since otherwise they repeat to infinity.

Now if periodicity and homogeniety are so different, why does the confusion arise? The POD provides the answer. For fields homogeneous in x, equation 10.3 can be shown to transform to

$$\int_{-\infty}^{\infty} \tilde{R}(r)\tilde{\phi}(x + r)dr = \tilde{\lambda}\tilde{\phi}(x) \tag{10.18}$$

Since the $\phi(x)$ on the right hand side is a function of x only, it can be included in the integral on the left. Since there is now no x-dependence left on the right hand side, it is immediately obvious that solution itself must eliminate the x-dependence on the left hand side. Therefore the eigenfunctions must be of the form $\tilde{\phi(x)} \sim \exp(ikx)$ where k is a wavenumber and *all* values of k are possible; *ie* $-\infty < k < \infty$. The coefficients, $\hat{u}(k)$, can be shown to be given by

$$\hat{u}(k) = \frac{1}{2\pi}\int_{-\infty}^{\infty} u(x)e^{-ikx}dx \tag{10.19}$$

and the velocity field can be reconstructed from them by

$$u(x) = \int_{-\infty}^{\infty} \hat{u}(k)e^{ikx}dk \tag{10.20}$$

Thus, as noted earlier, the optimized projection integral for homogeneous fields reduces to the familiar *Fourier transform* which depends on the continuous variable k, so the number of eigenfunctions is *non-denumerable*.

The situation for periodic fields is almost the same, but not quite — and that little difference is at the root of the confusion. Any periodic field, even a random one, can be represented by a *Fourier series*; *ie*

$$u(x) = \sum_{n=-\infty}^{\infty} a_n e^{i2\pi nx/L} \tag{10.21}$$

where the a_n are random and are determined in the usual manner. Using the orthogonality, the two-point correlation function can be written as

$$R(x,x') = \sum_{n=-\infty}^{\infty} < |a_n|^2 > e^{i2\pi n(x'-x)/L} \tag{10.22}$$

Thus the two-point correlation for periodic flows, like homogeneous flows, depends only on the difference variable $r = x' - x$. Hence the eigenvalue problem of the POD reduces to exactly the form of equation 10.18, except now the limits of integration are $(L/2, -L/2)$. It is easy to see that the POD modes must also be harmonic functions, like those for homogeneous flows. But there is a very important diffence which is obvious from the integral: for periodic flows the wavenumber must be given by $k = 2\pi n/L$ *and* n can only take integer values! Moreover, the number of POD modes is now *denumerably infinite* instead of being *non-denumerable* (*ie* continuous in k). Therefore *the POD modes and the Fourier modes are identical*. Thus the use of *Fourier series* to represent periodic fields is indeed optimal, at least in a mean square sense.

Now the relation between a boxed homogeneous field and a periodic field can be readily determined by noting that because the energy is made finite by the box, the Hilbert-Schmidt theory again applies; hence the number of eigenfunctions becomes denumerable. If the kernel of boxed field is now *in addition assumed to be periodic*, the Fourier series representation above follows immediately. Thus the periodic fields usually assumed for calculation are dynamically equivalent to a boxed homogeneous field with the additional assumption of periodicity of the *instantaneous* fields. The assumption of periodicity has not only made the eigenfunctions denumerable, but it has forced the phase relations of all the scales, and this must also be of particular concern for the largest ones.

Such calculations of bounded fields, like their experimental counterparts, can only be representative of homogeneous fields for scales of motion much smaller than the computational box (or lowest wavenumber) and for limited times. Whether current computations are acceptable is open to debate. My own view is that the best test of whether the field is a good model of a truly homogeneous flow is best measured by its departures (or lack of them) from similarity theory. We will talk about this in detail in the next chapter, but recognize that the whole subject is being debated right now, sometimes rather hotly. Who knows, you might be lucky enough find yourself in the middle of this debate quite soon.

10.6 Inhomogeneous fields of Infinite Extent

None of the approaches above applies to flows which are inhomogeneous, but of infinite extent (like most shear flows in the streamwise direction). In fact, it has not been at all clear until recently whether the integral of equation 10.3 even exists in such cases. All attempts to-date to apply the POD to the flow in these inhomogeneous directions have ended up applying the Hilbert-Schmidt

theory to artificially truncated, finite regions of the flow. And as a result, the eigenfunctions and eigenvalues found are dependent on the particular domain included in the decomposition. Clearly this is because it is the finite domain itself which is making the energy finite.

Recently, however, one of my Ph.d. students, Dan Ewing 1995 (see also Ewing and George 1995) was able to show that if similarity solutions of the *two-point* Reynolds stress equations were possible, then the POD could be applied *in similarity coordinates* and the eigenfunctions were harmonic functions in it. By using a logarithmic coordinate transformation he was able to identify a number of flows for which two-point similarity was possible, thus for these flows the eigenfunctions are known analytically. Most importantly, the eigenfunctions were independent of the domain, at least in principle. For the far axisymmetric jet, the appropriate modes were

$$u(\kappa, x) \sim x^{-1} \exp(-i\kappa\xi) \tag{10.23}$$

where

$$\xi \equiv \ln x/L_o \tag{10.24}$$

and L_o is prescribed by the initial conditions.[4] Thus two-point similarity and equation 10.3 have yielded an optimal set of eigenfunctions into which the flow can be decomposed. The two point correlations, $R_{ij}(x, x') =< u_i(x)u_j(x') >$, could all be expressed in the form,

$$R_{ij}(x, x') = Q(x, x')exp[i\kappa(\xi' - \xi)] = Q(x, x')exp[i\kappa \ln x'/x] \tag{10.25}$$

where $Q(x, x') = U_s(x)U_s(x')d\delta/dx$ and for this flow $U_s(x) \sim 1/x$ and $d\delta(x)/dx = constant$. Note the dependence of the correlation in similarity variables on $\xi' - \xi$, an obvious counterpart to the $x' - x$ dependence of homogeneous flows.

Now these functional forms are interesting for a couple of reasons. First, because they settle the question of whether equation 10.3 can be applied to a flow of infinite extent that is not homogeneous: It can! Second, for similarity flows of infinite extent, the optimal basis functions are analytical functions, and they are harmonic functions *in the similarity variable* $\xi = \ln x/L_o$. Third, there is a continuum of eigenfunctions since all values of the reduced wavenumber, κ, are possible; *ie* $-\infty < \kappa < \infty$. This last fact is the most interesting of all since it represents the counterpart of the homogeneous analysis above. Hence the denumerable POD modes of the Hilbert- Schmidt theory for an inhomogeneous finite energy flow have given way to the non-denumerable modes of Ewing. Thus, once again, the POD suggests that confining a flow changes the fundamental nature of it, consistent with observation.

There is at least one more interesting aspect of the these inhomogeneous eigenfunctions. It is easy to show by expanding the logarithm of equation 10.25 that the

[4]Interestingly, no length scale can be formed for a point source jet from the two parameters available, the kinematic viscosity and the rate at which momentum is added per unit mass. Hence L_o must depend on 'finite' source effects, like perhaps $(B_o^2/M_o)^{1/2}$ where B_o is the rate of mass addition per unit mass (v George 1989a).

limiting forms of at least these inhomogeneous eigenfunctions are ordinary Fourier modes. From its Taylor expansion about $x = x'$, $\ln x'/x = (x' - x)/x + \cdots$. It follows for small values of $(x' - x)/x$ that $R_{ij} \sim \exp[ik(x' - x]$ where k is the ordinary, but local, wavenumber defined by $k = \kappa x$. Thus the usual *assumptions* of *local* homogeniety and the use of spectral analysis for the small scale motions are justified, at least in this case. Whether this is a general property of the POD is still very much the subject of debate (*cf* Holmes *et al* 1996).

Bibliography

[1] Ewing D (1995) On Multi-point Simlarity Solutions in Turbulent Free-Shear Flows. PhD diss., Dept Mech Engr, SUNY/Buffalo, Buffalo, NY.a

[2] Ewing D and George WK (1995) Similarity Analysis of the Two-Point Velocity Correlation Tensor in the Turbulent Axisymmetry Jet. *Turbulence, Heat and Mass Transfer, Lisbon 1994* (Hanjalic and Pereira, eds.), Begell House Inc., NY, 49 – 56.

[3] Holmes P, Lumley JL and Berkooz G (1996) *Turbulence, Coherent Structures, Dynamical Systems and Symmetry* CUP, Cambridge, UK.

[4] George WK (1989b) Insight into the Dynamics of Coherent Structures from a Proper Orthogonal Decomposition. in *Zorin Zaric Symp on Near-wall Turbulence, Dubrovnik, Yug* (S.Kline ed), Hemisphere, NY.

[5] Lumley JL (1967) The Structure of Inhomogeneous Turbulent Flows. in *Atm Turb and Radio Wave Propag*, Nauka, Moscow.

Chapter 11

Decomposing Homogeneous Turbulence

Homogeneous turbulence provides us the only opportunity to study turbulence in the absence of turbulence transport and even more important, the absence of boundary conditions. Our study is facilitated by the results of section 10.4 which showed that homogenous turbulence is optimally decomposed into functions of exponential type. Thus the most natural way to analyze homogeneous flows is to use Fourier analysis. But because homogeneous flows are of necessity of infinite extent, clearly Fourier integrals in the ordinary sense will not work since the integrals involving instantaneous quantities will not converge. Clearly we will need to generalize the usual definitions in order to make them useful. The classic texts have mostly approached this problem by using so-called Fourier-Stieljes integration, which can be quite forbidding to the new student to the subject (and many older students as well). Fortunately there is another much simpler way to approach the subject using generalized functions. (Note that the reader who is unfamiliar with this subject might first want to study the appendices C, E, and F, which deal with temporal Fourier analysis only without the complications of a vector argument.)

11.1 Generalized functions

For homogeneous flows, we found that the appropriate choices of eigenfunctions to solve equation 10.3 were exponential functions. The coefficients of these complex exponential eigenfunctions, say $\hat{u}_i(\vec{k},t)$, were given by:

$$\hat{u}_i(\vec{k},t) = \frac{1}{(2\pi)^3}\int\int\int_{-\infty}^{\infty} u_i(\vec{x},t)e^{-i\vec{k}\cdot\vec{x}}d\vec{x}, \tag{11.1}$$

and the velocity field can be reconstructed from them by:

$$u_i(\vec{x},t) = \int\int\int_{-\infty}^{\infty} \hat{u}_i(\vec{k},t)e^{i\vec{k}\cdot\vec{x}}d\vec{k} \tag{11.2}$$

Now if you have studied Fourier transforms in an applied math course, you have probably already spotted one potential problem: the integrals of equations E.1 and E.2 may not even exist — at least *in the ordinary sense*. A truly homogeneous field has no spatial bounds and must be truly infinite. Moreover, since its statistical properties are independent of origin, the velocity fluctuations simply go on forever. Thus our random velocity field is really rather nasty, mathematically speaking, and most certainly the integrals *in the ordinary sense* become unbounded.

So we have a dilemma. Our attempt to find the optimal way to decompose this flow has led us to Fourier transforms, but they do not seem to apply to the very problem which gave rise to them — turbulence which is homogeneous. The answer lies in a major mathematical development of the 20th century — the theory of **generalized functions**.

There are numerous references which one can consult for a more proper mathematical treatment than the rather cursory and intuitive treatment here. (Lumley 1970, Lighthill 1955 are two of my favorites). In brief the basic idea is to replace functions whose integrals do not converge, with functions which do. Great idea, I'm sure you are thinking, but doesn't this require magic? In truth it is almost magic, since in the end we almost never worry about what we have done, and almost always just go on doing regular mathematics like nothing ever happened. Impossible, you say. Let's consider a simple example in one dimension.

Suppose I want to take the integral of the function, $f(x) = 1$, from $(-\infty, \infty)$. Obviously this integral does not exist. Nor, in fact does its Fourier transform exist (*in the ordinary sense*).

Now consider a second function, say:

$$g_L(x) = e^{-x^2/2L^2} \tag{11.3}$$

Now since the tails of this function roll-off exponentially, it certainly is integralable; in particular,

$$\int_{-\infty}^{\infty} e^{-x^2/2L^2} dx = \sqrt{2\pi} L \tag{11.4}$$

(You know this from Chapter 2, since $(1/\sqrt{2\pi}L)exp(-x^2/(2L^2)$ is exactly the Gaussian which integrates to unity.)

Our integrable function $g_L(x)$ also has a wonderful Fourier transform, wonderful in the sense that not only does it exist, all its derivatives exist also; i.e.,

$$\mathbf{FT}\{e^{-x^2/2L^2}\} = \frac{1}{2\pi}\int_{-\infty}^{\infty} e^{-ikx} e^{-x^2/2L^2} dx = \sqrt{2\pi} L e^{-k^2L^2/2} \tag{11.5}$$

This is easy to compute by completing the square.

So we have one nasty function, $f(x) = 1$, and one wonderful function, $g_L(x)$; the former has no integral, and hence no transform (*in the ordinary sense*), but the latter has both. Now note something interesting. The limit of $g_L(x) \to 1$ as $L \to \infty$, which is exactly the value of our nasty function, $f(x)$. In fact, we could just define a new function by the product $f_L(x) = f(x)g_L(x)$ and note that:

$$\lim_{L\to\infty} f_L(x) = \lim_{L\to\infty} f(x)g_L(x) = f(x) \tag{11.6}$$

In fact, even more interestingly, the Fourier transform of our new function, $f_L(x)$, also exists *in the ordinary sense*. In this case, it's just the Fourier transform of g_L itself.

Here is where one of the really good ideas of the last century appears[1], the magic if you will. Let's just **define** the Fourier transform of our nasty function, $f(x)$, **in the sense of generalized functions** to simply be the limit of the Fourier transform of $f_L(x)$ as $L \to \infty$; i.e,

$$\mathbf{FT_{gf}}\{f(x)\} = \lim_{L\to\infty} \mathbf{FT}\{f_L(x)\} = \lim_{L\to\infty} \frac{1}{2\pi}\int_{-\infty}^{\infty} e^{-ikx} f(x)g_L(x)dx \tag{11.7}$$

The Fourier transform of 1 *in the sense of generalized functions* is so useful, we have given it a special name, the 'delta-function'; i.e.,

$$\delta(y) \equiv \lim_{L\to\infty} G_L(y) \tag{11.8}$$

where $G_L(y)$ can be any function whose integral is unity and which becomes undefined at $y = 0$ and zero everywhere else in the limit as $L \to \infty$.

I'm sure you have seen δ before, but you may not have realized that it was a generalized function. In general, the generalized functions are not uniquely defined. For example, all the functions below are suitable for defining $\delta(y)$:

$$G_L(y) = \frac{1}{\sqrt{2\pi}} e^{-y^2/2L^2} \tag{11.9}$$

$$G_{2L}(y) = e^{-\|y|/L} \tag{11.10}$$

$$G_{3L}(y) = \frac{sin(\pi y/L)}{\pi y/L} \tag{11.11}$$

The first and last have continuous derivative everywhere, the second has a singularity at the origin. When working with Fourier transforms, it is generally best to define them in terms of functions which both go to zero exponentially fast, and which have all derivatives continuous. There is nothing in this course which needs anything more than $G_L(y)$, the Gaussian version, or $\sqrt{2\pi}L$ times it.

We can generalize this whole procedure to almost any arbitrary function, whether deterministic or random. For example, suppose we have a random homogenous function (in one variable), say $v(x)$. Then we can define its Fourier transform *in the sense of generalized functions* to be:

[1] One of the first to see this was the electrical engineer named Heaviside — and he invented the step function which bears his name.

$$\hat{v}(k) \equiv \mathbf{FT_{gf}}\{v(x)\} = \lim_{L\to\infty} \mathbf{FT}\{v(x)g_L(x)\} \tag{11.12}$$

$$= \lim_{L\to\infty} \frac{1}{2\pi}\int_{-\infty}^{\infty} e^{-ikx}v(x)g_L(x)dx \tag{11.13}$$

where $g_L(x)$ can be any function for which the product $v(x)g_L(x)$ is integrable and for which:

$$\lim_{L\to\infty} v(x)g_L(x) = v(x) \tag{11.14}$$

Obviously a suitable choice is the Gaussian function we started off with; i.e.,

$$g_L(x) = e^{-x^2/2L^2} \tag{11.15}$$

Exercise: Show that the Fourier transforms *in the sense of generalized functions* of e^{ikx_o}, $coskx_o$ and $sinkx_o$ are $\delta(x_o)$, $[\delta(x_o) + \delta(-x_o)]/2$ and $i[\delta(x_o) + \delta(-x_o)]/2$ respectively using the Gaussian version of $g_L(x)$ defined above.

Exercise: Compute the inverse transforms from the above example. Do NOT use the short-cut version where you assume the properties of a delta-function, but instead work with the actual transformed version of $f(x)g_L(x)$ under the limit sign, then take the limits.

For the rest of this course, we will simply agree that whenever there is any doubt, we always mean the Fourier transform in the sense of generalized functions. For example, when we take the three dimensional spatial Fourier transform of the velocity field, $u_i(\vec{x},t)$, we really mean the Fourier transform in the sense of generalized functions defined by:

$$\hat{u}_i(\vec{k},t) \equiv \mathbf{FT_{gf}}\{u_i(\vec{x},t)\} \tag{11.16}$$

$$= \lim_{L\to\infty} \frac{1}{(2\pi)^3}\int\int\int_{-\infty}^{\infty} e^{-i\vec{k}\cdot\vec{x}}[u_i(\vec{x},t)g_{L^3}(\vec{x})]d\vec{x} \tag{11.17}$$

where $g_{L^3}(\vec{x})$ is some suitably defined function which makes the integral exist. An excellent choice for $g_{L^3}(\vec{x})$ would be:

$$g_{L^3}(\vec{x}) = e^{-[x_1^2+x_2^2+x_3^2]/2L^2} \tag{11.18}$$

whose Fourier transform (in the ordinary sense) is given by:

$$G_{L^3}(\vec{k}) = \frac{L^3}{(2\pi)^{3/2}}e^{-[k_1^2+k_2^2+k_3^2]L^2/2} \tag{11.19}$$

We will use exactly this definition in Section 11.23 to show that Fourier coefficients in non-overlapping wavenumber bands are uncorrelated.

Exercise: Find the Fourier transform of 1 in three-dimensions using generalized functions, then show how you might represented it symbolically as a three dimensional delta-function, $\delta(\vec{k})$.

Exercise: If the Fourier transform can be represented in the sense of generalized functions as $\delta(|\vec{k} - \vec{k}_o|)$, find the inverse Fourier transform in the sense of generalized functions.

11.2 Fourier transforms of homogeneous turbulence

We have agreed already that we will always, when necessary, interpret our Fourier transforms *in the sense of generalized functions*. So if we agree to only transform over the space variables, we are left with the following Fourier transform vector pair:

$$\hat{u}_i(\vec{k},t) = \frac{1}{(2\pi)^3}\int_{-\infty}^{\infty} d\vec{x}\;\; e^{-i\vec{k}\cdot\vec{x}}\;\; u_i(\vec{x},t) \tag{11.20}$$

$$u_i(\vec{x}) = \int_{-\infty}^{\infty} d\vec{k}\;\; e^{+i\vec{k}\cdot\vec{x}}\;\; \hat{u}_i(\vec{k},t) \tag{11.21}$$

Note that we have represented a triple integral by a single integral sign and moved the differential, $d\vec{x}$ or $d\vec{k}$, next to the integral sign, so it will be obvious which variables are being integrated. Also it is understood that everything to the right of the differential is to be integrated over those variables.

There is still one little problem. We set out to find one deterministic vector function which best described our random field, and we have ended up finding not just an infinity of them (like for the inhomogeneous fields above), but in fact a continuum of them: the number of eigenfunctions is *non-denumerable*. As inconvenient as this might appear, that is the way things are. It is an inescapable consequence of the fact that we let the boundaries (and the energy) in the field go to infinity. But who cares, it is a small price to pay since we have this wonderful Fourier analysis tool to work with.

Now I'm sure you are asking: What is he so excited about? Why is the applicability of Fourier analysis such a BIG THING? There are two big reasons (among many). The first has to do with what happens when you take the inverse transform of equation F.9 at the point $\vec{x'}$, multiply it by the complex conjugate of the inverse transform at point $\vec{x}$, and average to get the two-point correlation, $R_{i,j}$; i.e.,

$$\begin{aligned} R_{i,j}(\vec{x'},\vec{x},t) &= \langle u_i(\vec{x},t)u_j(\vec{x}',t)\rangle \\ &= \int_{-\infty}^{\infty} d\vec{k'}\int_{-\infty}^{\infty} d\vec{k}\; e^{+i(k'_m x'_m - k_p x_p)}\langle \hat{u}_i(\vec{k'},t)\hat{u}_j^*(\vec{k},t)\rangle \end{aligned} \tag{11.22}$$

But we have assumed the field to be homogeneous so the two-point correlation can depend at most on the vector separation, $\vec{r} = \vec{x'} - \vec{x}$; i.e.,

$$R_{i,j}(\vec{x'}, \vec{x}, t) = B_{i,j}(\vec{r}, t) \tag{11.23}$$

Therefore equation F.3 is simply:

$$B_{i,j}(\vec{r}, t) = \int_{-\infty}^{\infty} d\vec{k'} \int_{-\infty}^{\infty} d\vec{k}\, e^{+i(k'_m x'_m - k_p x_p)} \langle \hat{u}_i(\vec{k'}, t) \hat{u}_j^*(\vec{k}, t) \rangle \tag{11.24}$$

and the left-hand side has no separate dependence on either $\vec{x}$ or $\vec{x'}$ separately, but is only a function of $\vec{r}$. Now look carefully at the right-hand side. Clearly, unless a miracle occurs in the integration, the right-hand side is going to always depend on $\vec{x'}$ and $\vec{x}$.

Guess what? You probably guessed it. A miracle DOES occur — well, not really a miracle, but even better than a 'miracle'. This 'miracle' can be proven to be true. The 'miracle' is that since both sides of equation F.3 MUST depend only on $\vec{r} = \vec{x'} - \vec{x}$, it follows immediately that *the Fourier components in non-overlapping wavenumber bands must be uncorrelated.*

Say what, you say? Exactly this:

$$\langle \hat{u}_i(\vec{k'}, t) \hat{u}_j^*(\vec{k}, t) \rangle d\vec{k'} d\vec{k} = \begin{cases} F_{i,j}(\vec{k}, t) d\vec{k} & , \vec{k'} = \vec{k} \\ 0 & , \vec{k'} \neq \vec{k} \end{cases} \tag{11.25}$$

or equivalently:

$$\langle \hat{u}_i(\vec{k'}, t) \hat{u}_j^*(\vec{k}, t) \rangle = F_{i,j}(\vec{k}, t) \delta(\vec{k'} - \vec{k}) \tag{11.26}$$

where $\delta(\ )$ is the familiar delta-function (not to be confused with the Kronecker delta tensor) and $F_{i,j}(\vec{k}, t)$ is a *deterministic* function called the **velocity cross-spectrum tensor**.

It is easy to see by substitution that our two-point velocity correlation function is the three-dimensional inverse Fourier transform (in the ordinary sense) of the velocity cross-spectrum tensor; i.e.,

$$B_{i,j}(\vec{r}, t) = \int \int \int_{-\infty}^{\infty} e^{ik_m r_m} F_{i,j}(\vec{k}, t) d\vec{k} \tag{11.27}$$

It is a bit more difficult to show that the cross-spectrum is the three-dimensional Fourier transform (in the ordinary sense) of the two-point velocity correlation function; i.e.,

$$F_{i,j}(\vec{k}, t) = \frac{1}{(2\pi)^3} \int \int \int_{-\infty}^{\infty} e^{-ik_m r_m} B_{i,j}(\vec{r}, t) d\vec{r} \tag{11.28}$$

Thus the cross-spectrum and the two-point correlation form a Fourier transform pair.

Exercise: Use the definition of $g_L(x)$ in the preceding chapter and prove that $\langle \hat{u}(k) \hat{u}^*(k') \rangle = F(k) \delta(k' - k)$ if $u(x)$ is a homogeneous random variable and $\hat{u}(k)$

is defined in the sense of generalized functions by:

$$\hat{u}(k) = \frac{1}{2\pi} \int_{\infty}^{\infty} dx \, e^{-ikx} u(x) \tag{11.29}$$

Exercise: Carry out the same exercise and derive equation F.8 using $g_{L^3}(\vec{x})$ as defined in the preceding chapter.

The implications of what we have accomplished become immediately obvious if we evaluate the inverse transform of equation F.9 at $\vec{r} = 0$ to regain the single-point cross-correlation; i.e.,

$$B_{i,j}(0,t) = \int_{-\infty}^{\infty} d\vec{k} \, F_{i,j}(\vec{k},t) \tag{11.30}$$

Clearly $F_{i.j}(\vec{k},t)$ is telling us how the single-point Reynolds stress, $\langle u_i u_j \rangle = B_{i,j}(0,t)$, is distributed over the various wavenumbers (or *scales of the turbulence*).

This is even more obvious if we contract the two indices by letting $i = j$, sum and divide by two to get the energy; i.e.,

$$\frac{1}{2}\langle q^2 \rangle = \frac{1}{2} B_{i,i}(0,t) = \frac{1}{2} \int_{-\infty}^{\infty} d\vec{k} \, F_{i,i}(\vec{k},t) \tag{11.31}$$

The contracted cross-spectrum is usually called simply the *energy spectrum*, and it tells us exactly how the turbulence energy is distributed with wavenumber. But this is almost what we wanted in the first place — a way to tell the energy associated with one scale from the energy associated with another.

11.3 The Three-dimensional Energy Spectrum Function

Now it really is a nuisance to have to deal with the energy spectrum, $F_{i,i}(\vec{k},t)$, defined above. Even though it is a scalar, it is still a function of four independent variables, $\vec{k}$ and t. This is, of course, a lot less nuisance than the full cross-spectrum tensor, $F_{i,j}(\vec{k},t)$). Nonetheless, it is still rather difficult to draw pictures of things that depend on even three-variables, much less show their time dependence. So theoreticians have defined another kind of spectrum, $E(k,t)$ which is defined as the *integral of* $F_{i,i}(\vec{k},t)$ *over spherical shells of radius* $k \equiv |\vec{k}|$; i.e.,

$$E(k,t) \equiv \frac{1}{2} \oint_{k=|\vec{k}|} dS(k) \, F_{i,i}(\vec{k},t) \tag{11.32}$$

where $\oint$ means a surface integral and $dS(k)$ is a spherical area element. This has the advantage of having only the scalar argument, k, defined by:

$$k^2 = k_1^2 + k_2^2 + k_3^2 \tag{11.33}$$

This new kind of spectrum is properly called the *three-dimensional spectrum function* (to distinguish it from the contracted cross-spectrum we used above). But most people simply refer to it as just the *spectrum* or the *energy spectrum*, which is fine as long as there is no confusion. (Be careful in skipping from book to book and paper to paper since some books do not include the factor of 1/2 in the definition.) Most of the time the surface integral of equation 11.32 is carried out in spherical coordinates, (k, θ, ϕ), so equation 11.32 becomes:

$$E(k,t) = \int_{\theta=0}^{2\pi} \int_{\phi=-\pi/2}^{\pi/2} F_{i,i}(\vec{k},t) k^2 sin\phi d\phi d\theta \tag{11.34}$$

where $F_{i,i}(\vec{k},t)$ must, of course, be written in spherical coordinates too. This has particular advantages for isotropic flow, as will be seen later.

It is easy to see that the integral of $E(k,t)$ over all wavenumbers yields the turbulence kinetic energy (per unit mass); i.e.,

$$\frac{1}{2}\langle u_i u_i \rangle = \int_{k=0}^{\infty} E(k,t) dk \tag{11.35}$$

This follows immediately from the fact that the integral of $F_{i,i}(\vec{k},t)/2$ over all wavenumbers yields the kinetic energy (per unit mass) and the fact that we have already integrated over two of the variables in the definition of $E(k,t)$. This is, of course, the reason why most people simply refer to $E(k,t)$ as the energy spectrum. Unfortunately there are a lot of other definitions of spectra which integrate to the energy which will shall learn about below, so be sure both you and the person you are talking to agree on your definitions.

Figure 13.1 shows an example of the energy spectrum function determined from an attempt using DNS to simulate isotropic turbulence in a computer. Figure **??** shows the energy spectrum function inferred from grid turbulence measurements of one-dimensional spectra (see below) at different positions downstream in a wind tunnel assuming isotropy (as described in a the next chapter).

The problem with $E(k,t)$ is that it is not simply related to the correlation functions, unless you are willing to make other assumptions like isotropy. This is because the value of $E(k,t)$ at a given wavenumber really has information from all three spectral components in it, so information as been smeared out, or averaged. But this is not 'averaging' in the sense that we have been using it — at least not without other hypotheses as noted below. It is really only exactly what it says it is: an integration of the energy spectrum over a surface of radius k.

11.4 DNS turbulence

In fact, researchers who do DNS with spectral codes take this 'average' over spherical shells of radius k quite literally and use it to their advantage in a very interesting manner. Since even a modest simulation of decaying turbulence takes

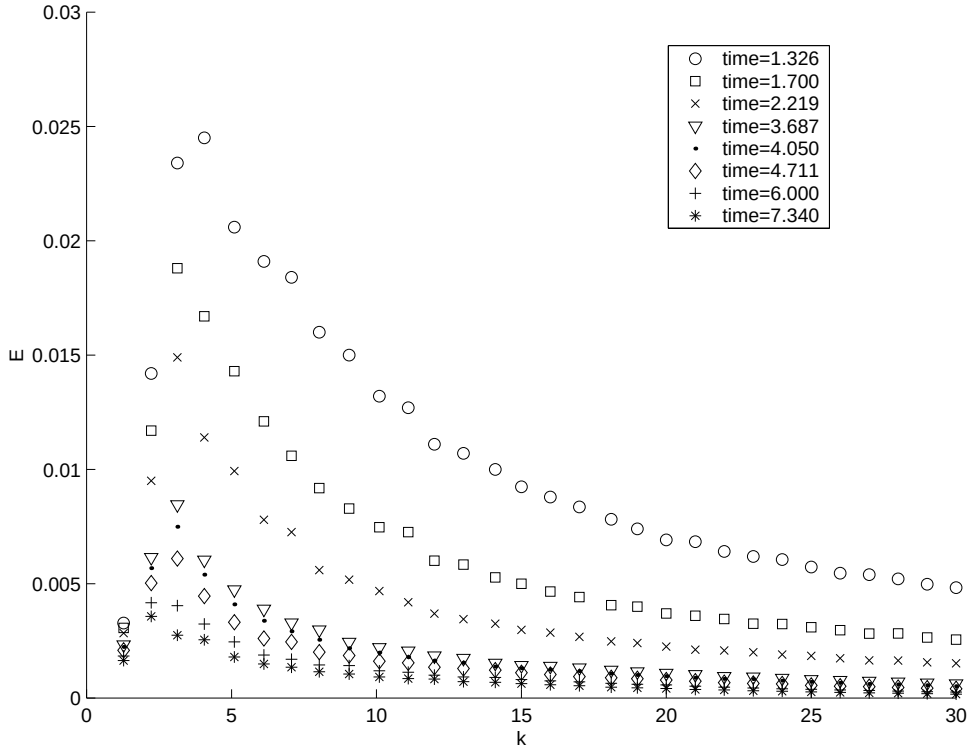

Figure 11.1: DNS data of Wray [**?**] for decaying isotropic turbulence showing how $E(k,t)$ decays with time. Note limited resolution at low wavenumbers.

hundreds of processor hours, it costs far too much to do more than a few runs. This means it is impossible to ever have enough data to do ensemble averages. One way to beat this problem is to compute so-called 'forced turbulence', in which the turbulence is forced continuously so the energy input exactly balances the dissipation rate. Such turbulence is then stationary, so the usual time averages can be performed.

Unfortunately, many interesting flows, like decaying turbulence or homogeneous shear flow turbulence, are not stationary. So what the DNS people do is to pick the starting spectrum, $E(k,0)$, then take the amplitude of their Fourier coefficients equal to the square root, so that the starting Fourier components are:

$$\hat{u}_i(\vec{k},0) = \left|\frac{E(k,0)}{(\Delta k)^3}\right|^{1/2} e^{i\alpha(k)} \tag{11.36}$$

where $\alpha(k)$ is initial phase and Δk is the resolution between the selected wavenumbers. (You will understand this better after we consider finite domain transforms in the next chapter, but for now simply think of $1/\Delta k^3$ as an approximations to the delta function $\delta(\vec{k}' - \vec{k})$ we encountered above.) They then use a random number generator to randomize the phases at each value of k. (Note that it is also important to make sure these initial values satisfy the incompressible continuity equation, which transformed becomes simply $k_i\hat{u}_i = 0$.) Once the calculation begins, the Fourier-transformed Navier-Stokes equations govern the evolution of both the amplitudes and the phases.

It is easy to see why these particular DNS techniques are still somewhat controversial, even after twenty years. You are working with only a single member of an ensemble, and a very special one at that. And you are interpreting the *integration* over the spherical shells of radius k as an *average* in the ensemble sense. Now this is really a very clever trick that makes the computations possible. But it assumes the turbulence evolves to a state independent of its initial conditions, consistent with the long held view about turbulence. Unfortunately even computations done in this way suggest quite strongly that the decay rate of the turbulence energy depends on how you begin; i.e., on the initial conditions. This is a very serious problem indeed, unless the only conditions that matter are the shape of the starting spectrum.

At this moment, most people believe (some vehemently) in the asymptotic independence, which is the traditional view of turbulence. I am of the opposite point of view, but suspect strongly that all the necessary information about the initial conditions is in the starting spectrum. You will have a chance to judge for yourself whose views are more reasonable from the examples in the following chapters. In spite of those who would like to pretend there is no problem, the next decade may prove very interesting as computers get more powerful and tougher questions are asked of the simulations. And who knows, maybe you will be among those who will provide the answers to questions that many now are afraid to ask.

11.5 One-dimensional spectra

There is another type of spectrum, the so-called one-dimensional spectrum, we need to consider before we press on to the applications. In truth, for the theory we really don't need this now; but I know you will all be thinking about how what we talk about relates to things we can measure, right? So we might as well put all the cards on the table at once.

The first thing you need to know is that NONE of the spectra we talked about above can actually be measured in a turbulent flow — or least haven't yet. Think about what would be required. You would have to make two-point correlation measurements of all three components of velocity in all three directions, then Fourier transform them in all three directions. And you would have to have enough of such measurements to satisfy statistical convergence criteria, and over a large enough spatial extent to not have a window problem, and with enough resolution to not alias — well you get the idea. The last two problems are tractable in most cases if special care is taken, but it's the three components of velocity with separations in three directions that is the killer (at least for now — maybe when holographic PIV techniques finally mature).

Now you might conclude from the above that spectral analysis is impossible. Not quite. If we can't do exactly what we want, we invent something else. It turns out that for turbulent flows in which there is a substantial mean velocity, say $\vec{U} = (U_1, 0, 0)$ and $|U_1|$ is a lot bigger than the rms turbulence velocity, the result of our measurement of a *frequency spectrum* with a fixed probe, is pretty close to the one-dimensional wavenumber spectrum defined by:

$$F_{i,j}^{(1)}(k_1) \equiv \int\int_{-\infty}^{\infty} F_{i,j}(\vec{k}, t) dk_2 dk_3 \tag{11.37}$$

In other words, the one-dimensional cross-spectrum is just the original cross-spectrum with two of the wavenumber directions integrated out. The superscript '1' is necessary to name the function so we can tell it apart from the original. (Remember: you can't name a function by its argument.) The superscript could be 1, 2, or 3, and is determined by the one variable that is NOT integrated out. The way this happens is that the fluctuations we see at a frequency f are mostly due to spatial disturbances of wavelength $\lambda = U_1/f$ being convected past us. Thus what shows up at frequency f is really a disturbance at wavenumber $k_1 = 2\pi f/U_1$. Really it is all the same as simply saying that $\partial/\partial t \approx U_1 \partial/\partial x_1$. This interpretation is called "Taylor's Hypothesis" and works pretty well as long as the *local* turbulence intensity is less than 10 – 20%. Above this the interpretation becomes very difficult.

Now one-dimensional spectra have some very funny and strange characteristics, which really drive non-turbulence people crazy. The most annoying feature is that they always end up with a finite value of the spectrum at zero wavenumber. This can be very misleading, since in fact there is no energy at zero wavenumber — ever! It has simply been aliased there by waves traveling sideways. This is illustrated

in Figure **??** which shows a probe traveling through a field of fixed waves, all of wavelength $\lambda_o = 2\pi/k_o$, but with their wavefronts aligned in different directions. Only those with wavefronts exactly perpendicular to the direction of travel of the probe get "measured" at the right wavenumber, k_o. All the rest are "seen" at $k_o \cos\beta$ where β is the angle of incidence.

Example: Consider a turbulent field to have all its energy concentrated on one shell at wavenumber, $|\vec{k}| = k_o$. This can be represented as $F_{i,i}(\vec{k}) = F_o\delta(|\vec{k}| - k_o)$. Apply the definition of equation 11.37 to show that $F^{(1)}_{i,i} = F_o[1 - k^2/k_o^2]$. Note that all of the energy in the field is at $|\vec{k}| = k_o$, there is none at k_o (or above) in the one-dimensional spectrum.

The one-dimensional spectrum does have several nice features, however. The first is that each one-dimensional spectrum is the one-dimensional Fourier transform of the corresponding two point correlation functions, $B_{i,j}(r,0,0)$, $B_{i,j}(0,r,0)$, and $B_{i,j}(0,0,r)$; i.e.,

$$F^{(1)}_{i,j}(k) = \frac{1}{2\pi}\int_{-\infty}^{\infty} e^{-ikr} B_{i,j}(r,0,0)dr \tag{11.38}$$

$$F^{(2)}_{i,j}(k) = \frac{1}{2\pi}\int_{-\infty}^{\infty} e^{-ikr} B_{i,j}(0,r,0)dr \tag{11.39}$$

$$F^{(3)}_{i,j}(k) = \frac{1}{2\pi}\int_{-\infty}^{\infty} e^{-ikr} B_{i,j}(0,0,r)dr \tag{11.40}$$

And in fact, these correlations can be shown to be the inverse Fourier transforms of the one-dimensional spectra; i.e.,

$$B_{i,j}(r,0,0) = \int_{-\infty}^{\infty} e^{+ikr} F^{(1)}_{i,j}(k)dk \tag{11.41}$$

$$B_{i,j}(0,r,0) = \int_{-\infty}^{\infty} e^{+ikr} F^{(2)}_{i,j}(k)dk \tag{11.42}$$

$$B_{i,j}(0,0,r) = \int_{-\infty}^{\infty} e^{+ikr} F^{(3)}_{i,j}(k)dk \tag{11.43}$$

Thus like there three-dimensional counterparts, they form a Fourier transform pair.

Proof of equation 11.39 Start with equation F.9 and set $\vec{r} = (r,0,0)$ to obtain:

$$\begin{aligned} B_{i,j}(r,0,0) &= \int\int\int_{-\infty}^{\infty} e^{ik_1 r} F_{i,j}(\vec{k},t)d\vec{k} \\ &= \int_{-\infty}^{\infty} dk_1 e^{ik_1 r}\left[\int\int_{-\infty}^{\infty} F_{i,j}(\vec{k},t)dk_2 dk_3\right] \end{aligned} \tag{11.44}$$

But the term in brackets is just $F^{(1)}_{i,j}(k_1)$.

Proof of equation 11.39 Start with the definition of equation F.10 and substitute from equation F.9 to obtain:

$$\begin{aligned} F^{(1)}_{i,j}(k_1) &= \int\int_{-\infty}^{\infty} F_{i,j}(\vec{k},t)dk_2dk_3 \\ &= \int\int_{-\infty}^{\infty}\left[\frac{1}{(2\pi)^3}\int\int\int_{-\infty}^{\infty} e^{-ik_m r_m}B_{i,j}(\vec{r},t)d\vec{r}\right]dk_2dk_3 \qquad (11.45) \\ &= \frac{1}{(2\pi)}\int_{-\infty}^{\infty} dr_1 e^{-ik_1r_1}\left\{\int\int_{-\infty}^{\infty} dr_2dr_3B_{i,j}(\vec{r},t)\delta(r_2)\delta(r_3)\right\} \end{aligned}$$

where the *delta*-functions result from the following double Fourier transform *in the sense of generalized functions* of 1; i.e.,

$$\frac{1}{(2\pi)^2}\int\int_{-\infty}^{\infty} e^{-ik_2r_2-k_3r_3}\ \ 1\ \ dk_2dk_3 = \delta(r_2)\delta(r_3) \qquad (11.46)$$

Integration over r_2 and r_3 yields immediately equation 11.39.

An interesting feature of the one-dimensional spectrum is that its value at the origin ($k = 0$) is proportional to an integral scale. For example, to obtain the longitudinal integral scale you would obtain from the two-point correlation, $B^{(1)}_{1,1}$, start with the corresponding one-dimensional spectrum. $F^{(1)}_{1,1}$ and set $k = 0$ to obtain:

$$\begin{aligned} F^{(1)}_{1,1}(0) &= \frac{1}{\pi}\int_0^{\infty} B_{1,1}(r,0,0)dr \\ &= \frac{\langle u_1^2\rangle L^{(1)}_{1,1}}{\pi} \qquad (11.47) \end{aligned}$$

where we have used the symmetry of $B_{1,1}(r,0,0)$ about $r = 0$. In fact, this is usually the best way to determine an integral scale, since you can use Fast Fourier Transform algorithms to speed up the computations (as shown in the appendices) and completely by-pass the computation of the correlation all together.

11.6 Spectral symmetries

The symmetries encountered in Section 9.4 all have their counterpart in spectral space. The Fourier representation, however, is generally complex; so what might be simply a symmetry about the origin shows up as a Hermitian property in the cross-spectrum.

For example, consider the cross spectrum which is the three-dimensional Fourier transform of the cross-correlation $B_{i,j}(\vec{r})$ and given by:

$$F_{i,j}(\vec{k}) = \frac{1}{(2\pi)^3}\int\int\int_{-\infty}^{\infty} e^{-ik_m r_m}B_{i,j}(\vec{r})d\vec{r}$$

$$\begin{aligned} &= \frac{1}{(2\pi)^3}\int\int\int_{-\infty}^{\infty} e^{-ik_m r_m} B_{j,i}(-\vec{r})d\vec{r} \\ &= \frac{1}{(2\pi)^3}\int\int\int_{-\infty}^{\infty} e^{+ik_m r_m} B_{j,i}(\vec{r})d\vec{r} \\ &= F^*_{j,i}(\vec{k}) \end{aligned} \tag{11.48}$$

since $B_{i,j}$ is real.

But also it follows that:

$$\begin{aligned} F_{i,j}(-\vec{k}) &= \frac{1}{(2\pi)^3}\int\int\int_{-\infty}^{\infty} e^{-ik_m r_m} B_{i,j}(\vec{r})d\vec{r} \\ &= \frac{1}{(2\pi)^3}\int\int\int_{-\infty}^{\infty} e^{+ik_m r_m} B_{i,j}(\vec{r})d\vec{r} \\ &= F^*_{i,j}(\vec{k}) \end{aligned} \tag{11.49}$$

This last property is called Hermitian and corresponds to symmetry of the cross-spectra.

11.7 Consequences of incompressibility

In section 9.5 we explored the consequences of the incompressible continuity equation on the two-point correlation tensor. To see the counterparts for Fourier analysis, consider first the continuity equation for just the instantaneous fluctuating velocity given by $\partial u_j/\partial x_j = 0$. Fourier transforming this *in the sense of generalized functions* yields:

$$\frac{1}{(2\pi)^3}\int\int\int_{-\infty}^{\infty} e^{-ik_m x_m}\left[\frac{\partial u_j(\vec{x},t)}{\partial x_j}\right] d\vec{x} = 0 \tag{11.50}$$

This can be integrated by parts to obtain:

$$\begin{aligned} \frac{1}{(2\pi)^3}\int\int\int_{-\infty}^{\infty} e^{-ik_m x_m}\left[\frac{\partial u_j(\vec{x},t)}{\partial x_j}\right] d\vec{x} &= [-ik_j]\frac{1}{(2\pi)^3}\int\int\int_{-\infty}^{\infty} e^{-ik_m x_m} u_j(\vec{x},t)d\vec{x} \\ &= [-ik_j]\hat{u}(\vec{k},t) \end{aligned} \tag{11.51}$$

Thus the counterpart to the instantaneous continuity equation in Fourier space is:

$$[-ik_j]\hat{u}_j(\vec{k},t) = 0 \tag{11.52}$$

Equations 9.43 and 9.44 can be Fourier transformed in a similar manner to obtain their counterparts in spectral space as:

$$k_j F_{i,j}(\vec{k}) = 0 \tag{11.53}$$

$$k_i F_{i,j}(\vec{k}) = 0 \tag{11.54}$$

Exercise Prove these.

11.8 Implications of Isotropy on Spectra

By direct analogy with the two-point correlations it follows that the most general forms of the two-point cross-spectral spectra in an isotropic field are given by:

$$F_{\theta,\theta}(\vec{k}) = F_\theta(k) \qquad (scalar) \tag{11.55}$$

$$F_{i,\theta}(\vec{k}) = F_{\theta L}(k)\frac{k_i}{k} \qquad (vector) \tag{11.56}$$

$$F_{i,j}(\vec{k}) = C(k)k_ik_j + D(k)\delta_{i,j} \qquad (tensor) \tag{11.57}$$

where F_θ, $F_{\theta L}$, C and C are all functions of $k = |\vec{k}|$ only.

It is straightforward to show (using continuity and the definitions) that $C(k)$ and $D(k)$ are simply related to the energy spectrum function, $E(k)$, so the most general form of the two-point vector-vector spectrum in an isotropic field is given by:

$$F_{i,j}(\vec{k}) = \frac{E(k)}{4\pi k^4}[k^2\delta_{ij} - k_ik_j] \tag{11.58}$$

Exercise: Prove equation 11.58 Hint: use the definition of $E(k)$ and change the surface integral to spherical coordinates using $dS(k) = k^2 \sin\phi d\phi d\theta$.

This isotropic spectral equation also has important implications for the one-dimensional spectra as well. In particular, it is straightforward to show that:

$$F^{(1)}_{1,1}(k_1) = \frac{1}{2}\int_{k_1}^{\infty} \frac{E(k)}{k^3}[k^2 - k_1^2]dk \tag{11.59}$$

$$F^{(1)}_{2,2}(k_1) = \frac{1}{4}\int_{k_1}^{\infty} \frac{E(k)}{k^3}[k^2 + k_1^2]dk \tag{11.60}$$

Exercises: Prove equations 11.59, and 11.60. Hint: substitute the general isotropic expression into the definition of the one-dimensional spectra and change to polar coordinates, noting that $\sigma d\sigma = kdk$ where $\sigma^2 = k_2^2 + k_3^2$.

It follows by repeated differentiation (and application of Leibnitz rule for differentiating under the integral sign) that:

$$E(k) = k^2\frac{d^2F^{(1)}_{2,2}}{dk^2} - k\frac{dF^{(1)}_{1,1}}{dk} \tag{11.61}$$

$$= k^3\frac{d}{dk}\left[\frac{1}{k}\frac{dF^{(1)}_{1,1}}{dk}\right] \tag{11.62}$$

Exercises: Prove equations 11.61 and 11.62.

Chapter 12

Measuring spectra from experimental and DNS data

12.1 Introduction

The theoretical considerations of the next chapters will make clear the importance of turbulence spectra. It is important both to be able to measure them experimentally, or alternatively, calculate them from DNS data. Unfortunately, there are several types of problems which one encounters, some of which are common to both, others unique to each. All are extremely important, and failure to properly understand the limitations can render the data useless.

The primary common problems for both DNS and experiments are the statistical errors one encounters from having only a limited number of samples, and the problems related to the finite spatial extent of the simulation or experimental facility. The sampling problems are the exact counterpart to those we encountered in Chapter 2 when making statistical estimates of single point quantities. This statistical uncertainty complicates all spectral data interpretation, especially the identification of spectral peaks and roll-offs. The finite domain problems arise from the fact that no experiment or simulation can be truly homogeneous, hence can at best be a model of homogeneous flows over some limited range of scales or times. It may seem that these differences are unimportant, but failure to recognize them can result in models for turbulence which depend more on the boundary conditions of the experiments (or DNS) than on the dynamics of the turbulence. Also, the finite size of measuring arrays or 'windows' can itself create spectral leakage

This chapter will focus on how to obtain a velocity spectrum from time-varying or spatially vary data from one or more probes. We will first examine how one processes data from time-varying signals, then we will discuss how such data can be interpreted as a space-varying using Taylor's hypothesis. Finally the ideas will be generalized to making spatial measurements directly.

12.2 Determining the wave-number spectrum from the spatial auto-correlation

The most obvious way to obtain a frequency spectrum is to measure the two-point correlation to as large a separation as possible, then Fourier transform it to directly obtain the corresponding one-dimensional spectrum. For example, suppose you have two probes, one fixed, the other movable, each measuring the streamwise component of the velocity. You would like to use them to measure $B_{1,1}(r,0,0)$ where:

$$B_{1,1}(r,0,0) \equiv < u_1(x_1,x_2,x_3)u_1(x_1+r,x_2,x_3) > \tag{12.1}$$

And you would then like to Fourier transform $B_{1,1}(r,0,0)$ to obtain the one-dimensional spectrum $F^{(1)}_{1,1}(k_1)$ where:

$$F^{(1)}_{1,1}(k_1) = \mathbf{FT}\{B_{1,1}(r,0,0)\} = \frac{1}{2\pi}\int_{-\infty}^{\infty} B_{1,1}(r,0,0)e^{-k_1 r}dr \tag{12.2}$$

But there is a limit to how far apart you can put your probes because of the finite extent of your facility. If your fixed probe is at the center, the most you can measure is $L/2 < r < L/2$; i.e, you can only obtain:

$$B_{1,1L}(r_1) \equiv \begin{cases} B_{1,1}(r_1,0,0) & , -L/2 < r < L/2 \\ 0 & , \text{otherwise} \end{cases} \tag{12.3}$$

Therefore you really can't perform the integration above, even though your estimate of $B_{1,1}$ is perfect for the separations you can measure (and of course it is never is, due to the statistical error we will discuss later). The most you can possibly compute is the *finite space transform* given by:

$$F^{(1)}_{1,1L}(k_1) = \frac{1}{2\pi}\int_{-L/2}^{L/2} B_{1,1L}(r_1)e^{-k_1 r_1}dr_1 \tag{12.4}$$

We can re-write this as the product of the true correlation, $B_{1,1}(r_1,0,0)$, and a '*window function*' as:

$$F^{(1)}_{1,1L}(k_1) = \frac{1}{2\pi}\int_{-\infty}^{\infty} B_{1,1L}(r_1)w_L(r_1)e^{-k_1 r_1}dr_1 \tag{12.5}$$

where $w_L(r)$ is the '*top-hat window function*' defined as:

$$w_L(r) = \begin{cases} 1 & , |r| \le L/2 \\ 0 & , |r| > L/2 \end{cases} \tag{12.6}$$

Parseval's Theorem tells us that the Fourier transform of the product of two functions is the convolution of their Fourier transforms. Thus our 'measured spectrum' is given by:

$$F^{(1)}_{1,1L}(k_1) = \int_{-\infty}^{\infty} F^{(1)}_{1,1}(k_1 - k)\hat{w}_L(k)dk = \int_{-\infty}^{\infty} F^{(1)}_{1,1}(k)\hat{w}_L(k_1 - k)dk \qquad (12.7)$$

where $\hat{w}(k)$ is the Fourier transform of the top-hat window function given by:

$$\hat{w}_L(k) \equiv \mathbf{FT}\{w_L(r)\} = \left(\frac{L}{2\pi}\right)\frac{sin(kL/2)}{(kL/2)} \qquad (12.8)$$

It is clear that in spite of our best efforts, we have not measured the true spectrum at all. Instead all we have obtained is a garbled version of it which filtered through the window function, $\hat{w}(k)$. The entire process is very much like looking through a glass-window at something on the other side. If the glass is not of high quality, then the image we see is distorted, perhaps even to the point where we cannot even recognize it. This can happen with spectra as well, so it is very important understand what the window has done.

Figure **??** shows both the top-hat and its Fourier transform. Note that most the area under $\hat{w}$ is between the zero-crossings at $k = \pm\pi/L$. But notice also the other peaks at higher and lower wavenumbers, and especially the rather strong negative peaks. These 'side-lobes' roll off as $|2/kL|$; but even so they can cause considerable leakage from high spectral values to low ones, and also cause false peaks due to the negative values. Obviously, the larger the domain $(L/2, L/2)$, the closer the narrower the filter, and the closer the window approaches a delta function, $\delta(k)$. In the limit of infinite L, the true spectrum is recovered, since convolution of any function with a delta function simply reproduces the original function.

True spectra can never be negative, of course. But 'measured' spectra can be, so they must be interpreted carefully. Usually it is desirable to reduce these unphysical and spurious values by introducing additional window functions into the data processing *before* Fourier transformation. (Afterwards is too late!) Popular choices are the 'hanning window', the 'hamming window', and the 'Parzen' window. All of these choice pre-multiply the measured correlation by a function which rolls off less abruptly than the top-hat. This reduces the side-lobes and their bad influences, usually by making them roll-off more rapidly. But it also reduces the resolution in wavenumber space by making the effective span-wise extent less and the 'band-width' greater. As a result, there is no simple 'best way' to process data. Each experiment must be considered separately, and each result carefully analyzed to see which peaks are real, which are false, which are reduced by leakage, which roll-offs are physical and which are not. Usually this is accomplished by analyzing the same data with several different windows. Then, with luck, it will be possible to infer what the real spectrum might be. But the entire process is really an art. Like any art skill, the more practice you have, the better you get at making the right choices. And like any newly acquired skill, **beginners be especially careful**.

12.3 The finite Fourier transform

There is another way to obtain the spectrum of a signal without first computing the autocorrelation — direct transformation of the incoming signals. The basic idea is quite simple and follows directly from the definition of the Fourier transform of the signal. For example, consider the same velocity component, $u_1(\vec{x}$, considered above with x_2 and x_3 held constant. The one-dimensional transform in the x_1 direction of this velocity component is given by:

Now again in the real world, our information is limited to a finite domain, say $(-L/2, L/2)$ as before. Therefore the most we can really compute from our data is:

12.4 Taylor's Hypothesis

12.4.1 The Frozen Field Hypothesis

12.4.2 The Effect of a Fluctuating Convection Velocity

12.5 Resolution and Spatial Filtering

Chapter 13

Dynamics of Homogeneous Turbulence

13.1 The Fourier transformed instantaneous equations

We are about ready to apply our results from Fourier analysis to the dynamical equations for homogeneous turbulence. Now with all the different types of spectra flying around it would be really easy to forget that this was, after all, the whole point of decomposing the instantaneous velocity in the first place. But our original purpose was to investigate the different roles that the different scales of motion play in the dynamics of the motion. And *dynamics* means the interplay of accelerations and forces; so back to the instantaneous equations we must go.

Now there are two ways we can proceed: We could Fourier transform the instantaneous equations for the fluctuations in a homogeneous flow. Then we could examine these, and from them even build equations for the energy spectra by using the Wiener-Kinchine relation. Alternatively we could build a set of equations for the two-point velocity correlations, and transform them to get the spectral equations. Either way, we end up in the same place — with a set of equations for the velocity cross-spectra, which we can then integrate over spherical shells of radius k to get an equation for $E(k,t)$. Let's try both, since each has a unique piece of information.

Let's begin by simply using equation 3.27 for the instantaneous fluctuating velocity. For now let's just assume there is no mean velocity at all and that the flow is homogeneous. If we substitute equation 11.21 for the instantaneous velocity and define a similar transform for the fluctuating pressure, the integrand of our transformed equation reduces to:

$$\begin{aligned} \frac{\partial \hat{u}_i(\vec{k},t)}{\partial t} &+ \int\int\int_{-\infty}^{\infty} (-ik'_j)\hat{u}_j(\vec{k'})\hat{u}_i(\vec{k'}-\vec{k},t)d\vec{k'} \\ &= -\frac{1}{\rho}k_i\hat{p}(\vec{k},t) - 2\nu k^2\hat{u}_i(\vec{k},t) \end{aligned} \tag{13.1}$$

The second term on the left-hand side is a convolution over the wavenumber vector and results from the fact that multiplication in space corresponds to convolution in wavenumber, and vice versa. Since we are assuming incompressible flow, the pressure term can also be expressed in terms of the velocity using the continuity equation. For an exercise see if you can show this.

Note that like the velocity fluctuation itself, the Fourier velocity coefficients, $\hat{u}_i(\vec{k}, t)$, are themselves random and of zero mean. Thus each realization of them will be different, and it is only the spectra formed from them which will be deterministic. This means averaging in some way is probably required at some point. But even without any kind of averaging, equation 13.1 is a very important equation because even a cursory examination tells us a lot about turbulence.

First note that the viscous terms are weighted by a factor of k^2, compared to the the temporal decay term. Obviously viscous effects are concentrated at much smaller scales (higher wavenumbers) than are inertial effects.

Second, note that the non-linear terms show up in a convolution involving *three* wavenumbers: $\vec{k}$, $\vec{k'}$, and also $\vec{k'} - \vec{k}$. This is the only place the non-linearity shows up. Since we know non-linearity is the essence of turbulence, then we can say for sure that turbulent non-linear interactions involve only "*triads*" of wavenumber vectors. Some possibilities are shown in Figure **??**. The study of which triads dominate the energy transfer has been important to turbulence for a long time. Although all triads can be important, it is generally believed that the *local* interactions are the most important; i.e., those for which all three wavenumbers have about the same magnitude. This can be very important in making models for the turbulence — like LES, for example.

So what have we learned so far? That the energetic scales decay primarily by the non-linear triad interactions which move the energy to higher and higher wavenumbers. Eventually the viscosity comes to dominate these high wavenumbers and the energy is dissipated — at the smallest scales of motion. Isn't it amazing how we can learn all this just by examining an equation without ever solving it? The neat thing is that once you learn to do this for turbulence you can do it for just about every field of science or engineering. The study of turbulence really has changed your life.

The discretized version of equation 13.1 is the basis for most spectral method DNS solutions (and pseudo-spectral) method solutions using very large parallel computers. Modern Fast Fourier Transform (FFT) algorithms allow huge arrays to be rapidly manipulated much more quickly than finite difference techniques. The emergence of these techniques, especially over the past decade, has been one of the most exciting aspects of turbulence research. And it gets even more interesting with each increase in computer capacity. Yet as we noted above, though, there are some fundamental questions which remain, some of which we will mention below.

13.2 The spectral equations

It is straight-forward to proceed from equation 13.1 to a set of spectral equations. It is worthwhile though to back up a step and arrive at the same point another way — via the two-point correlation equations. The procedure for deriving these equations are almost the same as those used to derive the single-point Reynolds stress equations, with only one difference: the instantaneous equations at one point are multiplied by the velocity component at another.

Thus the equation for the instantaneous fluctuating velocity at $\vec{x}$, say $u_i = u_i(\vec{x}, t)$, is multiplied by the fluctuating velocity at $\vec{x'}$, say $u'_i \equiv u_i(\vec{x'}, t)$; i.e.,

$$u'_i \left[\frac{\partial u_i}{\partial t} + \cdots = \cdots \right] \tag{13.2}$$

And vice versa,

$$u_i \left[\frac{\partial u'_i}{\partial t} + \cdots = \cdots \right] \tag{13.3}$$

These are averaged and added to obtain an equation for the two-point velocity correlation as:

$$\begin{aligned} &\frac{\partial < u_i u'_j >}{\partial t} + \frac{\partial < u_i u_k u'_j >}{\partial x_k} + \frac{\partial < u_i u'_j u'_k >}{\partial x'_k} \\ &= -\frac{1}{\rho} \left(\frac{\partial < p u'_j >}{\partial x_i} + \frac{\partial < p' u_i >}{\partial x'_j} \right) + \nu \left(\frac{\partial^2 < u_i u'_j >}{\partial x_k \partial x_k} + \frac{\partial^2 < u_i u'_j >}{\partial x'_k \partial x'_k} \right) \end{aligned} \tag{13.4}$$

Note that we used a "trick" to pull the derivatives outside the product: u_i is not a function of $\vec{x'}$, nor is u'_i a function of $\vec{x}$. Also we have assumed no mean velocity.

Now let's consider the implications of homogeneity. We know that this means that the two-point moments can only depend on $\vec{r} = \vec{x'} - \vec{x}$. For convenience let's define another variable, $\vec{\xi} = \vec{x'} + \vec{x}$, and then change variables from $\vec{x'}, \vec{x}$ to $\vec{\xi}, \vec{r}$. The chain-rule immediately implies that:

$$\begin{aligned} \frac{\partial}{\partial x'_i} &= \frac{\partial}{\partial \xi_j} \frac{\partial \xi_j}{\partial x'_i} + \frac{\partial}{\partial r_j} \frac{\partial r_j}{\partial x'_i} \\ &= \frac{\partial}{\partial \xi_i} + \frac{\partial}{\partial r_i} \end{aligned} \tag{13.5}$$

Similarly, it is easy to show that:

$$\frac{\partial}{\partial x_i} = \frac{\partial}{\partial \xi_i} - \frac{\partial}{\partial r_i} \tag{13.6}$$

Now this may seem like so much hocus-pocus until you realize that we are only differentiating functions of $\vec{r}$ only, so all the derivatives involving $\vec{\xi}$ are identically zero.

Thus homogeneity reduces our two-point Reynolds stress equation to:

$$\frac{\partial B_{i,j}(\vec{r},t)}{\partial t} = \frac{\partial}{\partial r_k}[B_{ik,j}(\vec{r},t) - B_{i,jk}(\vec{r},t)] \tag{13.7}$$

$$+ \frac{1}{\rho}\left[\frac{\partial B_{p,j}(\vec{r},t)}{\partial r_i} - \frac{\partial B_{i,p}(\vec{r},t)}{\partial r_j}\right] + 2\nu\frac{\partial^2 B_{i,j}(\vec{r},t)}{\partial r_k \partial r_k} \tag{13.8}$$

Don't lose heart yet, we are almost there. Now we could Fourier transform this directly, but since we are only going to work with the trace, let's contract the indices first, then Fourier transform. As usual, setting $i = j$ causes the pressure term to drop out, and we are left with:

$$\frac{\partial B_{i,i}(\vec{r},t)}{\partial t} = \frac{\partial}{\partial r_k}[B_{ik,i}(\vec{r},t) - B_{i,ik}(\vec{r},t)] + 2\nu\frac{\partial^2 B_{i,i}(\vec{r},t)}{\partial r_k \partial r_k} \tag{13.9}$$

We can immediately take the three-dimensional Fourier transform to obtain:

$$\frac{\partial F_{i,i}(\vec{k},t)}{\partial t} = G_{i,i}(\vec{k},t) - 2\nu k^2 F_{i,i}(\vec{k},t) \tag{13.10}$$

where $G_{i,i}$ contains the non-linear interactions and is related to the transform of the triple moment terms by:

$$G_{i,i}(\vec{k},t) = ik_l[F_{il,i}(\vec{k},t) - F_{il,i}(-\vec{k},t)] \tag{13.11}$$

What is arguably the most famous equation in turbulence theory results immediately by integrating over spherical shells of radius k and invoking the definition of the three-dimensional energy spectrum function, $E(k,t)$. The result is:

$$\frac{\partial E(k,t)}{\partial t} = T(k,t) - 2\nu k^2 E(k,t) \tag{13.12}$$

where $T(k,t)$ is non-linear spectral energy transfer defined as the integral over spherical shells of radius k of $G_{i,i}(\vec{k},t)/2$. Note that like all other averaged equations in turbulence, this equation is not closed since there are two unknowns but only one equation. Nonetheless, there will be much we can learn from it.

It is easy to show by integration that the left-hand side integrates to the left-hand side of equation 5.2, while the last term on the right-hand side integrates to the dissipation; i.e.,

$$\frac{1}{2} < q^2 > = \int_0^\infty E(k,t)dk \tag{13.13}$$

$$\epsilon = 2\nu \int k^2 E(k,t)dk \tag{13.14}$$

It follows that the integral of the spectral transfer term must be identically zero; i.e.,

$$\int_0^\infty T(k,t)dk = 0 \tag{13.15}$$

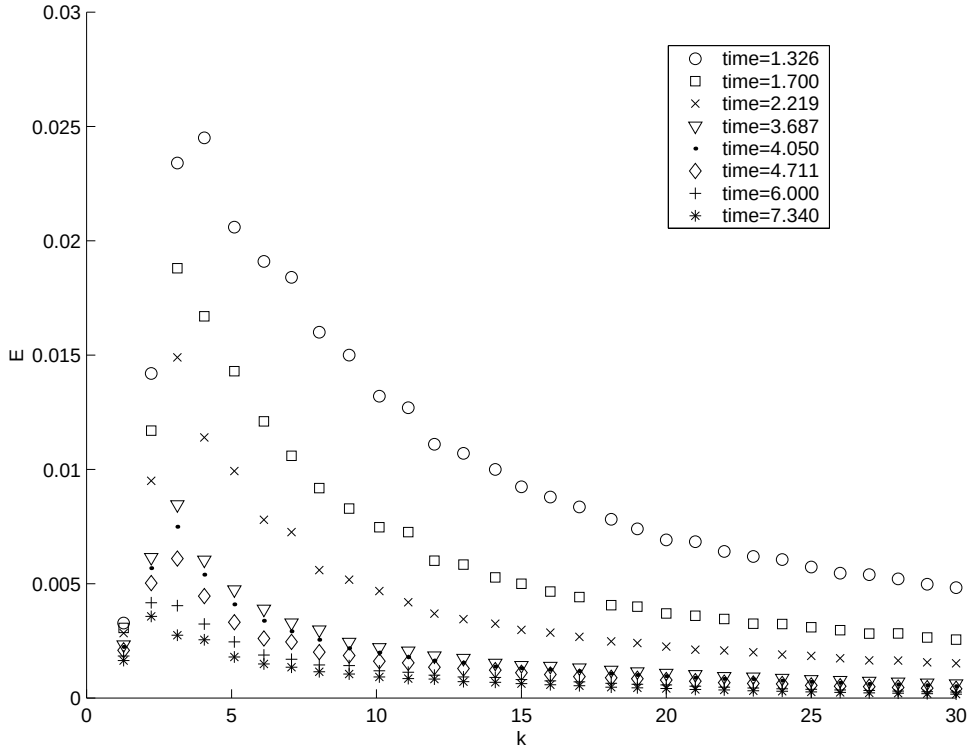

Figure 13.1: DNS data of Wray [**?**] for decaying isotropic turbulence showing how $E(k,t)$ decays with time. Note limited resolution at low wavenumbers.

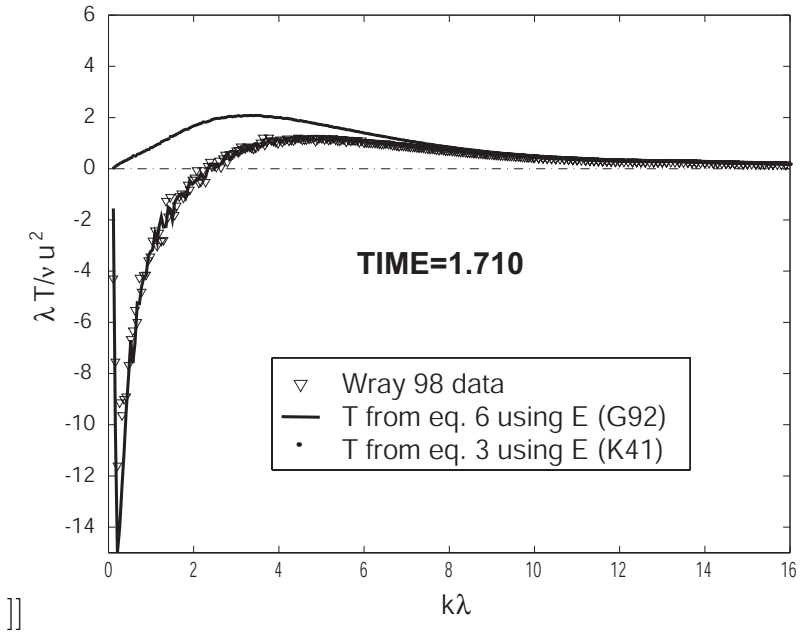

]]

Figure 13.2: DNS data of Wray [**?**] for decaying isotropic turbulence showing $T(k,t)$ and $2\nu E(k,t)$ at a single time.

(This can also be proven directly from the definition of T.) Thus the net effect of the spectral energy transfer term is zero. It can only act to move energy from one scale to another. In other words, it is exactly the term we were looking for, since it alone can move energy from the scales where they are generated to those where it can be dissipated.

13.3 The effect of Reynolds number on the spectral equations

We are now in a position to examine how turbulence changes during decay. Figure **??** depicts linear-linear plots of typical energy, dissipation and energy transfer spectra. The energy spectrum, $E(k,t)$, rises rather rapidly for small wavenumbers, probably as k^m where $1 < m < -5/2$ and is determined by the power law decay exponent of the energy. Most believe $E(k,t)$ peaks near $k \approx L^{-1}$ where L is the longitudinal integral scale. After this is rolls-off for a while as $k^{-5/3+\mu}$ where μ is very close to zero for large Reynolds numbers. Then finally it rolls off exponentially for wavenumbers above about one fifth the inverse of the Kolmogorov microscale. $1/\eta$. Since the kinetic energy of the turbulence is the integral under the energy spectrum, it is easy to see that most of the energy comes from the spectral region near the peak. Nonetheless, the contribution from the slow roll-off can not be neglected and must be considered in designing experiments (or simulations) to avoid underestimating the energy.

The dissipation spectrum is, of course, very closely related to the energy spectrum since it is the same spectrum multiplied by $2\nu k^2$. The effect of the pre-factor is weight the dissipation to the highest wavenumbers so most of the dissipation occurs at wavenumbers higher than the peak which is near $k \approx 0.2/\eta_K$. This means that experiments or simulations must carefully resolve wavenumbers to at least η_K (or higher) if the dissipation is to be accurately determined. Resolution requirements are much more severe for higher spectral moments.

The spectral transfer term does exactly what we thought it should do. The transfer term is negative for low wavenumbers and nearly equal to $-\partial E/\partial t$. Thus on the average, it takes energy from the energy-containing scales where there is very little dissipation and moves it somewhere. But where? The answer lies in the high wavenumbers, where the spectral transfer is positive and nearly equal to the dissipation.

13.4 Conflicting views of spectral transfer

Since Kolmogorov it has been believed that it is the ratio of the integral scale, L, to the Kolmogorov microscale, η_K, which determines the shape of the the spectra, and the separation between the energy and dissipation ranges. But there are recent indications that this may not always be true, if at all, as discussed below. For now, let's assume it is true.

Consider what happens as $R \equiv L/\eta_K$ becomes very large. The Kolmogorovian view of the energy, dissipation and transfer spectra for three different values of R are illustrated in Figure **??**. For $R \approx 100$ (which is typical of many simulations and laboratory experiments), the energy and dissipative ranges overlap, and there is really no region at all where the spectral transfer is near zero. By contrast, for $R > 10^4$, the dissipative ranges and energy-containing ranges are widely separated.

At low wavenumbers, the spectral decay is almost entirely due to the spectral transfer, and this region is virtually independent of viscosity. At high wavenumbers, there is virtually no energy, and the balance is almost entirely between spectral transfer and dissipation. And in-between the energy and dissipative ranges, there is an extensive spectral region where there is virtually no energy, no dissipation, and the spectral transfer is zero. This is the so-called inertial subrange of the spectrum which only emerges at very high wavenumbers, and will seen below to be the region characterized by the near $k^{-5/3}$ behavior noted above.

So where it the problem with this picture. The problem is that this picture has never been confirmed in any flow for which dE/dt was not identically zero due to stationarity. Figure **??** is taken from a paper by Helland et al. in 1977 and shows data taken in several wind tunnels, one the Colorado State University wind tunnel which is among the largest in the world. Figure **??** shows similar data in DNS of decaying turbulence taken from George and Wang (2002). These DNS data are at values of R_λ between 30 and 60, which is about the same as most of the wind tunnel data. The CSU data are at $R_\lambda \approx 240$. Clearly neither the DNS

nor the experiments in decaying turbulence show the expected region in which $T(k,t) \approx 0$. By contrast, the 'forced DNS' of Kaneda et al. (2002) does show an extensive range for which $T \approx 0$.

So we are left with the following dilemma: does the Kolmogorov picture appear to be correct for the forced turbulence only because of the absence of alternatives. In particular, forced turbulence is stationary, so above the wavenumber of the forcing, no other value of T is possible if the dissipative wavenumbers are large enough. Or would the results for decaying turbulence give the same results if the Reynolds number were high enough? If not, could it be that the whole idea of Kolmogorov is wrong and there is another idea which better describes the world as we find it? The next chapter explores such a possibility.

Chapter 14

'Kolmogorov' Turbulence

There are several different approaches to the spectral energy equation, each representing very different kinds of turbulence. This chapter presents and explores the classical theory, originally due at least in part to Kolmogorov (1941). It has been developed and refined by many. It was first presented in the form presented here by George K. Batchelor and his co-workers, and most eloquently in his now classic book 'Homogeneous turbulence' (Batchelor 1953). Most of the things we thought we knew about turbulence in the 20th century (including all turbulence models) are based at some level on these ideas. So even if they turn out not to be completely correct, it is important to learn about them – if for no other reason than to understand how and why the engineering models have developed the way they did. I've already given some hints in the previous chapters that I don't believe this so-called Kolmogorov view of turbulence to be the whole story. In fact, at this writing I have come to believe that there probably are three different kinds of turbulence, only one of which behaves like Kolmogorov. This is not a question of Kolmogorov's ideas being wrong, but instead my belief that the underlying assumptions do not apply to all flows. Therefore in preparation for the new ideas in subsequent chapters, I shall try to make it quite clear what what the underlying assumptions and hypotheses are.[1]

[1]Suprisingly, even the most ardent proponents and defenders of ideas in turbulence, especially those of Kolmogorov and his followers, often seem to have little understanding of what these underlying hypotheses are. Therefore they feel quite threatened when one suggests there might be problems. Unfortunately this seems to be a common phenomenon in the history of science, and has been described by Kuhn [**?**] as operating within a *paradigm* where everyone has agreed on a descriptive language of what they think they believe, but no one knows precisely what. This of course makes it almost impossible to challenge an existing theory, since no one really understands it. Thus science falls into a mode more like a religion than real (or at last ideal) science where hypotheses are tested and revised when found wanting.

14.0.1 The 'universal equilibrium' range

We shall start our discussion with the equation 13.12 for decaying homogenous turbulence, since it has all the features we need; i.e.,

$$\frac{\partial E(k,t)}{\partial t} = T(k,t) - 2\nu k^2 E(k,t) \tag{14.1}$$

where $E(k,t)$ is the three-dimensional energy spectrum function, and $T(k,t)$ is non-linear spectral energy transfer, also defined as the integral over spherical shells of radius k of the non-linear spectral transfer. It has already been noted that this equation is not closed since there are two unknowns but only one equation. Also remember that this equation assumes only *homogeneous turbulence*, and *not* isotropic turbulence. Also note that we could include extra terms to account of energy production and spectral scrambling by a mean velocity gradient, but we avoid for now this extra complexity. This neglect might seem to be a bit confusing, since we will follow (at least in this chapter) Kolmogov and suggest that the results apply to all flows, at least at scales of motion much smaller than that at which the energy is put into the turbulence and if the turbulence Reynolds number is high enough. But we will come back to this in subsequent chapters, so if things seem sometimes less than obvious, you will not be the first to think so. So save those thoughts.

Now the first thing we need to remind ourselves is what the basic terms in this equation are. The left-hand-side is just the rate at which energy changes (decays in this case) at any given wavenumber, so its integral over all wavenumbers is the rate of change of kinetic energy with time. The last term on the right-hand-side is the rate at which kinetic energy is converted to internal energy by viscosity and the deformation of fluid elements; i.e., the rate-of-dissipation, ε. Clearly this must equal the integral of the left-hand-side (since there is no production or transport in our simplified homogenous problem); i.e.,

$$\frac{d}{dt}\int_0^\infty E(k,t)dk = -2\nu\int_0^\infty k^2 E(k,t)dk = -\varepsilon \tag{14.2}$$

All of this, of course is a consequence of the fact that the integral of the non-linear transfer, $T(k,t)$ over all wavenumbers is exactly zero; i.e.,

$$\int_0^\infty T(k,t)dk = 0. \tag{14.3}$$

In words, there is no net transfer of energy due to the non-linear (or triadic) interactions; whatever is taken out at one wavenumber must be put back somewhere else (in wavenumber space).

The basis of Kolmogorov's ideas (or hypotheses) is that $T(k,t)$ takes energy out at low wavenumbers and puts it in at high wavenumbers. In fact, this is a probably a pretty good approximation for many flows since the energy is usually put into the flow at the large scales (the energetic scales corresponding roughly to the peak in the energy spectrum) and it is moved by the non-linear interactions

to scales where it can be dissipated. This is because in flows with mean shear the turbulence energy is produced by the working of the Reynolds shear stresses agains the mean flow gradient, and this happens preferentially at the energetic scales. You can see why in Figure 14.1 where the Reynolds stress spectrum peaks about where the energy spectrum does, but it falls off much more rapidly with increasing wavenumber. But the truth is though that we really don't know very much for sure about the non-linear energy fluxes, except for a few low Reynolds number DNS and two experiments in decaying turbulence (by Van Atta and his co-workers). The exception to this are the relatively recent high 4096k Reynolds number simulations of *forced turbulence DNS* carried out in Japan on their Earth Simulator by Kaneda, Ishihara and co-workers, which pretty much confirm the arguments of this chapter. We will postpone to Chapter **??** a discussion of the generality of their results and what they imply about all kinds of turbulence.

So the bottom line (at least for this chapter) is that even if we don't have a simple homogenous turbulence, the turbulence at sufficiently high-wavenumbers *might* behave as though we do – at least we can *hypothesize* that it might do so. In fact many flows actually do behave this way (at least approximately), even at modest Reynolds numbers. Note that as of this writing (in 2012) probably most workers in turbulence believe all of the above to be true for almost all flows. But they (like you) haven't seen or read the next two chapters.; and truth to tell would probably find them too threatening to believe anyway :-).

So here is the picture on which the 'classical' analysis is based: energetic scales of motion at wavenumbers of the same order of magnitude as the energy spectrum peak, say k_{peak}; and dissipation scales of motion mostly at much higher wavenumbers. And since obviously there has to be some means of getting energy from the large energetic scales to the smaller dissipative ones, this is carried out by the non-linear transfer among scales. In the classical picture the transfer has been generally been believed to accomplished by some type of energy cascade in which energy moves from one band of wavenumbers to higher bands, much like a waterfall (or cascade) where at each level the water is distributed over ever more smaller waterfalls (Tennekes and Lumley, 1972, chapter 8 provide a nice model for this 'leaky' cascade.) Originally the cascade in physical space was imagined to be a kind of progression in which large 'eddies' broke down into ever smaller eddies. This belief gave rise to the famous Richardson poem:

Big Whorls Have Little Whorls

Big whorls have little whorls
That feed on their velocity,
And little whorls have lesser whorls
And so on to viscosity."
– Lewis F. Richardson[2]

[2]For those of you who like to link pieces of history together, Lewis Richardson was a British Fluid Mechanicist of the early 20th Century, and was the uncle of Lord Julian Hunt, well-known

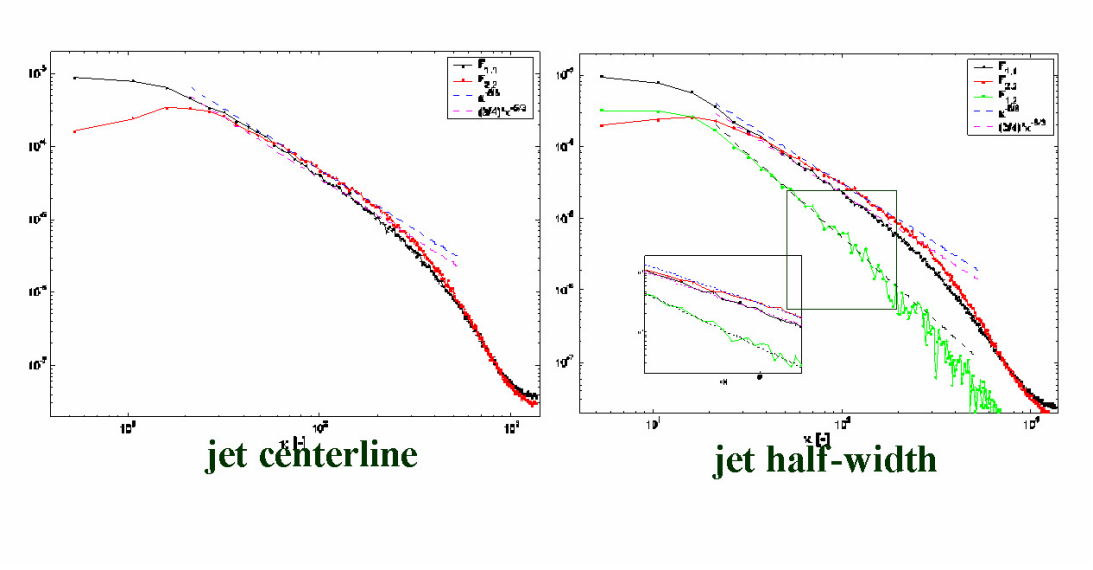

Figure 14.1: True spatial spectra from a 'transformed' turbulent jet at centerline and $\eta = r/\delta_{1/2} = 1$. Note the $k^{-5/3}$-range in both velocity components (u-black, v-red) and the $k^{-7/3}$-range for the Reynolds shear stress spectra (uv-green) at $\eta = 1$. The Reynolds shear stress is zero at the centerline. The faster rolloff at higher wavenumbers is mostly due to spatial filtering of the stereo PIV. From Wänström Ph.D. Thesis 2009, Wänström et al. 2011.

Now that we can actually see the vortical motions in at least some flows (thanks to DNS, PIV and wonderful flow visualization), we are not so sure of this picture any more, and the whole 'cascade' idea is questionable. Nonetheless, the energy definitely ends up at the dissipative scales, either by direct transfer from large to small or a progression of transfers, or some combination of both. Note that in the real world there can also be a reverse transfer from small scales to large, from high wavenumber to low. But since the largest velocity gradients are mostly at the smallest scales, the net effect is a transfer to smaller scales where viscosity wins.

We can develop this picture one step further. If most of the energy is at the smaller wavenumbers (the energetic scales), then these energetic scales will dominate the non-linear transfer (the triadic-interactions there). Moveover, since the fluctuating velocity gradients are relatively small at these low wavenumbers compared to those at much higher wavenumbers, then there is really very little dissipation down here at these wavenumbers where the energy mostly is. This can be easily seen by looking at the last term in equation 14.1 where the multiplication of $E(k,t)$ by k^2 skews its integral to much higher wavenumbers, and makes it nearly zero for low wavenumbers. So at least at sufficiently high Reynolds number (we will see which Reynolds number eventually), we can imagine a turbulence in which the energy is mostly at low wavenumbers (large scales) and the dissipation is mostly at much higher wavenumbers (small scales). And in our picture there is very little overlap.

14.0.2 The 'Universal Equilibrium Range' hypothesis

Now we are ready for Kolmogorov's fundamental hypothesis, on which all the other consequences of this theory are based: The *Universal Equilbrium Range Hypothesis*. But before stating it, remember that it was made long before we knew many of the things we know now. So while it was a brilliant intellectual triumph in the 1940's and was the basis for most our study of turbulence since, this does not mean it is necessarily correct. We must insist it stand on its own merits today. And in subsequent chapters we will do that and find that there are some problems. But first, what is it?

14.0.3 The basic argument

The equilibrium range hypothesis: In brief the hypothesis is that for wavenumbers sufficiently higher than the those characterizing the energy-containing range (say $k >> k_{peak}$), $\partial E(k,t)/\partial t \approx 0$. And most importantly, it is negligible relative to the non-linear transfer and dissipation.

The basic argument put forth to support this hypothesis is that the time scales of the smallest scales or eddies (or highest wavenumbers) are so much smaller than

---

British turbulence researcher from my generation.

the time scales of the energy-containing eddies (or energetic wavenumbers) that *the smallest scales are effectively in statistical equilibrium* (when measured in the time-frame of the energy-containing ones). Back in the 1940's we knew very little about the details of what turbulence actually looked like. In particular, it was quite reasonable to imagine many small eddies acting quite independently of large motions. So this whole line of reasoning which *assumes* that the small scales are adjusting in these short times, and not being locked instead in some way to the large scale structures, was quite reasonable. But modern flow visualization and DNS have given us a much better picture; and now we know a lot about coherent structures and the tendency of turbulence to appear as a nest of many small vortical structures. And we know that a long vortex which is being stretched along its axis clearly spins up, but the rate at which it does so is determined by the large scales that are doing the stretching. So even before the considerations of the next chapter, we can at least see a reason to be a bit suspicious of this line of argument. But let's pursue it anyway.

We can see why the equilibrium range hypothesis might be true by the following arguments. (Note that we will need to use information that we later derive from the consequences of Kolmogorov's hypothesis, so if you think we are assuming things we have not proven yet, we are. But hang in there for now – just don't forget your questions.) And note carefully that these are all *plausibility* arguments with very little quantitative about them. So as with all plausibility arguments we should be a bit suspicious, and for sure we should be willing to submit them any objective tests we can think of – even if they have appeared to be true for a long time.

We know from experience that most of the dissipation occurs for wavenumbers below $k\ \eta_{Kol} = 1$ (Typically about 99%.) And we have 'guessed' earlier that we can define a dissipative time scale from just the rate of dissipation of turbulence energy, ε, and the kinematic viscosity, ν; and it is given on dimensional grounds alone by $\tau_{Kol} = (\nu/\varepsilon)^{1/2}$. So let's compare τ_{Kol} to a time-scale characteristic of the energy-containing eddies, say $\tau_l \propto l/u \propto k_{peak}u/2\pi$ where $3u^2/2$ is the kinetic energy. Obviously we need an estimate for ε, so we will use another consequence of the theory we are deriving; namely we *define* $l = u^3/\varepsilon$ and hope that l is proportional to the size of the energetic scales (roughly the integral scale) or $l \propto 2\pi/k_{peak}$. Now we can substitute for $\varepsilon \propto u^3/l$ to obtain:

$$\frac{\tau_{Kol}}{\tau_l} = \left[\frac{ul}{\nu}\right]^{-1/2} = R_l^{-1/2} \tag{14.4}$$

where we have defined a *turbulence Reynolds number* as $R_l = ul/\nu$.

Clearly the larger the turbulence Reynolds number the smaller the ratio of time scales and the more the dissipative scales would seem to have a chance to be in equilibrium, at least relative to the energetic scales. For example, if we require the time scale ratio to be less than one-tenth, the turbulence Reynolds number, R_l, must be two orders of magnitude greater. So this doesn't look like it is a

very demanding criterion. BUT it only insures that the time scale ratio at the Kolmogorov microscale is small, not at the scales which are larger. To consider those we need to extend our ideas a bit further – and this leads us to the so-called *inertial subrange*.

14.1 The *inertial* subrange

14.1.1 A range without viscosity

Let's apply the same line of reasoning to wavenumbers that are much larger than k_{peak} but much smaller that $k = 1/\eta_{Kol}$; i.e., $k_{peak} << k << 1/\eta$. You can see that a much higher ratio of l/η is required to satisfy this inequality than for the time-scale ratio of equation 14.4 to be very small.

How do we know whether these might be (at least by the same arguments) in near statistical equilibrium? We can estimate a time-scale for an arbitrary wavenumber by simply using the energy spectrum itself and the local wavenumber. On dimensional grounds alone we define the local time scale to be:

$$\tau_k = [k^3 E(k,t)]^{-1/2} \tag{14.5}$$

Now we need to use another result of the theory we are about to derive, namely the form of the spectrum in the so-called *inertial subrange*, or more commonly, the $k^{-5/3}$-range. We will derive this later, but for now note that in it, $E(k,t) = \alpha_{Kol}\varepsilon^{2/3}k^{-5/3}$, where α_{Kol} is the so-called Kolmogorov constant which is usually assumed to be between 1.5 and 1.7. (The real miracle here is that the dissipation, ε, should make its way into an expression about the behaviour of the spectrum in a range in which there is assumed to be no dissipation, but save your questions about this till later – there is a reason.) Substituing this result into our local time scale leads to the time scale of 'eddies' in the inertial subrange as $\tau_k = \alpha_K^{-1/2}k^{2/3}\varepsilon^{1/3}$. Using $\varepsilon = u^3/l$ yields immediately the ratio of the time scale at given value of k in the inertial subrange to that of the energetic scales as:

$$\frac{\tau_k}{\tau_l} = \frac{1}{\sqrt{\alpha}}(kl)^{-2/3} \tag{14.6}$$

This can be much less than unity only if $kl >> 1$, to which we are of course willing to restrict ourselves; and simultaneously $k\eta_{Kol} << 1$.

14.1.2 Some problems already

It has been generally assumed, at least since the 1960's that this hypothesis of Kolmogorov's in fact describes all turbulence for scales much smaller than those at which the energy is put into the flow, no matter how generated. From their definitions, $l/\eta_{Kol} = R_l^{3/4}$. So both inequalities can be satisfied *only if* $R_l^{3/4} >>>> 1$. This is a very stringent requirement indeed. For example, the requirement is

only marginally satisfied if $R_l = 10^4$, since then $l/\eta_{Kol} = 10^3$. Very few lab experiments or DNS even come close to this.

Also this whole part of the spectrum has been widely assumed to be 'universal', hence the phase '*Universal Equilibrium Range*'. Nonetheless, we've had great difficulty pinning down exactly what that universal spectrum is, or even agree exactly what the value of α_{Kol} is. All of this has been complicated, of course, by our difficulties in trying to measure the dissipation. In fact, most of the time we just guess values of the dissipation that make the different spectra look like they agree at high wavenumbers. One of the few exceptions were the measurements in three different flows by Champagne 1978 shown in Figure **??**. Clearly these are not the same. Is the difference because the flows are different? Or because the Reynolds numbers are different and not high enough for the lower ones? Or because the theory is wrong? Or all three? As you can see, arguments to rationalize to the contrary, there is still much to be done in turbulence.

There are some other difficulties as well. Although there have been a number of experiments and simulations (using forced DNS) which purport to support the idea presented above, unfortunately it does not seem to have been noticed that there is one other very important circumstance under which Kolmogorov's hypothesis is satisfied exactly. In particular, *most experiments are in flows which are statistically stationary, so the left-hand-side of equation 14.1 is identically zero.*. Clearly you can't prove Kolmogorov's theory by using data from statistically stationary flows. But that is exactly what we have tried to do. And in fact it has been the non-stationary flows which have been the major problem for us, like decaying or growing turbulence in particular. Nonetheless, before examining them (in the next chapter), let's try to consider the full consequences of Kolmogorov's ideas.

14.1.3 The inertial subrange

Now let's assume Kolmogorov's ideas to be correct and that they indeed represent a spectral range which can be considered to be in statistical equilibrium. This of course presumes the Reynolds number to be sufficiently high, or more particularly $l/\eta_{Kol} >> 1$. If so then we can split the energy equation at some arbitrary wavenumber, say k_m, where k_m is some intermediate wavenumber simultaneously satisfying $k >> k_{peak}$ and simultaneously $k_m << 1/\eta_{Kol}$. Then if $k_{peak} <<<< 1/\eta_{Kol}$, we can safely assume there to be very little dissipation below $k < k_m$ so that the energy equation reduces simply to:

$$\frac{\partial E}{\partial t} \approx T, \qquad\qquad k < k_m \tag{14.7}$$

For convenience we can define a spectral flux, say $\varepsilon_k(k,t)$, so that:

$$\varepsilon_k(k,t) = -\int_0^k T(k',t)dk' \tag{14.8}$$

where k' is just a dummy integration variable (which we need since we have used k as the upper limit of integration). Note that many *confuse* this spectral flux, ε_k with the rate of dissipation of kinetic energy, ε. It is not! In fact it varies with wavenumber, k, and represents the net effect of the non-linear terms in 'removing' energy from wavenumbers smaller than k. So why you ask must we confuse things by calling it ε_k. The answer will come soon, and represents one of the most beautiful results in turbulence theory – and also one of the most poorly understood.

Now since $T(k,t)$ is the energy added (or removed if the sign is negative) at each wavenumber, it is easy to see that the spectral flux is the net energy crossing each wavenumber (from low to high since we have included the negative sign in the definition). Differentiation yields immediately the non-linear spectral transfer as the negative of the gradient of the spectral flux; i.e.,

$$T(k,t) = -\frac{d\varepsilon_k(k,t)}{dk} \tag{14.9}$$

We can integrate equation 14.7 from $0 \leq k \leq k_m$ to obtain:

$$\frac{d}{dt}\int_0^{k_m} E(k,t)dk = \int_0^{k_m} T(k,t)dk \tag{14.10}$$

But since we have assume almost all of the dissipation to occur at much higher wavenumbers than k_m and almost all of the energy to be at wavenumbers below k_m, it follows immediately that:

$$\frac{d}{dt}\int_0^{k_m} E(k,t)dk \approx \frac{d}{dt}\left[\frac{1}{2}\langle u_i u_i\rangle\right] = -\int_0^{k_m} \frac{d\varepsilon_k(k,t)}{dk}dk = -\varepsilon_k(k_m,t) \tag{14.11}$$

since by definition $\varepsilon_k(0,t) = 0$. In words, *the spectral flux crossing our intermediate wavenumber, k_m, is almost equal to the time derivative of the kinetic energy.*

Now let's examine what is happening at the higher wavenumbers. For $k > k_m$ the turbulence is assumed to be in in near statistical equilibrium so we can drop the time derivative on the left-hand-side and write approximately:

$$0 \approx T - 2\nu k^2 E, \qquad k > k_m \tag{14.12}$$

Integration from k_m to infinity yields:

$$0 \approx \int_{k_m}^{\infty} T(k,t)dk - 2\nu\int_{k_m}^{\infty} E(k,t)dk \tag{14.13}$$

But we already have observed that the integral of the non-linear spectral transfer, $T(k,t)$ over all wavenumbers is zero. Therefore

$$\int_{k_m}^{\infty} T(k,t)dk = -\int_0^{k_m} T(k,t)dk = \varepsilon_k(k_m,t) \tag{14.14}$$

Also since by hypothesis we have assumed the Reynolds number to be so high that there is relatively little dissipation for wavenumbers below k_m, it follows immediately that the last integral equation 14.13 is just approximately the dissipation; i.e.,

$$2\nu \int_{k_m}^{\infty} E(k,t)dk \approx \varepsilon \tag{14.15}$$

Thus the net spectral flux at our intermediate wavenumber, $\varepsilon_k(k_m)$ is approximately equal to the real dissipation of turbulence kinetic energy, ε. This is of course a consequence of the fact that we have assumed no dissipation at the low wavenumbers – just a net transfer out of the energy-containing eddies by the non-linear interactions to ever smaller scales.

It is but a small extension of our arguments to realize that if our underlying assumptions are correct (in particular the local equilibrium one), then these arguments are exact at infinite Reynolds number; i.e. when $l/\eta_{Kol} \to \infty$. In this limit, there can be no dissipation at the energy-containing scales, and no energy at the dissipative scales. If the latter seems counter-intuitive, then don't think of the limit, just the limiting process where less and less energy is available at the higher wavenumbers due to the vicous dissipation, and less and less dissipation at the smaller wavenumbers. And of course it is the non-linear terms (represented here by the spectral flux) that move energy from the low wavenumbers to the high ones. Exactly how they do this is not completely understood, but clearly it is through the non-linear triadic interactions.

One thing that is very important to note is that this whole line of argument seems to imply that there would be a finite rate of dissipation, even if the viscosity were identically zero (as opposed to simply getting smaller and smaller). This is because the energy decay appears to be (and in this model is) controlled only by the energetic scales of motion, and not be the viscous ones. The smallest scales simply respond to the amount of energy being fed to them by the non-linear interactions, and create whatever small velocity gradients are necessary to dissipate the energy. In fact, this is commonly assumed to be true. (But we shall see later that perhaps it is only true if the turbulence is statistically stationary, meaning that there must also be a continuous source of energy for this model of the dissipative scales to be true.)

14.2 Scaling the energy and dissipation ranges

From the consderations above we can infer two different scaling 'laws', one for high wavenumbers (or the dissipative scales of motion) and one for low wavenumbers (or the energetic scales of motion). This observation appears to have first been made by Batchelor in the late 1940's who synthesized the Kolmogorov ideas for the dissipative scales with the von Kármán/Howarth for the enegetic ones. Batchelor's synthesis became the standard belief among turbulence theorists after his own

book in the early 1950's, and especially after the eloquent and simple presentation by Tennekes and Lumley 1972. Indeed this is the 'religion' into which I was raised and spent much of my career. As you shall see in the next few chapters (and have had a few clues already) I've come to believe that maybe its time for a bit of heresy if we are to move forward in our understanding. Like everything else in this field, you can (and should) judge for yourselves. But be prepared for a bit of fight if you see the same problems I do, especially from those who are fearful that by having to revise their views they might have wasted their whole careers. Of course they most likely did not, but most still worry about it any time any old idea is challenged.

First, for the so-called energy-contaning range of scales we can see that the only important parameters (at least in the limit of infinite l/η_{Kol}) are u^2 and $l = u^3/\epsilon$. (Recall that the latter is really $l = u^3/\varepsilon_k(k_m)$, but since we are at assuming very high values of l/η_{Kol} we use ε instead.) Thus on dimensional grounds alone we would expect spectra to collapse at low wavenumbers when plotted as:

$$\tilde{E}(\tilde{k}) = \frac{E(k)}{u^2 l} \tag{14.16}$$

where we have dropped for now the dependence on t. $\tilde{E}(\tilde{k})$ is a non-dimensional spectrum and $\tilde{k} = kl$ is a non-dimensional wavenumber. This is the so-called 'energy-range' form of the spectrum and u^2 and l are referred to as 'energy-containing range' variables.

Exactly the same scaling can be applied to the one-dimensional spectra as well. Figure 14.2 shows spectra for different wavenumbers plotted in this manner. The particular plots shown actually use the measured spatial integral scales, $L^{(1)}_{1,1}$ and $L^{(1)}_{2,2}$ instead of the pseudo-integral scale l, so the collapse is actually a bit better than it would have been with l.[3] (More will be said about this later.) The collapse at low wavenumbers is quite impressive, and departure is gradual with increasing wavenumber until the near exponential roll-off with increasing Reynolds number as the ratio of l/η_{Kol} increases. The collapse is, of course, not perfect since we are not really at infinite Reynolds number (i.e., $l/\eta_{Kol} \to \infty$) and there are still small (but finite) viscous effects felt at all wavenumbers.

Now consider what happens for high wavenumbers. For this region of the spectrum dissipation dominates, and the entire equilibrium range is pretty much described by only ε and ν. We can use these to write another non-dimensionalized form of the spectrum as:

$$E^+(k^+) = \frac{1}{\nu^{5/4}\epsilon^{1/4}} E(k) \tag{14.17}$$

Now $E^+(k^+)$ is a non-dimensional spectrum of the dimensionless wavenumber, $k^+ = k\ \eta_{Kol}$. This is the so-called (and famous) 'Kolmogorov non-dimensional spectrum' and the spectrum is said to be normalized in Kolmogorov variables.

[3]The original Mylarski/Warhaft paper uses $l = u^3/\varepsilon$ instead.

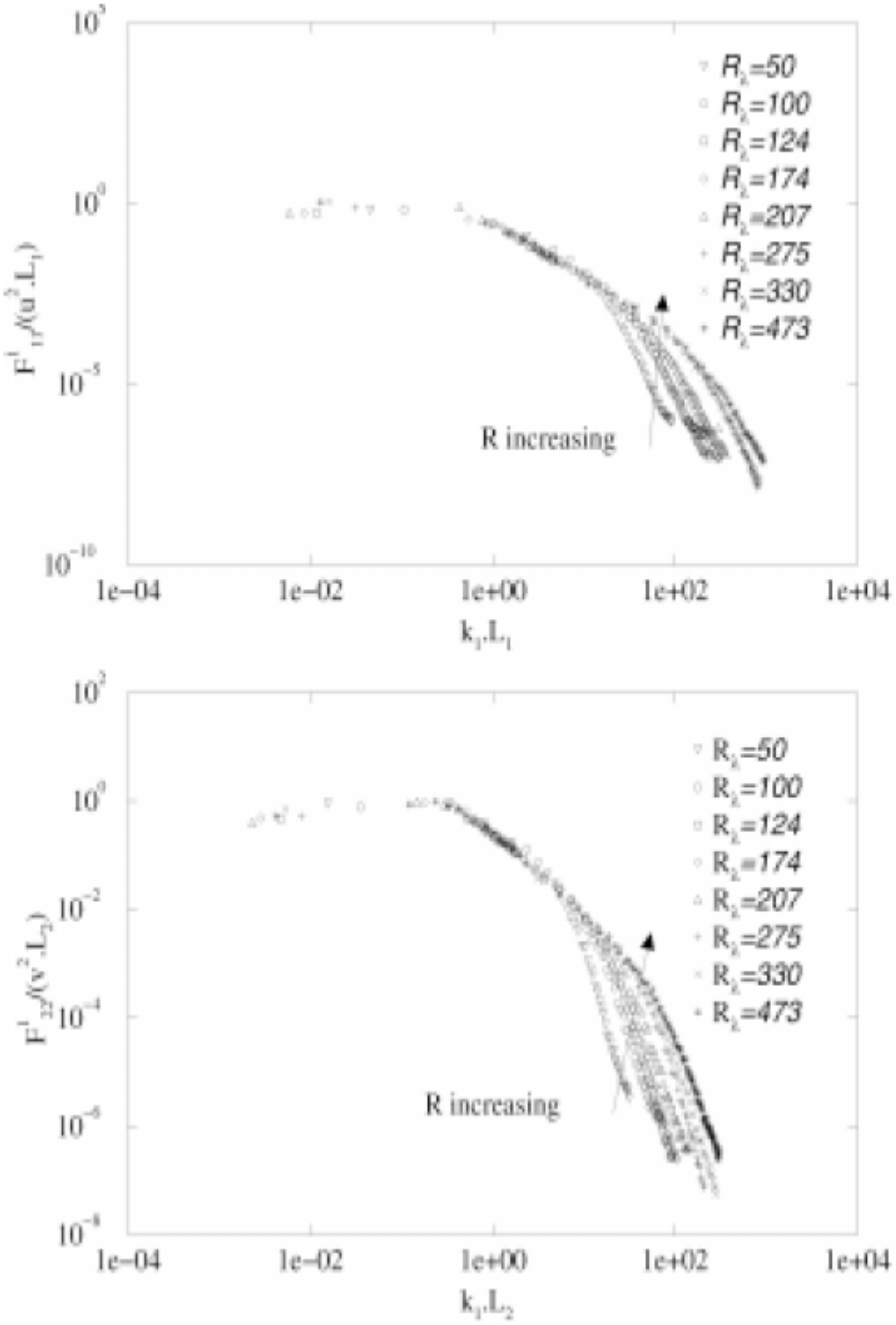

Figure 14.2: Plots of streamwise and lateral one-dimensional spectra measured downstream of grid, plotted in energy-containing range variables (data of Mydlarski and Warhaft 1996, from Gamard and George 2000).

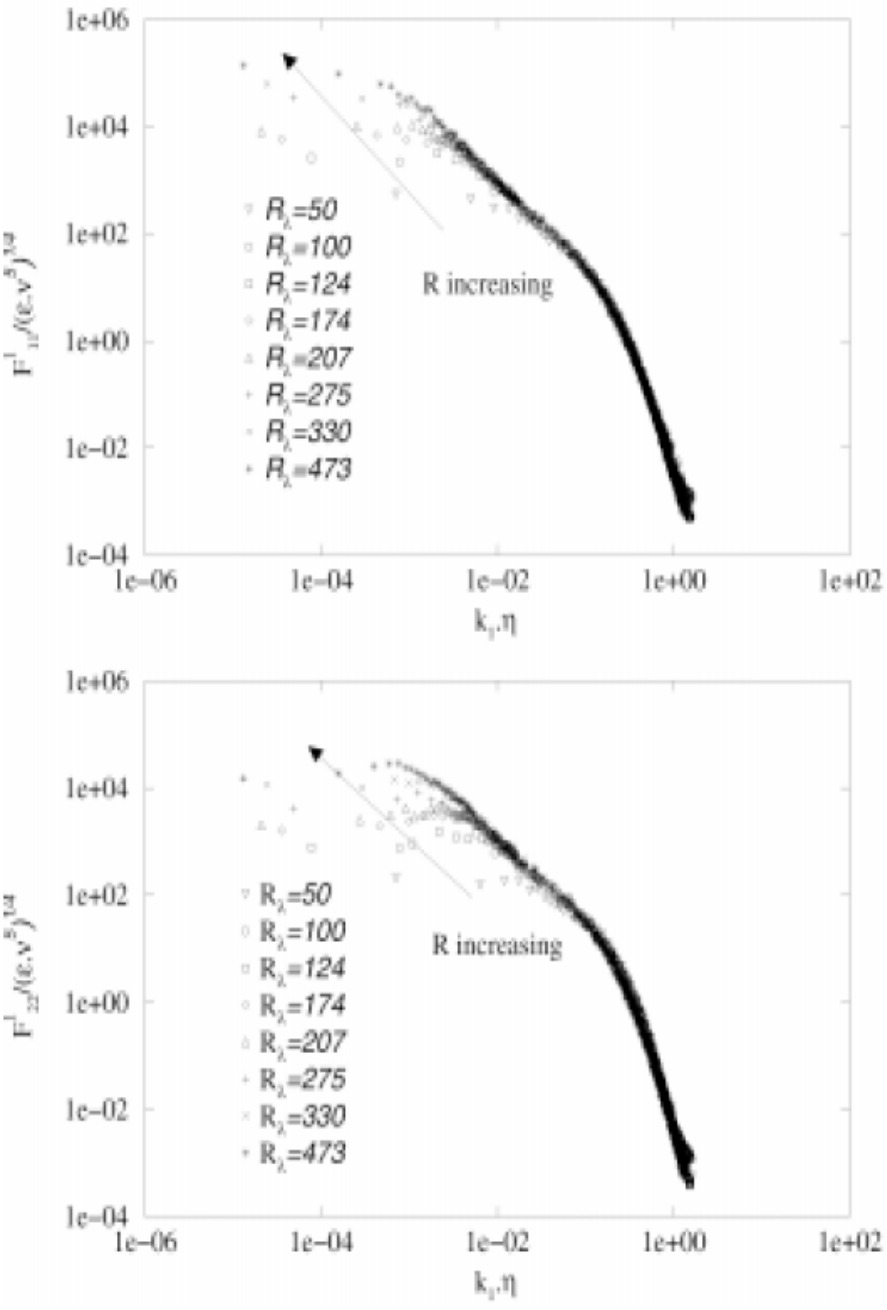

Figure 14.3: Plots of streamwise and lateral one-dimensional spectra measured downstream of a grid, plotted in Kolmogorov variables (data of Mydlarski and Warhaft 1996, from Gamard and George 2000).

Figure 14.3 shows the same one-dimensional spectral data as shown in Figure 14.2, but this time plotted in Kolmogorov variables. Note the near collapse at high wavenumbers, but the clear variation with l/η_{Kol} at the low wavenumbers. Also clear from both figures is that there seems to be range of wavenumbers between both extremes (say $1/l << k << 1/\eta_{Kol}$) where both the high and low wavenumber scalings work pretty well. This, as we shall see below, is the 'inertial subrange' where the famous Kolmogorov $k^{-5/3}$ law will be seen to live.

14.2.1 The $k^{-5/3}$ and $r^{4/3}$ laws

One of the main reasons for the acceptance[4] of Kolmogorov's ideas about the local equilibrium (and even universality) of the small scale (or high wavenumber) turbulence was the success of the the inertial subrange prediction. As we shall see below, a slight extension of the arguments above leads immediately to prediction that the spectrum in the inertial subrange should vary as $E(k) = \alpha_{Kol}\ \varepsilon^{2/3}\ k^{-5/3}$. Similar considerations for the velocity structure functions yields $\langle [u_i(\vec{x} + \vec{r}) - u_i(\vec{x}]^n \rangle = \beta_i^{(n)}\ \varepsilon^{n/3}\ r^{n/3}$. If it is assumed that the turbulence in this equilibrium range is also universal (meaning it is the same in all flows and the Reynolds number is high enough), then the coefficients are also presumed to be universal constants. The third-order structure function is the most interesting of all, since it can be shown directly from the dynamic equation for the second-order structure function that the coefficient is exactly 4/5; i.e $\langle [u(x+r) - u(x)]^3 \rangle = (4/5)\ \varepsilon\ r$. It is often forgotten that all of these results (if true at all) can be strictly true only in the limit as $l/\eta_{Kol} \to \infty$.

Now the truth is that in spite of the enthusiasm for these ideas (actually it's more like religious fervor[5]), they seem to work really well only some of the time, and not so well other times. One reason for this 'not-so-great' behavior is completely obvious. The Reynolds number (i.e., l/η_{Kol}, the ratio of integral scale to Kolmogorov microscale) of many flows, especially those we generate in our laboratories and computers, is not nearly at high enough for the theory to even begin to apply. Thus in most flows we can measure or compute there really is no inertial subrange in which $\varepsilon_k \approx \varepsilon$. Nor sometimes is the Reynolds number even high enough for there to be an equilibrium range at all! Even so, many researchers still draw $k^{-5/3}$ lines on their measured spectra, and seem to take comfort in the

[4]This didn't happen immediately, and it really wasn't until the tidal channel measurements of Grant et al. reported in a famous 1962 Marseille turbulence meeting and the measurments in a jet of M.M. Gibson 1963 that people began to generally accept them. Batchelor and others, of course, believed them much earlier, probably because of their theoretical elegance, but without much experimental confirmation. But even Kolmogorov himself was beginning to doubt and in the same meeting produced another version that included intermittency. This latter has come to be known as Kolmogorov 1963 or just K63, while his earlier theory is usually just referred to as K41. It is K41 that is the focus of this chapter.

[5]I just saw the results of recent study that suggests the more poorly people actually understand something and the less confident they are that the data actually support it, the more intensely they will defend it. This happens in turbulence too.

fact there is always a point of tangency.

But there are other reasons for the failure of the theory as well. First there seem to be flows which march to a different drummer entirely, especially non-equilibrium flows. We shall discuss some of these in the next chapter. And also there are flows in which energy is being put into or taken out of the inertial subrange directly by the mean flow or from other sources like buoyancy or energy production from the mean flow by the Reynolds stresses. In these cases the spectral flux is not constant but increases or decreases with wavenumber, so this at very least causes a departure from the $k^{-5/3}$-behavior, even if all the other assumptions are satisfied. Sometimes even when this happens we can make a different spectral model, still in part based on Kolmogorov's ideas. We shall include an example in the next section where finite Reynolds number effects can be in part accounted for.

And there seem to also be effects of internal intermittency; i.e., effects arising from the fact that the dissipation is not uniformly distributed throughout the flow but is sometimes highly concentrated into compact regions (like spaghetti or lasagna). Actually it was Kolmogorov himself in 1962 who first built a model for this based on the assumption that the dissipation was log-normally distributed. There has been much work on this over the past four decades (see the book by Frisch 1996, for example); and although it is important, we shall not discuss it here since it will lead us too far from our story. The bottom line though is that internal intermittency will cause a slight Reynolds number dependence in the inertial subrange exponents (e.g., from $-5/3$ to $-5/3 + \gamma(Re)$ where $\gamma(Re) > 0$. Note that this is the opposite of the low Reynolds number effects considered later which cause $\gamma < 0$).

14.2.2 Dimensional and physical analysis

In section 14.1.3 we argued for the existence of a spectral range, the *inertial subrange*, in which for any wavenumber, k_m, the spectral flux, $\varepsilon_k(k_m)$ was constant and approximately equal to the actual rate of dissipation, ε. Moreover we argued that in the limit of infinte Reynolds number that $\varepsilon_k(k_m) = \varepsilon$ exactly. This was an immediate consequence of our assumption that there was no dissipation at the lower wavenumbers or in our inertial range, and therefore any energy dissipated had to be passed through to the dissipative range.

Now look at the consequence for the spectrum $E(k)$ in this inertial subrange. The only parameter surviving in the equations is $\varepsilon_k \approx \varepsilon$. There is effectively no energy here, so u^2 and l can not be important here; nor are there any viscous effects so we can forget about ν also. This means that $E(k)$ must be entirely determined by k and ε alone, the latter ONLY because it is equal to the spectral flux in the inertial range, ε_k. To emphasize this point we shall write ε_k below in our derived result, and set it equal to ε only at the very end. (This may seem rather silly to you now, but it will save you much agonizing later when you try to figure out whether these theoretical results should apply to the flows you encounter which don't seem to behave this way – like in turbomachinery, or in

geophysical fluid dynamics, or in flows with a mean shear, or even those 'unusual' flows that insist on being at finite Reynolds number :-).)

Now we apply the Buckingham-Π theorem which in its simplest form says the number of *independent* dimensionless ratios possible is equal to the number of parameters minus the number of dimensions. We have three parameters ($E(k)$, k and ε_k) and two dimensions (length and time). Therefore we know immediately that $E^a \varepsilon_k^b k^c = const$ and must be dimensionless. Since the dimensions of E are $length^3/time^2$, ε are $length^2/time^3$ and k is $1/length$, clearly the constant can be dimensionless only if $E(k) \propto \varepsilon_k^{2/3} k^{-5/3}$. Moreover if the spectrum itself is 'assumed' to be universal[6], then so must be the coefficient, say α_{Kol}, which is why it is commonly referred to as the *universal Kolmogorov constant.*[7]

Exercise Prove using dimensional analysis that if there is a range of scales in physical space for which ε and r are the only parameters, then the n^{th}-order structure function must be given by $\langle [u_i(\vec{x}+\vec{r}) - u_i(\vec{x}]^n \rangle = \beta_i^{(n)}\ \varepsilon\ r^{n/3}$.

The results for the structure function and spectrum are generally assumed to be equivalent, but I must confess I have a certain uneasiness about the latter. My reason is that in spectral space we know that the spectral coefficients in non-overlapping bands are uncorrelated. So when we make arguments about spectral flux we can pretty much be sure that we are talking about something that corresponds to the mathematical decomposition of the equations, with energy being transferred from the eigenfuntion at one wavenumber to that at another. It is not so obviously true (at least to me) in structure function space, since we for sure can not say that turbulence at one physical scale is uncorrelated with that at another. But maybe I'm just being a bit pedantic here, since I'm not aware that anyone else seems too worried about this. It does make a difference, however, when one thinks about closure in LES (Large Eddy Simulations). In particular, can one apply Kolmogorov's ideas to small volumes of fluid below some cutoff size with the same degree of confidence one could make a truncation in wavenumber space above some wavenumber? My personal opinion is: probably not.

14.2.3 Deduction of $k^{-5/3}$-range from asymptotic analysis

There is another way to deduce the existence of the $k^{-5/3}$-range by working with the scaling laws for low and high wavenumber spectra (equations 14.16 and 14.17).

[6]This is a nice hypothesis, but the rationale for it usually involves some sort of so-called 'cascade' model in which the turbulence loses its memory as the energy is passed through interactions among progressively smaller triads of wavenumbers that are mostly the same size (see Tennekes and Lumley, Chapter 8 for a really nice model). The problem comes in when there is no cascade and there are interactions over all wavenumbers – as for example in non-stationary flows.

[7]One might think after more than a half-century we could agree with some certainty what the 'universal value' would be, but apparently not. Should make us think at bit. It just might be a smoke signal that something is wrong.

It has the advantage that it really is useful in highlighting that our deductions are really valid only at very high Reynolds number, in fact infinite to be precise. This approach was to the best of my knowledge first presented by Tennekes and Lumley in their pioneering book "An First Course in Turbulence", which even though out-dated is still well well worth studying (but with proper scepticism since many years have passed and our understanding has changed). What they do particularly correctly is to recognize that both the inner and outer scaled forms of the spectrum are valid **everywhere** *if you retain the Reynolds number dependence in the functional expressions*, in their case $R = l/\eta_{Kol}$ where they used $l = u^3/\varepsilon$ for their low wavenumber scaling. Thus both the following expressions for $E(k)$ are completely valid at all wavenumbers when written as:

$$E(k) = u^2 l E^+(k^+, R) \tag{14.18}$$
$$E(k) = \nu^{5/4}\varepsilon^{1/4}\tilde{E}(\tilde{k}, R) \tag{14.19}$$

where $k^+ = k\,\eta_{Kol}$ and $\tilde{k} = k\,l$ and $R = l/\eta_{Kol}$. The dependence on the parameter R inside the functional relationship is what makes the energy variables scaled spectrum start deviating at high wavenumbers, and *vice versa* for the high wavenumber scaled spectrum. For example, in Figures 14.2 and 14.3, R (but defined using L instead of l) is the parameter that labels the individual curves. Note how the individual curves depart from collapse as R changes – at high wavenumbers when scaled in energy-scaled variables, and at low in Kolmogorov variables. It is more subtle to realize that they really don't perfectly collapse at any wavenumber at finite values of R, only approximately.

Now if the spectra have to be equal, so must their derivatives with respect to wavenumber; i.e., using the chain-rule we can write:

$$\frac{dE}{dk} = u^2 l\,\frac{d\tilde{E}}{d\tilde{k}}\,\frac{d\tilde{k}}{dk} \tag{14.20}$$
$$\frac{dE}{dk} = \nu^{5/4}\varepsilon^{1/4}\,\frac{dE^+}{dk^+}\,\frac{dk^+}{dk} \tag{14.21}$$

But $d\tilde{k}/dk = l$ and $dk^+/dk = \eta_{Kol}$. Hence the derivatives can be equal only if:

$$u^2 l^2\,\frac{d\tilde{E}}{d\tilde{k}} = \nu^{5/4}\varepsilon^{1/4}\eta_{Kol}\,\frac{dE^+}{dk^+} \tag{14.22}$$

We can eliminate u^2 by substituting using $\epsilon = u^3/l$, which must be true, at least at infinite Reynolds number. Doing this, using the definition of $\eta_{Kol} = (\nu^3/\varepsilon)^{1/4}$, and multiplication of both sides by $k^{8/3}$ yields after some rearrangement:

$$\tilde{k}^{8/3}\,\frac{d\tilde{E}(\tilde{k}, R}{d\tilde{k}} = k^{+-8/3}\,\frac{dE^+(k^+, R)}{dk^+} \tag{14.23}$$

Now comes the 'trick' part, which is the same trick used to derive the log or power law solutions to the boundary layer. We argue that in the limit as $R = l/\eta_{Kol} \to \infty$, the ratio of $\tilde{k}/k^+$ becomes undefined. Therefore in this limit, both sides of equation 14.23 must equal the same constant, which for convenience we define to be $-(3/5)\ \alpha_{Kol}$; i.e.,

$$\lim_{R\to\infty} \tilde{k}^{8/3}\ \frac{d\tilde{E}(\tilde{k}, R}{d\tilde{k}} = -\frac{3}{5}\alpha_{Kol} \tag{14.24}$$

$$\lim_{R\to\infty} k^{+-8/3}\ \frac{dE^+(k^+, R)}{dk^+} = -\frac{3}{5}\alpha_{Kol} \tag{14.25}$$

But since the right-hand side of both equations is a constant we can integrate immediately to obtain:

$$\tilde{E}_\infty(\tilde{k}) \ = \ \alpha_{Kol}\ \tilde{k}^{-5/3} \tag{14.26}$$

$$E^+_\infty(k^+) \ = \ \alpha_{Kol}\ k^{+-5/3} \tag{14.27}$$

Thus we have recovered the inertial subrange we obtained by dimensional analysis. But we now recognize that it is not just '*in-between*' the energy-containing range and the dissipative range, **it is an extension of both of them**! It is truly a 'matched' layer (overlap region) that comes from stretching and matching two solutions in the limit of infinite Reynolds number. Clearly, even if all theoretical assumptions are correct, we should expect to find α_{Kol} strictly constant and universal in the real world only at very, very high Reynolds numbers. Also we should expect spectra at low wavenumbers to collapse with u^2 and l, BUT to only collapse the low wavenumber range nearly perfectly at very, very high Reynolds numbers. And the same for the Kolmogorov scaled spectra at high wavenumbers: collapsing with increasing Reynolds number, but with only perfect collapse at very very high Reynolds number.

In the next section we shall examine what happens if we relax this requirement on the Reynolds number a bit.But before we do, let's see what happens if we try putting the high wavenumber and low wavenumber spectra together to form a composite spectrum. The basic idea is to write one of them in the variables of the other, multiply them together and divide by the common part (a trick I learned from Chuck Van Atta, a highly respected turbulence experimentatlist at UC San Diego, now deceased). For example, we can write the high wavenumber spectrum using $k^+ = \tilde{k}/R$. The common part of both the high and low wavenumber spectra (in $\tilde{k}$ variables) would be just be equation 14.26 above. Thus our composite spectrum in energy variables would just be:

$$\tilde{E}_{composite}(\tilde{k}, R) = \tilde{E}_\infty(\tilde{k})\ E^+_\infty(\tilde{k}/R)\ [\alpha_{Kol}\tilde{k}^{-5/3}]^{-1} \tag{14.28}$$

Note the substitution of $\tilde{k}/R$ for k^+ inside the function E^+. As the value of $\tilde{k}$ increases, the increasing viscous effects included in E^+ will cut off the composite

spectrum at very high wavenumbers, exactly like happens in nature. And the higher the value of R, the higher the value of $\tilde{k}$ before this happens.

Of course, we could just as easily write the composite spectrum in high wavenumber variables by substituting for $\tilde{k}$ using k^+/R The result is:

$$E^+_{composite}(k^+, R) = \tilde{E}_\infty(k^+/R)\ E^+_\infty(k^+)\ [\alpha_{Kol} k^{+-5/3}]^{-1} \tag{14.29}$$

14.2.4 The inertial range at finite Reynolds numbers

review Gamard/George contribution here.

14.3 Models for the spectrum in the universal equilibrium range

For the high wavenumber part of the spectrum there actually are many semi-empirical models that have been developed. Several of these were put forth shortly after World War II as scientists from many countries became aware of Kolmogorov's equilibrium range hypothesis. Among the most famous were those due to Heisenburg (of uncertainty principle fame and Nobel Prize winner), Onsager (another Nobel Prize winner), and Kovasznay (who came to Johns Hopkins later as Professor and had an influence on my career as well).[8] All of these models have been well discussed in most other books, and none are particularly good, so I won't go into detail discussing them here. The exception is perhaps Heisenberg's, which while not particularly useful for computing spectra has found a new life in closing off truncated sets of equations using POD and other decomposition techniques (see for example the book by Holmes, Lumley and Berkooz). Basically what Heisenberg did was to use the small scales to create an eddy viscosity to act on the strain rates of the larger scales. This same idea is the basis of modern LES closures as well. One thing to note is that every closure model successfully reproduced the $k^{+-5/3}$-range, but as we have noted this hardly can be used to justify any model since it can be obtained from simple dimensional analysis alone.

Kovasznay model Even though Kovasznay's model is not very good and leads to a unphysical spectral cut-off (and negative spectra thereafter), it is a good point to start our discussion of how one can build a high-wavenumber model which has the right physical ideas in it. What Kovasnay suggested was that maybe the spectral flux depended on just $E(k)$ and k alone. If so the only dimensionally correct possibility was

$$\varepsilon_k = \gamma\ k^{5/2}\ [E(k)]^{3/2} \tag{14.30}$$

[8] Among the many things I remember him telling me was his comment after I congratulated him on assuming the job of Department chairman. He responded in his Hungarian accent: 'Beel, you must understand that the most important task of the Department Chairman is to make sure there is toilet paper in the johns.' He always did have a unique perspective on life :-)

where γ is a constant of proportionality. Now it is pretty straight-forward to substitute this into equation 14.12 and solve for $E(k)$. You indeed find a $k^{-5/3}$ for small values of k, which then rolls off eventually as k^{-7}. Unfortunately it then actually gets to zero and goes negative, which is quite unphysical (since energy can never be negative).

Exercise: Do exactly what is suggested above. Show that indeed in the low-wavenumber limit (i.e., $k \to 0$) you do recover the $k^{-5/3}$-range and use this fact to relate γ to α_{Kol}. Also show that the spectrum has a viscous range that rolls-off as k^{-7} and a cut-off value beyond which the spectrum is negative.

Now sometimes people who do experiments like to show k^{-7} lines on their spectral plots, but mostly it indicates that they really don't know very much about turbulence. You really should NEVER use this spectrum, since it clearly has some pretty serious deficiencies, the negative value and cut-off being the worst. BUT the idea is still useful to us, especially the idea that the spectral flux should depend some way on the spectrum itself.

Pao-Corrsin model By the 1960's hot-wires had improved enough that spectral measurements could be made at wavenumbers approaching $k\ \eta_{Kol} \approx 1$. And it was becoming clear that none of the spectral models were showing the right behavior, which appear to be like an exponential roll-off. Yih-Ho (Mike) Pao[9] and his thesis advisor (and my spiritual turbulence father) Stanley Corrsin realized that the only way to get an exponential roll-off was to make the spectral flux itself depend linearly on the spectrum. Given this then, on dimensional grounds alone the spectral flux must be given by:

$$\varepsilon_k(k) = C\ \varepsilon^{1/3}\ k^{5/3}\ E(k) \tag{14.31}$$

where C is a constant. Note the $\varepsilon^{1/3}$ is exactly what is needed to make $\varepsilon_k = \varepsilon$ in the inertial subrange. Also it should be obvious that C has to be equal to α_{Kol}^{-1} for the same reason.

It is quite straightforward to plug this into equation 14.12 above and find the so-called Pao-Corrsin spectrum which is given by:

$$E(k) = \alpha_{Kol}\ k^{-5/3}\ \exp\left[-2\alpha_{Kol}(k\ \eta_{Kol})^{4/3}/(4/3)\right] \tag{14.32}$$

Note that integration constant coefficients have been evaluated by plugging equation 14.32 into the dissipation integral, then choosing them so it gives the correct dissipation.

Exercise: Carry out the steps indicated above and derive the Pao-Corrsin spectrum.

[9]Mike Pao finished his Ph.D. at the Johns Hopkins University and took a position at Boeing Research Lab in Seattle. When they decided to shut it down in the late 60's Mike took a part of the lab and formed what we now know as Flow Research and a few other spin-off companies.

Exercise: Use the Pao-Corrsin model to compute the one-dimensional spectra for the streamwise and cross-stream velocity components. Note that you of course will have to assume isotropy and carry out a difficult integration with singularities. If you are clever you can do the problem in cylindrical coordinates using and use $\sigma d\sigma = kdk$ where $k^2 = k_1^2 + \sigma^2$, etc.

Lin-Hill spectrum

In spite of the simplicity of its derivation, the Pao-Corrsin spectrum seemed at first to be a great solution to the need for an empirical spectrum. I used it myself in my Ph.D. dissertation to derive the spatial filtering imposed by the finite size of an LDA scattering volume on spectral measurements. And my former students Dan Ewing and Hussein Hussein have done the same when trying to calculate the effects of hot-wires on derivative measurements. Nonetheless, it became clear in the early 1980's that there still was too much energy in the dissipative range. The reason was apparently due to the fact that the roll-off of the spectrum itself did not cut back the spectral flux fast enough. Moreover, spectra measured at high Reynolds numbers were showing what looked like a small k^{-1}-range after the $k^{-5/3}$-range, just before the exponential roll-off.

A simple solution was proposed by Lin and Hill which cut back the spectral flux as the Kolmogorov microscale was approached:

$$\varepsilon_k(k) = \alpha_{Kol}\ \varepsilon^{1/3}\ k^{-5/3}\ [1 + (k\eta_{Kol})^{2/3}]^{-1} E(k) \tag{14.33}$$

Note how the term in square brackets reduces the spectral flux as $k\eta_{Kol}$ increases towards unity.

It is again a simple matter of substitution and integration to show that the spectrum is now given by:

$$E(k) = \alpha_{Kol}\, \varepsilon^{1/3}\, k^{-5/3}[1+(k\eta_{Kol})^{2/3}]\ \exp\{-2\alpha_{Kol}[(k\eta_{Kol})^{4/3}/(4/3) + (k\eta_{Kol})^2/2]\} \tag{14.34}$$

Once again the integration constants have been chosen so that the dissipation integral gives the correct result.

Exercise Substitute the Lin-Hill model for the spectral flux into the local equilibrium spectral equation and solve for $E(k)$. Show that it satisfies the dissipation if the integration constants are chosen appropriately.

14.4 A useful empirical low wavenumber spectral model

There really are no known analytical solutions to the spectral energy equation, so when one is needed we have to resort to empirical ones. For the low wavenumber

spectral models, these are only a little more than just 'fits' to data, but they should try to get the physics more or less right. For example, one popular choice for an spectrum in the energy-containing range (originally proposed by von-Karman and Howard 1938) is given by:

$$E(k) = [u^2 l] \frac{C_4 k^4}{[1 + (k/k_e)^2]^{17/6}} \tag{14.35}$$

For small k this will start off as k^4, which is consistent with the controversial Loitsianskii invariant.[10] And for $k >> k_e$ it rolls off as $k^{-5/3}$, which is consistent with the upper limit of the energy scaled spectrum in the limit of infinite Reynolds number, $E^+_\infty(k^+)$. The coefficient C_4 and parameter, k_e are usually chosen so the the spectrum integrates to the all the kinetic energy, $3u^2/2$ and gives the right value of α_{Kol} in the limit of large k; i.e.,

$$\frac{3}{2}u^2 = \int_0^\infty E_\infty(k,t)dk \tag{14.36}$$

and $u^2 l C_4 k_e^{17/3} = \alpha_{Kol}$. Obviously you will need to use the infinite Reynolds number relationship $\varepsilon = u^3/l$.

Exercise: Find the value of C_4 and $k_e l$ which satisfies these constraints. (Hint: non-dimensionalize the wavenumber by k_e, then you will discover the integral to be one of the standard tabulated integral (a gamma-function actually). Then solve for the values of $k_e l$ and C_4 that give you the right kinetic energy, $3u^2/2$, and α_{Kol}. Try two values of α_{Kol}: 1.5 and 1.7. Do you see any problems with this?)

Substitute equation 14.35 into the isotropic spectral relations and show that the corresponding one-dimensional spectrum is given by:

$$F^{(1)}_{1,1}(k_1) = \frac{C}{[1 + (k_1/k_e)^2]^{5/6}} \tag{14.37}$$

What are the values of C and $k_e l$ for the two cases above? (Remember the one-dimensional spectrum should only integrate to u^2, and from the isotropic relation between the three-dimensional spectrum function and the one-dimensional spectrum, the 'one-dimensional' Kolmogorov constant is $(9/55)\ \alpha_{Kol}$.)

It is possible to generalize the result above into more variations. One used by Wang and George, JFM 2003 (see their appendix) writes:

$$E(k) = [u^2 L] \frac{C_p (kL)^p}{[1 + (kL/k_e L)^2]^{5/6 + p/2}} \tag{14.38}$$

Here L is the physical (or real integral scale) and the values of C_p and $k_e L$ are chosen so that the energy and integral scale spectral integrals give the correct

[10] Note that one could easily use different powers for the low wavenumber exponent (e.g. k^2) and modify the exponent for the denominator accordingly.)

p	1	1.34	2	3	4
$k_{peak}L$	1.3630	1.2943	1.2272	1.1804	1.1570
k_eL	1.7597	1.4437	1.1203	0.8798	0.7468
k_{peak}/k_e	0.7746	0.8965	1.0954	1.3416	1.5492
C_p	0.3229	0.4535	0.8455	2.2249	6.2528

Table 14.1: Spectral parameters as function of p

values. The same trick of non-dimensionalizing the wavenumber by k_e allows both integrals to be expressed exactly as beta-functions. Values of $k_{peak}L$, k_eL, k_{peak}/k_e and C_p are tabulated in Table 1 for $p = 1$, 1.34, 2, 3 and 4. Note that this method of choosing the coefficients (i.e., insisting the integral scale be correct as well as the energy) does not allow an independent determination of the Kolmogorov 'constant' (as you probably figured out from the exercise above).

Finally, Gamard and George (2000 J. Flow, Turbulence and Combustion, see the appendix) used a slightly modified version with near asympototics which actually allows for finite Reynolds number departures from the infinite Reynolds number solutions; e.g.,

$$E(k, L/\eta_{Kol}) = [u^2L]\frac{{C_p}'(kL)^p}{[1 + (kL/k_eL)^2]^{5/6+p/2-\mu/2}} \tag{14.39}$$

where μ is a function of $1/(\ln L/\eta_{Kol})$. As discussed in the next section they were able to find the functional form by looking at the interdependence of the coefficients and the Reynolds number dependence ratio of $\varepsilon L/u^3$, then fit experimental spectral data to determine the coefficients.

The whole point is that even an empirical expression like this can be of enormous value in trying to understand some of the finer points of turbulence and turbulence measurement. For example, Reynolds (Ann. Rev. Fluid Mech. 1976) uses Equation 14.38 to examine how turbulence modeling constants depend on the energy spectrum assumed. George et al. 1984 use a slightly different version to obtain an excellent fit to the one-dimensional velocity and pressure spectra in a jet mixing layer. Wänström et al. (2007 ASME paper and in her Ph.D. dissertation) even used equation 14.35 to evaluate how the finite spatial dimensions of a PIV interrogation volume affected the mean square value of different components of the velocity. This worked in her case because the spatial filtering was cutting off in the inertial subrange, so the viscous range was not important. The bottom line is: don't be too analytically lazy to be creative. It is amazing how much you can learn from a simple empirical model thoughtfully applied.

fill in from Gamard and George 2000

14.5 Some problems

Non-stationarity

Energy is mostly in the $k^{-5/3}$ range

Appendices

Appendix A

Signal Processing

Foreword: This appendix was largely taken from the notes from courses on turbulence measurement at the Danish Technical University and Chalmers developed by Knud Erik Meyer, Peter B.V. Johansson and William K. George.

Most things that we measure are what we called random processes. In measurements of fluid flows, turbulence is one example of very important random component. To get useful results from measurements from a random process we need to use statistical tools since we do not have much use for a collection of instantaneous values alone. This is not always simple to do in practice, but the underlying ideas are quite straightforward. This chapter is about the process of getting from a physical quantity to a numerical estimate of the quantity. For more reading on data from random processes, we recommend the very thorough book by Bendat and Piersol [**?**]. Several special details related to flow measurements are covered in [**?**].

A.1 Signals

We define a signal as the variation in time and space of any relevant physical quantity occurring in a useful system or device. The signal itself is formed by a series of measurements of the quantity. We can divide signals from random processes into three different types:

Stationary: a signal whose *statistical* properties do not vary with time. This means that it does not matter *when* you choose to do your measurement. This is a fundamental assumption in most experiments and also an assumption that we will do throughout this chapter.

Periodic: a signal that repeats itself after a finite amount of time. Common examples occur in rotating machinery. Sometimes such a signal can be treated as though it were 'locally' stationary statistically by dividing each period into small "time-slots". Data from the same time-slot from many periods

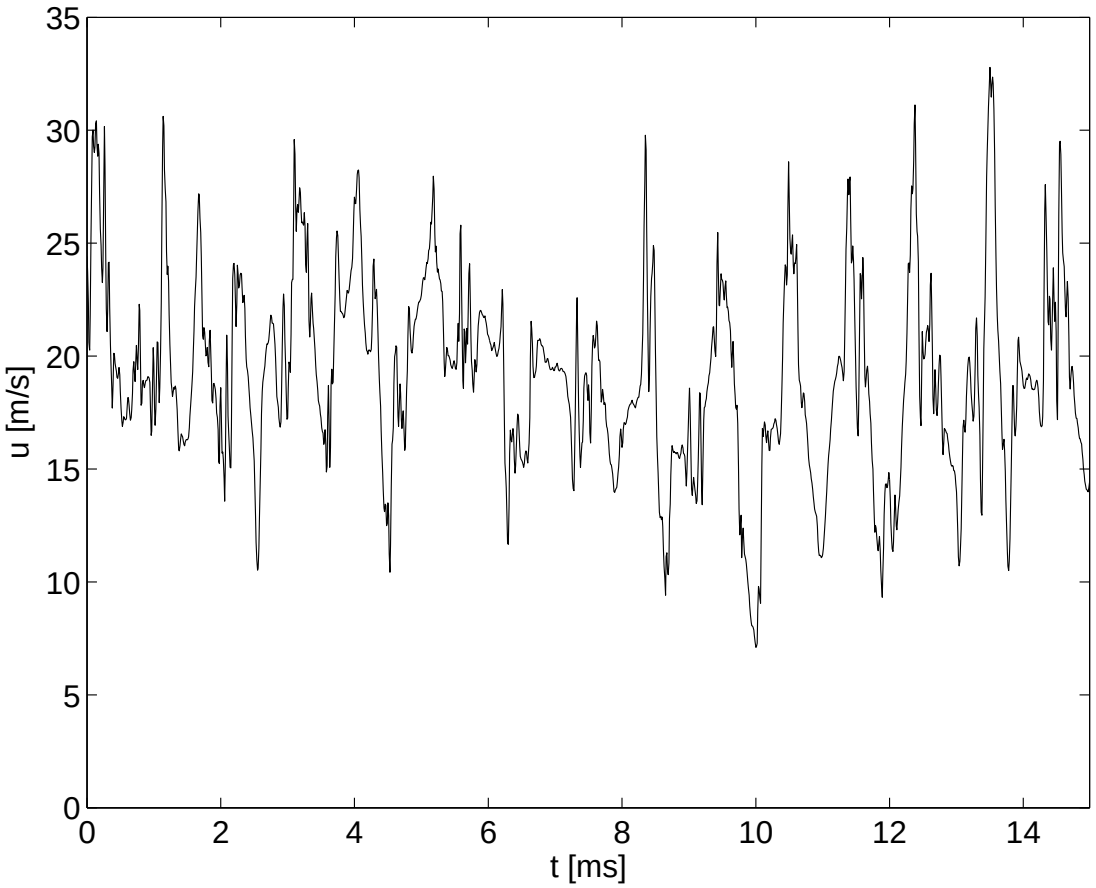

Figure A.1: Hot-wire measurement of the main flow velocity component in a turbulent flow behind a cylinder sampled at 100 kHz. Data from [**?**].

can then be treated as a stationary signal. Usually though, when doing statistical analysis, it is better to treat such signals by using only information from exactly the same phase of the signal (called phase-averaging).

Transient: a signal that only exists for a finite amount of time, usually short. An example could be a sudden close of a valve in a flow system. If the process creating the signal is repeatable, the signal can sometimes be treated as a periodic signal.

There can of course be signals that do not fall within these three types; e.g., signals that are not repeatable. For such a signal, many of the statistical tools discussed in the present chapter are not applicable and it is only possible to average between different realizations of the same experiment; i.e., the experiment must be repeated over and over.

An example of a signal is shown in figure A.1. Even though the signal does seem to have some repeating patterns, the signal has a strong random component

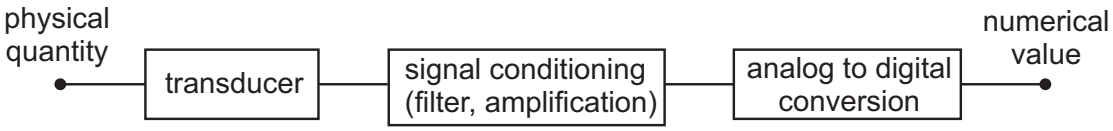

Figure A.2: The measurement chain

due to flow turbulence. There are many questions we could try to answer using the data shown in figure A.1. A few of them are:

- What is the mean velocity?
- Is the data record long enough for an accurate estimate?
- Can we estimate the turbulence intensity?
- How accurate will our estimate be?
- Is there a dominant frequency in the signal due to vortex shedding from the cylinder? And if so, how can we estimate it?
- What would the optimal sampling frequency be for the questions above?

These questions and several more can be answered using the statistical tools that we present in these appendices.

A.2 The measurement chain

Before we look at the statistical tools, we think it is instructive to understand the basic elements of a measurement. Any measurement can be described by the measurement chain shown in figure A.2. Here the measurement is divided into three steps. The first step is a transducer (based on some physical principle) that converts the physical quantity into another physical quantity suitable for further signal processing. This is very often a voltage, but there are other possibilities as well; e.g., a displacement or an optical signal. Then there is nearly always some sort of signal conditioning. The converted signal might be amplified. It is also both unavoidable and desirable to have some filtering of the signal. Sometimes this is inherent to the transducer. Finally, before a measurement is usable, it should be converted into a numerical value. This is accomplished by an analog-to-digital (A/D) converter.

For a simple example: consider the measurement of the temperature in room by a glass thermometer. The transducer is an enclosed amount of fluid whose volume changes with temperature (e.g., ethanol). When the fluid (mostly in the bulb) changes its volume to adjust to the temperature around it, this change is amplified by letting the change in volume cause a thin column of the fluid to rise or fall in a very thin pipe. The temperature can then read be comparing

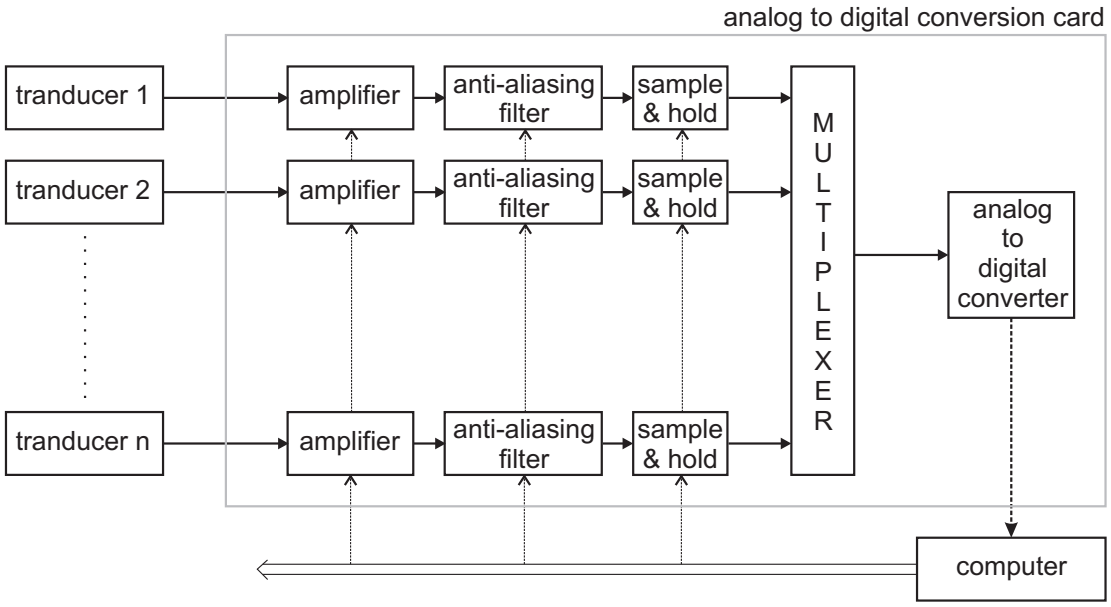

Figure A.3: Schematics of an analog-to-digital card

the height of the column to a calibrated scale placed along the thin pipe. The conversion to a numerical value is done by you when you compare the column height to the scale. If the thermometer is moved into a cold air stream from a an open window, it will not instantly show the new temperature. You will need to wait at least a few minutes to read the new temperature. It is inherent to the construction of the thermometer that it filters out fast (or high frequency) variations of the temperature, and only follows slower variations. Thus in signal processing terminology, the thermometer is acting like a low-pass filter on the temperature fluctuations, the net effect of which is to integrate out the faster time-dependent variations. The amplification (sensitivity of column movement) and the filtering properties have been fixed by the design of the thermometer, and by your choice of the type of thermometer to use. You are also making some decisions about the conversion to numerical values. You can choose to report the temperature as 21°C, as 21.4°C or as 21.43°C depending on number of divisions on the scale and on your ability to interpolate between divisions.

In the example with the glass thermometer of the preceding section, the conversion to a numerical value was the last step before the final result. A few decades ago, a large part of the data processing was done by analog systems using specially built electrical circuits to evaluate quantities like mean values or frequency content. Today, the strategy is usually to convert measurements to a digital form as early as possible and perform data processing digitally. This is partly because digital processing has become very cheap, but in many cases, it is also because digital processing is much more flexible. In the following section, we will therefore only consider digital data processing.

When a measurement variable is converted into digital form, it is discretized in three different ways:

- The value of the variable is discretized into a number of bit levels
- The variable is discretized in time by sampling
- The variable is discretized in space by selection of measurement points.

The consequences of this discretization will be discussed in the subsequent sections.

In any measurement, you will need to make some decisions regarding all three elements in the measurements chain. We will cover the properties of different transducers in the discussion of the different measurements techniques and we will cover the use of filters in section G.2. In the next section we will examine how an analog-to-digital converter works and what options are available.

A.3 Analog-to-digital conversion

If you are sampling data with a computer, most investigators today use an "analog-to-digital card" (A/D card). A schematic of typical components is shown in figure A.3. An A/D card will typically have several data channels so that it can be connected to several transducers. Each channel has its own signal conditioning. The conversion to a digital number will be only for a fixed voltage range; e.g., from 0.0 to 10.0V or from -5.0V to 5.0V. The signal from the transducer must therefore be first amplified (or attenuated) to match this voltage range. Often an offset value should be added to place the mean value near the middle of the range, thereby minimizing the possibility of instantaneous values outside it.

Depending on what will be done with the data, an important element can be an *anti-aliasing* filter. This is just a low-pass filter that removes high frequency parts of the signal *before* digitization. This filter is essential for spectral analysis of digital time-series data,and will be discussed in detail in section G.2. The basic problem it prevents is called *aliasing*, which means that frequencies of the digitized data show up at different frequencies than they should. **Once data has been sampled incorrectly and is *aliased*, it is nearly impossible to de-alias or correct it**; so proper choice (and use) of anti-aliasing filters can be quite crucial to the success or failure of the experiment. Three considerations are primary: First, do the filters roll-off (or cut-off) rapidly enough to really remove the parts of the signal that might otherwise be aliased? Second, are the filters for different channels phase-matched so their effect on all channels is the same? And finally, are the phase changes at different frequencies that are introduced by the filters acceptable. Since the more severe the cut-off, the more the phase changes with frequency, generally some trade-offs must be made. A popular compromise choice is the Bessel filter whose phase variation with frequency is linear, which corresponds to a simple time delay.

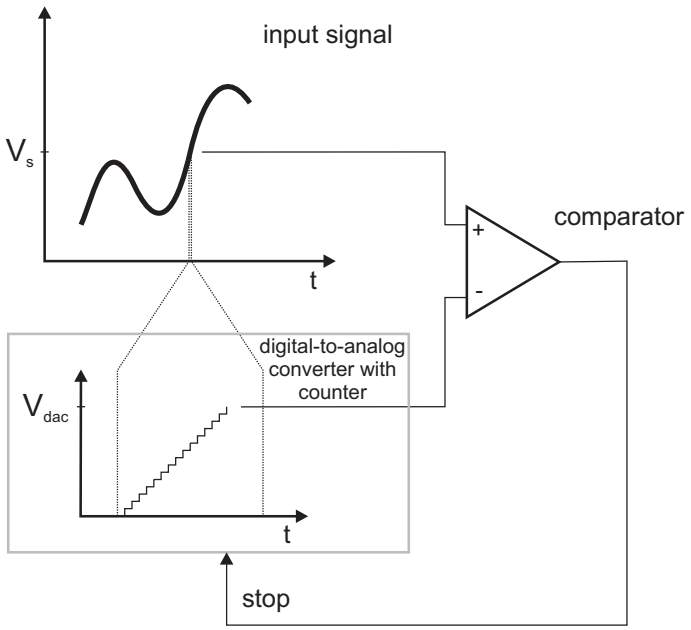

Figure A.4: Principle of an analog-to-digital converter

Most A/D cards only have one analog-to-digital converter (A/D converter). The A/D converter is therefore connected (or multiplexed) to the data channels through a multiplexer which only connects the A/D to one channel at a time. This means that the channel signals are not converted at the same time, which can create phase problems in the data analysis if they are to used together. It is often desirable to take samples from all channels at exactly the same time. Therefore some A/D cards have a "sample-and-hold" component for each channel just before the multiplexer. At a trigger pulse or at a fixed frequency, each channel voltage is stored, and then the stored channel voltages can be read one by one by using the multiplexer and the A/D converter. But even sample-and-hold will not fix the problem if the anti-aliasing filters are not properly phase-matched to each other.

The principles of an A/D converter are illustrated in figure A.4. The A/D converter determines the current signal voltage V_s by comparing the voltage to voltage generated by a digital-to-analog converter (DAC). A common method is to increment the D/A using a digital counter count from zero until the corresponding voltage from DAC matches the signal voltage. A comparator will then send a stop signal to the counter. The digital number in the counter will then be the digital representation of the signal voltage. It is obvious that the conversion takes some time and also that the more bits in the converted value (resolution of voltage), the longer the time needed for the conversion. Some A/D converters use more sophisticated and thus faster algorithms. The basic specification of an A/D converter is the number of conversions per second and the number of bits in the

bits	levels	resolution
8	$2^8 = 256$	0.4%
12	$2^{12} = 4096$	0.02%
16	$2^{16} = 65536$	0.002%

Table A.1: Common resolution of AD cards

converted digital value.

A number of properties should be evaluated when an A/D card or an A/D converter is selected for measuring task:

Resolution: The resolution of the full range is determined by the number of bits in the converted digital value. Common values are shown in table A.1. Converters with as low as 10 bits or as high as 22 bits are also available. Even conversion to a 8 bit number has a resolution better than 1% of full range, and this is sometimes sufficient with proper pre-conditioning of the signal (e.g., offset, amplification, etc.). A/D cards or converters with 16 bits are quite affordable today and can be very convenient; e.g., for signal that has small fluctuations around a large mean value. Sometimes a 16 bit card can measure directly without as much signal conditioning as one with fewer bits.

Sampling rate: General purpose 12 bit A/D cards are available with sampling rates up to 1000 kHz; i.e., up to 1.000.000 data samples per second can be obtained. If such an A/D card is connected to 5 channels, this means that each channel with be sampled with 200 kHz. Dedicated 8 bit converters can have sample rates up 1000 MHz. Cards may have local memory buffers and can then only sample at the highest sample rates until the buffer is full.

Channels: As mentioned above, general purpose A/D cards multiplex several channels into a single A/D converter. Channels can be "single ended" or "differential". Single ended channels use a common ground and therefore only one wire is connected for each channel. This always introduces ground loops in the system, which can substantially increase the electronic noise and greatly complicate analysis. Much to be preferred are differential channels which connect each pair of wires separately, so that all channels can be electrically isolated from each other. A general purpose card often comes with either 16 single ended channels or 8 differential channels. The sample-and-hold option illustrated in figure A.3 will increase the cost of the card.

Sensitivity: The sensitivity is limited by the number of bits and the range over which conversion is performed. When electronic noise is negligible, the effective 'noise' on the system is set by the volts/bit. This is the so-called *quantization noise*. Since it appears on the digitized data as broadband

noise, it must be insured to be well below any signal of interest. The important control factors here are the signal conditioning (offset, amplification and filtering), and the general noise specifications of the A/D card.

Appendix B

Random Processes

Foreword: This section overlaps considerably (at this point at least) the material in Chapter 8. It was largely taken from the notes from courses on turbulence measurement at the Danish Technical University and Chalmers developed by Knud Erik Meyer, Peter B.V. Johansson and William K. George.

Many processes we wish to measure are in fact random processes, meaning that one can not guess exactly future values by looking at it past values. Some processes really are deterministic (meaning that for fixed initial conditions and boundary values the same answer will be obtained every time in the process), but they behave chaotically and appear to be random. Turbulence is a good example of this. But even processes that are not really random, appear to us as random when we try to measure them because of our measurement (or computational) errors. Thus just about everything we encounter can be treated as random processes.

We will call a variable measured from a random process a *random variable*. In the following, we will denote the random variable as u, since we often measure a velocity or velocity component. The variable could just as well be anything else, like local pressure, temperature, etc. And it could be a function of time and space, and most certainly which (of possibly many) experiments we performed. But to make statistics we need to be able to deal with *independent events*. The easiest way to understand this is to imagine doing the same experiment quite independently in many different universes simultaneously. Then we could compare what happened at exactly the same place at the same time in each universe, or 'average' the results together. When we can compute such an average, the 'true' average, we denote it by $\langle u \rangle$. Even though we have still not defined the 'true average, we will presume it to exist. In fact we shall see that the only way to get a 'true' average is to have an infinite number of universes in which we are simultaneously performing an identical experiment in each.

We will call our i^{th} attempt to measure our random variable as the i^{th}-realization, and denote it as $u^{(i)}$. In the paragraphs below we shall assume each realization to be statistically independent from all others. This is discussed in detail in sec-

tion 2.4.3 of chapter 2, which provides a definition in terms of the joint probability density function. But for our purposes the most important consequence is that if two random variables, $u^{(i)}$ and $u^{(j)}$, are statistically independent, then are *uncorrelated*. This means that $\langle u^{(i)}u^{(j)}\rangle = 0$ if $i \neq j$. (Note that the inverse is not necessarily true; i.e., lack of correlation does not imply statistical independence.)

Usually the first thing we want to know about a random variable, u, is its mean value, $\langle u\rangle$. This is really not a simple as it might seem, since the best we can ever do is *estimate* the true mean value (which we have presumed to exist for any random process). The reason is obvious if we look at the definition of the ensemble mean (or true) mean (or average):

$$\langle u\rangle = \lim_{N\to\infty} \frac{1}{N}\sum_{i=1}^{N} u^{(i)} \tag{B.1}$$

Clearly one can never have an infinite number of independent universes (other than in our imaginations). And in fact we can never even have an infinite number in the one universe we have.

Your first thought is probably: Do we really need an infinite number? What's wrong with just taking a finite number, say U_N given by:

$$U_N = \frac{1}{N}\sum_{i=1}^{N} u^{(i)} \tag{B.2}$$

Our problem is that this *estimator* (or 'estimate of the mean) is itself a random variable. This means that our every attempt to measure the mean will most likely produce a different result. Obviously we need to know a couple of things for measurements to make any sense. First, is there some reason to believe that the mean of our estimates is close to the true mean of the underlying random process? And second, is there hope that by making more estimates or for longer times that we have a better chance of getting closer to the correct answer? These two questions are usually asked this way: Is the estimator biased? And does the estimator converge with increasing time or number of samples? The first question is generally addressed by examining the *bias*, the second by examining its *variability*. We shall examine both of these in the following subsections.

The problem is that in a real measurement, we never have the true mean, say $\langle u\rangle$, but can only use an estimator for the ensemble average based on a finite number of realizations, say N; i.e.,

$$U_N = \frac{1}{N}\sum_{i=1}^{N} u^{(i)} \tag{B.3}$$

Since $u^{(i)}$ is a random variable then U_N is also a random variable. This means that if we repeat the experiment, we should not expect to get two values of U_N that are exactly the same.

There are two important questions to investigate when an estimator is used.

1. Does the average of our estimator give the right average; i.e., does $\overline{U}_N \to \langle u \rangle$? If this is the case, the estimator is an *unbiased* estimator.

2. Does the estimator converge towards the true value as we take more and more samples? We talk about *convergence*.

It is straightforward to see that U_N is an unbiased estimator by comparing eqs. (B.10) and (B.3). We can analyze the convergence by looking at the *variability* defined as

$$\epsilon_N^2 = \frac{(U_N - \langle u \rangle)^2}{\langle u \rangle^2}. \tag{B.4}$$

If we insert the definition of our estimator from eq. (B.3), we get that

$$\epsilon_N^2 = \frac{1}{N} \frac{\text{var}(u)}{\langle u \rangle^2} = \frac{1}{N} \frac{\sigma_u^2}{\langle u \rangle^2} \tag{B.5}$$

where the *variance* is estimated as

$$\text{var}(u) = \frac{1}{N} \sum_{i=1}^{N} (u^{(i)} - \langle u \rangle)^2 \tag{B.6}$$

and the *standard deviation*, σ_u is the square root of the variance.

Sometimes the variability is expressed using the turbulence intensity $\text{Tu} = \sigma_u / \langle u \rangle$ (here u *is* a velocity) as

$$\epsilon_N = \frac{1}{\sqrt{N}} \frac{\sigma_u}{\langle u \rangle} = \frac{\text{Tu}}{\sqrt{N}}. \tag{B.7}$$

Looking at eq. (B.5) or (B.7), we see that $\epsilon_N \to 0$ as $N \to \infty$. We also see that $\epsilon_N \sim 1/\sqrt{N}$; i.e., if we increase the number of samples N four times, we should expect the confidence interval between our estimated mean value and the true mean value to get 50% smaller.

As discussed in detail in section 2.5 of chapter 2, ϵ_N is an estimator of the standard deviation of U_N (but only if the N samples are *uncorrelated*). Thus ϵ_N is a measure of the uncertainty caused by the limited number of samples, and it is therefore an important parameter for the design of an experiment.

B.1 Time-averaged statistics

As discussed in section A.1, most experiments are random processes designed to be stationary.

B.1.1 Time mean value

The time-averaged mean value for stationary signal is defined as

$$\langle u \rangle \equiv \lim_{T\to\infty} \frac{1}{T} \int_0^T u(t)dt. \tag{B.8}$$

We have used the same symbol for the average as for the true average defined above, since if the process is stationary, both time and ensemble averages are the same. Like the true average though, this expression can not be evaluated in a real experiment since we can not measure for an infinite time. So instead we are forced to deal with an estimator for the time average, say U_T, defined by:

$$U_T \equiv \frac{1}{T} \int_0^T u(t)dt. \tag{B.9}$$

Also usually we will not represent the signal as analog (or continuous), but instead use a discrete representation. The latter problem can be easily solved by rewriting equation (B.8) into a discrete form using values $u_1, u_2 \ldots u_N$ of u sampled with a constant time between samples Δt,

$$U_T \approx \frac{1}{N\Delta t} \sum_{i=1}^{N} u^{(i)} \Delta t = \frac{1}{N} \sum_{i=1}^{N} u^{(i)} \tag{B.10}$$

since $T = N\Delta t$. Thus our discrete time average estimator looks exactly like our estimator for independent realizations from before. Therefore we can approximate the time average value this way, and it does not depend on the time between samples, Δt, *as long as they are statistically independent.*

In a real measurement, of course, we can only take a limited number of samples, N. Moreover, our random process is a continuous process with its own memory of how it was at an earlier time (since the flow at one time is linked to other times by the governing equations). How then can any two samples be truly statistically independent? Given this question, we obviously need to worry about the same things we did before: Does our time average estimator converge? And does it converge to the right value?

By comparing eqs. (B.8) and (B.9), it is easily seen that the estimator is unbiased; i.e., $\overline{U}_T \to \langle u \rangle$ as $T \to \infty$. The question of convergence is addressed as before by studying the variability, which is given in this case by:

$$\epsilon_T^2 = \frac{var\{U_T\}}{\langle u \rangle^2} = \frac{\langle (U_T - \langle u \rangle)^2 \rangle}{\langle u \rangle^2} \tag{B.11}$$

(Note that in practice we use U_T instead of $\langle u \rangle$ in the integral above.)

After some effort involving multiple integrations, it can be shown that the relative error in estimating the mean is given by:

$$\epsilon_T = \sqrt{\frac{2I}{T}} \frac{\sqrt{var\{u\}}}{\langle u \rangle} = \sqrt{\frac{2I}{T}} \frac{\sigma_u}{\langle u \rangle} \tag{B.12}$$

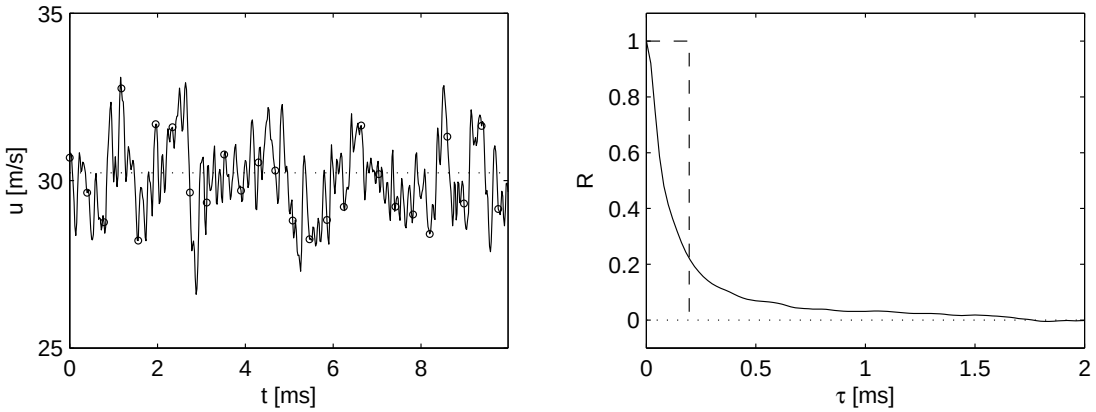

(a) sample of velocity data (b) autocorrelation function

Figure B.1: Hot-wire measurement downstream of a grid.

where I is the integral time scale for the process defined by:

$$\overline{[u - \langle u \rangle]^2} I = \int_0^\infty \overline{[u(t) - \langle u \rangle][u(t+\tau) - \langle u \rangle]} d\tau \tag{B.13}$$

Note that the integrand is the two-time correlation (or autocorrelation function) for the process defined by:

$$R(\tau) = \overline{u(t)u(t+\tau)}. \tag{B.14}$$

Also the variance in the continuous formulation can be estimated using its finite time estimator as:

$$var_T\{u\} = \frac{1}{T}\int_0^T [u(t) - \langle u \rangle]^2 dt. \tag{B.15}$$

Comparing equation B.12 to equation (B.7) it can be seen that $T/2I$ corresponds to the N of our independent samples above. This means that

- To have uncorrelated measurements, the time between samples should be at least two times the integral time scale ($T/N \geq 2I$).
- If you have measured with a time between samples that is shorter than two times the integral time scale, you can estimate the standard deviation of the mean value using eq. (B.12).
- Said in another way, you will not get better convergence for the estimate of the mean value by sampling faster than one sample every $2I$.

Example: Autocorrelation from hot-wire measurement

Figure B.1 shows a hot-wire measurement made downstream of a grid in a wind tunnel. The data is taken with a single wire probe with a sampling frequency of

50 kHz. The total data record is 2.6 seconds long (131072 samples). The first 10 ms of the record is shown in figure B.1(a). The mean value of the total record is $\langle u \rangle = 30.23$ m/s (here assumed to be the true mean value) and this is indicated as a horizontal dotted line in the figure. Figure B.1(b) shows the autocorrelation found by evaluating eq. (B.14) for the total data record. By integrating the autocorrelation, the integral time scale is found to be $I = 0.20$ ms. This is indicated in figure B.1(b) as a dashed rectangle with the same area as the area below the autocorrelation curve. In figure B.1(a) samples taken with a distance of $2I = 0.4$ ms is shown with the symbol $\circ$. The 10 ms record of the flow therefore corresponds to 25 statistically independent samples. The standard deviation of u can be calculated from the data to be $\sigma_u = 1.24$ m/s and relative value of the standard deviation of the mean value can therefore be estimated using eq. (B.12) as

$$\frac{\sigma_{U_T}}{\langle u \rangle} = \epsilon_T = \sqrt{\frac{2I}{T}} \frac{\sigma_u}{\langle u \rangle} = \sqrt{\frac{2 \cdot 0.20\,\mathrm{ms}}{10\,\mathrm{ms}}} \frac{1.24\,\mathrm{m/s}}{30.23\,\mathrm{m/s}} = 0.8\%$$

or a value of $\sigma_{U_T} = 0.25$ m/s. The actual mean value of the sample shown in figure B.1(a) is $U_T = 30.06$ m/s or a deviation from $\langle u \rangle$ of 0.6%. The mean value of the first 25 samples marked with the symbol $\circ$ figure B.1(a) is $U_N = 29.98$ m/s or a deviation from $\langle u \rangle$ of 0.8%. Both of these deviations are clearly with in the statistical variation indicated by the value of ϵ_T.

B.1.2 Higher moments

We often want to characterize our data using higher order moments. A higher moment is defined as

$$\langle u'^n \rangle = \lim_{T \to \infty} \frac{1}{T} \int_0^T \left(u'(t) \right)^2 dt \tag{B.16}$$

where we have defined the fluctuation, $u'(t)$, to be;

$$u'(t) = u(t) - \langle u \rangle \tag{B.17}$$

Using our previous results, we can get an error estimate for an arbitrary moment by substituting u' with u'^n and N with $T/2I$ in eq. (B.5) to obtain

$$\epsilon^2_{u'^n} = \frac{2I}{T} \frac{\mathrm{var}(u'^n)}{\langle u'^n \rangle^2} = \frac{2I}{T} \frac{\langle u'^{2n} \rangle - \langle u'^n \rangle^2}{\langle u'^n \rangle^2} \tag{B.18}$$

For the second moment (the variance of u) we get

$$\epsilon^2_{u'^2} = \frac{2I}{T} \left(\frac{\langle u'^4 \rangle}{\left(\langle u'^2 \rangle \right)^2} - 1 \right) \tag{B.19}$$

Thus in order to estimate the error of the second moment, we need to know the fourth! For the third moment (the skewness) we get

$$\epsilon^2_{u'^3} = \frac{2I}{T} \left(\frac{\langle u'^6 \rangle}{\left(\langle u'^3 \rangle \right)^2} - 1 \right) \tag{B.20}$$

For the fourth moment (the flatness or sometimes called the kurtosis) the error estimate becomes

$$\epsilon^2_{u'^4} = \frac{2I}{T}\left(\frac{\langle u'^8\rangle}{\langle u'^4\rangle^2} - 1\right) \tag{B.21}$$

Equations (B.19–B.21) are very hard to compute from measured data. Therefore it is customary to estimate these using the approximation that the random process can take an analytical form. The most common form used in turbulence is to assume the process to be *Gaussian*. A random process is Gaussian if the probability density function $p(u')$ can be expressed as

$$p(u') = \frac{1}{2\pi\sigma}\exp\left(-\frac{u'^2}{2\sigma^2}\right) \tag{B.22}$$

where σ is the standard deviation, $\sigma = \sqrt{\langle u'^2\rangle}$.

Using the probability density function, the moments can be alternatively defined as

$$\langle u'^n\rangle = \int_{-\infty}^{\infty} u'^n p(u')du' \tag{B.23}$$

This can be used together with the definition of the Gaussian to obtain a simple analytical form for the error of each moment. For a Gaussian process, the odd moments like the skewness is identical zero, so one can only obtain numbers for the second and forth moments

$$\epsilon^2_{u'^2,G} = \frac{4I}{T} \tag{B.24}$$

$$\epsilon^2_{u'^4,G} = \frac{22I}{T} \tag{B.25}$$

Example: Deciding sampling times

We want to measure in a turbulent flow and preliminary measurements have estimated a turbulence intensity of Tu = 20% and an integral time scale of $I =$ 1.5 ms. We want to measure the mean velocity with a an error not larger than 1%.

If we assume the errors to be distributed according to a Gaussian random process, a 1% error corresponds to two times the standard deviation and is sometimes expressed as a 95% confidence interval. We therefore want to estimate the necessary sample times for the standard deviation of the estimated mean value to be $\epsilon_T = 0.5\%$. Using equations (B.7) and (B.12) we find the sample time to be

$$T = \frac{2I(\mathrm{Tu})^2}{\epsilon_T} = \frac{2\cdot 1.5\cdot 10^{-3}\,\mathrm{s}\cdot 0.2^2}{0.005^2} = 4.8\,\mathrm{s}$$

corresponding to an effective number of samples of

$$N = \frac{T}{2I} = \frac{4.8\,\mathrm{s}}{2\cdot 1.5\cdot 10^{-3}\,\mathrm{s}} = 1600$$

Statistically it does not matter if we take more samples during the 4.8 seconds of sampling. The optimal sampling rate f_s can therefore be considered to be

$$f_s = \frac{N}{T} = \frac{1600}{4.8\,\mathrm{s}} = 333\,\mathrm{Hz}$$

We can use eqs. (B.24) and (B.25) to estimate the uncertainty for the higher moments for a sample time of $T = 4.8$ s. Using a factor of two on the standard deviations corresponding to a 95% confidence interval, we find the uncertainty on the second moment (the variance) to be 7% and for the fourth moment to be 17%. To obtain one percent uncertainty on the fourth moment, we must have a total sampling time equal to at least 1320 seconds (22 minutes!) corresponding to 1,750,000 uncorrelated samples!

Appendix C

Fourier analysis of time varying signals

Foreword: This appendix was largely taken from the notes from courses on turbulence measurement at the Danish Technical University and Chalmers developed by Knud Erik Meyer, Peter B.V. Johansson and William K. George.

There are two ways of looking at how a signal evolves in time. One way is to look at the signal as a sequence of events (e.g., opening and closing a valve). Another way is to characterize the signal in terms of *frequencies* being present. An example is how we perceive sound. If we are listening to somebody talking, we understand words by listening to the sequences of different sounds in the words. However, the single sounds in the words (corresponding to letters in written words) are characterized by the combinations of frequencies in the sound – which is a result of how we form the sound with our mouth. It is also interesting that we are able to recognize people we know only by a small sample of their voice. We simply recognize the combination of frequencies that characterize their voice.

The human ear is a sophisticated analyzer of frequencies in a sound signal. The sound sensing organ has about 15 000 "hair cells" that each are tuned to a specific frequency. The brain therefore receives a measurement of the content of each frequency present in a sound. When we want to do a similar analysis of a measured signal we usually use *Fourier analysis*. This is an important tool to characterize data from a measurement from a turbulent flow, but it is also an important part of many optical measurement systems where the raw transducer signal is a frequency. The frequency is often determined by a Fourier analysis. In this section we focus on Fourier analysis in time, but it can just as well be done in space (e.g., if instantaneous data along a line is available) .

C.1 Fourier series

If we have a periodic signal (i.e., a signal that repeats itself every time interval T) it can be developed in a Fourier series as:

$$u(t) = A_0 + \sum_{n=1}^{\infty} A_n \cos\left(2\pi n \frac{t}{T}\right) + \sum_{n=1}^{\infty} B_n \sin\left(2\pi n \frac{t}{T}\right) \tag{C.1}$$

The frequencies present in this decomposition, $f_n = n/T$, are *harmonics* (or integer multiples) of the fundamental frequency $1/T$. The Fourier coefficients, A_n and B_n, are given by:

$$A_n = \frac{1}{T} \int_{-T/2}^{T/2} u(t) \cos\left(2\pi n \frac{t}{T}\right) dt \tag{C.2}$$

$$B_n = \frac{1}{T} \int_{-T/2}^{T/2} u(t) \sin\left(2\pi n \frac{t}{T}\right) dt \tag{C.3}$$

Example: Square wave

Consider the square wave signal shown in figure C.1. Show that it can be reconstructed using the following expression:

$$u(t) = \frac{4}{\pi} \sum_{n=1,3,5\ldots}^{\infty} \frac{1}{n} \sin\left(2\pi n \frac{t}{T}\right) \tag{C.4}$$

Figure C.1 illustrates that for $n = 1$ (dashed curve) the result is just a sine curve. As the Fourier components for increasing values of n are added, however, the resulting curve approaches the square wave signal.

It is sometimes convenient to use a complex notation in the formulation of Fourier series. We can define a complex coefficient as $C_n = A_n - iB_n$ and rewrite equations (C.2–C.3) as:

$$C_n = \frac{1}{T} \int_{-T/2}^{T/2} u(t) e^{-i2\pi nt/T} dt \tag{C.5}$$

The ratio between the real and imaginary values can provide phase information about the signal.

It is also convenient to introduce negative values of n. This corresponds to negative frequencies (which can be thought of as waves going backwards in time). Then the values are symmetric in the sense that $A(-n) = A(n)$ and $B(-n) = B(n)$. The use of negative values of n means that the reconstruction formula now can be written very compactly as

$$u(t) = \sum_{n=-\infty}^{\infty} C_n e^{+i2\pi nt/T} \tag{C.6}$$

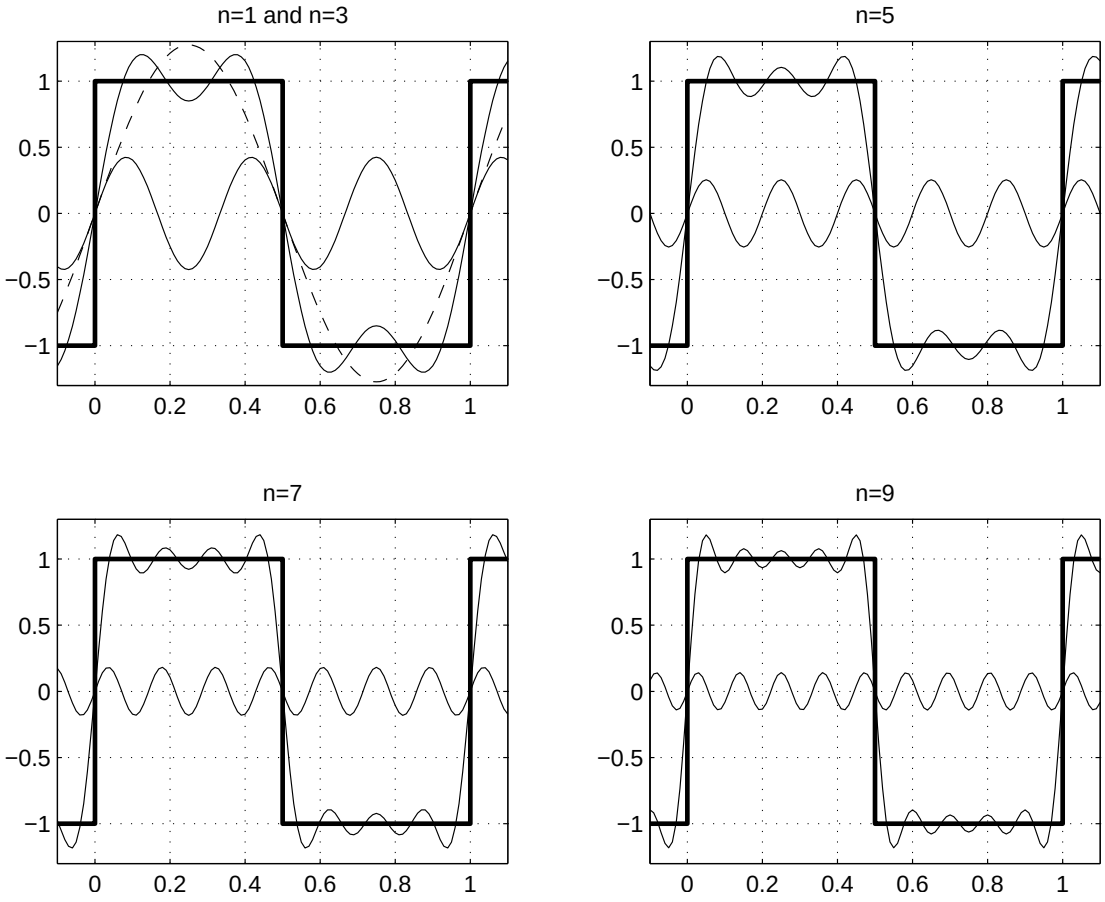

Figure C.1: Reconstruction of square wave signal using Fourier series

C.2 Fourier transform

The Fourier series discussed in the previous section only applies for a periodic deterministic signal; i.e., a signal that is exactly the same from period to period. But sometimes we must deal with a single pulse or even a random processes. We therefore need to be able to decompose a signal that is not repeatable. We can overcome this by using the *Fourier transform*. This can be viewed as a Fourier series in the limit for which the period, T becomes infinite, and the corresponding values of n/T become a continuous range of frequencies f, meaning that all frequencies are now possible.

We define then, the *Fourier transform* of the function $u(t)$ as:

$$\hat{u}(f) = \int_{-\infty}^{\infty} e^{-i2\pi ft} u(t) dt \tag{C.7}$$

These are really the continuous counterpart to the Fourier series coefficients of a periodic signal, and can similarly be used to reconstruct the original signal. We call this reconstruction the *inverse Fourier transform* and define it as:

$$u(t) = \int_{-\infty}^{\infty} e^{+i2\pi ft} \hat{u}(f) df \tag{C.8}$$

As in the complex Fourier series, we use negative values of the frequency f.

An implicit assumption is that the integrals converge. This is, of course, never true for a stationary random process, so we need to use the idea of generalized functions to insure that they do. These are discussed in detail in section E, and will be important when we consider stationary random processes. In practice, however, these Fourier integrals exist for all experimental signals, sincethe time domain over which the integral can be performed is finite. Some of the consequences of this truncation in time are discussed under the sections about filtering and windows below.

C.3 Convolution

A convolution is an operation on two functions f and g defined as:

$$f \otimes g = \int_{-\infty}^{\infty} f(\tau) g(t - \tau) d\tau \tag{C.9}$$

A convolution is an integral that expresses the amount of overlap of one function g as it is shifted over another function f. It therefore "blends" one function with another. We have already seen one example of a convolution in the autocorrelation function defined in section 8.2. The use of windows discussed in the next section can also conveniently be expressed in terms of convolutions.

For the Fourier transform, some important relations for convolutions exist. Here, we will let $\mathcal{F}$ denote the Fourier transform and $\mathcal{F}^{-1}$ denote the inverse

Fourier transform. The most important results are:

$$\begin{aligned} \mathcal{F}[f \otimes g] &= \mathcal{F}[f]\mathcal{F}[g] && \text{(C.10)} \\ \mathcal{F}(f\, g) &= \mathcal{F}[f] \otimes \mathcal{F}(g) && \text{(C.11)} \\ \mathcal{F}^{-1}[\mathcal{F}(f)\mathcal{F}(g)] &= f \otimes g && \text{(C.12)} \\ \mathcal{F}^{-1}[\mathcal{F}(f) \otimes \mathcal{F}(g)] &= f\, g && \text{(C.13)} \end{aligned}$$

In words, this means that the convolution of two functions in the time space corresponds to the product of the transformed functions in the frequency space – and vice versa.

C.4 The finite Fourier transform

In any application of Fourier analysis we are always limited by the length of the time record, T. This means that the most we can expect to be able to transform is the finite time transform given by:

$$\hat{u}_{iT}(f) = \int_{-T/2}^{T/2} e^{-i2\pi ft} u(t) dt \tag{C.14}$$

where for convenience we have written it over the symmetric interval in time $(-T/2, T/2)$.

Now with a little thought, it is clear that we are actually taking the Fourier transform of the product of two functions, the correlation (the part we want) plus the window function; i.e.,

$$\hat{u}_{iT}(f) = \mathcal{F}[u(t)w_T(t)] = \int_{-\infty}^{\infty} e^{-i2\pi ft} u(t) w_T(t) dt \tag{C.15}$$

where $w_T(\tau)$ is defined by:

$$w_T(\tau) = \begin{cases} 1, & -T/2 \le \tau \le T/2 \\ 0, & |\tau| > T/2 \end{cases} \tag{C.16}$$

From the results of the preceding section we immediately recognize that the Fourier transform we seek is the convolution of the true Fourier transform with the Fourier transform of the window function; i.e,,

$$\begin{aligned} \hat{u}_{iT}(f) &= \hat{u}_i(f) \otimes \hat{w}_T(f) \\ &= \int_{-\infty}^{\infty} \hat{u}(f - f')\hat{w}_T(f') df' \\ &= \int_{-\infty}^{\infty} \hat{u}(f')\hat{w}_T(f - f') df' \end{aligned} \tag{C.17}$$

Obviously the Fourier transform at a given frequency is contaminated by the Fourier transform at all other frequencies, the exact amount depending on the window function, the Fourier transform of which is given by:

$$\hat{W}_T(f) = T\frac{sin(\pi fT)}{\pi fT} \tag{C.18}$$

(See if you can show this.) The so-called side-lobes have their zeros at frequency which are multiples of $1/T$ and roll-off only as f^{-1}; moreover, every other side-lobe is negative.

We shall see later that windows play a very important role in spectral analysis. Unfortunately their importance is poorly understood by many (even texts) which erroneously confuse Fourier transforms and Fourier series. For example, if you simply imagine a finite piece of record to be repeated periodically, you will completely overlook the fact that your spectral analysis has been corrupted by the finite time window.

C.5 The shift theorem

Consider a signal, $u(t)$, which is shifted in time by amount Δ to obtain $u(t+\Delta)$. Sometimes this is unavoidable; e.g., in a multichannel A/D converter without simultaneous sample-and-hold where the channels are scanned sequentially. And sometimes we introduce time lags deliberately; for example, to maximize the correlation with another signal. Or as another example, in the next section it will be seen to be convenient to consider the Fourier transform over the interval $(0, T)$ instead of $(-T/2, T/2)$.

It is straightforward to show that time-lags introduce a phase-shift on the Fourier transform which is linear with frequency. From the definition of the Fourier transform, it follows immediately that:

$$\mathcal{F}[u(t+\Delta)] = \int_{-\infty}^{\infty} e^{-i2\pi ft} u(t+\Delta)dt \tag{C.19}$$

But we can define $x = t + \Delta$ and transform the integral to obtain:

$$\begin{aligned} \mathcal{F}[u(t+\Delta)] &= \int_{-\infty}^{\infty} e^{-i2\pi f(x-\Delta)} u(x)dx \\ &= e^{+i2\pi\Delta} \int_{-\infty}^{\infty} e^{-i2\pi fx} u(x)dx \\ &= e^{+i2\pi\Delta}\mathcal{F}[u(x)] = e^{+i2\pi\Delta}\hat{u}(f) \end{aligned} \tag{C.20}$$

Note that $F[u(x)] = \mathcal{F}[u(t)]$ since both t and x are just dummy integration variables in the integrals.

If we look at the phase of the Fourier transform, we see immediately that our time displacement corresponds to a phase shift which is linear with frequency; that is:

$$\phi_{shifted}(f) = tan^{-1}\left[\frac{Im}{Re}\right] = \phi_{unshifted} + 2\pi f\Delta \tag{C.21}$$

It is easy to show the the inverse is also true: a linear phase shift corresponds to a simple time delay in the signal. This can sometimes be used to great advantage in designing measurement systems.

Appendix D

Digital Fourier transforms

Foreword: This appendix was largely taken from the notes from courses on turbulence measurement at the Danish Technical University and Chalmers developed by Knud Erik Meyer, Peter B.V. Johansson and William K. George.

D.1 Aliasing of periodically sampled data

Before considering what happens if we digitally sample an signal for a finite length time interval, let's consider first what happens if we digitally sample an infinitely long record. The easiest way to think about this is to make a simple model for the analog-to-digital conversion process in which the digitally sampled signal is treated as the limit of a continuously varying one. Although this involves generalized functions (which are treated in detail in section E), the only result we need to use here is the familiar delta-function, $\delta(t)$ which is infinite at $t = 0$, zero everwhere else, and in the limit as $\epsilon \to 0$ has the following properties:

$$\int_{-\epsilon}^{+\epsilon} \delta(t)dt = 1 \tag{D.1}$$

$$\int_{-\epsilon}^{+\epsilon} f(t)\delta(t)dt = f(0) \tag{D.2}$$

$$\int_{-\epsilon}^{+\epsilon} f(t)\delta(t-t_o)dt = f(t_o) \tag{D.3}$$

Using these we can define a sampling function, say $g(t)$ as:

$$g(t) = \Delta t \sum_{n=-\infty}^{\infty} \delta(t - n\Delta t) \tag{D.4}$$

where Δt is the distance between samples. (Note that multiplication by Δt makes $g(t)$ dimensionless, since the delta-function of time has dimensions of inverse time.) Now we can represent our 'sampled' signal as:

$$u_s(t) = u(t)g(t) \tag{D.5}$$

It is easy to see that this has all of the properties of a sampled time series. For example, the time average over the interval from 0 to T is given by:

$$\begin{aligned} U_T = \frac{1}{T}\int_0^T u_s(t)dt &= \frac{1}{T}\int_0^T u(t)\left\{\Delta t \sum_{n=-\infty}^{\infty}\delta(t-n\Delta t)\right\}dt \\ &= \frac{1}{N}\sum_{n=1}^{N} u(n\Delta t) \end{aligned} \tag{D.6}$$

since $T = N\Delta t$ is the record length. But this is exactly the digital approximation given by equation B.10.

Similarly we can examine the Fourier transform of our digitally sampled signal which is given by:

$$\begin{aligned} \mathcal{F}[u_s(t)] &= \int_{-\infty}^{\infty} e^{-i2\pi ft}u_s(t)dt \\ &= \int_{-\infty}^{\infty} e^{-i2\pi ft}u(t)g(t)dt \end{aligned} \tag{D.7}$$

Since the right-hand side is the Fourier transform of the product of two functions, we know immediately that the result is the convolution of the Fourier transform of each function individually; i.e.,

$$\mathcal{F}[u_s(t)] = \{\mathcal{F}[u(t)] \otimes \mathcal{F}[g(t)]\} = \int_{-\infty}^{\infty}\hat{u}(f-f')\hat{g}(f')df' \tag{D.8}$$

where as shown below, $\hat{g}(f)$ is given by:

$$\hat{g}(f) = \sum_{n=-\infty}^{\infty}\delta(f - n/\Delta t) : \tag{D.9}$$

Proof of equation D.9 First note that $g(t)$ is periodic, so it can be represented by a Fourier *series*. If we center the delta function over one period in the interval $(-\Delta t/2, \Delta t/2)$, the Fourier series coefficients are given by;

$$C_m = \frac{1}{\Delta t}\int_{-\Delta t/2}^{\Delta t/2} e^{-i2\pi mt/\Delta t}\Delta t\delta(t)dt = 1 \tag{D.10}$$

Thus the Fourier series representation of $g(t)$is given by:

$$g(t) = \sum_{m=-\infty}^{\infty} e^{+i2\pi mt/\Delta t} \tag{D.11}$$

Now take the Fourier *transform*, term by term, of this Fourier series representation which is given by:

$$\begin{aligned} \mathcal{F}\left[\sum_{m=-\infty}^{\infty} e^{+i2\pi mt/\Delta t}\right] &= \sum_{m=-\infty}^{\infty}\int_{-\infty}^{\infty} e^{-i2\pi ft}e^{+i2\pi mt/\Delta t}dt \\ &= \sum_{m=-\infty}^{\infty}\delta(f - m/\Delta t) \end{aligned} \tag{D.12}$$

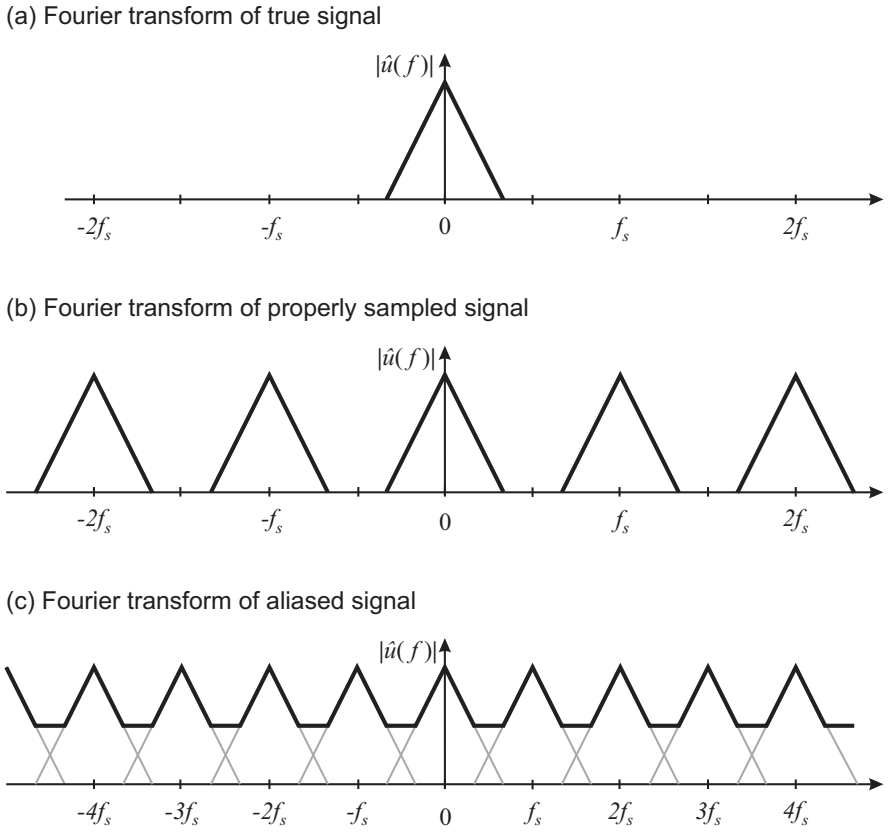

Figure D.1: Relation between aliasing and sample frequency $f_s = 1/\Delta t$

It follows immediately that the Fourier transform of our sampled signal is given by:

$$\begin{aligned}
\mathcal{F}[u_s(t)] &= \int_{-\infty}^{\infty} \hat{u}(f - f')\hat{g}(f')df' \\
&= \sum_{m=-\infty}^{\infty} \int_{-\infty}^{\infty} \hat{u}(f - f')\delta(f' - m/\Delta t)df \\
&= \sum_{m=-\infty}^{\infty} \hat{u}(f - m/\Delta t) \qquad \text{(D.13)}
\end{aligned}$$

Thus the Fourier transform of our sampled signal is an infinitely repeated version of the Fourier transform of the original signal.

This is illustrated in figure D.1. We will assume that figure D.1(a) shows the real Fourier transform of our signal. Note that the signal is symmetric around $f = 0$ as we have just discussed. The result of a discrete Fourier transform with data sampled with a sample frequency f_s that is three times the maximum frequency present in the signal is shown in figure D.1(b). We see that the result

is repeated with a period of f_s. If we instead use a sample frequency that is only 1.5 times the maximum frequency in the signal, we get the result shown in figure D.1(c). The result from the true distribution is still repeated with a period of f_s, but there now is an overlap between the periods. The result (shown as a thick line) is an incorrect (or *aliased*) distribution in the regions of overlap.

This is an important problem called **aliasing**. If we sample too slowly, the results get corrupted – lower frequencies get a contribution from higher frequencies and vice versa. This is also illustrated in figure D.3 of section D.3. The sine signal has period frequency of 0.7 the sampling frequency. However, two other sine signals with period time of 0.3 and 1.3 of sampling frequency, respectively, also match the data samples. After sampling, there is no way of determining what the real signal really was.

The key to avoiding aliasing is to satisfy the so-called "Nyquist criterion": *A signal must be sampled with a sample rate that is at least twice the maximum frequency present in the signal.* In figure D.3 this means that only the slowest signal (period frequency of 0.3 time the sampling rate) would be correctly sampled with the illustrated sampling; i.e., there is no sine function with a frequency lower than 0.3 that matches the sampled data. You may think that you are only interested in the lower frequencies and therefore do not have to worry about higher frequencies. This is wrong. If you proceed this way it is quite likely that the lower frequencies will be corrupted by the higher frequencies! Worse, you will have little chance of detecting the problem and you will have no way of fixing the problem after the data is taken. You may argue that you don't know what the highest frequencies are in your signal. There is always some noise that we cannot control. Well, it is *your* task to ensure this is not a problem! This is the reason why most A/D cards have a low pass filter *before* the sampling and the A/D conversion. To be safe, the filter frequency should be 3–5 times lower than the sampling frequency. We will have a closer look on filters in section G.2.

D.2 The Discrete Fourier transform

As in section B.1, the problem is both that the signal is only known at discrete points and that we only will have data for a limited time period. Now we will look at how a discrete formulation can be made. First we have to change eqs. (C.7) to a finite time estimate,

$$\hat{u_T}(f) = \int_0^T e^{-i2\pi ft} u(t) dt \tag{D.14}$$

Note that we have deliberately shifted the time axis by $+T/2$. This introduces a linear phase shift equivalent to multiplying the Fourier coefficients by $e^{+i\pi fT}$ compared to the symmetric finite transform of the previous chapter. Generally this will not present a problem, but should not be ignored.

This is not exactly what we want, since we have sampled the velocity at discrete

times. We really have

$$u_n = u(n\Delta t) \qquad n = 0, 1, 2, \ldots, N-1 \tag{D.15}$$

Using the basic definitions of integral calculus, we can discretize the integral of equation (D.14) as:

$$\hat{u_T}(f) = \sum_{n=0}^{N-1} e^{-i2\pi f n\Delta t} u_n \Delta t \tag{D.16}$$

N is the total number of samples and $T = N\Delta t$ is the total sample time. The time between samples, Δt, is given by the sampling frequency, $\Delta t = 1/f_s = T/N$. This is, of course, an approximation which becomes exact in the limit as the number of points, N, becomes infinite and as the interval between them, Δt, goes to zero.

Now since we only have N data points, we can only calculate N independent Fourier coefficients. In fact, since we are in the complex domain, we can only calculate $N/2$, since the real and imaginary parts are independent of each other. So we might as well pick the frequencies for which we will evaluate the sum of equation D.16 for maximum convenience. For almost all applications this turns out to be integer multiples of the inverse record length; i.e.,

$$f_m = \frac{m}{T} = \frac{m}{N\Delta t} \qquad m = 0, 1, 2, \ldots, N-1 \tag{D.17}$$

Substituting this into equation D.16 yields our discretized Fourier transform as:

$$\hat{u}_T(f_m) = T\left\{\frac{1}{N}\sum_{n=0}^{N-1} e^{-i2\pi mn/N} u_n\right\} \qquad m = 0, 1, 2, \ldots, N-1 \tag{D.18}$$

This equation can be evaluated numerically for each of the frequencies f_m defined in eq. (D.17). The Fourier coefficients, $\hat{u}_T(f_m)$, found from eq. (D.18) are complex numbers. For future reference note they negative frequencies are mapped into $f_m = N-1, N-2, N-3, N-m$ instead of at negative values of m, as illustrated in Figure D.1.

It is easy to show the original time series data points can be recovered by using the inverse discrete Fourier transform:

$$u_n = \frac{1}{T}\left\{\sum_{m=0}^{N-1} e^{+i2\pi mn/N} \hat{u_T}(f_m)\right\} \tag{D.19}$$

The real and imaginary value of at frequency f_m corresponds to the coefficients of the cosine and sine parts respectively, in a reconstruction of the signal. In fact if we divide $\hat{u_T}(f_m)$ by T, then it is exactly the Fourier series coefficient that would represent a periodic signal of period T, but equal to our piece of the record over the interval $0, T$. Thus the algorithms for treating a discretized periodic signal and a discretized piece of an infinitely long signal are the same. Because of this the

terms in brackets of equations D.18 and D.19 are so important they are usually written as a pair like this:

$$\hat{u}_m = \frac{1}{N}\sum_{n=0}^{N-1} e^{-i2\pi mn/N} u_n \tag{D.20}$$

$$u_n = \sum_{m=0}^{N-1} e^{+i2\pi mn/N} \hat{u}_k \tag{D.21}$$

Equations D.20 and D.21 are computationally very demanding since they require N^2 operations. Fortunately if N is an integer power of 2, 3 or 5, there is an algorithm called the "Fast Fourier Transform" (or simply the **FFT**) that is computationally very efficient and requires only $N \ln N$ operations.[1] The FFT algorithm is available in many software packages for numerical calculations. Hardware solutions (dedicated electronic devices) are also available and are used in several measurement instruments.

Example: Look up the FFT implementation in MATLAB. Note that MATLAB uses a slightly different definition with the indices n and m running from 1 to N instead of from 0 to $N-1$, with corresponding different arguments inside the summations. A change of variables $m' = m+1$ and $n' = n+1$ in eq. (D.18) yields exactly the same definition as used in the MATLAB implementation.

D.3 An Example

Let us try to do an FFT analysis on a very simple signal: we will sample a cosine function with 10 samples per period and we will use $N = 32$ samples and put them into a vector `u`. The samples are illustrated with the symbol $\circ$ in figure D.2(a). Assuming a unit time between samples, the frequency in the signal is $f = 0.1$. The theoretical result in the frequency domain should therefore be a single peak at $f = 0.1$ and zero value of f everywhere else. The result of running an FFT on these 32 samples is shown in figure D.2(b) as the magnitude of $\hat{u}(f)$. The MATLAB command used for the calculation is simply `uf=abs(fft(u))`. The values of the frequency are found using equatiob (D.17) by dividing the vector index with N. The result is probably a bit surprising. We do get a clear peak at the signal frequency $f = 0.1$. However, the result also show some frequency content at all other frequencies. Furthermore we see that the result is perfectly symmetric around $f = 0.5$ and that we therefore also have a clear peak at $f = 0.9$.

To understand the symmetry, remember that we introduced the concept of negative frequencies in the definition of the Fourier Transform. If we instead calculated the frequencies using an index range from $-N/2$ to $N/2$, we would have gotten a result that was symmetric around $f = 0$. Actually, we can evaluate eq. (D.18) for any value of m. However, since cosine and sine give the same values

[1] See [**?**] for more details on the FFT.

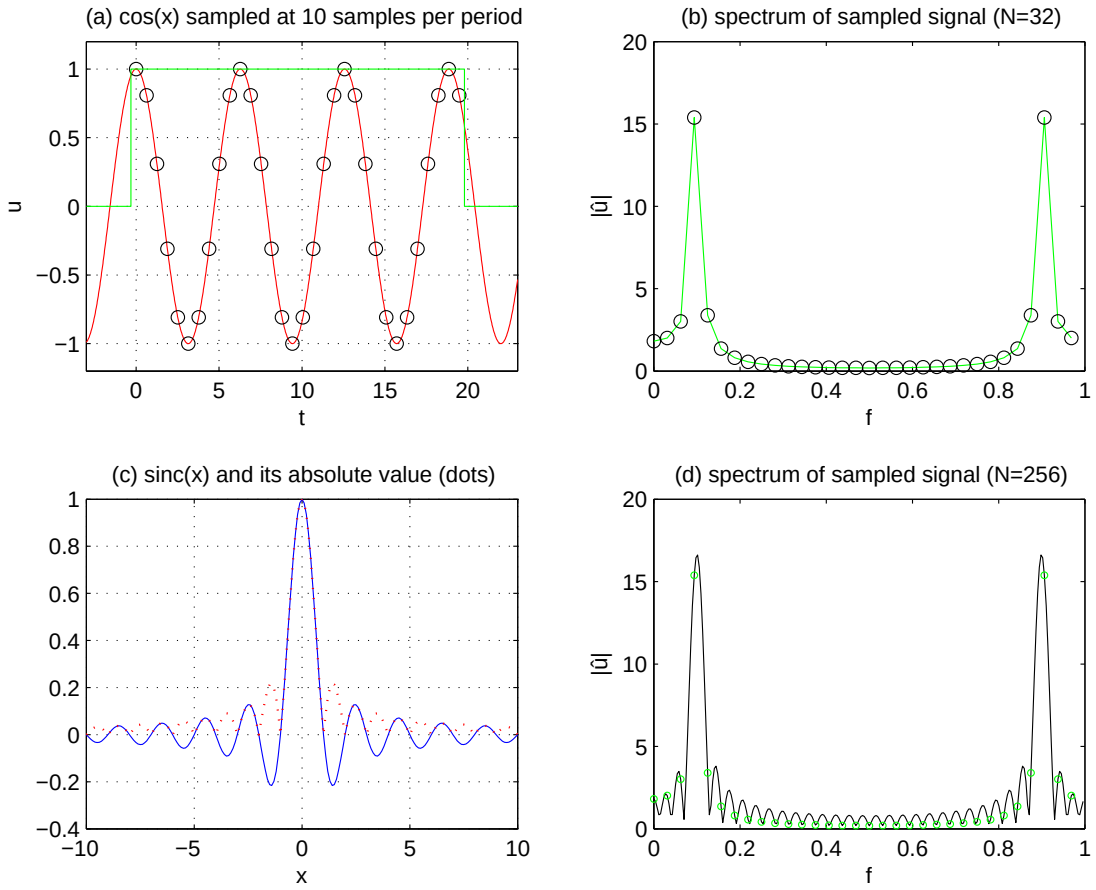

Figure D.2: FFT on sampled cosine signal

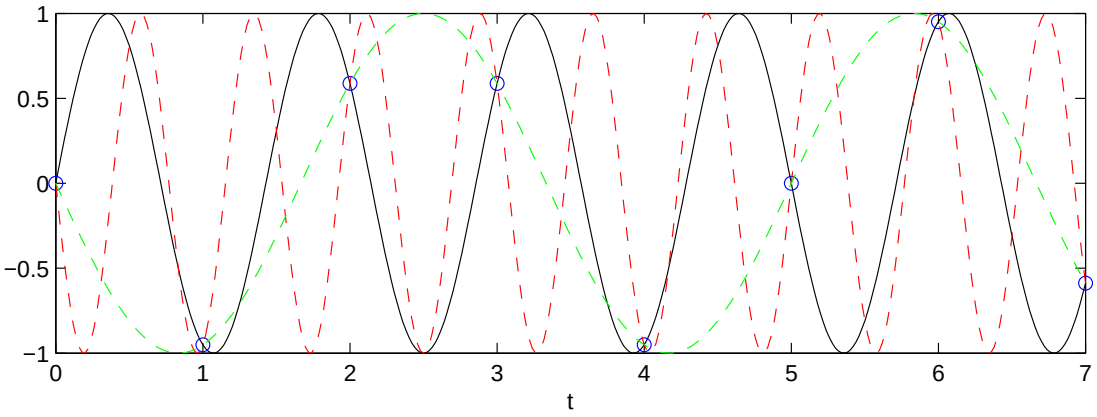

Figure D.3: Sine signal (solid curve) with frequency 0.7 sampled at unit time between samples – sine curves with frequencies 0.3 and 1.3 also matches sampled data.

for arguments that have a difference of 2π, the result will repeat itself every time m is increased with N.

Returning to figure D.2(b), we see that the reason why we get a symmetry around $f = 0.5$ is that we see the real, positive frequencies in the region from $f = 0$ to $f = 0.5$ and then the negative frequencies from the next period of the result (repeated with $f_s = 1$) in the region from $f = 0.5$ to $f = 1$. The symmetric part is only there because it is a technical convenient way of doing the calculations. When we present the results, we therefore only need to present the first half of the result corresponding to "positive" frequencies.

Appendix E

Generalized functions

In Appendix C we defined the Fourier transform and Inverse Fourier Transform by equations C.7 and C.8 respectively. The Fourier coefficients $\hat{u}(t)$, of the signal, $u(t)$ were given by

$$\hat{u}(t) = \int_{-\infty}^{\infty} e^{-i2\pi ft} u(t) dt \tag{E.1}$$

From them the original signal can be reconstructed using inverse Fourier transform by:

$$u(t) = \int_{-\infty}^{\infty} e^{+i2\pi ft} \hat{u}(t) df \tag{E.2}$$

Now if you have studied Fourier transforms in an applied math course, you have probably already spotted one potential problem: the integrals of equations E.1 and E.2 may not even exist — at least *in the ordinary sense*. Figure E.1 illustrates the problem. For example, a stationary random process has no bounds (unless we arbitrarily truncate it over some interval). Moreover, since its statistical properties are independent of origin, the fluctuations simply go on forever. Thus our random signal is really rather nasty, mathematically speaking, and most certainly the integrals *in the ordinary sense* become unbounded.

There are, of course, many other kinds of signals for which the integrals do not converge either, some of which are of great interest to us. Examples include: $u(t) = 1$, $u(t) = cos(2\pi f_o t)$, $u(t) = sin(2\pi f_o t)$, to cite but a few. So we have a dilemma. Our decomposition of signals using Fourier transforms does not seem possible, since the integrals do not converge. The resolution to our dilemma lies in a major mathematical development of the 20th century — the theory of **generalized functions**.

There are numerous references which one can consult for a more proper mathematical treatment than the rather cursory and intuitive treatment here. (Lumley 1970, Lighthill 1955 are two of my favorites). In brief the basic idea is to replace functions whose integrals do not converge with functions which do. Great idea, I'm sure you are thinking, but doesn't this require magic? In truth it is almost magic, since in the end we almost never worry about what we have done, and almost always just go on doing regular mathematics like nothing ever happened.

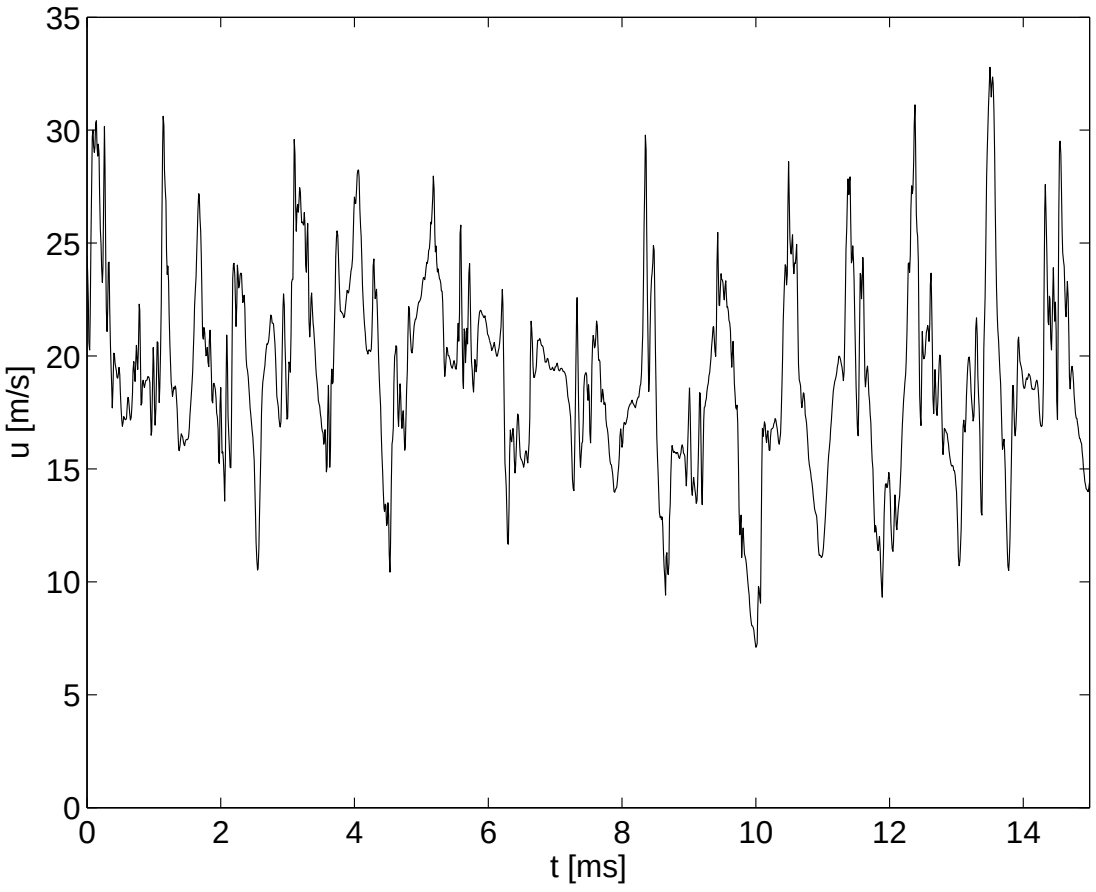

Figure E.1: Hot-wire measurement of the main flow velocity component in a turbulent flow behind a cylinder sampled at 100 kHz. Data from [**?**].

Only rarely will we have to actually consider that we are working with *generalized functions*. Impossible, you say.

Let's consider the following simple example. Suppose I want to take the integral of the function, $f(t) = 1$, from $(-\infty, \infty)$. Obviously this integral does not exist. Nor, in fact does its Fourier transform exist, at least (*in the ordinary sense*).

Now consider a second function, say:

$$g_T(t) = e^{-t^2/2T^2} \tag{E.3}$$

Now since the tails of this function roll-off exponentially, it certainly is integrable. And in fact the integral is given by:

$$\int_{-\infty}^{\infty} e^{-t^2/2T^2} dt = \sqrt{2\pi}T \tag{E.4}$$

(You know this from Chapter 2, since $(1/\sqrt{2\pi}T)exp(-t^2/(2T^2)$ is exactly the Gaussian which integrates to unity.)

Our integrable function $g_T(t)$ also has a wonderful Fourier transform, wonderful in the sense that not only does it exist, all its derivatives exist also; i.e.,

$$\mathbf{FT}\{e^{-t^2/2T^2}\} = \int_{-\infty}^{\infty} e^{-i2\pi ft} e^{-t^2/2T^2} dt = \sqrt{2\pi}Te^{-(2\pi fT)^2/2} \tag{E.5}$$

This is easy to compute by completing the square.

So we have one nasty function, $f(t) = 1$, and one wonderful function, $g_T(t)$; the former has no integral, and hence no transform *in the ordinary sense*, but the latter has both. Now note something interesting. The limit of $g_T(t) \to 1$ as $T \to \infty$, which is exactly the value of our nasty function, $f(t)$. In fact, we could just define a new function by the product $f_T(t) = f(t)g_T(t)$ and note that:

$$\lim_{T\to\infty} f_T(t) = \lim_{T\to\infty} f(t)g_T(t) = f(t) \tag{E.6}$$

In fact, even more interestingly, the Fourier transform of our new function, $f_T(t)$, also exists *in the ordinary sense*. In this case, it's just the Fourier transform of $g_T(t)$ itself.

Here is where one of the really good ideas of the last century appears[1], the magic if you will. Let's just **define** the Fourier transform of our nasty function, $f(t)$, **in the sense of generalized functions** to simply be the limit of the Fourier transform of $f_T(t)$ as $T \to \infty$; i.e,

$$\mathbf{FT_{gf}}\{f(t)\} = \lim_{T\to\infty} \mathbf{FT}\{f_T(t)\} = \lim_{T\to\infty} \int_{-\infty}^{\infty} e^{-i2\pi ft} f(t)g_T(t)dx \tag{E.7}$$

The Fourier transform of 1 *in the sense of generalized functions* is so useful, we have given it a special name, the 'delta-function'; i.e.,

[1]One of the first to see this was the electrical engineer named Heaviside — and he invented the step function which bears his name.

$$\delta(t) \equiv \lim_{T\to\infty} G_T(t) \tag{E.8}$$

where $G_T(t)$ can be any function whose integral is unity and which becomes undefined at $t = 0$ and zero everywhere else in the limit as $T \to \infty$.

I'm sure you have seen δ before, but you may not have realized that it was a generalized function. In general, the generalized functions are not uniquely defined. For example, all the functions below are suitable for defining $\delta(t)$:

$$G_T(t) = e^{-t^2/2T^2} \tag{E.9}$$
$$G_{2L}(t) = e^{-|t|/T} \tag{E.10}$$
$$G_{3L}(t) = \frac{sin(\pi t/T)}{\pi t/T} \tag{E.11}$$

The first and last have continuous derivative everywhere, the second has no derivative at the origin. When working with Fourier transforms, it is generally best to define them in terms of functions which both go to zero exponentially fast, and which have all derivatives continuous. There is nothing in this course which needs anything more than $G_T(t)$, the Gaussian version, or $\sqrt{2\pi}T$ times it.

We can generalize this whole procedure to almost any arbitrary function, whether deterministic or random. For example, suppose we have a stationary random process of time, say $v(t)$. Then we can define its Fourier transform *in the sense of generalized functions* to be:

$$\hat{v}(f) \equiv \mathbf{FT_{gf}}\{v(t)\} = \lim_{T\to\infty} \mathbf{FT}\{v(t)g_T(t)\} \tag{E.12}$$
$$= \lim_{T\to\infty} \int_{-\infty}^{\infty} e^{-i2\pi ft} v(t) g_T(t) dt \tag{E.13}$$

where $g_T(t)$ can be any function for which the product $v(t)g_T(t)$ is integrable and for which:

$$\lim_{T\to\infty} v(t)g_T(t) = v(t) \tag{E.14}$$

Obviously a suitable choice is the Gaussian function we started off with; i.e.,

$$g_T(t) = e^{-t^2/2T^2} \tag{E.15}$$

Exercise: Show that the Fourier transforms *in the sense of generalized functions* of $e^{i2\pi f_o t}$, $cos(2\pi f_o t)$ and $sin(2\pi f_o t)$ are $\delta(f_o)$, $[\delta(f_o)+\delta(-f_o)]/2$ and $i[\delta(f_o)+\delta(-f_o)]/2$ respectively using the Gaussian version of $g_T(t)$ defined above.

Exercise: Compute the inverse transforms from the above example. Do NOT use the short-cut version where you assume the properties of a delta-function, but

instead work with the actual transformed version of $f(t)g_T(t)$ under the limit sign, then take the limits.

For the rest of this course, we will simply agree that whenever there is any doubt, we always mean the Fourier transform in the sense of generalized functions. For example, when we consider homogeneous random processes in three-dimensions, we consider the three dimensional spatial Fourier transform of the velocity field, $u_i(\vec{x},t)$, defined by:

$$\hat{u}_i(\vec{k},t) = \frac{1}{(2\pi)^3}\int\int\int_{-\infty}^{\infty} e^{-i\vec{k}\cdot\vec{x}} u_i(\vec{x},t)d\vec{x} \tag{E.16}$$

(Note the factors of 2π appear in a spatial transform because we are transforming over the wavenumber vector, $\vec{k}$, instead of f.) Since we are transforming functions for which the integrals do not converge, we really mean the Fourier transform *in the sense of generalized functions* defined by:

$$\begin{aligned} \hat{u}_i(\vec{k},t) &\equiv \mathbf{FT_{gf}}\{u_i(\vec{x},t)\} && \text{(E.17)} \\ &= \lim_{T\to\infty} \frac{1}{(2\pi)^3}\int\int\int_{-\infty}^{\infty} e^{-i\vec{k}\cdot\vec{x}}[u_i(\vec{x},t)g_{L^3}(\vec{x})]d\vec{x} && \text{(E.18)} \end{aligned}$$

where $g_{L^3}(\vec{x})$ is some suitably defined function which makes the integral exist. An excellent choice for $g_{L^3}(\vec{x})$ would be:

$$g_{L^3}(\vec{x}) = e^{-[x_1^2+x_2^2+x_3^2]/2L^2} \tag{E.19}$$

whose Fourier transform (in the ordinary sense) is given by:

$$G_{L^3}(\vec{k}) = \frac{L^3}{(2\pi)^{3/2}} e^{-[k_1^2+k_2^2+k_3^2]L^2/2} \tag{E.20}$$

We have used exactly this definition to show that Fourier coefficients in non-overlapping wavenumber bands are uncorrelated.

Exercise: Find the Fourier transform of 1 in three-dimensions using generalized functions, then show how you might represented it symbolically as a three-dimensional delta-function, $\delta(\vec{k})$.

Exercise: If the Fourier transform can be represented in the sense of generalized functions as $\delta(|\vec{k}-\vec{k}_o|)$, find the inverse Fourier transform in the sense of generalized functions.

Appendix F

Spectral analysis of random signals

Stationary random processes commonly arise in the study of random signals, and especially in the study of turbulence. As we shall see below, Fourier transforming a random signal leads to a Fourier transform that is itself random; i.e., the Fourier coefficients associated with any frequency are random and will be different for each realization. Thus we must use statistical analysis in conjunction with Fourier transformation if we wish to examine the frequency content of our signals. This could be quite complicated were it not for the implications of stationarity. As introduced in Chapter 8, a stationary random process is one for which all the statistics are independent of origin in time. Of particular interest to us in this appendix will be the autocorrelation given by $\langle u(t)u(t+\tau)\rangle$ and its Fourier transform, the *spectrum*.

F.1 The Fourier transform of a random signal

The Fourier transform and the inverse Fourier of a vector function of time, say $u_i(t)$, form a transform pair given by:

$$\hat{u}_i(f) = \int_{-\infty}^{\infty} dt \;\; e^{-i2\pi ft} \;\; u_i(\vec{x},t) \tag{F.1}$$

$$u_i(t) = \int_{-\infty}^{\infty} df \;\; e^{+i2\pi ft} \;\; \hat{u}_i(f) \tag{F.2}$$

Note that we have moved the differentials, dt and df, next to the integral sign, so it will be obvious which variable is being integrated. Also it is understood that everything to the right of the differential is to be integrated over those variables. Finally, note that although we have chosen in this section to talk about vector functions of time, everything can be directly applied to scalar functions of time as well – just eliminate the subscripts.

Now I'm sure you are asking: Why is the applicability of Fourier analysis such a BIG THING? There are two big reasons (among many). The first has to do with what happens when you take the inverse transform at the time t, multiply it by the complex conjugate of the inverse transform at time t', and average to get the two-point correlation, $R_{i,j}(t,t')$; i.e.,

$$\begin{aligned} R_{i,j}(t,t') &= \langle u_i(t)u_j(t')\rangle & \text{(F.3)} \\ &= \int_{-\infty}^{\infty} df \int_{-\infty}^{\infty} df'\, e^{+i2\pi(f't'-ft)}\langle \hat{u}_i^*(f)\hat{u}_j(f')\rangle & \text{(F.4)} \end{aligned}$$

But we have assumed the field to be stationary, so the two-point correlation can depend at most on the time separation, $\tau = t' - t$; i.e.,

$$R_{i,j}(t,t') = B_{i,j}(\tau) \tag{F.5}$$

Therefore equation F.3 is simply:

$$B_{i,j}(\tau) = \int_{-\infty}^{\infty} df' \int_{-\infty}^{\infty} df\, e^{+i2\pi(f't'-ft)}\langle \hat{u}_i^*(f)\hat{u}_j(f')\rangle \tag{F.6}$$

and the left-hand side has no dependence on either t or t' separately, but is only a function of $\tau = t' - t$. Now look carefully at the right-hand side. Clearly, unless a miracle occurs in the integration, the right-hand side is going to always depend on t' and t.

Guess what? You probably guessed it. A miracle DOES occur — well, not really a miracle, but even better than a 'miracle'. This 'miracle' can be proven to be true by using the generalized functions of the previous section. The 'miracle' is that since both sides of equation F.3 MUST depend only on $\tau = t' - t$, it follows immediately that *the Fourier components in non-overlapping frequency bands must be uncorrelated.*

Say what, you say? Exactly this:

$$\langle \hat{u}_i^*(f)\hat{u}_j^*(f')\rangle df df' = \begin{cases} S_{i,j}(f)df & , f' = f \\ 0 & , f' \neq f \end{cases} \tag{F.7}$$

or equivalently:

$$\langle \hat{u}_i^*(f)\hat{u}_j(f')\rangle = S_{i,j}(f)\delta(f' - f) \tag{F.8}$$

where $\delta(\ )$ is the familiar delta-function (not to be confused with the Kronecker delta tensor) and $S_{i,j}(f)$ is a *deterministic* function called the **velocity cross-spectrum tensor**.

It is easy to see by substitution that our two-point velocity correlation function is the inverse Fourier transform (in the ordinary sense) of the velocity cross-spectrum tensor; i.e.,

$$B_{i,j}(\tau) = \int_{-\infty}^{\infty} e^{i2\pi f\tau} S_{i,j}(f)df \tag{F.9}$$

It is a bit more difficult to show that the cross-spectrum is the Fourier transform (in the ordinary sense) of the two-point velocity correlation function; i.e.,

$$S_{i,j}(f) = \int_{-\infty}^{\infty} e^{-i2\pi f\tau} B_{i,j}(\tau) d\tau \tag{F.10}$$

Thus the cross-spectrum and the two-point correlation form a Fourier transform pair.

Exercise: Use the definition of $g_T(t)$ in the preceding chapter and prove that $\langle \hat{u}_i^*(f)\hat{u}_j(f')\rangle = S_{ij}(f)\delta(f'-f)$ if $u_i(t)$ is a stationary random variable and $\hat{u}_i(f)$ is defined in the sense of generalized functions by:

$$\hat{u}_i(f) = lim_{T\to\infty} \int_{-\infty}^{\infty} dt\; e^{-i2\pi ft} u_i(t) g_T(t) \tag{F.11}$$

(Hint: The solution is in the next section. But see if you can work it out before looking at it.)

The implications of what we have accomplished become immediately obvious if we evaluate the inverse transform of equation F.9 at $\tau = 0$ to regain the single-point cross-correlation; i.e.,

$$B_{i,j}(\tau) = \int_{-\infty}^{\infty} df\; S_{i,j}(f) \tag{F.12}$$

$S_{i.j}(f)$ is telling us how the single-point Reynolds stress, $\langle u_i u_j\rangle = B_{i,j}(\tau)$, is distributed over the various frequencies.

This is even more obvious if we contract the two indices by letting $i = j$, sum and divide by two to get the energy; i.e.,

$$\frac{1}{2}\langle q^2\rangle = \frac{1}{2} B_{i,i}(0,t) = \frac{1}{2}\int_{-\infty}^{\infty} df\; F_{i,i}(f) \tag{F.13}$$

Clearly the contracted cross-spectrum (usually called simply the *energy spectrum*) is telling us exactly how the turbulence energy is distributed with frequency.

F.2 Proof of Wiener-Khinchin Theorem using generalized functions

Start with the definition of the Fourier transform *in the sense of generalized functions*:

$$\begin{aligned} \hat{u}_i(f) &=_{gf} \int_{-\infty}^{\infty} e^{-i\ 2\pi ft} u_i(t) dt \\ &= lim_{T\to\infty} \int_{-\infty}^{\infty} e^{-i\ 2\pi ft} u_i(t)\ g_T(t) dt \end{aligned} \tag{F.14}$$

where we choose for convenience:

$$g_T(t) = e^{-[t^2/2\ T^2]} \tag{F.15}$$

Now examine the product $\langle \hat{u}_i^*(f)\ \hat{u}_j(f')\rangle$. Substitution from equation F.14 and changing the dummy variable under the integral sign yields:

$$\langle \hat{u}_i^*(f)\ \hat{u}_j(f')\rangle = lim_{\mathrm{T}\to\infty}\ \langle \hat{u}_i^*(f)\ \hat{u}_j(f')\rangle_T \tag{F.16}$$

where $\langle \hat{u}_i^*(f)\ \hat{u}_j(f')\rangle_T$ is defined to be the integral before taking the limit; i.e.,

$$\langle \hat{u}_i^*(f)\ \hat{u}_j(f')\rangle_T = \int\int_{-\infty}^{\infty} e^{-i\ 2\pi\ [f't'-ft]}\langle u_i(t)u_j(t')\rangle e^{-t^2/2T^2}\ e^{-t'^2/2T^2}dtdt' \tag{F.17}$$

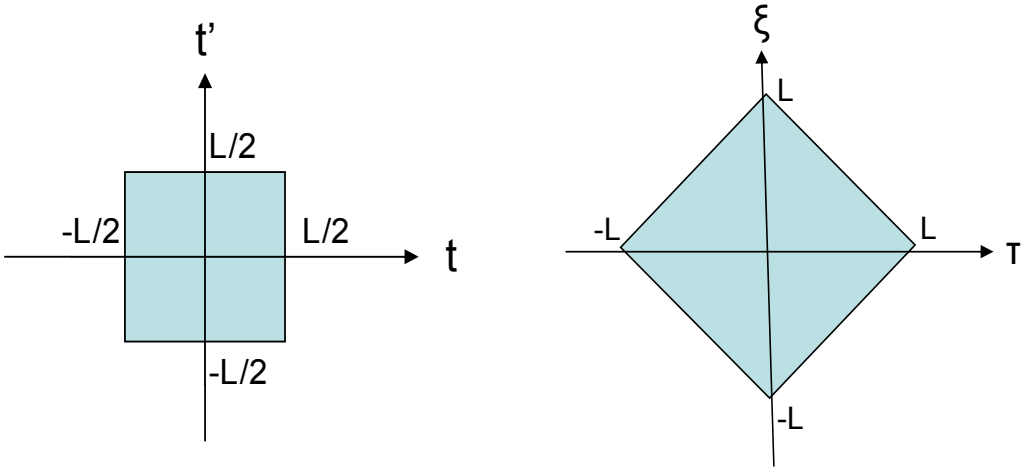

Figure F.1: Leftmost: original domain. Rightmost: transformed domain.

If $u_i(t)$ is a stationary random process, then the two-time correlation is a function only of $\tau = t' - t$ only; i.e. $\langle u_i(t)u_j(t')\rangle = B_{i,j}(\tau)$. So we need to transform the integral to reflect this. For convenience we also define a second new independent variable as $\xi = t' + t$. The original and transformed domains can be viewed as the limits as $L \to \infty$ of the finite domains shown in Figure F.1. For $\tau \geq 0$, $-L+\tau \leq \xi \leq L-\tau$ and $\tau \leq 0$, $-L-\tau \leq \xi \leq L+\tau$. Defining $\Delta f = f' - f$ and transforming the integral yields:

$$\begin{aligned}
&\langle \hat{u}_i^*(f)\ \hat{u}_j(f')\rangle_T \qquad\qquad (F.18)\\
&= lim_{L\to\infty}\frac{1}{2}\left\{\int_0^L d\tau\ e^{i\ [2\pi f'+\pi\Delta f]\tau}\ B_{i,j}(\tau)\ e^{-\tau^2/4T^2}\ \int_{-L+\tau}^{L-\tau} d\xi\ e^{i\ \pi\Delta f\xi}\ e^{-\xi^2/4L^2}\right.\\
&\qquad \left. + \int_{-L}^0\ d\tau e^{i\ [2\pi f'+\pi\Delta f]\tau}\ B_{i,j}(\tau)\ e^{-\tau^2/4T^2}\ \int_{-L-\tau}^{L+\tau} d\xi\ e^{i\ \pi\Delta f\xi}\ e^{-\xi^2/4T^2}\right\}
\end{aligned}$$

Taking the limit as $L \to \infty$ and recombining the integrals yields immediately:

$$\langle \hat{u}_i^*(f)\ \hat{u}_j(f')\rangle_T = \int_{-\infty}^{\infty} d\tau\ e^{i\ [2\pi f' + \pi\Delta f]\tau} B_{i,j}(\tau)\ e^{-\tau^2/4T^2} \int_{-\infty}^{\infty} d\xi\ e^{i\ \pi\Delta f\xi}\ e^{-\xi^2/4T^2} \quad \text{(F.19)}$$

The factor of 1/2 comes from the Jacobian since we have mapped into a domain with twice the area. It is easy to see that the inner integral is just the Fourier transform of a Gaussian with standard deviation $\sqrt{2}T$ and transform variable $\Delta f/\sqrt{2}$, so it reduces to:

$$\int_{-\infty}^{\infty} d\xi\ e^{i\ \pi\Delta f\xi}\ e^{-\xi^2/4T^2} = 2\sqrt{\pi}Te^{-[2\pi\Delta fT]^2} \quad \text{(F.20)}$$

which when integrated over all Δf has integral unity. Therefore in the limit as $T \to \infty$ this will become our delta-function, $\delta(\Delta f) = \delta(f' - f)$. Since it is independent of τ we can move it in front of the integral over τ to obtain:

$$\begin{aligned} \langle \hat{u}_i^*(f)\ \hat{u}_j(f')\rangle &= lim_{T\to\infty}\ \langle \hat{u}_i^*(f)\ \hat{u}_j(f')\rangle_T \quad \text{(F.21)} \\ &= lim_{T\to\infty} 2\sqrt{\pi}Te^{-[2\pi\Delta fT]^2} \int_{-\infty}^{\infty} d\tau\ e^{i\ [2\pi f' + \pi\Delta f]\tau}\ B_{i,j}(\tau)\ e^{-\tau^2/4T^2} \end{aligned}$$

By taking the limit as $T \to \infty$ it is easy to see that this reduces to:

$$\langle \hat{u}_i^*(f)\ \hat{u}_j(f')\rangle = S_{i,j}([f' + f]/2)\delta(f' - f) \quad \text{(F.22)}$$

Since the delta function kills of anything for which $f \neq f'$, this is equivalent to:

$$\langle \hat{u}_i^*(f)\ \hat{u}_j(f')\rangle = S_{i,j}(f)\delta(f' - f) \quad \text{(F.23)}$$

where $S_{i,j}(f)$ is the spectrum given by the Fourier transform of the autocorrelation function; i.e.,

$$S_{i,j}(f) = \int_{-\infty}^{\infty} e^{-i2\pi f\tau}\ B_{i,j}(\tau)d\tau \quad \text{(F.24)}$$

F.3 The finite Fourier transform

We saw earlier in section D.2 that in reality we are always limited to a finite domain. This means that the most we can expect to be able to transform is the finite time transform given by equation D.14; i.e., for a vector field:

$$\hat{u}_{iT}(f) = \int_{-T/2}^{T/2} e^{-i2\pi ft} u_i(t)dt \quad \text{(F.25)}$$

where for later convenience we have written it over the symmetric interval in time. Note that this introduces a linear phase shift equivalent to multiplying the Fourier coefficients by $e^{+i\pi fT}$. Clearly if $u_i(t)$ is random, then so is $\hat{u}_{iT}(f)$, just as was $\hat{u}_i(f)$ above for the infinite domain. What is not so obvious is the relation between the spectrum associated with $\hat{u}_i(f)$ and that associated with $\hat{u}_{iT}(f)$. Note that equation F.8 is not particularly useful to us in actually computing the spectrum, since it contains the generalized function, $\delta(f' - f)$, and thus has meaning only in the limit.

F.3.1 An indirect method

Of course we could take the data and compute from it $\langle u(t)u(t+\tau)\rangle$ for all the time-lags available to us on the interval $0, T$. For example if we have a stationary random process we could define an estimator for the correlation from a time average like this:

$$B_{i,jT}(\tau) = \frac{1}{T}\int_0^{T-|\tau|} u_i(t)u_j(t+\tau)dt \tag{F.26}$$

Note that it may seem strange to divide by T when the integration is over the interval $T - |\tau|$ since this produces a biased estimator, but it actually has a lower variability this way. (See if you can show this.) Also, one disadvantage of this method it is considerably more computationally intensive than the method outlined in the following section, the number of multiplications being proportional to N^2 for N point records.

Once we compute $B_{i,jT}(\tau)$, we can Fourier transform it to get a spectral estimator, i.e.,

$$S_{i,jT}(f) = \int_{-T/2}^{T/2} e^{-i2\pi f\tau} B_{i,jT}(\tau)d\tau \tag{F.27}$$

where we have made the interval symmetrical since we need both positive and negative time lags. Note that we have completely avoided the need for generalized functions, since our correlation estimator is an ordinary function.

The problem with this method can be seen by re-writing the spectral estimator using a window function like this;

$$S_{i,jT}(f) = \int_{-\infty}^{\infty} e^{-i2\pi f\tau} B_{i,jT}(\tau)W_T(\tau)\rangle d\tau \tag{F.28}$$

where $W_T(\tau)$ is defined by:

$$W_T(\tau) = \begin{cases} 1, & -T/2 \le \tau \le T/2 \\ 0, & |\tau| > T/2 \end{cases} \tag{F.29}$$

Now it is clear that we are actually taking the Fourier transform of the product of two functions, the correlation (the part we want) plus the window function. Thus the spectrum we obtain is not the spectrum we seek, but the convolution of the true spectrum with the window function; i.e,,

$$S_{i,jT}(f) = S_{ij}(f) \otimes \hat{W}_T(f) = \int_{-\infty}^{\infty} S_{i,j}(f - f')\hat{W}_T(f')df' \tag{F.30}$$

In other words, the spectrum at a given frequency is contaminated by the spectrum at all other frequencies, the exact amount depending on the window function. This window function is given by:

$$\hat{W}_T(f) = T\frac{sin(\pi fT)}{\pi fT} \tag{F.31}$$

The so-called side-lobes have their zeros at frequency which are multiples of $1/T$, but roll-off only as f^{-1} which is much slower than most spectra. Moreover, every other one is negative, which means you can actually compute negative spectral values for some frequencies. This is of course, quite unphysical. Although other windows (e.g., Hanning, Hamming and Parzen) can be introduced to improve things, the best approach is to avoid this method if at all possible.

F.3.2 A direct method

Another better way to proceed is to work directly with the finite transform of equation F.25, and create the spectral estimator defined by:

$$S_{i,jT}(f) = \frac{\hat{u}^*_{iT}(f)\hat{u}_{jT}(f)}{T} \tag{F.32}$$

The spectrum generated by a single record of data will of course be random, since the $\hat{u}_i$'s are random. But the trick is to sub-divide a very long record into blocks of data which are transformed separately, then averaged the spectral estimators for each block. The more independent blocks that are averaged together, the smoother the resulting spectral estimates (i.e., the more blocks, the lower the variability).

We can show directly that this makes sense by substituting from equation D.14 into the definition of equation F.32 to obtain:

$$S_{i,jT}(f) = \frac{1}{T}\left\{\int_{-T/2}^{T/2} e^{+i2\pi ft}u_i(t)dt\right\}\left\{\int_{-T/2}^{T/2} e^{-i2\pi ft'}u_j(t')dt'\right\} \tag{F.33}$$

where we have changed the dummy integration variable in the second expression to t' since we want to put the integrals together. Combining the integrals and averaging yields:

$$S_{i,jT}(f) = \frac{1}{T}\int_{-T/2}^{T/2}\int_{-T/2}^{T/2} e^{-i2\pi(f't'-ft)}\langle u_i(t)u_j(t')\rangle dtdt' \tag{F.34}$$

But because the process is statistically stationary, the cross-correlation depends only on the time difference, $t' - t = \tau$; i.e., $\langle u_i(t)u_j(t')\rangle = B_{ij}(\tau)$ only. Thus, we can use the same trick we used in section 8.7 to transform the integrals, then integrate one of them out to obtain:

$$S_{i,jT}(f) = \int_{-T}^{T} e^{-i2\pi f\tau}B_{i,j}(\tau)\left[1 - \frac{|\tau|}{T}\right]d\tau \tag{F.35}$$

It is easy to see that as $T \to \infty$ this estimator reduces to exactly equation F.10, so this estimator (unlike the one of the previous section) is unbiased. But like it, it is also clearly the convolution of the spectrum we want with a window. This time, however, the window is given by the Fourier transform of:

$$W_T(\tau) = \begin{cases} 1 - \dfrac{|\tau|}{T}, & -T \leq \tau \leq T \\ 0, & |\tau| > T \end{cases} \tag{F.36}$$

It is straightforward to show that in this case $\hat{W}_T(f)$ is given by:

$$\hat{W}_T(f) = T \left[\frac{sin(\pi f T)}{\pi f T} \right]^2 \tag{F.37}$$

So the sidelobes have their zeros at multiples of $f = 1/T$ just like the top-hat window of section F.3.1, but they roll off as f^{-2}. Moreover, they are always positive, meaning that it is impossible to produce negative spectral values.

F.4 An example: digital spectral analysis of random data

We will now use Fourier analysis on some real data. First, we will use the first 1024 samples data shown in figure A.1 (first 10 ms of data). The data are taken 4 diameters downstream of a cylinder in a turbulent cross flow. Flow settings were matched to a vortex shedding frequency of 1000 Hz. Putting the velocity data into a vector `u`, we use to following MATLAB commands:

```
N=1024;                          % number of samples
dt=0.00001;                      % time between samples
uf=fft(u(1:N));                  % do fft
f=[0:N-1]/(N*dt);                % make frequency axis
uf2=abs(uf).^2/(N*dt);           % calculate spectrum
loglog(f(2:N/2),uf2(2:N/2));  % loglog plot of result
```

The result is shown in figure F.2 (marked "first record"). The six MATLAB script lines make the following operations: First we define number of samples to be 1024 and the time between samples to be 0.01 ms (i.e. sample frequency of 100 kHz). We do the fast Fourier transport on the first 1024 samples and store them in vector `uf`. The frequency axis is then computed using eq. (D.17)), and the power spectrum is calculated using eq. (F.32)). Finally, the plot is made. Note that the plot only is produced for indices from 2 to $N/2$. The first index correspond to $f = 0$ or $m = 0$ in eq. (D.18)), and (as can easily been seen from the FFT algorithm), it corresponds to the mean value of u and not a real frequency. It is therefore not included in the plot. If we wish to obtain the real zero frequency we must estimate it by extrapolation from the lowest frequencies we have. As discussed in section D.3, the result is symmetric around $N/2$ and we therefore

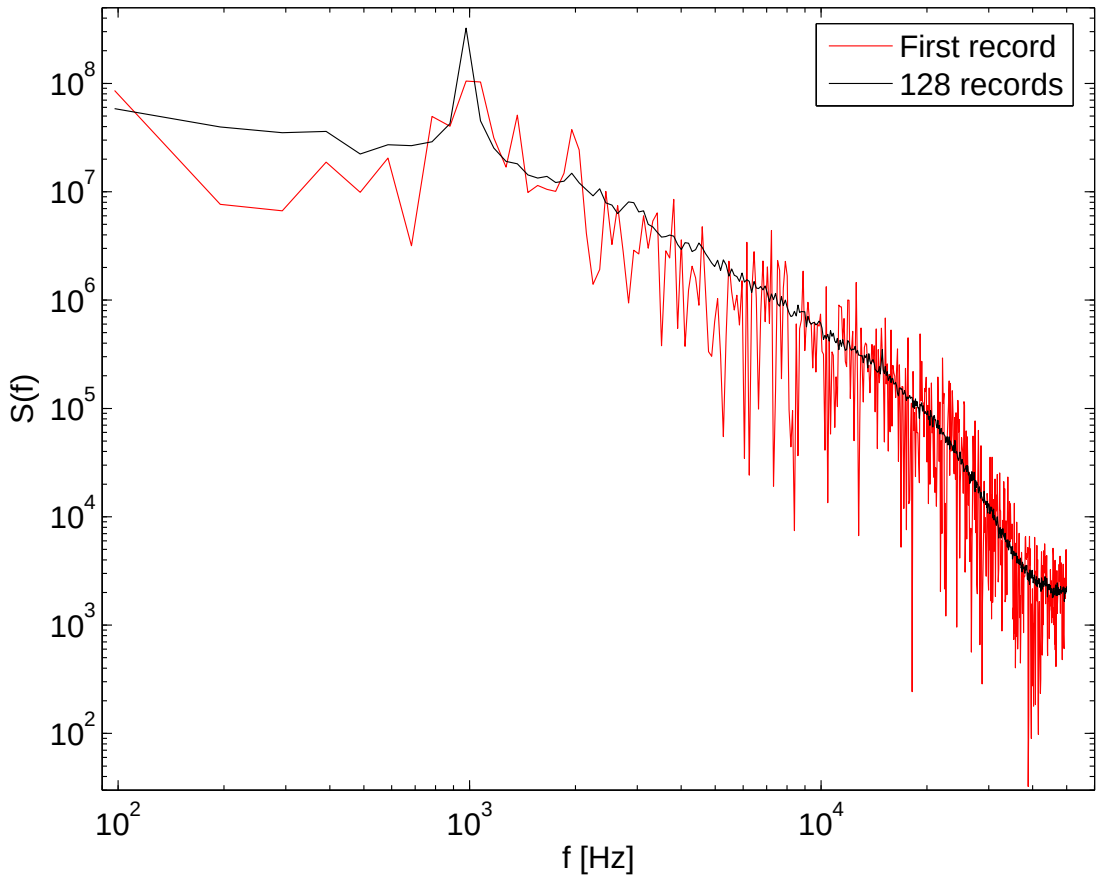

Figure F.2: Power spectrum of the data presented in figure A.1.

only present the first half of the result. The results are usually plotted in a double logarithmic plot since both axis cover several decades.

The result of this analysis is shown as "first record" in Figure F.2. The result is not very satisfying. We do see a peak near 1000 Hz, but also other large peaks. Basically the the result seem very noisy. What we have done is to estimate 1024 frequencies using 1024 data samples. Our input data is a random data set, and therefore the result is just another random data set. To get a better estimate we clearly need to use much more input data. But using a longer data record will not by itself solve the problem, since we will also get more frequencies in the result (increase the resolution of the frequency axis). We there need to do some sort of averaging. One methods is to average adjacent frequencies, which is reduces the variability just like averaging any random numbers. It also decreases the frequency resolution by 'smoothing' the data. Another approach is to divide the original data record into a number of shorter records of the same length and then take the average of the results. The full data series of the data shown in Figure A.1 consists of 131 072 samples (1.3 seconds). This can be split into 128 records of each 1024 samples. The average of the results of FFT analysis of each of these records is also shown in Figure F.2. The result is much smoother and now has a single dominant peak at 1000 Hz. But no matter which way we do it, the resulting spectrum has approximately the same resolution.

Appendix G

Windows and Filters

Foreword: This appendix was largely taken from the notes from courses on turbulence measurement at the Danish Technical University and Chalmers developed by Knud Erik Meyer, Peter B.V. Johansson and William K. George.

G.1 Windows

The other problem in figure D.2(b) was the frequency content outside the signal frequency. It turns out that this is related to the limited number of samples that we have. The Fourier transform is really an integral from $-\infty$ to ∞, not a limited time. We can describe what we do by using the concept of a *window*. We will use a "top hat" window. This can be defined as

$$w_T(t) = \begin{cases} 1; & -T/2 < t < T/2 \\ 0; & \text{otherwise} \end{cases} \tag{G.1}$$

We can now describe the finite time sampling of the real signal $u(t)$ by multiplying with this window function,

$$u_T(t) = u(t)w_T(t) \tag{G.2}$$

and in the frequency domain we find

$$\hat{u}_T(f) = \mathcal{F}[u_T(t)] = \mathcal{F}[u(t)w_T(t)] \tag{G.3}$$

Using eq. (C.11), we find that

$$\hat{u}_T(f) = \hat{u}(f) \otimes \hat{w}_T(f) = \int_{-\infty}^{\infty} \hat{u}(f-f_1)\hat{w}_T(f_1)df_1 = \int_{-\infty}^{\infty} \hat{u}(f_1)\hat{w}_T(f-f_1)df_1 \tag{G.4}$$

We see that our transformed signal gets contaminated with all other frequencies coming from the convolution with the transformed window function $\hat{w}_T$.

This can be seen in the example with the cosine function in figure D.2. The t axis limits in eq. (G.1)) can be changed to suit the actual sampling. This is

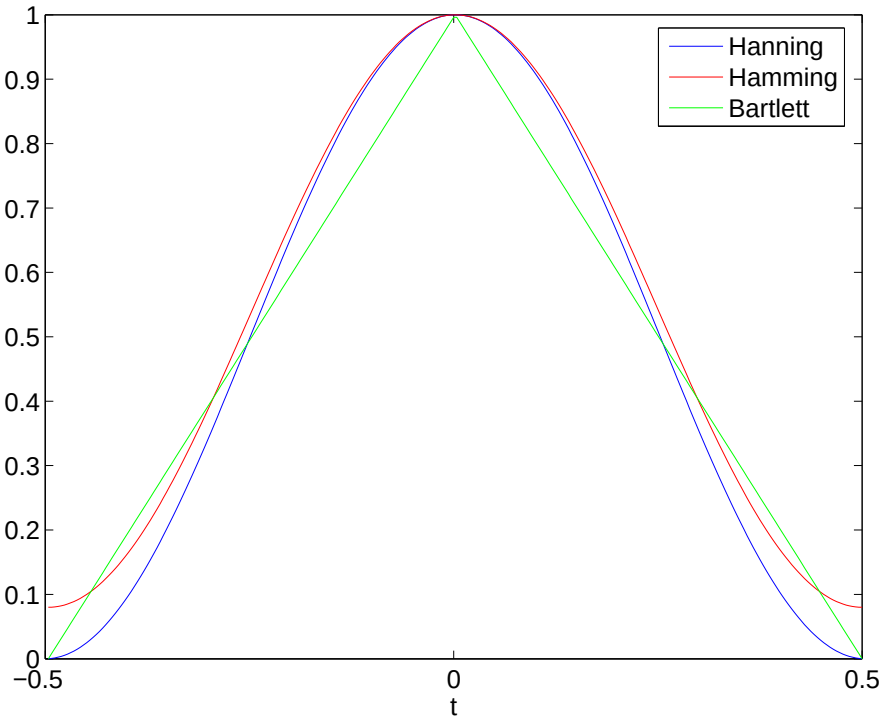

Figure G.1: Examples of common window functions

shown in figure D.2(a). The Fourier Transform of the top-hat window function defined in eq. (G.1) is the function $\mathrm{sinc}(x) = sin(x)/x$. This function is shown in figure D.2(c) where the absolute value of the function is also shown as a dotted curve. We can see how the sinc function is convoluted by the original cosine frequency by doing a new FFT calculation with so-called "zero-padding". This means that samples with the value zero after the original 32 sampled data. This will increase the resolution of the frequency. In MATLAB, zero-padding to a total record of 256 is simply done by the command `uf=abs(fft(u,256))`. The result of this command is shown in figure D.2(d). This result is very close the the analytic result of our sampling procedure. We see how the original frequency at 0.1 has been convolved with the sinc function. The points from figure D.2(b) are shown in figure D.2(d) as small green rings. We see that the courser calculation are samples of the more detailed curve. The lobes of the sinc function falls of as $1/f$ and therefore in the example of figure D.2 moves spectral energy from the "real" frequency into a large range of the total spectrum.

There are several ways to fix the window problem. The best way is to make the record length (the window length) longer. Of course, this requires planning before you do the experiment. Another way is to multiply the sampled data with a window function with no sharp corners. Examples of some common window functions are shown in figure G.1. It may seem strange to take perfectly good data and weight it. One effect of windows is to smooth out real peaks (reduce

resolution). There might also be bias effects, i.e. energy is put into the wrong frequencies. Even though weighting windows can solve problems, they can also create them, so they should therefore be used with care.

G.2 Filters

We can describe filters in the frequency domain in way similar to how we used windows in the time domain. We could define a very simple filter (low-pass sharp cut-off filter) as

$$\hat{w}_{LP}(f) = \begin{cases} 1; & |f| < f_L \\ 0; & \text{otherwise} \end{cases} \tag{G.5}$$

We find the new frequency distribution as

$$\hat{u}_{LP}(f) = \hat{u}(f)\hat{w}_{LP}(f) \tag{G.6}$$

The filtered signal in the time-domain is then found using the inverse Fourier Transform on $\hat{u}_{LP}(f)$. If we apply such a filter to, for example, a square wave signal, we would get a result similar to what we see in figure C.1. If the cut-off frequency f_L is a slightly above a frequency of 9 times the square wave period time, we would get the result shown in the last plot of figure C.1 (marked $n = 9$). We get some distortion of the signal in terms of "ringing". Often this is not desirable and a sharp cut-off filter is therefore not a practical solution. Instead, a much smoother filter function should be used.

Filters and other electronic component (e.g. amplifiers) are often described by the relative change on a logarithmic scale. Traditionally the unit "deciBel" (dB) is used. This unit was originally used in acoustics, where it is a measure for the ratio between two sound intensity levels (measured in $\mathrm{W/m^2}$). If I_2 is a reference level (e.g. the smallest sound intensity sensed by the human ear), the level of an intensity I_1 is found in dB as

$$I_n = 10 \log \frac{I_1}{I_2} \tag{G.7}$$

From this definition, we see that 1 dB corresponds to a 25.9% increase in intensity level. If I_1 is two times I_2 we get $I_n = 3.01$ dB. In electronics, this correspond to differences in power levels. Often we want instead to describe differences in voltage levels. We can find the corresponding ratio N by relating two voltages V_1 and V_2 to the ratio power levels the voltages will make in a resistor R,

$$N = 10 \log \frac{V_1^2/R}{V_2^2} = 20log\frac{V_1}{V_2} \tag{G.8}$$

For voltages we find, that if V_1 is two times V_2 then $N = 6.02$ dB.

Simple filters can be made with combinations of condensers (capitors), coils (inductors) and resistors. A filter that removes high frequencies is called a low-pass filter, and a filter that removes low frequencies is called a high-pass filter. A

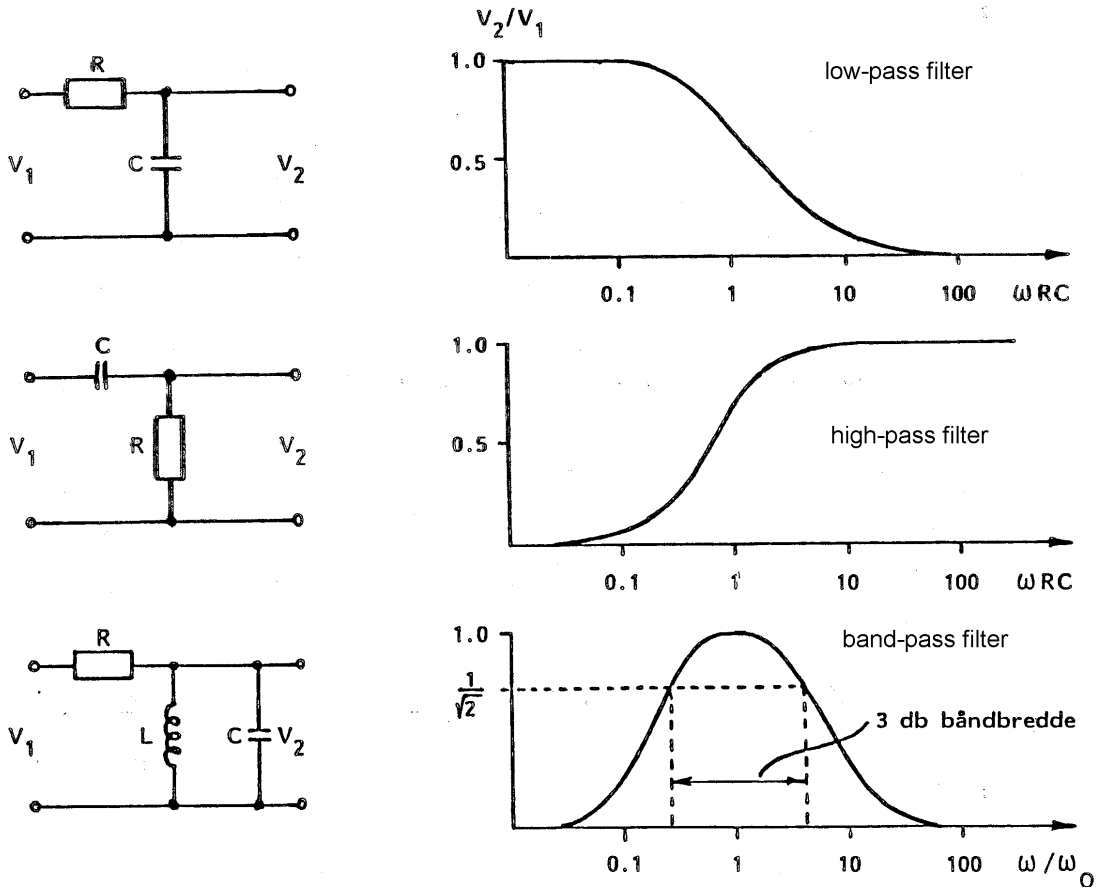

Figure G.2: Simple first order filters

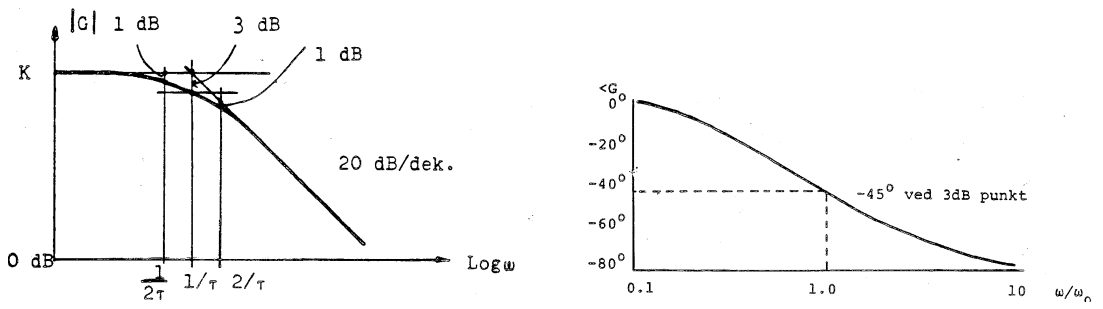

Figure G.3: Amplitude characteristics (left) and phase characteristics (right)

high-pass and a low-pass filter can be combined into a band-pass filter. The filters that can be described by first order differential equations are therefore called first-order filters. A first order low-pass filter rolls off at -6 dB/octave, a second order at -12 dB/oct, and so on. As illustrated in figure G.3, a filter can be described by characteristics of amplitude and phase of the output signal compare to input signal as a function of the frequency. A filter is characterized by a cut-off frequency (frequency where attenuation is 3 dB) and then the slope of the characteristic in dB/decade. As it can be seen, filters change not only the amplitude but also the phase of the output signal. Usually this is not a problem, but if two signals are to be compared after passing two different filters, care should be taken.

More advanced filters with different slopes in dB/decade can be built. Filters that roll-off at -48 dB/octave or more are not uncommon, and can be very useful in preventing aliasing. Details are not covered here, but can be found in signal processing books.